REGIONAL DIAGENETIC POROSITY CHANGE IN PALAEOCENE OILFIELD SANDSTONES, U.K. NORTH SEA

A thesis submitted for the degree of
Doctor of Philosophy

by
Robert Neill Traill Stewart
B.Sc. Edinburgh University

Department of Geology and Applied Geology
University of Glasgow

February 1995

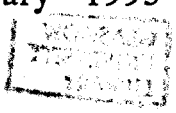

PAGE NUMBERING AS ORIGINAL

Declaration

The material presented in this thesis is the result of research carried out between October 1990 and January 1995 in the Department of Geology and Applied Geology, Galsgow University. The thesis is based upon my own independent research and any published or unpublished material used by me has been given full acknowledgement in the text.

Robert N. T. Stewart
February 1995

Co-authors declaration

The papers presented in this thesis are the product of independent research by Robert N. T. Stewart. Any contributions we have made to the papers are no more than those normally provided during the course of Ph.D. supervision

Dr. R.S. Haszeldine

Dr. A.E. Fallick

ABSTRACT

Palaeocene Montrose Group sandstones form a regionally extensive sequence of stacked sandbodies within the Central North Sea. The diagenetic sequence has been characterised as chlorite; micro-dolomite; pyrite; early carbonate concretions; dissolution of feldspars; steady precipitation of kaolinite during burial; quartz overgrowths increasing during deep burial; late calcite concretions; illite.

Epigenetic chlorite, and pyrite precipitated within depositional marine porefluids ($\delta^{18}O$ -0.9‰SMOW). During the late Palaeocene-early Eocene, shortly after deposition of the Montrose Group, a dramatic sea-level fall and eastward delta progradation of the Moray group resulted in the regional meteoric flushing of the Montrose Group sands. This flushing is recorded in the isotopic signatures of early carbonate concretions, which indicate that aquifer waters had light meteoric $\delta^{18}O$ values. Many of these concretions precipitated from bacterially-mediated reactions. This included fermentation and shallow anaerobic oxidation of hydrocarbons migrating 3km vertically from the underlying Kimmeridge Clay. Examination of 115 well logs shows that locations of vertical migration were structurally controlled, above faulted graben edges, or above thick shales along graben axes. Strontium ratios indicate that dissolution of detrital calcite supplied the calcium.

Kaolinite volumes are usually 2-4%; anomalously high volumes of kaolinite (up to 12%) are found close to deltaic palaeo-shorelines and may represent precipitation during vigorous meteoric flushing of the sandstones. Kaolinite isotopic compositions throughout the Central North Sea indicate that precipitation took place within mixed meteoric-marine pore fluids, whilst surrounding marine shales compacted into a meteoric aquifer, over a temperature range of 30-85°C. Deuterium values are unusually depleted -53 to -76, and suggest a combination of meteoric water and organic interaction.

Quartz cement appears to be generally depth-controlled and forms about 4% at 8,500ft burial. There is also a possibility of 8% quartz overgrowth adjacent to salt diapirs. Secondary porosity does not vary much with depth, always being 2-4%. This indicates that any increase in porosity due to dissolution of feldspars has been thwarted by continued compaction and no net increase of porosity has occurred.

During precipitation of late calcite concretions, pore-water $\delta^{18}O$ was isotopically marine and C supplied by decarboxylation. This indicates that porewaters had become dominated by the introduction of evolved-marine compactional waters from overlying Palaeogene mudrocks. Late carbonate concretions contain up to 10% $MnCO_3$ and are enriched in radiogenic ^{87}Sr compared to Palaeocene shell ratios. This trend is similar to that noted in cements from the underlying Chalk. It is possible that strontium-rich fluids may have been transferred vertically into the Palaeocene from the deeper-buried Jurassic sequence.

Porosity-depth profiles from conventional core analysis data in 42 wells show porosities of 22-36%, with permeabilities of 40-3,000mD at 5,700-9,200ft. The dominant controls are depositional facies, and compaction. Dewatering structures can reduce vertical permeability by 10x. Authigenic chlorite maintains high porosities, but with permeability reduced by 10x. Vertical gradients of porosity and of permeability with depth exhibit "bow curves", which decrease at the top and base of each channel sand unit. Shorter core lengths give systematically higher rates of porosity decline, due to insufficient sampling of depositionally thick channels, whereas cores longer than 30m give gradients of 5-13%.km^{-1}. Porosity varies regionally, but no regional variation of decline-gradient was found.

R.N.T.Stewart PhD University of Glasgow 1996
Regional diagenetic porosity changes in Palaeocene oilfield sandstones, UK North Sea

CHAPTER 1 INTRODUCTION

Figures

CHAPTER 2 ISOTOPIC COMPOSITIONS OF OILFIELD DIAGENETIC CALCITE WITHIN PALAEOCENE SANDSTONES, CENTRAL NORTH SEA.

Figures

CHAPTER 3 DISTRIBUTION OF CARBONATE CONCRETIONS

CHAPTER 4 KAOLINITE GROWTH DURING PORE-WATER MIXING: ISOTOPIC DATA FROM PALAEOCENE SANDS, NORTH SEA UK.

CHAPTER 5 POROSITY AND PERMEABILITY CHARACTERISTICS OF THE PALAEOCENE CLASTIC SEQUENCE, CENTRAL NORTH SEA, UK SECTOR

Figures

Tables

CHAPTER 6 COMPARISON OF DIAGENESIS BETWEEN PALAEOCENE MONTROSE GROUP AND JURASSIC SANDSTONES, NORTH SEA, UK

CHAPTER 7 CONCLUSIONS

Figures

CHAPTER 1 INTRODUCTION

Figures

1.1 Introduction

1.1.1 Importance of diagenesis

As oil production world-wide has progressed to reservoirs at deeper burial depths, it has become apparent that diagenetic mineral cements have an important effect upon rock properties. These non-depositional authigenic minerals affect sandstone reservoir quality in the North Sea reservoirs; for example quartz cements reduce porosity (Giles et a1.1992), hairy illite reduces permeability (Goodchild & Whitaker 1986), authigenic chlorite prevents quartz cementation (Tonkin & Fraser 1991), and extensive carbonate sheets result in compartmentalisation of sandstone reservoirs (Sommer 1978; Blackbourn 1984).

In the UK, the rise in interest inte diagenesis resulted from the combined factors of; the search for petroleum within British waters **Figure 1.1, 1.2,** (Bain 1993), and improvements in laboratory instruments, particularly the scanning electron microscope (Waugh 1970, Pittman 1972). Offshore drilling has enabled recovery of in-situ unweathered rock samples (up to 5km burial, 200°C), and a sense of urgency and relevance to discover the rock properties of sandstones. The effects of deep burial are important so that at least the range in porosities and permeabilities of an undrilled prospect can be assessed. However the wide spread of porosities and permeabilities remains a problem, and additional methods of reducing the uncertainties of poroperm predictions are still needed.

Diagenetic studies within North Sea sandstones have concentrated on the Rotliegendes eolian gas reservoir of the southern North Sea (Glennie et al. 1978; Arthur et al. 1986) and the shallow marine-deltaic mid-Jurassic Brent Group sandstones (Hancock & Taylor 1978; Giles et al. 1992). In particular, the vast amount of data generated from studies into the diagenesis of Brent sandstones has provided diagenetic models from which to compare other reservoir horizons. There are several factors to be taken into consideration when interpreting data which may have affected diagenetic processes. Such factors are detrital mineralogy, facies architecture, pore-water evolution, organic content of sediments. Perhaps surprisingly, although identical data is used, interpretations from diagenetic workers can be at loggerheads;- a) One debate concerns the source of porewaters; this relates to interpretations of oxygen isotopic compositions of authigenic minerals and interpretations of the palaeo-temperatures of quartz overgrowth derived from fluid inclusion measurements. Are porewaters modified by meteoric influx into reservoir horizons during sea-level fall, and fluid inclusions reset during burial (Haszeldine et al. 1992; Osborne & Haszeldine 1993)? b) Are these porefluids influenced by hot brines expelled upwards along faults by underlying compacting sediments, (Burley et al. 19S9; Burley 1993) or can authigenic minerals precipitate without requiring unusual conditions? c) Another debate concerns the open-ness of the geological system. Is the sandstone dosed (Bjorlykke 1984) or open (Gluyas & Coleman 1992) to export and import of ions during cementation?

1.1.2 Rationale for this study

The chemical and isotopic signatures of authigenic minerals are often specific to precipitation processes. To understand why these minerals are present, it is necessary to undertake detailed petrography and chemical and isotopic analysis of mineral separates. Results are normally interpreted in terms of; i) detrital mineralogy ii) mineral-organic reactions iii) differing hydrogeological regimes iv) burial history. Sufficient studies have

now been carried out within the Jurassic sandstones of the Northern North Sea, **Figure 1.3** (Brown 1991), so that ancient hydrogeological regimes can now be reconstructed and modelled with a certain degree of confidence (Haszeldine et al. 1992; Macaulay et al. 1993). Not so the Palaeocene. Although the Montrose Group, **Figure 1.4** (Deegan & Scull 1977), forms the most important reservoir horizon, by volume of oil, within the Central North Sea (and second only to the Brent Group in the North Sea as a whole), neither sufficient individual studies have been undertaken nor any regional studies. Thus it was decided to undertake a regional diagenetic study of the Montrose Group sandstones, **Figures 1.1,1.4** (Rochow 1981). The Montrose Group forms a particularly relevant unit for study as it forms a widespread composite sandbody sub-cropping at burial depths of a few hundred metres in the Moray Firth to three thousand metres in the Central North Sea.

Diagenetic studies have previously concentrated on the important Brent Group reservoirs within the Northern North Sea, and hence diagenetic processes are primarily deduced from data gathered within this unit. The Montrose Group provides an opportunity to test these concepts, by way of examining shallow-buried sandstones which overlap with the Brent Group in burial depth and also by examining sandstones deposited after any possible effects of Palaeocene volcanism. Is there a fundamental difference in cementation between the Brent and Montrose Groups, or was cementation in each Group controlled by burial temperature in a locally closed system?

1.2 Geology

The UK Sector of the North Sea has been divided into Quadrants which are futher divided into 30 Blocks. Quadrants boundaries are defined by longitude and latitude single degrees. Quadrants are divided into 6 (vertical) x 5 (horizontal) array of Blocks. The convention for identifying individual Blocks is to use the Quadrant number and the Block number (1-30) separated by a slash; i.e. 15/20 is Block 20 in Quadrant 15. Individual wells are separated by a dash and are numbered in consequetive order; i.e. 16/28-6 is the sixth well drilled in Block 28 of Quadrant 16.

1.2.1 Pre-Montrose Group

This is described in Glennie (1992). The late Triassic Cimmerian 'orogeny' records rifting at the creation of the Witch Ground Graben, Central Graben and Viking Graben systems. The Triassic here is represented by thin continental red beds of mudstone and siltstone. Tectonic activity is evident from the presence of conglomerates, composed of red-bed boulders and pebbles, along fault block scarps. These grabens began to subside rapidly during the Triassic when development of the East Shetland Platform was initiated. They reached their maximum structural development by. the beginning of the Cretaceous as a result of Mid-Jurassic domal uplift and widespread erosion, especially centred over the axis of the Central Graben.

Late Jurassic to earliest Cretaceous strike-slip movements and fault-block and minor rotations within and adjacent to the Viking and Central Grabens probably coincided with the opening of the central Atlantic and rifting between Iberia and Newfoundland. Lower Jurassic rocks are absent within the Central North Sea and mid-late Jurassic clastic rocks are represented by thin transgressive marine sandstones. These may be absent over contemporaneous dominant positive structural features such as the Fladen Ground Spur and the Forties Montrose High, probably through non- deposition. The late Jurassic

clastic sequence is overlain by the organic-rich marine Kimmeridge Clay Formation, the source rock for hydrocarbons. The thickness and distribution of the clay appears to have been controlled by syn-depositional faulting.

A thin sequence of early Cretaceous claystones and marls marks the continuation of rifting and the onset of Cretaceous marine incursion. Deepening and onlap of the Cretaceous sea during thermal sag after rifting, led to the deposition of the Upper Cretaceous marls and chalks. Chalk sedimentation continued into the Danian as represented by the Ekofisk Formation.

1.2.2 Montrose Group

The early Tertiary marked the transition from late Cretaceous and Danian pelagic carbonate sedimentation, with low terrigineous input, to the accumulation of vast thicknesses of clastic sediment deposited in deltaic, shelf and submarine-fan environments (Stewart 1987). This rapid change is believed to be the result of uplift, erosion and the eastward tilting of the Shetland Platform, **Figure 1.5.** This was located to the north-west, and uplift was associated with the last phase of the opening of the North Atlantic Ocean.

The pre-Tertiary structural configuration controlled the deposition of the early Tertiary sediments. Consequently the early Montrose Group sediments accumulated in the axial regions of the Mesozoic grabens, with no or little sedimentation over the previously emergent highs such as the Forties Montrose High. The Montrose Group consists of three lithostratigraphic units, the Maureen, Andrew and the Forties Formations, **Figure 1.4.** These were deposited as major sand-bodies during separate falls of relative sea-level.

The Formations were deposited as high density gravity flows in sand-dominated channels. These were fed from a series of sediments from the Moray Firth. The Montrose Group was ultimately derived from Devonian-Carboniferous deposits on the Fladen Ground Spur platform, and some first cycle Highland metamorphic terrane debris (Morton 1979; Morton 1982; Morton 1984; Morton 1993).

The basal Maureen Formation was sourced from north of the Halibut Horst and off the East Shetland Platform. The sandstones are generally thin within the Central North Sea area (~20m thick) but form laterally continous sand-rich lobes in the Central Graben area. Abutting the Jaeren High is an 80m thick section of Maureen sandstones which apparently bypassed basin margins during deposition. The Maureen Formation contains a high proportion of chalk detrital material.

The Andrew Formation is by far the largest sandbody and reaches its greatest thickness within the Witch Ground Graben (440m) though generally >120m thick within the study area. It was sourced from the north and south of the Halibut Horst. Overall sand-mud ratios are high throughout the Central North Sea (>40%) and at least >60% within the Witch Ground Graben and into the upper blocks of UK Quadrant 22.

The Forties Formation is present within the Witch Ground Graben as a series of thin mudstones and sandstones (<60m), but thickens considerably within the Central Graben to reach a thickness of 120m. These sands in the Central Graben were apparently

sourced from south of the Halibut Horst. There is more pronounced sediment by-pass of basin margins with sand:mud ratios increasing into the Central Graben. Ratios are >60% within this area though linear sand lobes several km across are apparent.

One of the most controversial aspects of early Tertiary sedimentation in the North Sea basin is the question of water depth. Parker (1975) and Zeigler (1981) argue for water depths up to 915m (3000ft) but not less than 180m (600ft). Beggren & Gradstien (1981) indicate that palaeo-bathymetry did not control the faunal assemblage. Agglutinated foraminifera could develop in water depths as little as 200m but depths of 300 to 500m are equally likely. Morton (1982) argues that similar sedimentary facies occur on either side of the basin margin in the southern Viking Graben and sediment flowed depositionally northwest to southeast. Consequently water depths could not have been deep in the basin centre. He suggests that these water depths could have reached between 300 to 400m (1000ft to 1,300ft). Jones & Milton (1994) suggest a 800m (2625ft) relative sea-level fall during the progradation of Moray Formation deltaic deposits, indicating that they consider the early Palaeocene Central North Sea was a deep basin. This concept was generated by seismic stratigraphic analysis.

Volume balance of sediment supply calculated by Den Hartog Jager et al. (1993) indicates that less than 1km uplift on the East Shetland Platform and Scottish Highlands is necessary to supply Palaeogene sediments to balance sediment budget estimated for the Central North Sea.

1.2.3 Post-Montrose Group Geology

Disconformably overlying the Montrose Group within the Outer Moray Firth is the Upper Palaeocene clastic deposits of a prograding deltaic sequence, the Moray Group (Deegan & Scull 1977; Rochow 1981). This is up to 500m thick and contains some in-situ delta-plain lignite. A thin veneer of mudstones is present at this horizon in the rest of the Central North Sea. Towards the close of Palaeocene subsidence, in the axial part of the graben system, mudstones of the Sele Formation were deposited in dysaerobic conditions. Deposition of the tuffaceous claystones and mudstones of the Balder Formation followed at the end of the Palaeocene. This formation is a wide-spread Palaeocene-Eocene boundary marker. The Hordoland Group, of Eocene to late Miocene age and the Nordland Group of late Miocene to Pliocene age were deposited as basinal muds with localised channel sands and turbidity flows. The two groups have a combined thickness of 1524m (5000ft) to 1829m (6000ft). A composite sub-aerial unconformity cut down into late Eocene deposits in the Outer Moray Firth, and extended into UK Quadrant 15 around 40Ma.

1.3 Previous work - diagenesis

Relatively few papers relating to Lower Tertiary reservoir sandstone diagenesis have been published (Pagan 1980; Stewart et al. 1993; Watson 1993; Stewart et al. 1994). Within descriptions of individual oilfields, the diagenesis is usually considered as slight, and there are no detailed published studies on the effects of compaction and the cementation in these sandstones.

Early papers concerned with diagenetic alteration within Tertiary sediments of the North Sea discussed the dissolution of detrital heavy minerals (Morton 1979; Morton 1982; Morton 1984; Morton et al. 1993). Three conclusions from these papers which are of

interest to clastic diagenetic studies are:- i) during burial, provenance heavy minerals dissolved out as a result of increase in temperature (Morton 1982). ii) the presence of apatite deep within the Palaeocene (3000m burial) was seen being an indication that acidic pore-fluids had never been present within the sands.(Morton 1982). iii) in parts of the Outer Moray Firth (Morton 1984), within the prograding Moray Formation deltaic sequence, (Deegan & Scull 1977), early diagenetic dissolution of minerals such as epidote, staurolite and sphene was attributed to flushing by acidic groundwaters.

The occurrence of carbonate cemented horizons within the sandstones forms a notable feature and is commonly referred to in papers relating to Montrose Group sandstones. Even the earliest paper on lower Tertiary sandstones (Thomas et al. 1974) mentions the presence of hard-cemented impermeable calcite layers within massive sandstones. Carman and Young (1981) added little in their later study on Forties Field, 21/10, 22/6 indicating the occasional presence of carbonate cements in massive sandstones, at 2300m (7540ft) present day burial.

In the most comprehensive review of North Sea fields (Abbotts 1991) details of several Palaeocene Central North Sea fields are summarised. The most detailed descriptions come from:- Maureen Field (Cutts 1991) (16/29, ~8700ft, 2650m burial depth). Here the brief paragenetic sequence is:-
- early calcite cementation
- minor quartz overgrowths
- minor kaolinite cementation
- chlorite cementation
- late calcite cementation
-minor grain dissolution/welding (throughout diagenetic history).
Overall diagenesis is described as 'mild' which resulted in good preserved porosities. The principal diagenetic event is recognised as chlorite cementation. Although this occurs in minor quantities it has a significant detrimental effect on permeability by occluding pore throats. Calcite cemented horizons within massive sandstone units are also noted. These cements are described as being common at sandstone/shale contacts.

In the study of Arbroath and Montrose Fields, 22/17, 22/18, (~8250ft, 2510m burial depth) diagenesis is described as a late event (Crawford et al. 1991). Authigenic phases are quartz, calcite, kaolinite and chlorite cements. None of the cements are significant porosity occluders, the main effect has been to reduce permeability. However, though not noted, large concretions several feet in diameter are clearly present in their type log (their figure 6).

The main diagenetic feature in the Balmoral Field, 16/21, (~7000ft 2130m burial; Tonkin & Fraser 1991) is the presence of calcite cemented zones which act as permeability 'baffles'. These can be up to 5ft thick but of unknown lateral extent and are presurned by the authors to have precipitated from the early breakdown of organic material. Early diagenetic chlorite and illite grain coating clays is reported to have prevented precipitation of quartz overgrowths.

Another Forties Field paper, (Wills 1991), 21/10, 22/6, refers to sandstones as poorly lithified with minor cementation. Authigenic phases; kaolinite, illite and chlorite are not abundant and have only minor detrimental effect on reservoir properties. In the Nelson

Field (22/11), diagenesis is mentioned as being moderate (~7500ft, 2290m present day burial; Whyatt et al. 1991). The cementing phase throughout the sands is quartz overgrowth. However volumetrically the most important phase is ferroan calcite, occurring as randomly distributed concretions, 0.3 to 2m in diameter.

Palaeocene reservoir sandstones of the Everest trend, 22/9, 22/10, (-8500ft, 2590m burial) have been studied by O'Connor and Walker (1993). Reservoir properties relate to depositional environment. Low porosity/permeability sandstones are affected by secondary ferroan calcite which is the dominant control on porosity/permeability. These cemented sandstones are generally near to the base of the sequence and the relate the increase in calcareous cement as being due to the proximity of alkaline, calcitic pore waters derived from the underlying chalk of the Ekofisk Formation. Secondary porosity exists within the Forties Formation as leached feldspar grains and large dissolution voids.

1.4 Aims of thesis

The aims of this thesis are to -
- explain the main processes controlling porosity and permeability within the sands,
- regionally characterise isotopic compositions of authigenic carbonate cements,
- regionally characterise the isotopical compositions of authigenic kaolinites,
- relate composition of authigenic cements to pore-fluid histories taking into account basin geometry and geological history,
- compare the paragenesis and diagenetic processes of Palaeocene sandstones with the intensely studied Brent province.

1.5 Analytical Techniques

Analytical facilities available during this project were
- standard petrography
- cathodoluminescence petrography
- scanning electron microscopy was used on rock stubs to determine morphologies and habits of authigenic minerals. Polished thin-sections were made for back scattered analysis on the SEM.
- X-ray diffraction was used to determine purity of mineral /separate
- computer programs were used to create crossplots on MacIntosh computers (Kaleidegraph v2.0).
- carbon and oxygen isotope extraction lines for carbonate separates, at Scottish Universities Research and Reactor Centre (SURRC), East Kilbride. CO_2 gas produced was purified and then analysed on a VG Isogas SIRA-10 mass spectrometer for carbon and oxygen isotopic compositions.
- oxygen and hydrogen isotope extraction lines for clay separates at SURRC. A VG Isogas SIRA-10 mass spectrometer was used to analyse resultant CO gas for oxygen isotopic compositions. Hydrogen was analysed on a VG-Isotopes Micromass 602 spectrometer.
- $^{87}Sr/^{86}Sr$ analysis of carbonate separates using standard ion exchange columns at SURRC. Strontium was analysed on a VG- Isomass 54E thermal ionisation mass spectrometer.
-core examination and BP poroperm data.

1.6 Summaries of chapters in this thesis

1.6.1 Chapter 2

This chapter concentrates on interpreting the isotopic compositions of carbonate concretions. These were sampled from 10 wells spread across the Central North Sea from depths ranging from 830m (2725ft) to 2750m (9022ft) burial. Minus-cement porosities indicate that concretions grew at a variety of depths. Data were divided into four groupings based on isotopic values; these also coincided with geographical areas, defined by geological structures.

Early concretions precipitated from organic mediated reactions; sulphate reduction, anaerobic hydrocarbon oxidation and fermentation. Oxygen isotope compositions of early concretions indicate that sulphate reduction took place within marine porefluids while the later concretions grew in predominantly meteoric water. Late concretions in areas distal to palaeo-landmass have constrained carbon isotope values $\delta^{13}C = -10$ to +2‰PDB indicating that carbon supply was by way of decarboxylation and detrital carbonate dissolution. Here the oxygen isotope compositions suggest that pore-waters were marine during precipitation.

Strontium ratios of concretions can also be divided. Early concretions have values close to that of detrital Palaeocene carbonates. Late concretion values indicate that these contain an additional radiogenic component either from the dissolution of radiogenic silicates or from Zechstein salt waters.

1.6.2 Chapter 3

This examines the regional distribution of carbonate cements in the Montrose Group. 100 cored and non-cored wells were selected to span the geography of the Central North Sea. Signatures from electric logs were used to define the sandstones themselves, and the thicknesses of concretions within sandstones. The distribution of concretions is illustrated on a map. This shows that concretionary horizons generally forms between 3 - 7% of core thickness. However there are three broad areas where there is enhanced carbonate cementation. These are along graben flanks, along graben axes and distally down palaeoflow towards the graben system. Combined with earlier isotopic data from sampled concretions, the processes forming these cements are tentatively ascribed to have resulted from i) the higher percentage of detrital carbonate material carried into the graben systems, ii) the interaction of hydrocarbons with meteoric influx into the sands; carbonate cements precipitated within the mixing zone of these two fluids. The hydrocarbons are suggested to by oil migrating from the deeper Kimmeridge Clay Formation, and iii) organic acids created earlier by decarboxylation influenced by higher heat flows around salt diapirs or from deep fluids moving vertically from underlying sediments through fractures created by salt domes.

1.6.3 Chapter 4

This examines the origin of porewaters affecting growth of diagenetic kaolinite clay. Kaolinite is a ubiquitous mineral within Montrose Group sandstones. It is present in two morphologies, as a ragged vermiform habit, and as booklet kaolinite. Booklet kaolinite is predominant within deeper wells, while vermiform kaolinite is present within shallower wells. With depth the precipitation habit changes from vermiform kaolinite to the booklet morphology. Within most wells kaolinite makes around 2% of rock volume. However in wells 15/26-3 and 15/26-4 distinctly ragged, vermiform kaolinite makes up to 12% of the rock volume. Isotopic analysis indicates that there is very little variation in composition between the two kaolinite morphologies. On an interpretative δD-$\delta^{18}O$

crossplot, temperatures of precipitation vary from 45 to 70°C within a porewater of between $\delta^{18}O$ = -5 and -3‰SMOW. The simple interpretation is that both kaolinites grew at overlapping temperatures within pore-water modified by meteoric influx. Meteoric waters are presumed to have entered the sandstones during relative sealevel fall in the late Palaeocene-early Eocene.

1.6.4 Chapter 5

This uses compilations of laboratory measurements of porosity and permeability from 115 cored wells. The same depositional facies - channel-sandstones was examined in all cases. Porosity variations of the sandstones are controlled by depositional de-watering structures which define the upper boundary of individual flow units. Gradients of porosity-decline, vertically within the Palaeocene, are similar to shallow buried Brent and to trends of shallow buried sandstone in the Norwegian sector of the North Sea. However at depths greater than 2591m (8500ft) burial, gradients of porosity-decline increase rapidly in a manner similar to that of Brent sandstones. Within the East Central Graben area however porosity gradients decline at a higher rate. This may be due to decrease in sorting or an increase in authigenic minerals.

1.6.5. Chapter 6

The relatively shallow burial of the Palaeocene sandstones provides an opportunity to compare processes controlling diagenesis and early paragenetic sequences with those which operated in more deeply buried Brent sandstones. This enables testing of the hypotheses that diagenesis within the Brent sandstones was either affected by unusual geological events, or was controlled by temperature (depth) driven reactions.

The wide range of isotopic, $\delta^{13}C$ and $\delta^{18}O$, compositions within early concretions from the Palaeocene are similar to that of the Brent Group indicating that a similar range of organic reactions controlled early precipitation within both sandstones. However no late ankeritic carbonates are seen within the Palaeocene, even though these are commonly seen within the Brent Group. Late carbonates in the Montrose Group, precipitated by processes of decarboxylation, enclosing quartz overgrowth are Mn-calcite.

While kaolinite volumes are low within most wells, the ragged vermiform kaolinite morphology and large volumes within Palaeocene wells close to palaeo-shorelines are similar to Brent kaolinites. This suggests that processes precipitating kaolinites within these reservoir horizons were similar.

Quartz cement volumes at 2740m (9000ft) are similar (<5%) to that of shallow Brent Group sandstones. At burial depths around 2590m (8500ft) volumes start to increase suddenly. Within Brent Group sandstones this increase in quartz cement commences at 2740m (9000ft). This may be a depth/temperature controlled reaction within both sequences. Within Montrose Group shallow sandstones (2250m, 7380ft) in close proximity to underlying Zechstein salt-domes, quartz cements form volumes similar to that expected at 2740m (9000ft). This may be related to either higher heat flow around the vicinty of salt domes accelerating pressure solution reactions and/or organic fluids produced within organic-rich muds in the Palaeocene or introduced into the Montrose Gorup from underlying Jurassic sediments through fractures created by salt diapirsm.

Exceptionally saline pore-waters in porewaters of Montrose Group sandstones in the vicinity of salt diapirs indicates some degree of vertical cross-formational flow.

1.7 Conclusions

In summary, Montrose Group sandstones show similar processes of compaction and diagenetic cementation to mid-Jurassic Brent Group sandstones. Unexpected findings from this study include the evidence for cross-formational flow of hydrocarbon. Fractions of these hydrocarbons were oxidised to bicarbonate which later precipitated calcite cements. Also the evidence for cross-formational flow of saline fluids - which are somehow linked to additional quartz cementation. Poroperm within sandbodies is controlled primarily by depositional subfacies. Calcite cements in particular nucleate onto de-watering concentrations of fines at the top of sandstones. Meteoric water displaced depostional marine water at an early stage of burial. However it is not likely that continuous long term flow through the Montrose Group occurred. Secondary porosity has formed continually from early burial, but has been controlled by distinct processes of fluid flow in a shallow open system, followed by deeper dissolution in porewaters made acid by hydrocarbon maturation.

References

Abbotts I.L. (editor) 1991 *United Kingdom Oil and Gas Feilds: 25 Years Commemorative Volume, Geol. Soc. Mem.* **14**, London.

Arthur T.J., Pilling D., Bush D. and L. Macchi 1986 The Leman Sandstone Formation in UK Block 49/28: Sedimentation, diagenesis and burial history. In: *Habitat of Palaeozoic Gas in N.W. Europe.* J. Brooks, J.Goff and B. Van Hoorn (eds) *Geol. Soc. Spec. Publ.*, **23**, 251-266.

Bain J.S. 1993 Historical overview of exploration of Tertiary plays in the UK North Sea. In: *Petroleum Geology of Northwest Europe.* J.R. Parker (ed) Geol Soc., London, 5-14.

Berggren W.A. and F.M. Gradstein 1981 Agglutinated benthonic foramminiferal assemblages in the Palaeogene of the central North Sea: their biostratigraphical and depositional environmental significance In: *Petroleum Geology of the continental shelf of north-west Europe.* L.V. Illing and G.D. Hobson (eds), Heyden & Son, 282-285.

Bjorlykke K. 1984 Secondary Porosity: how important is it? Am. Assoc. Pet. Geol. Mem. **37**, 277-286.

Blackbourn G.A. 1984 Diagenetic history and reservoir quality in a Brent sand sequence. *Clay Minerals*, **19**, 377-389.

Brown S. 1991 Stratigraphy of the oil and gas reservoirs: UK Continental Shelf. In : *United Kingdom Oil and Gas Fields: 25 Years Commemorative Volume,* I.L. Abbotts (ed), *Geol. Soc. Mem.***14**, 9-18.

Burley S.D., Mullis J. and A. Matter 1989 Timing diagenesis in the Tartan Reservoir (UK North Sea): constraints from combined cathodoluminescence microscopy and fluid inclusion studies. *Marine and Petroleum Geology*, **6**, 98-120.

Burley S.D. 1993 Models of burial diagenesis for deep exploration plays in Jurassic fault traps of the Central and Northern North Sea. In: *Petroleum Geology of Northwest Europe: Proceedings of the 4th Conference*, J.R. Parker (ed), Geol. Soc., London, 1353- 1375.

Crawford R., Littlefair R.W. and L.G. Affleck 1991 The Arbroath and Montrose Fields, Blocks 22/17, 18, North Sea. In: *United Kingdom Oil and Gas Fields, 25 Year Commorative Volume*, I.L. Abbotts (ed), *Geol. Soc. Mem.* **14**, 211-217.

Cutts, P.L. 1991 The Maureen Field, Block 16/29a, UK North Sea. In: *United Kingdom Oil and Gas Fields, 25 Years Commemorative Volume*, I.L. Abbotts (ed), *Geol. Soc. Mem.* **14**, 347-352.

Deegan, C.E. and B.J. Scull 1977 A standard lithostratigraphic nomenclature for the central and northern North Sea. *Inst. Geol. Sci. Report* **77/25**.

Den Hartog Jager, D., Giles, M.R., and G.R. Griffiths 1993 Evolution of Paleogene submarine fans of the North Sea in space and time. In: *Petroleum Geology of Northern Europe: Proceedings of the 4th Conference in London*, J.R. Parker (ed), Geol. Soc., London, 59-71.

Giles, M.R., Stevenson, S., Martin, S.V., Cannon, S.J.C., Hamilton, P.J., Marshall, J.D., and G.M. Samways 1992 The reservoir properties of the Brent Group: a regional perspective. In: *Geology of the Brent Group*, A.C. Morton, R.S. Haszeldine, M.R. Giles and S. Brown, (eds), *Geol Soc. Spec. Publ.* **61**, 289-327.

Glennie K.W., Mudd G.C. and P.J.C. Nategaal 1978 Depositional enviroments and diagenesis of Permian Rotliegendes sandstones in Leman Bank and Sole Pit areas of the UK southern North Sea. *J. Geol. Soc.*, **135**, 25-34.

Glennie K.W. 1992 *Introduction to the Petroleum Geology of the North Sea* (3d edition) Blackwell Scientific Publications, Oxford.

Gluyas J.G. and M.L. Coleman 1992 Material flux and porosity changes during sandstone diagenesis. *Nature*, **356**, 52-554.

Goodchild M.W. and J.McD. Whitaker 1986 A petrographic study of the Rotliedendes Sandstone reservoir (Lower Permian) in the Rough Gas Field. *Clay Minerals*, **21**, 459-477.

Hancock N.J. and A.M. Taylor 1978 Clay diagenesis and oil migration in the Middle Jurassic Brent Group Sand Formation. *J. Geol. Soc. Lond.* **135**, 69-71.

Haszeldine, R.S., Brint, J.F., Fallick, A.E., Hamilton, P.J. and S. Brown 1992 Open and restricted hydrologies in Brent Group diagenesis: North Sea. In: *Geology of the Brent Group*, R.S. Haszeldine, A.C. Morton, M.R. Giles and S. Brown (eds), *Geol. Soc. Spec. Publ.* **61**, 401-419.

Jones, R.W. and N.J. Milton 1994 Sequence development during uplift: Palaeogene stratigraphy and relative sea-level history of the Outer Moray Firth, UK North Sea. *Marine and Petroleum Geology*, **11**, 157-165.

Knox R.W.O. and R. Harland 1979 Stratigraphical relationships of the early Palaeogene ash-series of NW Europe. *J. Geol Soc. Lond*, 136, 463-470.

Macaulay C.I., Fallick A.E. and Haszeldine R.S. 1994 Textural and isotopic variations in diagenetic kaolinite from the Magnus Oilfield Sandstones. *Clay Minerals*, **28**, 625-639.

Morton A.C. 1979 Surface features of heavy mineral grains from Palaeogcene sands of the central North Sea. *Scottish Journal of Geology*, **15**, 293-300.

Morton A.C. 1982 Lower Tertiary sand development in Viking Graben, North Sea. *Bull. Am. Assoc. Pet. Geol.*, **66**, 1542-1559.

Morton A.C. 1984 Stability of detrital heavy mineral in Tertiary sandstones from the North Sea Basin. *Clay Minerals*, **19**, 287-308.

Morton, A.C., Halsworth, C.R. and G.C. Wilkinson 1993 Stratigraphic evolution of sand provenance during Palaeocene deposition in the Northem North Sea area. In; *Petroleum Geology of Northwest Europe: Proceedings of the 4th Conference*, J.R. Parker (ed), Geol. Soc., London, 73- 84.

O'Connor S.J. and D. Walker 1993 Palaeocene reservoirs of the Everest trend. In: *Petroleum Geology of Northwest Europe*. J.R. Parker (ed) Geol. Soc., London, 73-84.

Osborne M. and R.S. Haszeldine 1993 Evidence for resetting of fluid inclusion temperatures from quartz cements in oilfields. *Marine and Petroleum Geology*, **10**, 271- 278.

Pagan M.C.T. 1980 *Diagenesis of the Forties Field.* M. Phil. Thesis, University of Edinburgh.

Parker J.R. 1975 Lower Tertiary sand development in the Central North Sea. In: *Petroleum and the continental shelf of northwest Europe*, John Wiley, New York, 447-453.

Pittman E.D. 1972 Diagnenesis of quartz in sandstones as revealed by scanning electron microscopy. *Earth. Sci. Rev.* **26**, 69-112.

Rochow K.A. 1981 Seismic stratigraphy of the North Sea 'Palaeogene' deposits. In*: Petroleum Geology of the Continental Shelf of North- West Europe*, I.V. Illing and G.D. Hobson (eds), Heyden, London, 225-266.

Sommer F. 1978 Diagenesis of Jurassic sandstones in the Viking Graben. *J. Geol. Soc. Lond.* **135**, 63-67.

Stewart, I.J. 1987 A revised stratigraphic interpretation of the Early Palaeogene of the Central North Sea. In: *Petroleum Geology of North West Europe*, J. Brooks and K.W. Glennie (eds), Graham and Trotman, London, 557-577.

Stewart, R.N.T., Haszeldine, R.S., Fallick, A.E., Anderton, R. and R. Dixon 1993 Shallow calcite cementation in a submarine fan: biodegradation of vertically migrating oil? *Am. Assoc. Pet. Geol. Annual Convention*, 186.

Stewart, R.N.T., Fallick, A.E. and R.S. Haszeldine 1994 Kaolinite growth during pore-water mixing: isotopic data from Palaeocene sands, North Sea, UK. *Clay Minerals*, **29**, 627-636.

Thomas A.N., Walmsley P.J. and D.A.L. Jenkins 1974 Forties Field, North Sea. *Bull. Am. Assoc. Pet. Geol.*, **58**, 396-406.

Tonkin P.C. and A.R. Fraser 1991 The Balmoral Field, Block 16/21, UK North Sea. In: *United Kingdom Oil and Gas Fields: 25 Years Commemorative Volume*, I.L. Abbotts (ed), *Geol. Soc. Mem.* **14**, 237-243.

Watson R. 1993 The Forth Field, British Sector, North Sea: evidence for palao-oil leakage in a near surface reservoir. Am. Assoc. Pet. Geol. Annual Convention, 198.

Waugh B. 1970 Petrology, provenance and silica diagenesis of the Penrith Sandstone (Lower Permian) of northwest England. *J. Sed. Pet.*, **40**, 1226-1240.

Whyatt M. and J.M. Bowen 1991 Nelson successful application of a development geoscience model in North Sea Exploration. *First Break*, **9**, 265-280.

Wills J.M. 1991 The Forties Field, Block 21/10, 22/6a, UK North Sea. In: *United Kingdom Oil and Gas Fields, 25 Year Commemorative Volume*, I.L. Abbotts (ed), *Geol. Soc. Mem.* **14**, 301-308.

Ziegler P.A. 1981 Evolution of sedimentary basins in north-west Europe. In: Petroleum geology of the continental shelf of north-west Europe. L.V. Illing and G.D. Hobson (eds), Heyden & Son, London, 3-39.

Figure captions

Figure 1.1 Regional map of the North Sea: WGG - Witch Ground Graben, SHH - South Halibut Horst, FBB - Fisher Bnk Basin.

Figure 1.2 Palaeocene and Eocene oilfields discovered within the North Sea showing number of Quadrants (Bain 1993)

Figure 1.3 Stratigraphic column of the North Sea (Bain 1993)

Figure 1.4 Stratigraphic column of the Palaeocene to Recent (Deegan & Scull1977)

Figure 1.5 Palaeogeographical map during the Palaeocene (Rochow 1981).

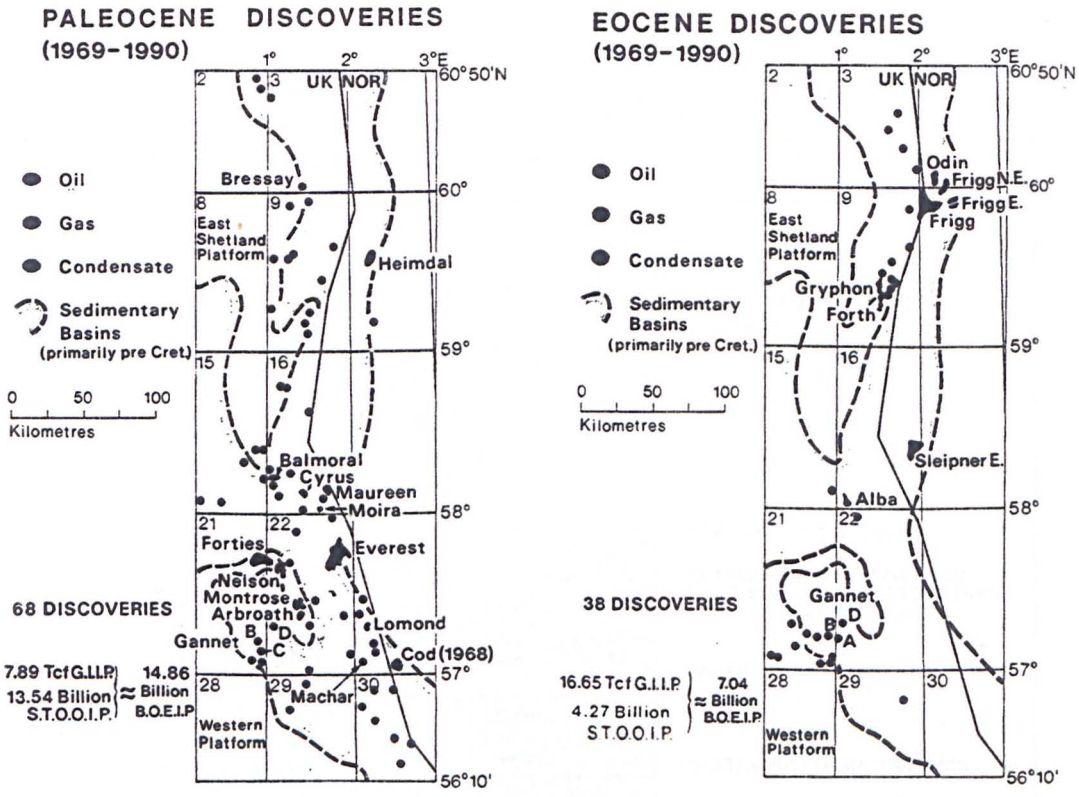

Figure 1.2

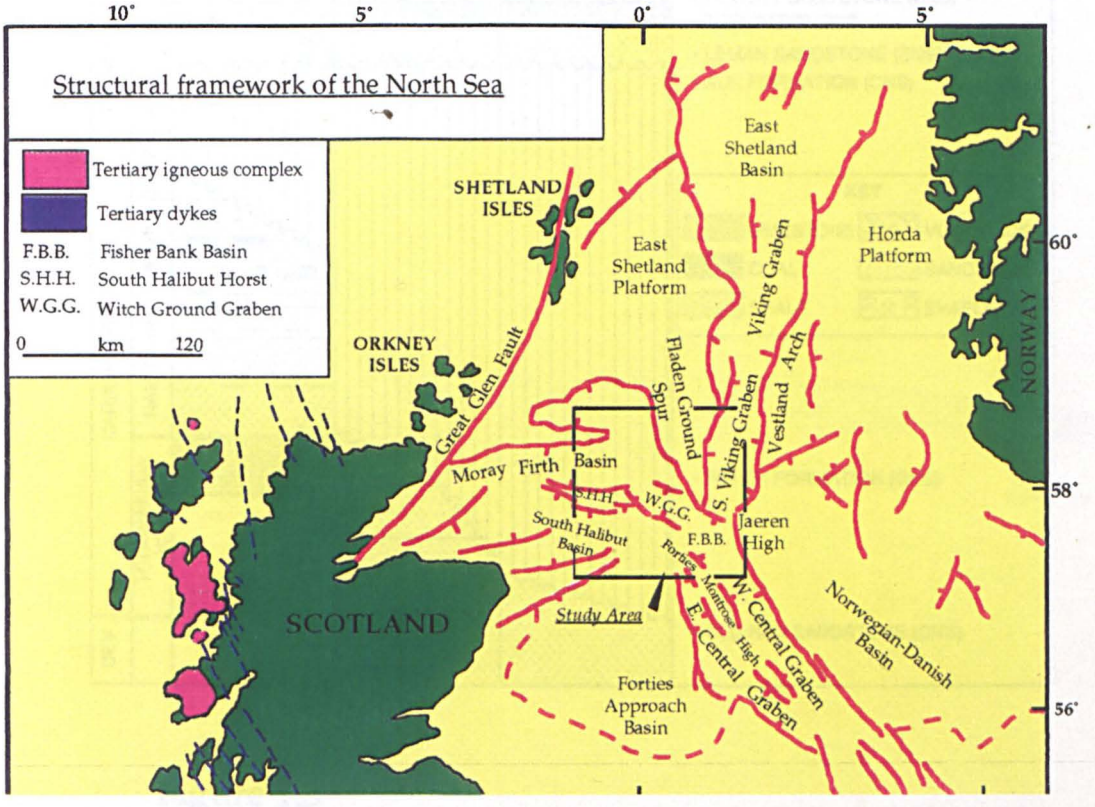

Figure 1.1

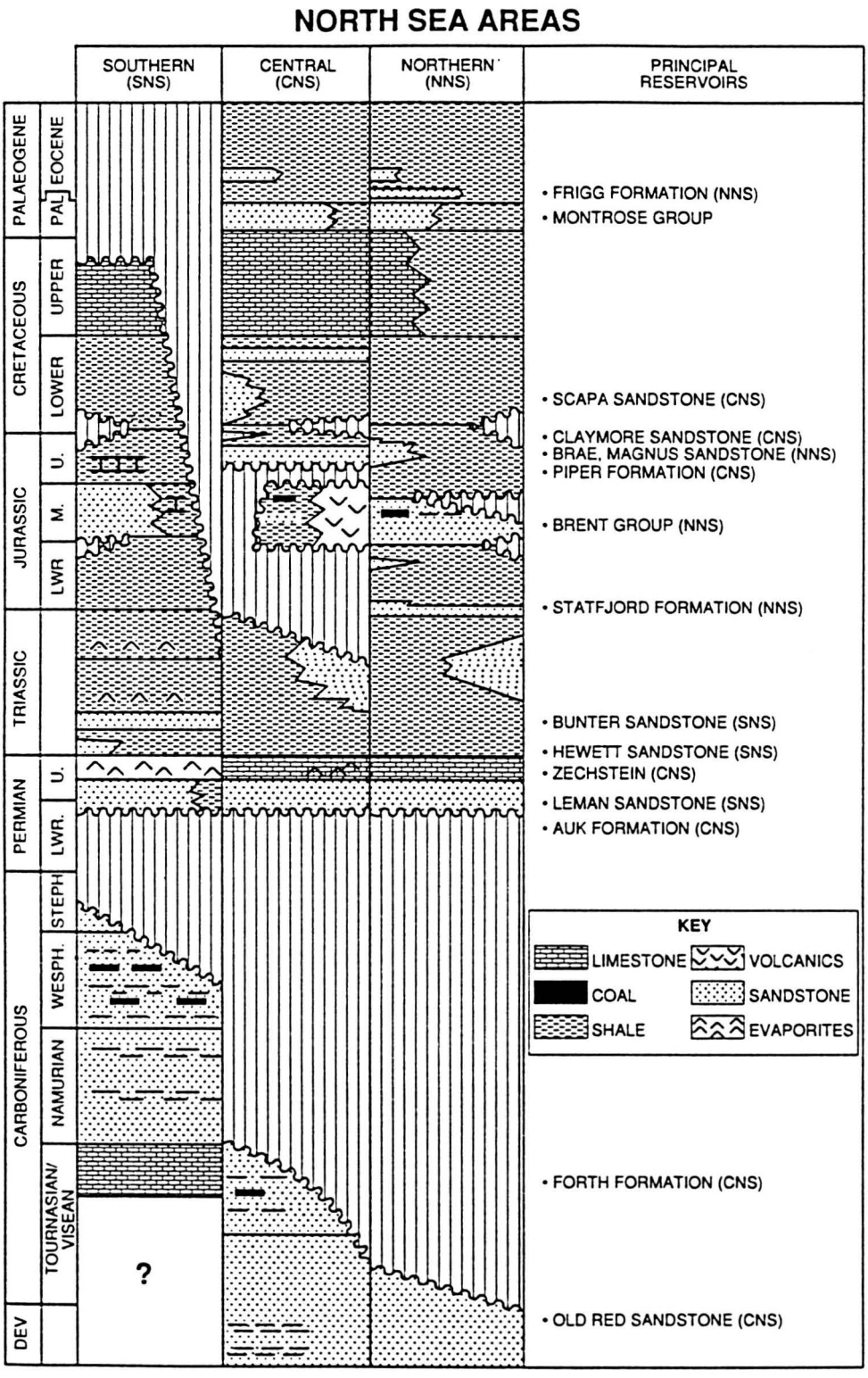
NORTH SEA AREAS
SOUTHERN (SNS)
CENTRAL (CNS)
NORTHERN (NNS)
PRINCIPAL RESERVOIRS
PALAEOGENE
EOCENE
PAL
CRETACEOUS
UPPER
LOWER
JURASSIC
U.
M.
LWR
TRIASSIC
PERMIAN
U.
LWR.
CARBONIFEROUS
STEPH.
WESPH.
NAMURIAN
TOURNASIAN/ VISEAN
DEV
?
• FRIGG FORMATION (NNS)
• MONTROSE GROUP
• SCAPA SANDSTONE (CNS)
• CLAYMORE SANDSTONE (CNS)
• BRAE, MAGNUS SANDSTONE (NNS)
• PIPER FORMATION (CNS)
• BRENT GROUP (NNS)
• STATFJORD FORMATION (NNS)
• BUNTER SANDSTONE (SNS)
• HEWETT SANDSTONE (SNS)
• ZECHSTEIN (CNS)
• LEMAN SANDSTONE (SNS)
• AUK FORMATION (CNS)
• FORTH FORMATION (CNS)
• OLD RED SANDSTONE (CNS)
KEY
LIMESTONE
VOLCANICS
COAL
SANDSTONE
SHALE
EVAPORITES

Figure 1.3

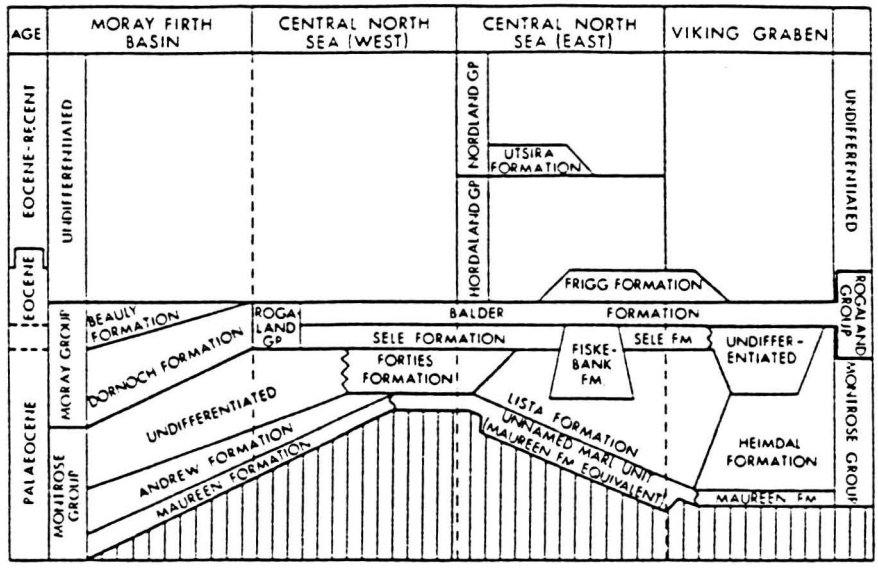
AGE
MORAY FIRTH BASIN
CENTRAL NORTH SEA (WEST)
CENTRAL NORTH SEA (EAST)
VIKING GRABEN
EOCENE-RECENT
EOCENE
PALAEOCENE
UNDIFFERENTIATED
MORAY GROUP
MONTROSE GROUP
NORDLAND GP
HORDALAND GP
UTSIRA FORMATION
FRIGG FORMATION
UNDIFFERENTIATED
ROGALAND GROUP
MONTROSE GROUP
BEAULY FORMATION
DORNOCH FORMATION
UNDIFFERENTIATED
ANDREW FORMATION
MAUREEN FORMATION
ROGALAND GP
BALDER FORMATION
SELE FORMATION
FORTIES FORMATION
FISKE-BANK FM
SELE FM
UNDIFFER-ENTIATED
LISTA FORMATION
UNNAMED MARL UNIT (MAUREEN FM EQUIVALENT)
HEIMDAL FORMATION
MAUREEN FM

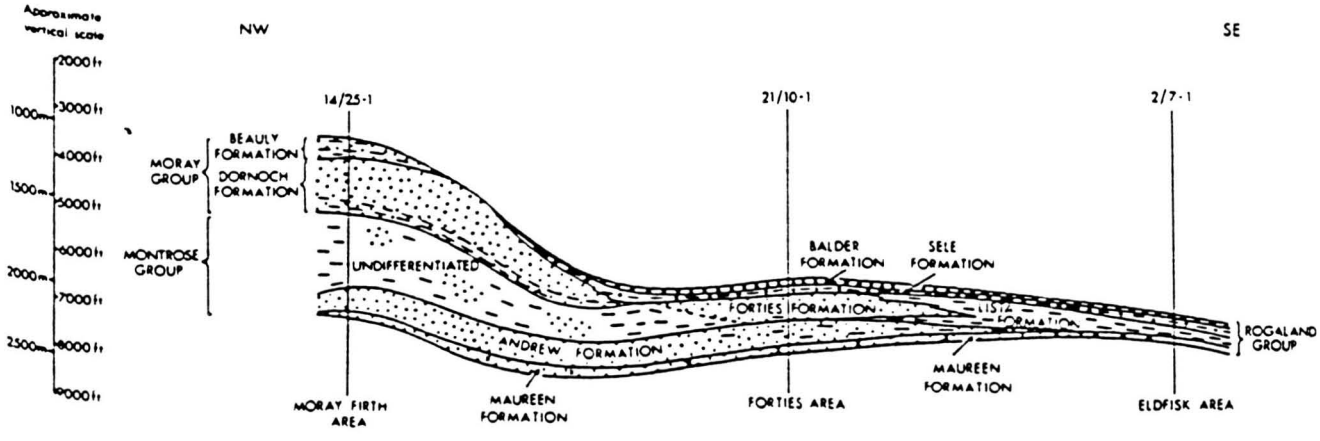
Approximate vertical scale
2000 ft
3000 ft
1000m
4000 ft
1500m
5000 ft
6000 ft
2000m
7000 ft
2500m
8000 ft
9000 ft
NW
SE
14/25-1
21/10-1
2/7-1
MORAY GROUP
BEAULY FORMATION
DORNOCH FORMATION
MONTROSE GROUP
UNDIFFERENTIATED
ANDREW FORMATION
MAUREEN FORMATION
BALDER FORMATION
SELE FORMATION
FORTIES FORMATION
LISTA FORMATION
MAUREEN FORMATION
ROGALAND GROUP
MORAY FIRTH AREA
MAUREEN FORMATION
FORTIES AREA
ELDFISK AREA

Figure 1.4

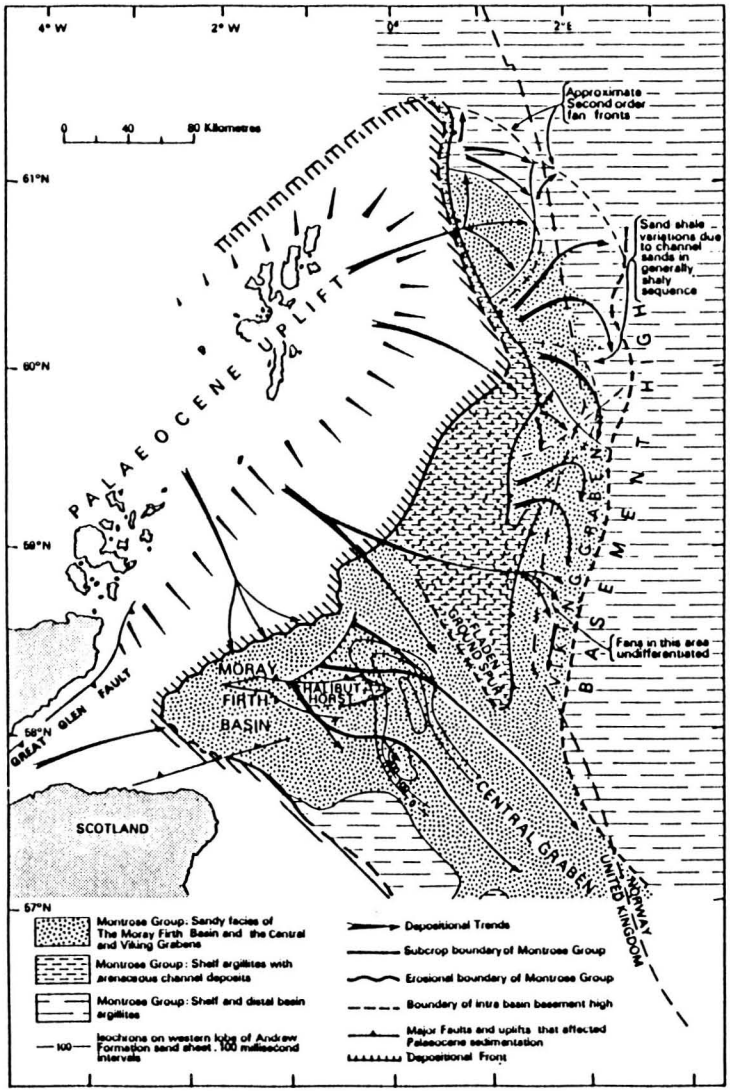

Montrose Group subcrop map.

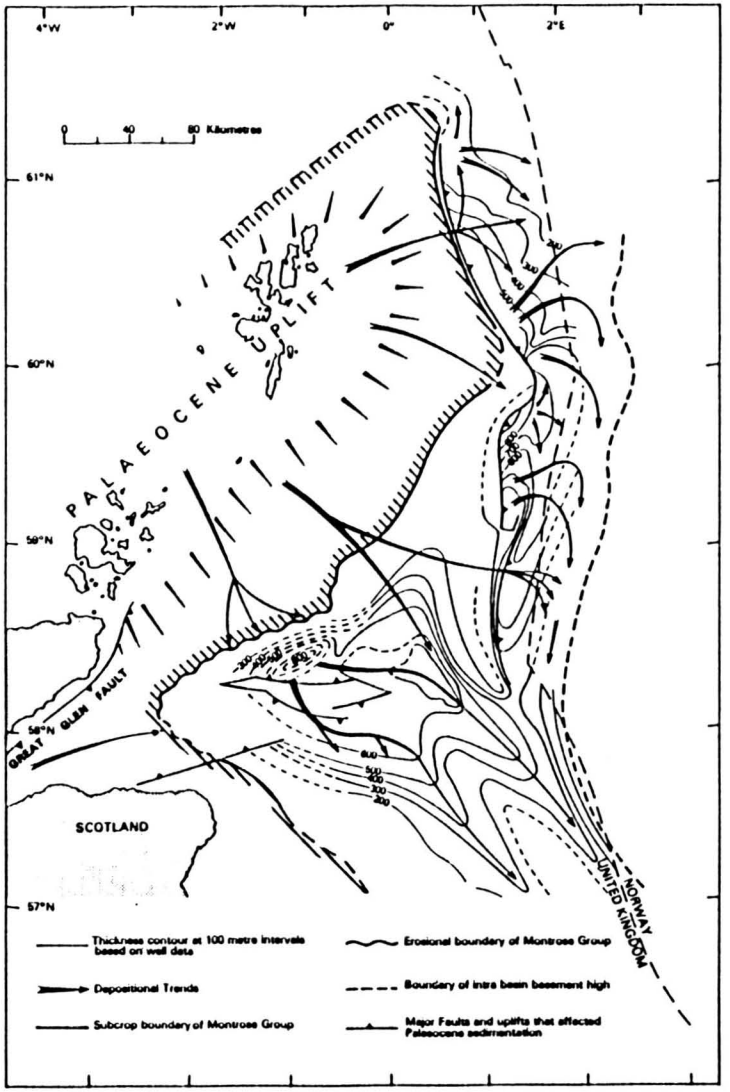

Montrose Group isopach map.

Figure 1.5

CHAPTER 2 ISOTOPIC COMPOSITIONS OF OILFIELD DIAGENETIC CALCITE WITHIN PALAEOCENE SANDSTONES, CENTRAL NORTH SEA.

Figures

CHAPTER 2 ISOTOPIC COMPOSITIONS OF OILFIELD DIAGENETIC CALCITE WITHIN PALAEOCENE SANDSTONES, CENTRAL NORTH SEA.

2.1 Abstract

Carbonate concretions from ten wells cored in the Palaeocene Montrose Group sandstones, Central North Sea have been studied. Petrographic and isotopic ($^{13}C/^{12}C$, $^{18}O/^{16}O$ $^{87}Sr/^{86}Sr$) analyses have been carried out.

Four regional groups have been defined dependent on carbon and oxygen isotopic compositions: (1) A shallow burial proximal setting where calcite has been precipitated during sulphate reduction and shell/chalk dissolution within cool predominantly depositional marine fluids. (2) A graben axis setting, where calcite precipitated as a result of the interaction of meteoric water flushing and hydrocarbon degredation. Anaerobic oxidation of hydrocarbon has taken place which resulted in calcite precipitation (-30 to -15‰PDB) during shallow (<500m) burial. Bituminous stains within these concretions indicate that the hydrocarbon source may have been early migrating oil. (3) A graben flank setting, distant from the early oil migration path characterised by high $\delta^{13}C$ compositions +9 to +12‰PDB. Fermentation of detrital organic material and shell dissolution supplied carbon within predominantly meteoric water. (4) A distal setting where petrographically late calcite concretions were sourced from the dissolution of detrital carbonate and decarboxylation of organic carbon within depositional marine pore-fluids. $^{87}Sr/^{86}Sr$ ratios for groups (1), (2), and (3) are similar to detrital carbonate ratios (Cretaceous Chalk and Lower Palaeocene shells). Group (4) wells have a radiogenic component indicating that there was an input from the dissolution of silicate minerals.

2.2 Introduction

Understanding the geochemistry of carbonate cemented horizons within clastic sequences is of interest to petroleum geologists, as the timing of carbonate cementation can be important for predicting the effect on poroperm across a reservoir. Concretionary horizons can reduce permeability/porosity, act as barriers or baffles to fluid flow (oil migration or production), and if extensively developed result in compartmentalisation (Bryant et al. 1988; Smalley et al. 1989; Bjorkum & Walderhaug 1990; Giles et al. 1992). Within the North Sea, many geochemical studies of authigenic carbonates have been undertaken, particularly on the economically important mid-Jurassic Brent Group sandstones (5.56 Bbbl ultimate recoverable reserves, North Sea UK Sector Brennand et al. 1990; Hamilton et al. 1987; Burley et al. 1989; Haszeldine et al. 1992; Giles et al. 1992; Glasmann 1992). However for the similarly important Palaeocene reservoir sandstones (2.99Bbbl ultimate recoverable reserves, Brennand et al. 1990), surprisingly few studies exist devoted to diagenesis and the construction, and interpretation of paragenetic sequences (Pagan 1980; Stewart et al. 1993; Watson 1993).

In this paper authigenic carbonate concretions from the Montrose Group sandstones are described. Carbonate separates have been analysed for their geochemical and isotopical compositions. This is integrated with petrographic data and palaeo-geographic location to interpret pore-fluid evolution in the Paleocene sandstones.

2.3 Geological Setting

The Palaeocene Montrose Group, (Deegan & Scull 1977), is a sequence of submarine fan systems which form extensive sand- rich basin-floor aprons in the Central and Witch Ground Grabens (Stewart 1987), **Figure 2.1.** The sands are similar to braided channel deposits laid down in mid-fan suprafan lobes as described by Walker (1978). The Montrose Group has been divided into three similar stacked lithostratigraphic units; the Maureen, Andrew and Forties Formations (Deegan & Scull 1977), **Figure 2.2.** The similar sand-rich massive lithofacies and submarine channel depositional facies which make up these formations make formation boundary identification a contentious issue. Published regional thickness estimations are based upon seismic stratigraphy.

The basal Maureen Formation overlies Cretaceous Chalk and contains a high proportion of carbonate debris and marls. The maximum thickness of the Maureen Formation varies between 100-150m (Sequence 2 of Stewart, 1987); and 80-100m (sandstone thickness T20, Roger Anderton, BP Exploration, Aberdeen, pers. comm). The Andrew Fan is more extensive than the younger Forties Fan though both are centred over the Outer Moray Firth and Central Graben. In cross section the Andrew Formation displays a giant wedge shaped geometry which is at its thickest within the Witch Ground Graben; 400-500m (Sequence 3 of Stewart, 1987); 700m (Andrews Fan of Den Hartog Jager et al., 1993); 440m (sandstone thickness T30, unpublished BP data Roger Anderton BP Exploration, Aberdeen pers. comm.).

Within the Witch Ground Graben area the Andrew Formation is overlain by thin Forties Formation equivalent silt/mudstone unit. Within the Central Graben, the Forties Formation is built up of isolated channel systems (approximately 2.5-4km wide) enclosed by levee and hemi-pelagic muds with resultant low connectivity between channel systems (Den Hartog Jager et al. 1993). The maximum thickness according to different authors is between 100-200m (Sequence 7 of Stewart 1987); up to 410m (Forties Fan, Den Hartog Jager, 1993); 120-140m (T40 sandstone thickness, Roger Anderton, BP Exploration, Aberdeen pers. comm.).

The ability of these sandstones to transport fluid over regional distances has been the result of four factors; regionally high sand/mud ratios (Stewart 1987), hydrostatic pressure of the Lower Palaoecene sandstones (becoming overpressured moving east and south towards Quadrants 23, 29, and 30) (Cayley 1987), lack of major faulting since deposition, and high connectivity between sand bodies resulting from stacked channel systems, though this decreases within the Forties Formation particularly within the Central Graben (Den Hartog Jager et al. 1993).

Within the Palaeocene sands, the result of rapid deposition and recycling of Mesozoic sandstones from the East Shetland Platform resulted in regionally high sand/mud ratios within the Montrose Group (Knox et al. 1981). Sand percentages within most of the Central North Sea for Andrew Formation equivalent, Unit B according to Knox et al. (1981) are greater than 50%.

Lower Palaeocene sandstones are predominantly hydrostatically pressured (Cayley 1987). The widespread hydrostatic pressure throughout most of the Central Graben gives way to increasing abnormal pressure as the sands dies out to the south and east in quadrants 23, 29 and 30. Local pressure increases associated with Tertiary salt diapirs

may be due to deep charging (Cayley 1987). Produced formation waters from the Tertiary oil fields in the East Central Graben are highly saline (Crawford et al. 1991, Maliva et al. 1995), indicating that waters associated with Zechstein have also migrated vertically (Bjorlykke & Gran 1994).

No major faults cross the Palaeocene sandstones (Milton et al. 1990). Sand deposition was within and along pre-existing Mesozoic graben systems. The lack of major faults crossing the Tertiary clastic system means that on a regional scale the normally pressured aquifer system remains laterally continuous and not compartmentalised.

The extensive sheet-like morphology of the submarine fan deposits show high-energy amalgamated channelised sands, interbedded with deposits representing lower energy unconfined flows. The Palaeocene submarine fans especially the Andrew Fan and the base of the Forties Fan have these characteristics. The Andrew Formation is made up of amalgamated submarine channels of high connectivity between them (Den Hartog Jager et al. 1993). Higher parts of the Forties Formation bear more resemblance to a channel level complex with more confined channels (Den Hartog Jager et al. 1993). These deep water fans comprise a thick net/gross stacked channel sequence in Quadrants 21 and 22 which shale out to the south-east in Quads 29 and 30. Thin distal turbidites fringe the main sand lobes (Cayley 1987). Distinct channel bodies within the Forties Formation are present over a large area, even in the more distal parts of the fan, such as the Cod Field (Parsley 1990).

The term, Outer Fan, is applied to deposits of unconfined dilute turbidite currents which are responsible for at least part of the deposition of silts, sands muds in basinal areas. In general sand content seems to drop rapidly at the fan fringes and in most cases the Outer Fan is effectively a non-reservoir.

Field studies of individual fields indicate that on a meso-scale connectivity may be restricted by mudstone barriers or diagenetic carbonate doggers. Within the Forties Field there is sufficient permeability restriction across claystones units to cause significant pressure differences during production, though no differences in oil composition is seen between pressure compartments (Wills 1991). Within the Montrose Field, is noted a less effective aquifer support during production within field area with stratified sediments (Crawford et al. 1991). Within the Maureen field, Block 16/29, although the reservoir geometry shows rapid sandstone pinchouts and apparently laterally extensive claystones within the field area, production history for several years strongly suggests that these non-reservoir units do not form vertical or lateral barriers to fluid flow, the reservoir behaving like a single unit (Cutts 1991).

Provenance and paleogeographical studies indicate that the sources for detrital grains were Palaeozoic or Mesozoic sediments from the southern part of the East Shetland Platform, **Figure 2.1**, (Morton et al. 1993), and possibly eroded Dalradian schists from the Scottish Highlands (Morton et al. 1993). Sediments were transported eastwards to be deposited in the subsiding Central North Sea along pre-existing Mesozoic grabens (Knox et al. 1981) with an intermittent supply of volcanic debris (basaltic clasts and wind-blown ashes) carried over the water-shed from the west of Scotland igneous centres (Jacque & Thouvenin 1975).

After deposition the sediments experienced a relatively simple sag pattern of subsidence (Barnard & Bastow 1992). Interpretation of seismic reflection data suggests that no major faults cut the Palaeocene sequence (Milton et al. 1990). Thus the original depositional aquifer connections are intact without tectonically induced fluid barriers or conduits.

2.4 Methodology and analytical procedure

Ten cored wells (**Table 2.1**) with carbonate-cemented horizons were selected to give regional coverage across the sub-crop of the Lower Paleocene sandstones within the Central North Sea.

Wells were chosen after comparing available composite logs; high sonic velocity 'carbonate concretions' greater than 25cm thick are readily identified within the thick-bedded and structureless sands which maintain fairly uniform log traces. Samples for thin-sectioning and isotopic analysis were taken across concretions and also at regular intervals within the cored sandstones. Blue-stained epoxy-resin impregnated polished thin-sections were stained for carbonates following the techniques of Friedman (1959). They have been examined using standard petrographic techniques including point count analysis (500 points) to quantify detrital mineralogy, authigenic cements and porosity. Double polished wafers were made from concretions in wells 15/20-4 and 16/28-6 for fluid inclusion analysis. Cold-stage cathodoluminescence (CL) was carried out to identify carbonate zoning. Rock stubs were examined using a scanning electron microscope (SEM) to determine the morphology, composition and distribution of the authigenic minerals. X-ray diffraction (XRD) analysis was undertaken on whole rock samples and separates to determine the composition of carbonate phases. Where possible, concretion samples were disagreggated and size separated and the carbonate-rich size fraction (53-75μm) was then purified using heavy liquid, and electromagnetic separation to around 70% purity. Where samples were too small to separate out the carbonate, crush samples were used. Samples of CO_2 gas for stable isotopic measurements were obtained by reacting plasma-ashed carbonate samples with 100% phosphoric acid using the method outlined by McCrea (1950). Calcite was left to react overnight at 25+0.1°C in a thermostated bath. Samples of CO_2 gas were analysed on a VG SIRA 10 mass spectrometer. Standard deviation of replicate analyses was less than 0.04‰ for carbon and 0.2‰ for oxygen. Carbon isotope results are reported in the delta per mil notation ($\delta^{13}C$) relative to Peedee belemnite (PDB). Oxygen isotope results are reported in the delta per mill notation ($\delta^{18}O$ relative to Standard Mean Ocean Water; SMOW). Strontium was separated using standard cation exchange chromatography and analysed by isotope dilution (Smalley et al. 1992); concentrations and $^{87}Sr/^{86}Sr$ ratios were determined using a solid-source mass spectrometer on a VG Isomass 54E. Replicate analyses of NBS 987 gave $^{87}Sr/^{86}Sr$ values of 0.71022 +2(2σ).

2.5 Petrography

Most wells are dominated by massive sandstones deposited from high-density turbidity currents and this facies generally makes up to 80% of the cores. The three basic rock types are massive sandstones, interbedded sandstones and claystones, and silty claystones. The facies under study is the economically productive massive facies. The massive sandstones are characterized by elongate sheet-like geometries with good lateral and vertical connectivity. Individual beds are 1m to several 10m's thick with high porosities (>20%) and permeabilities (>100mD). Locally they grade into pebbly

sandstones at the base of units. Dewatering dish-and-pillar structures (Lowe 1982) are seen between amalgamated beds. The sandstones are generally poorly lithified with only minor cementation. Reservoir geometries within distal, reaches, (Block 16/29), indicate that rapid sandstone pinchouts and apparently extensive claystone exist. However production histories indicate that non-reservoir units do not form vertical or lateral barriers to fluid flow (Cutts 1991).

The massive facies consists of generally very fine-to-medium grained and poor-to-moderately sorted sandstones. Detrital clay content is low (<5%). In all wells sampled is seen a clay with a diagenetic boxwork habit protruding from the detrital clay background. The 'box' sides are up to 4microns across. Back-scattered electron microscopy and qualitative XRD analysis indicate that the overall detrital clay fraction has an indistinct smectitic-illitic chloritic composition with broad peaks covering these compositions. It is impossible to separate the clay with the boxwork habit from the detrital clay by way of XRD analysis. It is assumed that these boxwork clays represent the gradual neomorphism of detrital clay into illite (Eslinger & Peaver 1988). The sandstones are generally sub-lithic in composition (Folk 1974). Rock fragments are generally quartzite and quartz/mica/feldspar composite grains with a schistose fabric reflecting the Scottish Highland hinterland (Morton et al. 1993). Igneous clasts and extrusive fragments are also frequent. These are often dissolved leaving secondary pores (~2% rock volume) outlined by opaque grains. There is generally little detrital carbonate within the sandstones (<0.4% by volume) though within sampled Maureen Formation sandstones there are occasional beds containing chalk clasts and rich in chalky fines. Muscovites and altered biotite are present in small volumes (<2% by volume). Carbonaceous material now pyritised (<2.5% by volume) is also present.

2.6 Habit of carbonate concretions

Outwith concretions authigenic minerals are developed in only low abundances and do not significantly affect the reservoir quality of the sandstones. However concretions do locally reduce both porosity and permeability to negligible levels.

Carbonate occurs as a concretionary cement, **Figure 2.3**. It is also occasionally seen as traces within the host sandstone associated with expanded mica flakes, similar to those seen by Boles & Johnson (1983). Small incipient feldspar and quartz overgrowths (<5μm) and small dolomite rhombs associated with pyrite pre-date concretion formation, **Figure 2.4**. In most wells traces of small vermiform kaolinite (<20μm) associated with splayed mica are also seen within concretions or forming patches adjacent to corroded feldspars. Slight corrosion of detrital framework grains is also apparent and within well 14/13-3 igneous lithic clasts are particularly susceptible to calcitisation. Within wells 22/20-3 and 16/29-2 noticeable silicate diagenesis pre-dates concretion precipitation. Within wells 22/17-4, 22/20-3 and some of 23/16-4 carbonate concretions are not tightly cemented . Compacted framework grains within these particular concretions have quartz overgrowths on detrital grains.

Calcite grain size varies from coarse poikilitic to microcrystalline **Table 2.2**. Small grain size results from the presence of many nuclei during carbonate cementation (Putnis & McConnell 1980).

Thickness of concretion and total thickness of cemented zones varies between wells. Within wells 15/26-3, 15/26-4, 16/28-6 and 21/10-1, calcite cemented zones make up between 3-7% of core length while in wells 16/29-2, 22/20-3, 15/20-4 and 23/16-4 calcite cemented zones make up to 10% of cored length. Concretion thicknesses are generally 10's of cm but can be considerably larger, eg. 1.2m thick in 15/26-4, 2m thick in 16/28-6, 2.7m thick in 16/29-2 and 2.75m thick in 22/17-4. In most cases it is unclear whether these exceptionally thick zones consist of coalesced nodules. However within well 16/28-6, the 2m thick concretion had concentric isotopic compositions suggesting that it was a single concretion.

2.7 Mineralogy

Back-scattered analysis of polished thin-sections indicates that concretionary carbonates range from Fe-calcites, Mn-calcites, ankerites to non-ferroan calcites, **Table 2.3, Figures 2.5,6,7.**

14/13-3 Two concretions (824.9m and 830.3-4m) sampled have Mn (0.64 to 1.80%) and Fe (2.02 to 4.14%) inversely correlated with some anomolously high Mn concentration, up to 9.4% Mn in one sample **Figures 2.5,6,7.** On the scale of sampling no trends for Mg (0.29 to 4.01%) concentrations with Fe or Mn are seen . The presence of tuffaceous debris within the core would indicate that supply of metal ions is likely to come directly from dissolving volcanic material.

15/20-4 (2012.5) Fe-calcite (purple stained) concretion (Fe=1.69 to 2.23%) has relatively high concentrations of Mg (2.75 to 4.08%) and Mn (2.50 to 3.42%) **Figures 2.5,6,7.** Source of metal ions is unknown but the presence of tuffaceous material at 2013.55m would suggest that supply of material would be local.

15/26-3 (1877.9 to 1878.3m) ankerites. Mn concentration are low within the concretion (0.15 to 0.68%) but show slight increase towards the margins of the concretion, **Figure 2.8a.** Fe and Mg concentrations are irregular at 1878m within the concretion but are constant in the rest of the concretions. The irregular concentration indicate that supply of Fe and Mg are local on a thin section scale. Fe and Mg concentrations are strongly inversely related suggesting dissolution from a single ferromagnesian source.

(1894.3 to 1895.2m) 2 samples from Fe-calcite (1.10 to 3.70%) concretion rims **Figure 2.8b.** Upper rim has higher concentrations of Fe, lower Mn concentrations and lower Mg concentrations.

15/26-4 (2274-2274.74) calcite concretion. Both Fe and Mg concentrations in the centre of the concretion (1.03 to 1.38% and 0.97 to 1.88% respectively) decrease towards the rims of the concretion (00.00 to 1.03% and 0.71 to 1.66% respectively) **Figure 2.8c.** Mn concentrations are low (<0.62%) during growth and show no trend. The similar trends in Fe and Mn concentrations indicate a similar source of ions which is likely to be dissolution of ferromagnesian minerals.

16/28-6 Fe-calcite concretion (2681.6 to 2683m) shows local increase in Fe and Mg concentration from the centre of the concretion (0.93 to 1.36% and 0.25 to 1.19% respectively) towards the upper (1.49 to 1.83% and 3.70 to 4.80% respectively) and lower rims (1.16 to 1.56% and 0.83 to 2.70% respectively) **Figure 2.8d.** Mn

concentrations do not follow this trend but show a decrease in concentration towards the upper margin (0.88 to 0.95%) and an increase towards the lower margin (1.52 to 1.86%). The Fe and Mg appear to be associated and again local supply from dissolution of ferromagnesian minerals is inferred.

16/29-2 Mn-calcite concretion (2642.5 to 2645.5m) **Figure 2.8e.** There is a slight increase of low Fe and Mg concentration during growth from concretion centres to concretion rims. Centre Fe=0.16 to 0.73 % and Mg=0.10 to 0.51 %; upper rim Fe=0.89 to 1.46% and Mg=0.71 to 0.95% ; lower rim Fe=0.63 to 1.06% and Mg=0.58 to 1.19%. Fe and Mn appear to be related to each other. Relatively high concentration of Mn are irregular throughout the concretion

(2664.9 to 2666.9m) Mn-calcite concretion, **Figure 2.8f.** Mg and Fe concentrations remain low throughout the concretions (Fe=0.47 to 1.20% ; Mg=0.01 to 0.95%) and no trend is evident. Mn concentrations are irregular on the thin-section scale (2.52 to 8.42%) and show no trend within the concretion.

21/10-1 Strongly Fe-calcite concretion (3.46 to 4.74%) at 2220 to 2242.8m, **Figures 2.5,6,7.** No trends apparent from analysis taken. Mg concentration are constant, 0.92 to 1.50%, whereas Mn concentration are irregular on a thin-section scale, 0.06 to 1.54%.

22/17-4 Mn-calcite (4.99 to 5.27%) concretion at cored depth 3107 -43110m, **Figures 2.5,6,7.** Fe and Mg concentration a are low (0.81 to 1.31% and 0.30 to 0.67% respectively). Source of Mn is problematic as no source of Mn is apparent within the sandstones. Mn was either imported into the sands or source of Mn within sandstones has completely dissolved out.

22/20-3 Mn-calcite concretion (1.2 to 6.5 %) at 2689.45 - 2689.7m **Figures 2.5,6,7.** No correlation is apparent between Fe, Mg and Mn.

23/16-4 As clastic amalgamated units are less than 10's cm within the core concretions cannot be individually recognized. Samples aware taken at cemented intervals within the core.

There is an overall decrease Mn concentration with depth (2155m, Mn=5.14 to 6.18%; to 2316m, Mn=0.57 to 1.36%), **Figure 2.8g.** Fe concentration also decrease down the well from 1.72 to 2.13% to 0.93 to 1.43%. Mg percentage stays relatively constant from 0.36 to 1.36% at 2155.9m to 0.19 to 1.20% at 2316.5m. The low concentrations of Mn, Fe and Mg in the lower sections of the core coincide with chalky debris and it is likely there-precipitation of detrital carbonate supplied ions.

Mn source

The source of manganese in concretions from wells 16/29-2, 22/17-4, 22/20-3 and 23/16-4 is puzzling. These petrographically late concretions are predominantly Mn-calcites. There is currently no apparent source of Mn available in the sandstones. Mn supply during concretion precipitation could have come from; dissolution of ferromagnesion minerals rich in Mn, dissolution of diagenetic Mn-oxides which had

precipitated on the sea floor, external introduction of Mn-rich fluids into the Montrose Group.

Dissolution of detrital ferromagnesian minerals - Concretions from 14/13-3 which are present within sediments originally rich in ferromagnesian minerals have strong Fe and Mg components as well as Mn. It is likely that the Mn component within these concretions came from detrital ferromagnesian mineral dissolution. For the other wells this hypothesis is unsatisfying, as Fe% and Mg% are generally less than 2%, **Figure 2.7.**

Dissolution of diagenetic Mn rich minerals - The distribution of Fe-hydroxides and Mn-hydroxides within sediments is related to the position of the oxygen-minimum and the concentration of the ionic species in contemporary seawater. Mn-hydroxide formation and minerals are poorly understood as a result of the many reduced states of manganese and its reactions in differing Eh-pH conditions (Burdige 1993). Manganese concentrations increases within sediments which are influenced by *black smoker* fluids. Mn-rich sea water may have been carried by currents from the active Tertiary volcanic province in the West of Scotland. There is no recorded evidence of thermal spring activity or active spreading areas in the Palaeocene North Sea itself. The Palaeocene North Sea is known to have been partially anoxic, and perhaps restricted, as illustrated by the presence of green mudstones and black mudstones which characterise the Andrews and the Forties Formations respectively (Knox et al. 1993). Manganese in solution or present as Mn-hydroxides is likely to have been precipitated as Mn-oxides within the sulphate reduction zone during shallow burial (Burdige 1993). The increase in Mn component in diagenetic carbonates towards the top of the Montrose Group in well 23/16-4 may be related to either greater anoxicity within the Forties Formation or a rise in black smoker activity on the west coast of Scotland. Real Eh-pH changes within relatively deep buried sediments are poorly understood and it is proposed that chemical alteration within the Montrose Group porefluids resulted in the dissolution of the diagenetic Mn-oxides during burial, the manganese becoming incorporated into diagenetic carbonates.

Introduction of Mn-rich fluids externally into the Montrose Group - Pressure release from underlying overpressured Jurassic sediments by way of fluid migration has been proposed by some authors (Burley et al. 1993). Tranferring this hypothesis it can be proposed that Mn-rich fluids may have been introduced during hydrocarbon migration or pore-fluid release/migration. Fluids rich in Mn may have come from dissolution of ferromagnesian minerals in the underlying sediments and then introduced through fractures in the Cretaceous relating to salt diapirism. As there is no complementary increase in Fe or Mg within the carbonates this hypothesis is seen as unlikely.

Minor dolomite crystals a few microns across were common within wells. Compositions of dolomites were measured within well 16/28-6 which had dolomite crystals sufficiently large enough (10microns) to produce reliable data by way of backscattered SEM imaging. **Figure 2.4, Figure 2.8h Table 2.3.** Dolomite Fe and Mg components vary within each slide by up to 6%. This indicates that Fe and Mg was sourced locally on a thin-section scale. Mn concentrations are low 0.43 to 1.48%.

2.8 Cathodoluminescence

None of the concretions sampled showed distinct concentric zoning, **Figure 2.9.** Within well 16/29-2 faint sector zoning was observed within large >150micron poikilotopic calcite grains **Figure 2.10.** Back-scattered electron BSE images of polished thin-sections showed no compositional zoning present within any concretion. Luminescence colour are a uniform dull orange-brown to dull brown. Bioclasts and carbonate chalk debris luminesce a brighter orange signifying a non-ferroan calcite while calcified lithic grains have a dull brown luminescence.

2.9 Minus-cement porosity

The depth at which these concretions grew can be estimated by point counting the cement volumes between detrital sand grains, assuming that this represents primary porosity (Baldwin & Butler 1985; Haszeldine et a1.1992).

Sclater & Christies (1980) sandstone porosity/depth relationship was the best fit straight lime generated from a log porosity-depth plot showing surface porosity data (Pryor 1973), porosity from Palaeocene wells within the Central Graben (Selley 1978) at depths between 2000-3000m burial, and supplemented with data calculated using observed sonic velocities and the velocity/porosity table of Schlumberger (1974). Selley's (1978) porosity data came from the hydrostatically pressured North Sea Palaeocene oilfields. No equation was added to Sclater & Chrisite's (1981) figure. Sclater & Christies (1981) chose an exponential to describe porosity decrease within the Central North Sea as such an exponential decrease proved satisfactory using Atwater & Miller's (1965) sandstone porosity data from Louisiana (depth range 0.5 to 6km) and Pryor's (1973) surface sand porosity data. Baldwin & Butler (1985) later interpreted Sclater & Christie's (1980) sandstone porosity diagram as a logarithmic equivalent.

$$\text{Burial depth (in km)} = 3.7\ln[0.49/(1-S)] \quad \text{(where S=1-porosity)}$$

For sandstones that do not change porespace within the upper 10-100m, this form of equation provides a reasonable description for predicting porosities of hydrostatically pressured Central North Sea Palaeocene sandstones. Palmer & Barton's (1987) study of shallow buried (780m maximum burial) uncemented sandstones (Holocene to mid Jurassic) indicate that porosities reduce rapidly to around 35% during the first 200m of burial. Therefore Baldwin & Butler's (1985) porosity-depth curve may underestimate the rapid decline in burial in porosities. It is worth noting Baldwin & Butler's (1985) 'sandstone-envelope' depth range 0.5-7.0km created from Maxwell's (1964) data encompasses sandstones of widely differing ages at similar burial depths, sandstones of different facies though all are quartzose sandstones, from basins of different geothermal gradients, and the strong likelihood of different pressure regimes though no pressure data is given for study areas. There is always the possibility of misinterpreting porosities in terms of potential burial depths generated by empirical porosity depth equations

These pre-cement porosities are superimposed on a general compaction curve for Central North Sea sandstones generate by Sclater & Christie (1980) and interpreted in a logarithmic form by Baldwin & Butler (1985). Although this compaction curve is only an approximation we can nevertheless still use it to demonstrate that from simple

textural relationships, calcites have precipitated at different depths within the study area, **Table 2.4, Figure 2.11.** The concretions in wells 22/17-4, 22/20-2 and some of 23/16-4 were not tightly cemented. The earliest calcite concretions are found within proximal and graben axis study wells, 14/13-3, 15/20-4, 15/26-4 and 16/28-6 which formed prior to 1km burial. Within these concretions, contacts between detrital grains are rare and it is apparent that most of this calcite formed before significant compaction. Later concretions are within flank and distal wells 15/26-3 and 16/29-2 while the concretions with the least minus-cement porosities are found within distal Central Graben wells 21/10-1 and 23/16-4 which grew in more compacted sediments at depths greater than 1km.

2.10 Location of concretions

Concretions within the sands have been noted as both isolated spherical concretions within study cores and as permeability restricting calcite-cemented layers (Tonkin & Fraser 1991; Emery & Robinson 1993a). Cores from wells 15/26-3, 15/26-4, 16/29-2, 21/10-1 and 23/16-4 all have calcite cemented horizons within beds (<20cm) rich in marls and chalk clasts. These are believed to be laterally continuous. Bjorkum and Walderhaug (1990), in an isotopic study of the Bridgeport Sand shallow marine sandstone, suggested that the spatial distribution of concretions is controlled by the distribution of detrital carbonate. Shell-rich beds with stratified detrital carbonate are more likely to be cemented than structureless sands where potential nuclei are dispersed. Visual analyses of composite and sedimentological logs indicate that concretions within massive sands consisting of amalgamated units are more likely to be present adjacent to dewatering dish-and-pillar structures (see Chapter 5). These dish-and-pillar structures are outlined by detrital fines. These fines are likely to contain calcite microfossils and micas, and so be potential nucleation points for concretions (Boles & Johnson 1983; Bjorkum & Walderhaug 1990). Within well 16/29-2 concretions are noted to be found adjacent to shale/sandstone boundaries (Cutts 1991).

2.11 Carbon isotopes:

Carbon isotopic compositions range widely from -29.7‰ PDB to +12.7‰ PDB **Figure 2.12,** ($\delta^{18}O$ = 15.2 to 29.4‰SMOW) **Table 2.5.**

Carbon isotopes can be used to indicate the source of the carbonate (CO_3^{2-}) in a cement. As sediment undergoes shallow burial (<1.5km), CO_2 is released through biochemical and chemical reactions. Because the starting composition of detrital organic material is usually close to $\delta^{13}C$ PDB~-25‰, the composition of CO_2 for any specific reaction process is known (Irwin et al. 1977).

With depth the reactions are:- aerobic oxidation ($\delta^{13}C$ PDB~ -25‰), bacterial sulphate reduction ($\delta^{13}C$ PDB~ -25‰), fermentation ($\delta^{13}C$ PDB ~ +15‰) and abiotic thermal decarboxylation ($\delta^{13}C$ PDB~-15‰) (Irwin et al. 1977). Detrital carbonates such as high-Mg calcites and aragonite can also undergo dissolution during burial releasing bicarbonate with $\delta^{13}C$ near to 0‰. Taylor & Lapre (1987) in their study of Cretaceous Chalk Ekofisk Formation diagenesis within the Central North Sea, indicated that pressure solution due to compaction of chalky deposits is expected to take place at depths of 100m onwards.

Unfortunately, the results of $\delta^{13}C$ analyses are sometimes ambiguous because carbonates commonly contain carbon from a mixture of sources, and different processes can result in similar mineral $\delta^{13}C$ values.

2.12 Results

From a $\delta^{13}C$-$\delta^{18}O$ plot, the study wells can be divided into four different isotopic groups which also define regional areas: well 14/13-3 on the south side of the East Shetland Platform cored within proximal to source area shallow buried friable sandstones; wells 15/20-4 and 16-28-6 within the axis of the Witch Ground Graben core Andrew Formation sandstones, wells 15/26-3 and 15/26-4 situated on the south flank of the Witch Ground Graben , and a grouping of wells with similar $\delta^{18}O$ and $\delta^{13}C$ isotopic compositions though geographically separate wells 16/29-2 (Maureen Formation sandstones), 21/10-1, 22/17-4, 22/20-2 (Forties Formation sandstones) and 23/16-4 (Montrose Group Sandstones)

2.12.1 Shallow proximal area

The well 14/13-3 is located in the shallow buried Montrose Group in the Outer Moray Firth the southern edge of the East Shetland Platform (cored depth 825.4-830.8m). High minus-cement porosities (37.2 to 46.2%) indicate that concretions precipitated during early burial, **Figure 2.11.**

The light isotopic carbon compositions ($\delta^{13}C$ PDB = -14.2 to -3.1‰, **Table 2.5**) are not reaction specific but indicate a combination of carbon sources. Because of the <830m burial of these sandstones, abiotic decarboxylation (-15‰ PDB, Irwin et al. 1977) is not considered to have contributed carbon as this reaction requires temperatures in excess of 40°C. Shallow bacterial sulphate reduction ($\delta^{13}C$ PDB = -25‰; e.g. Irwin et al. 1977; Curtis 1986; Glasmann et al. 1989) is probably the main component. Authigenic pyrite indicative of sulphate reduction reactions is abundant and forms around 0.4 to 2.6% by volume (mean 1.2% by volume) of concretion volume and is present in smaller quantities (<0.2% by volume) outside the concretions. The other contribution to carbon is likely to come from the dissolution of detrital shells and/or chalk debris (-0 to +3‰ PDB, Taylor and Lapre 1987). In CL petrography detrital calcite grains are clearly identified within these concretions and so could have acted as nucleation sites and contributed to $\delta^{13}C$ values.

The $\delta^{13}C$ signature of concretions increases by 4-12‰PDB from the centre to the rims, **Figure 2.13a, b.** This could result from a reduction in SO_4^- concentration within pore-waters and declining input of sulphate reduction carbonate ($\delta^{13}C$~ -25‰). Correspondingly, there would be a resultant increase in the component from detrital carbonate dissolution.

2.12.2 Witch Ground Graben axis

The two wells 15/20a-4 and 16/28-6 (cored depths 1949.7- 2019.4m and 2585.8-2736.4m) are located on the southern tip of the Fladen Ground Spur and in more distal reaches of the Witch Ground Graben, **Table 2.5.**

Plotting minus-cement porosities on a porosity-depth curve indicates that these concretions may have grown at depth up to 1100m. Five out of seven minus-cement

porosities from these two wells are >45% and this suggests that precipitation took place during early burial **Figure 2.11.**

Concretions within study wells are characterised by exceptionally low carbon isotope compositions, $\delta^{13}C$ = -30 to -15‰PDB. Such depleted values can result during sulphate reduction (Irwin et al. 1977), oxidation of methane (Jorgensen 1989), thermally induced abiotic decarboxylation (Irwin et al. 1977) and anaerobic oxidation of oil (Donovan et al 1974; Dimitrakopolous & Muehlenbachs 1987; O'Brien & Woods 1994).

Enclosed within concretions, pre-dating calcite cementation are disseminated authigenic dolomite grains (<10μm) intimately associated with pyrite (<10μm), **Figure 2.4.** The small size of the dolomite grains and the small volume of dolomite within the calcite concretions (<2% BV in all samples) precluded isotopic analysis but the association of dolomite with pyrite indicates that dolomite formed within the sulphate reduction zone. Dolomite forms discrete crystals with euhedral faces. There is no gradual change form dolomite to calcite precipitation. The different chemistries, habit of precipitation, and the concretions $\delta^{18}O$ ratios suggests that the Fe-calcite precipitated deeper that the sulphate reduction zone. The lack of similar disseminated pyrite within the calcite concretions (unless seen with dolomite) indicates that available sulphate was used up prior to calcite precipitation.

The presence of weakly luminescent organic fluid inclusions and brown bituminous inclusions leads to the proposition that anaerobic oxidation/biodegradation of early migrating hydrocarbons took place during concretion precipitation. Such oils have $\delta^{13}C$ signatures of -30 to -25‰PDB (Gould & Smith 1978). Fluid inclusion analysis of fluid inclusion wafers from well 15/20-4 indicated the presence of short chain hydrocarbons (pers. comm. G.MacLeod, Univ Newcastle, 1994)

In various studies biodegradation of hydrocarbons has been held responsible for similar depleted $\delta^{13}C$ compositions of sandstone-hosted concretions (Donovan et al. 1974; Dimitrakopolous & Muehlenbachs 1987; Watson 1993; O'Brien & Woods 1994). Dimitrakopolous and Meuhlenbachs (1987) studied carbonates from the Cretaceous heavy oil deposits of Alberta. They suggest that meteoric water with dissolved O_2 interacted with petroleum, and aerobic bacteria degraded hydrocarbons, to release acids, alcohols and ketones. These organic compounds were then anaerobically oxidised to produce CO_2 with $\delta^{13}C_{PDB}$-depleted signatures. This resulted in the precipitation of isotopically light ($\delta^{13}C$ PDB) carbonates. It is suggested that similar processes were taking place during concretion growth in wells 15/20-4 and 16/28- 6.

The increasingly negative $\delta^{13}C$ component, $\delta^{13}C$ = -15 to -30‰PDB, in composition from concretion centres to rims suggests that the influence of isotopically light hydrocarbon increased during growth of the concretions, **Figure 2.13c,i.** Concomitantly another component with a more positive carbon isotope values (shell material/chalk, $\delta^{13}C$ = 0 to +3‰PDB) or fermentation, $\delta^{13}C$ =+15‰, was decreasing.

Petrographic and SEM stub analyses of samples found no detrital calcite outside concretions but only inside the concretions **Figure 2.14.** This suggests that detrital

calcite was only preserved within concretions as these calcite clasts were engulfed during concretion precipitation.

2.12.3 South Witch Ground Graben flank

These data are from wells 15/26-3 and 15/26-4 located on the south flank of the Witch Ground Graben in the Outer Moray Firth area (cored depths 1874.6-1929.75m and 2066.4-2476m respectively). Minus-cement porosities indicate that these cements grew at 0 to 600m, but at predominantly shallow depths during burial as all are >42 % minus-cement porosity. Concretions near the top of the Montrose Group from both study wells have distinctive positive isotopic compositions, $\delta^{13}C$ = +9.8 to +13.5‰PDB, with excursions to negative values at the rim of the concretions, $\delta^{13}C$ = -18.9 to -18.5‰PDB. At the base of the core or where analyses were taken of cement within chalk rich matrix have $\delta^{13}C$ =-6.7 to +2.6‰PDB, **Figure 2.13h, 2.15a,b, Table 2.5.**

Positive values indicate that the cements formed within the fermentation zone (10-1000m depths, Irwin et al. 1977; Saigal and Bjorlykke 1987), where CO_2 gas generated by methanogenesis has generally a value of around +15‰PDB. **Figures 2.13c,d, e, f.** The rim of two concretions have carbonate ratios around -20‰PDB, **Figures 2.13e, f.** This could indicate the reintroduction of sulphate reduction by a change to porewaters rich in sulphate.

No hydrocarbons are seen in fluid inclusions. From this it is suggested that oil migration had not reached wells 15/26-3 and 15/26-4 during concretion growth. Therefore negative $\delta^{13}C$ compositions suggest formation within the sulphate reduction zone ($\delta^{13}C$ ~ -25‰PDB) or organic degradation ($\delta^{13}C$ ~ -25‰PDB). Concretions near the base of both of these cores are in a layer rich in Cretaceous chalk debris. These mixed chalk/authigenic cements have values close to detrital marine carbonate (0 to +3‰PDB Taylor & Lapre 1987). It is likely that detrital calcite was the source for carbonate cement.

2.12.4 Distal Wells

These wells' locations are characterised by their distal nature to provenance area, most of the wells except for 16/29-2 are located within the Central Graben area. They are wells 16/29-2 (2623.2-2688.8m) and 23/16-4 (2150.19-2320.69m) and samples from 21/10-1, 22/17-4 and 22/20-3. Minus-cement porosities show that cements grew from around 700 to 1800m burial **Figure 2.11.**

16/29-2 (2642.6 to 2645.3m concretion). Three analyses over the upper half of this concretion show no trend **Figure 2.13j.** Carbon values vary from -5.4 to +2.7‰PDB.

16/29-2 (2664.9 to 2666.9m concretion). Rims have similar low negative carbon values; upper rim -1.1 PDB, lower rim 3.2 to -2.7‰PDB, **Figure 2.13k.** A slight increase in carbon ratios as the lower rim is approached (-3.2 to -2.7‰PDB)

16/29-2 Cemented zone at depth 2683.5 and vein at 2682.2m have very similar vales -0.7 to -0.4‰PDB and -0.7‰PDB respectively **Figure 2.13l.** The source of carbonate for these cements are likely to be detrital chalk debris.

22/17-4 (3106.8 to 3110.5m concretion). Three analysis in the upper half of the concretion have values between -11.1 and -3.7‰PDB **Figure 2.12.**

22/20-3 sample from 2689.4 and 2689.7m have values between -4.7 and -4.3‰PDB **Figure 2.12.**

Both 16/29-2 and 23/16-4 have similar trends with depth. Carbon isotope values around zero, $\delta^{13}C$ =-0.5 to +2.0‰PDB at the bottom of the over become gradually more negative upwards, $\delta^{13}C$ = -9 to -6‰PDB **Figure 2.15c,d.** Well 23/16-4 has a top zone where carbon compositions are near zero $\delta^{13}C$ = -1 to +2‰PDB.

Carbon isotope values near the base are likely to be influenced by detrital chalk debris: $\delta^{13}C$=0 to 3‰PDB. Towards the top an organic influence (ie more negative values) could have resulted from sulphate reduction $\delta^{13}C$=-25‰PDB or decarboxylation $\delta^{13}C$=-15‰PDB. Decarboxylation becomes effective at temperatures in excess of 60°C. (Irwin et al. 1977). Such temperatures are near to current burial temperatures of these sample wells indicating that carbonate precipitation is a very late diagenetic phase. Decarboxylation temperatures are also in excess of that predicted from minus-cement porosities. However the errors within depths predicted from minus-cement porosity are likely to be large and precipitation depths should be interpreted as being qualitative rather than quantitative. At the top of well, 23/16-4 $\delta^{13}C$ values near zero indicate that carbon came from detrital carbonate.

2.13 $\delta^{18}O$ overview

The mineral $\delta^{18}O$ values record the dual influences of growth temperature and of pore-water. Using the fractionation equation of Friedman & O'Neill (1977) a plot was constructed relating $\delta^{18}O$‰SMOW(calcite), $\delta^{18}O$‰SMOW(pore-water) and growth temperature, **Figure 2. 16.** $\delta^{18}O$ SMOW of Palaeocene seawater (Shackleton & Kennet 1974) and early Tertiary meteoric water (Forester & Taylor 1977) are illustrated **Figure 2.16.** Difficulties are faced when interpreting very low $\delta^{18}O$ values for calcite cements within shallow buried marine sands. How can these concretions have precipitated within marine pore-waters, as the low $\delta^{18}O$ values of calcite ($\delta^{18}O$= 15.2 to 29.4‰SMOW) clearly cannot reflect equilibrium during very early diagenesis? Oxygen isotope compositions for authigenic concretionary calcite within marine sediments are often problematic to interpret (Mozley & Burns 1993; Osborne 1994). Common values for seemingly petrographically early calcites precipitated within marine sediments are between 20.6 and 30.9‰SMOW (Mozley & Bums 1993). Such values suggest that pore-waters during precipitation were isotopically lighter than seawater ($\delta^{18}O$ ~ 0‰SMOW). If depositional marine water is chosen as a potential pore-water, precipitation temperatures can often be hotter than maximum burial temperatures inferred from minus-cement porosities (Moore et al. 1992).

There are five explanations:-

1) Isotopic alteration of seawater in a closed system.
2) Meteoric water influx.
3) Recrystallisation of calcites after growth.
4) Precipitation at anomalously high temperatures
5) Elevated Palaeocene surface water temperatures

2.13.1 Precipitation of ^{18}O enriched minerals within a closed system

The viability of the water rock interaction mechanism is difficult to evaluate because the mode of concretion growth and environment of formation are imperfectly understood. In a closed system the effect of mineral precipitation could be substantial. For example the alteration of volcanic ash to smectite is very likely to have occurred in these Palaeocene sediments. For this reaction, shifts in marine pore-water $\delta^{18}O$ composition relative to SMOW as great as -8‰ have been reported (Lawrence & Gieskes 1981). But in the Montrose Group sandstones the amounts of volcanic debris may only have been 2 to 4% of the rock, so mass balance suggests that this is not likely to have affected Palaeocene porewaters in most cases. Moore et al (1992) attributed low $\delta^{18}O$ values from carbonates in modem marine coastal marsh sediments to be the product of precipitation in a closed hydrogeological system. The degree of alteration depends on a) amount and reactivity of volcanic sediments, b) water-sediment ratio, and c) extent of diffusional exchange of oxygen between the sediments and overlying seawater (Morad & De Ros 1994; Prosser et al. 1994).

2.13.2 Meteoric water influx

A common interpretation of $\delta^{18}O$ values for low temperature precipitation requires influx of meteoric water (Galloway 1984; Haszeldine et al. 1992). This hypothesis is frequently invoked within the Northern North Sea to explain low oxygen values of stratified calcite cements (Giles et al. 1992; Haszeldine et al. 19.9). To allow meteoric water to penetrate the sediments requires a suitable sediment and basin geometry. For a concretion that formed relatively near to shore such a mechanism is more likely than for that offshore. Meteoric influx can occur due to sea-level fall and subaerial erosion, uplift of hinterland creating a head or delta progradation (Longstaffe 1989; Wilkinson 1991; Haszeldine et al. 1992; Macaulay et al. 1992). For the Palaeocene sands, relative sea-level fall and delta progradation over the sands in the Moray Firth shortly after deposition could have resulted in meteoric water flushing.

2.13.3 Recrystallisation

If concretions undergo recrystallisation their isotopic compositions can re-equilibrate with ambient conditions. Dix & Mullins (1987) in their study of Middle Devonian concretions, indicated that late septarian blocky calcite had the same $\delta^{13}C$ but different $\delta^{18}O$ values as concretionary cements. They interpreted oxygen isotope compositions as resulting from recrystallisation at depth without being affected by meteoric water influx. Recrystallisation can be ruled out where there is preservation of microfabrics and small scale isotopic zoning (Carpenter et al. 1988). Within the Montrose Group concretions there is no petrographic evidence for multiple phases of calcite precipitation, even when within the same concretion there may be different $\delta^{13}C$ and $\delta^{18}O$ compositions. Variations in composition can be satisfactorily explained in terms of solute supply and pore-water change.

2.13.4 Precipitation at anomalously high temperatures

Several papers have indicated the possibility of elevated thermal gradients during the early Tertiary (Pearson & Small 1988; Burley 1993). This is suggested to have occurred during the creation of the North Atlantic during the end-Cretaceous to Palaeocene. Illitisation of smectite is reported to be thermally controlled (Hower et al. 1976). Within the North Sea the onset of smectite-illite to illite transformation appears

to coincide with the Palaeocene-Eocene boundary (Pearson & Small 1988). They suggested that this may indicate that palaeo-temperatures, within the wells sampled, reached a maximum within several hundred metres burial in the Eocene. This is not considered likely as problems of heat supply and water circulation are created by this proposal. We suggest that this is a stratigraphic control (Dypvik 1983). Other inferences of increased palaeo-temperatures are based on fluid inclusion temperatures which may themselves be reset (Osborne & Haszeldine 1993).

2.13.5 Elevated Palaeocene surface water temperatures

There is strong isotopic and fossil evidence that surface waters within the mid-Eocene were substantially warmer than during the Paleocene times during deposition of the Montrose Group. The warming of bottom waters which would affect the shallow geothermal gradient is dependent upon the non-existence of a thermoclime within the Eocene North Sea which is dependent on the depth and circulation patterns of the Eocene North Sea.

Burchadt (1978) assemble Tertiary mollusc isotopic data from southern England, Holland, Germany, Denmark and southern Sweden. Equivalent day molluscs live at depths of 30-150m. Simple interpretation of the oxygen isotopic ratios of these fossils indicate that surface waters during mid-Eocene peak at 53-42Ma. This interpretation indicated that surface water temperatures were between 22-28°C during this period having risen from 10-14°C during the Thanetian. No information is given in this paper about locality, depth of burial of samples (outcrop versus well data) or general condition of samples. Schrag et al (1995) consider that the oxygen isotopic ratios of carbonate fossils can be strongly affected by any diagenetic effects and have in the past lead to misleading interpretation of high Eocene lower-equatorial precipitation temperatures.

The range in $^{18}O/^{16}O$ ratios can alternatively be in interpreted as mixing of marine and isotopically light meteoric water within semi-closed Eocene North Sea (Schmitz & Hailmann -Clausan (1993). However this warming period has been recognised in isotopic analysis of ODP cores from around the world (Corfield 1993).

The depth of the Paleocene North Sea is a matter of current debate . If the Eocene seas were shallower than 200m the thermoclines may not have been established. Providing bottom circulation is present, temperature profiles of sea present at present-day mid-latitudes indicate that water temperatures rapidly drop within the first 10's of metres depth (15-20°C surface temperatures to 5-10°C and drop even more rapidly as higher latitudes are reached (Open University 1989)). The temperatures of bottom waters of the Paleocene is unknown but there is the possibility that they may have been affected by the accepted Eocene warming. If the Palaeogene North Sea had elevated bottom waters temperatures then it is expected that such a strong effect would impose itself upon shallow geothermal gradients in the porous clastic sequence within a short geological timescale.

2.14 Oxygen isotopes; results

Oxygen isotopic compositions range from 15.2 to 29.4‰SMOW. These data can conveniently be discussed in geographical groupings identical to those used for understanding $\delta^{13}C$, **Figure 2.12, Table 2.5**

2.14.1 Shallow proximal area

Well 14/13-3 (cored depth 825.4-830.8m). $\delta^{18}O$ compositions vary from 23.0‰ to 28.2‰SMOW **Table 2.5.**

If depositional marine water (Lower Palaeocene marine water $\delta^{18}O$ = -0.9‰SMOW, Shackleton & Kennet 1974) was present during precipitation, then precipitation temperatures were 22- 48°C (mean 32°C), **Figure 2.16.** Alternatively temperatures of precipitation would be less than 5°C for meteoric pore-waters (early Tertiary meteoric water, $\delta^{18}O$ = -10‰SMOW, Forester and Taylor 1977).

Isotopic composition trends within concretions are similar, with a 2 to 3‰ decrease from the centre of the concretions to the rims, **Figure 2.13a, b.** In a pore-water of constant composition such a 2 to 3‰ change is equivalent to a 10 to 15°C increase during precipitation, equivalent to a 280-420m burial (assuming a 35°C/km geothermal gradient). However if precipitation temperatures are constant then this oxygen shift could also result from precipitation within progressively isotopically lighter pore- fluid to create a fluid 2 to 3‰ lower. Such a fluid could be created by mixing depositional fluids with; a) meteoric water (with low SO_4^- concentrations) or b) from the alteration of volcaniclastics to smectite (Lawrence & Gieskes 1981). Smectitic clays are common in the Montrose Group sandstones and this core is particularly tuffaceous and rich in igneous clasts (average 8% lithic fragments by volume). The tuffs are not layered but were depositionally carried into the sands forming a detrital mud matrix component in the sands. Weathering and degradation had taken place prior to deposition. This volcanic alteration hypothesis is a possible explanation for the Montrose Group concretion compositions to explain the shift in oxygen compositions of concretions within this well. It is concluded that porewaters were predominantly marine during concretion precipitation though later modifications were made to lighten porewater compositions, either due to meteoric water introduction or alteration of igneous detritus to smectite clays.

2.14.2 Witch Ground Graben axis

These are wells 15/20-4 and 16/28-6 (cored depths 1949.7 to 2019.4m and 2585.8 to 2736.4m). $\delta^{18}O$ composition varies from 20.0 to 20.5‰ and 20.0 to 22.1‰SMOW respectively, **Figure 2.13c, i, Table 2.5.**

Assuming calcite growth in depositional marine waters gives temperatures of 55 to 70°C. Alternatively, early Tertiary meteoric water (-10‰SMOW, Forester and Taylor 1977) gives precipitation temperatures of 10 to 18°C, **Figure 2.16.** The higher precipitation temperatures of 55 to 70°C are unlikely as such temperatures approach maximum burial temperatures of 70°C (well 15/20-4) and 95°C (well 16/28-6). Calcite is also amongst the earliest authigenic phases in these paragenetic sequences. Blocky kaolinite and the bulk of quartz overgrowths both post-date concretion growth. It is suggested that lower temperatures are more consistent with the petrographic evidence for shallow concretion growth and possible biodegradation processes.

In both wells sampled there is an increase in $\delta^{18}O$ values 20.3 to 20.5‰SMOW and 20.90 to 22.2‰SMOW respectively. This corresponds to either an increase in pore-waters $\delta^{18}O$ values or an increase in temperature, in porewaters of constant

composition, of ~2°C and ~12°C at precipitation temperatures less than 40°C. For geothermal gradient of 35°/km this can be interpreted as burial of 70 and 420m during precipitation.

Early precipitation of calcite is commonly explained by the presence of meteoric pore-water. During the early Tertiary within the Central North Sea (Milton et al 1990; Mudge & Copestake 1992) a combination of delta progradation and sea level fall (Jones & Milton 1994; Reynolds 1994) did occur shortly after deposition of Montrose Group sandstones and is likely to have provided sufficient head for meteoric flushing (Timbrell 1993; Stewart et al. 1994), **Figure 2.17.** This took place before significant burial (<500m) and before the compaction of overlying muds creating an impermeable seal. Within the Witch Ground Graben sufficient connectivity exists within the regionally extensive Andrew Formation to act as an aquifer for pore-water movement (Den Hartog Jager et al. 1993). Other evidence for the meteoric flushing during the Tertiary (Barnard and Bastow 1992) is the distribution of degraded hydrocarbons within Palaeocene sandstones in the Northern North Sea. Oils uniformly decrease in API° towards coastlines, indicating that bacterial degradation processes were more important in those palaeo-geographies. Although $\delta^{13}C$ values indicate hydrocarbon degradation, no evidence of deep basin waters are found in $\delta^{18}O$ distributions.

2.14.3 South Witch Ground Graben flank

These cements are from wells 15/26-3 and 15/26-4 (cored depths 1874.6-1929.75m and 2066.4-2476m respectively). $\delta^{18}O$ varies from 18.0 to 22.8‰SMOW. and 15.2 to 29.4‰SMOW respectively, **Figure 2.12, Table 2.5.**

Oxygen composition of concretions with positive carbon ratios from these two wells have remarkable consistent oxygen isotopic ratios. The values fall in a narrow range between 20.3 to 22.8‰SMOW. The maximum variation within a single concretion is 0.8‰ SMOW which is equivalent to about 8°C variation in temperature. During precipitation at temperatures less than 40°C in porewaters of constant isotopic composition. Assuming marine pore-waters for these carbonates yields precipitation temperatures of between 45-65°C, **Figure 2.16,** and assuming meteoric water, this results in precipitation temperatures of between 5-15°C.

Carbon isotope ratios from these cements indicate definitely that cement formed within the fermentation zone (2.12.3). Although fermentation and sulphate reduction can take place concomitantly, fermentation dominates when waters are lacking in available sulphate. This can happen either when sulphate is used up in marine pore-fluids during burial, or when pore-waters are meteoric and low in SO_4^- concentrations. Fermentation takes place at a general temperature range of 10m to 1000m, 5-40°C (Irwin et al. 1977).

Therefore mixed pore-waters with a strong meteoric component are suggested, because of the δ^{13} C evidence for cementation within the fermentation zone. These cores underly a major late Palaeocene deltaic complex (Moray Formation; Deegan & Scull 1977) which prograded into the Palaeocene Central North Sea shortly after deposition of these cored sandstones. Influx of meteoric water is suggested to have occurred during this time.

Samples taken from chalky rich clastic beds have oxygen isotopes ratios from 24.8 to 31.6‰SMOW (and $\delta^{13}C$= -2.7 to +0.6‰PDB and one at -14.0‰PDB). Such values indicate precipitation from marine pore-waters at temperatures between 10-40°C. Two samples from well 15/26-4 at 2468.5 and 2469.9 within chalky rich beds have $\delta^{18}O$ = 17.9 and 15.2‰SMOW respectively with slight negative carbon isotopic ratios of -1.8 and -3.6‰PDB respectively. This suggests that re-precipitation of calcite from chalk has taken place during high water-rock ratios in the presence of meteoric water at low temperatures less than 40°C

2.14.4 Distal Wells

These are wells 16/29-2 (2623.2 to 2688.8m) and 23/16-4 (2150.19 to 2320.69m) and samples from 21/10-1, 22/17-4 and 22/20-3. Minus-cement porosities suggest growth at depths of 700-1200m.

16/29-2 2642.6 to 2643.5m concretions has very similar oxygen values 18.0 to 18.3‰SMOW **Figure 2.13j.** 2664.9 to 2666.9 concretion again has slight variation in oxygen composition, 17.9 to 19.5‰SMOW **Figure 2.13k.** Samples from a concretion within a chalky rich bed (2683.5m) has values of 18.0 and 18.2‰SMOW, **Figure 2.13l.** An adjacent calcite vein (2682.8m) has $\delta^{18}O$=17.5‰SMOW. A sample from a concretion at the top of the core (2638.0m) has oxygen values of 18.0 and 23.6‰SMOW **Figure 2.15c.** The 23.6‰SMOW value may be result of experimental error. The value of concretions around 18.0 indicate precipitation at temperature of 82°C within Tertiary marine pore-waters or 26°C within Tertiary meteoric water. The calcite vein indicates precipitation temperatures of 87°C within marine pore-waters or 30°C in meteoric water.

21/10-1 oxygen values for Fe-calcite are between 19.2 and 22.1‰SMOW
22/17-4 oxygen values for the Mn-calcite are between 19.2 and 19.8‰SMOW
22./20-3 oxygen values for the two Mn-calcite samples are 22.3 and 23.0‰SMOW

For these wells if marine pore-waters are chosen, then precipitation temperatures are 45-70°C, by contrast meteoric water suggests 5-25°C **Figure 2.16**

23/16-4 Most samples taken from cemented horizons have oxygen values between 20.3 and 21.8‰SMOW and $\delta^{13}C$=-88.2 to -0.4‰PDB **Figure 2.15d.** Precipitation temperatures are 55-70°C for marine pore-fluids and 10-15°C for meteoric pore-fluids **Figure 2.16.** Samples taken near the top of the Montrose Group at 2156m and at further down the core at 2316.5m which have $\delta^{13}C$ around zero (-0.3 to +0.6‰PDB have $\delta^{18}O$ values around 17.5 to 18.2‰SMOW. This suggests that precipitation temperatures in marine pore-fluids were 80-88°C and 25-30°C for meteoric fluids. A calcite vein at 2316.6m has $\delta^{18}O$ = 18.1‰SMOW.

A chalk sample at 2369.4m has $\delta^{18}O$ =24.5‰SMOW which suggests precipitation temperature of 40°C from marine porewaters and 2°C for meteoric waters pore-fluids.

For all these wells pore-waters with a purely meteoric composition is an unlikely pore-fluid during precipitation because of the low temperatures inferred. Carbonate are

petrographically late and post-date quartz and kaolinite precipitation. Kaolinite predates calcite growth and isotopic compositions $\delta^{18}O$‰SMOW kaolinite=11-20) indicate that mixed meteoric -marine porewaters were present during precipitation Chapter 4. This implies that by the time of late carbonate precipitation, porewaters isotopic compositions had reverted to marine water compositions. Present day compositions of Forties Field porewaters are between $\delta^{18}O$ =-0.9 to +1.7‰SMOW (Emery & Robinson 1993b). This reversion towards marine water compositions was probably due to saline compactional waters from surrounding mudrocks mixing with and pushing out mixed meteoric -marine were during burial. Water of a marine-dominated isotopic composition are compatible with conditions or precipitation.

Palaeo-temperatures derived from oxygen isotope ratios can only be used to predict depth of precipitation if geothermal gradients and surface temperatures are constant throughout burial. Palaeo-temperatures within the Montrose Group must have been elevated during the Eocene global warming (Burchardt 1978). If temperatures were raised by 10°C during shallow burial (<1km) then depth of precipitation suggested by precipitation temperatures using bottom water temperatures of 5°C and standard 35°/km for the Palaeocene sandstones may be misleading. Depth of precipitation if temperatures were 10°C higher would raise precipitation depth by 300m. Palaeotemperatures may also have been raised in the close vicinity of Zechstein salt diapir . The high thermal conductivity of salt transfers heat rapidly vertically to locally raise burial temperatures. Precipitation depth generated from simple interpretation of $\delta^{18}O$ values from wells 22/20-3 and 23/16-4 close to salt diapirs may be deeper than is actually the case.

2.15 Strontium

Data have been plotted on $^{87}Sr/^{86}Sr$- $\delta^{13}C$, Sr(ppm)-Rb(ppm) and $^{87}Sr/^{86}Sr$ -Sr(ppm), plots, **Figure 2.18.** $^{87}Sr/^{86}Sr$ ratios range from 0.70771 to 0.70985 and Sr concentrations range from 313.8ppm to 1138.6ppm, **Table 2.6.**

Strontium is incorporated as a minor component into carbonate minerals, substituting for Ca. Strontium is chemically very similar to Ca and the $^{87}Sr/^{86}Sr$ ratio is thus taken to record the source of both Sr and Ca Strontium in marine carbonate has a low ratio (0.707 to 0.709) reflecting the Sr composition of seawater whereas Sr derived from silicate minerals has a much higher, more radiogenic $^{87}Sr/^{86}Sr$ ratio commonly 0.720 or greater (Halliday et al. 1979; Hamilton et al. 1987) **Table 2.6b.**

There are 5 possible sources for strontium included in Palaeocene sandstone concretions;:-

2.15.1.1 Palaeocene seawater

Palaeocene seawater values vary from 0.70772 to 0.70780 (Smalley et al. 1994). The $^{87}Sr/^{86}Sr$ curve generated by Smalley et al. (1994) has been compiled from Sr analysis of unaltered fossils. $^{87}Sr/^{86}Sr$ ratios are precise enough to deduce age dates to <2M.a. in the Cenozoic.

2.15.1.2 Dissolution of Palaeocene shell

Palaeocene shells will have the same ratios as Palaeocene seawater, ie 0.7072 to 0.70780. Concentration of Sr in shells is commonly 100's to 1000's ppm.

2.15.1.3 Dissolution of detrital chalk

Ekofisk Field chalks (primary calcite free from cement) are 0.70778 to 0.70793 (Smalley et al. 1992). Sr concentrations are 300 to 3000ppm (Taylor & Lapre 1987).

2.15.1.4 Water imported into the sandstones

Meteoric water contains negligible Sr, so any Sr would have to have come from the dissolution of Sr bearing minerals (carbonate, feldspar and mica) during flow. An example of this was illustrated by Smalley et al. (1994) who identified meteoric flushing for 25km away from outcrop (50m vertical head), within a limestone bed (40m maximum thickness). Sr concentrations up to 2mg/l increased away from outcrop.

2.15.1.5 Dissolution of Sr-containing detrital minerals

Detrital Caledonian feldspars from within the provenance region typically have $^{87}Sr/^{86}Sr$ of 0.705 to 0.745 and strontium concentrations of 125-1000ppm (Halliday et al. 1979; Haughton et al. 1991) **Table 2.6b**. Very radiogenic strontium can be supplied by the dissolution of micas ($^{87}Sr/^{86}Sr = 0.79$; Halliday et al. 1979). The dissolution of detrital micas and feldspars within Brent Group sands is held responsible for the high $^{87}Sr/^{86}Sr$ ratios found in authigenic carbonates (Brint 1989; Haszeldine et al. 1992).

2.15.2 Results

Well samples in this study can be divided into two general groups

a) those with $^{87}Sr/^{86}Sr$ values similar to that of Palaeocene shells

b) those with a strong radiogenic component

A chalk clast sample analysed from well 23/16-4 ($^{87}Sr/^{86}Sr = 0.70793$, $\delta^{13}C = 0.83‰$PDB) falls close to the Ekofisk Formation range (Smalley et al. 1992; Taylor & Lapre 1987).

Samples from wells 14/13-3. 15/20-4, 15/26-3, 15/26-4, 16/28-6 and 16/29-2

Carbonate samples from these wells have $^{87}Sr/^{86}Sr$ ratios that are within recorded strontium ratios measures from unaltered Palaeocene and Cretaceous carbonate shell fossils. It is likely that all these samples derived Sr from the dissolution of detrital carbonate **Figure 2.18, Table 2.6.** In the case of wells 15/20-4 and 16/28-6, concretions in both samples increase in radiogenic component towards the concretion edge during precipitation. The lack of correlation between Sr and Rb concentrations also makes a contribution from feldspar dissolution unlikely, **Figures 2.18b, c.**

Samples from wells 21/10-1, 22/17-4 22/20-3 and 23/16-4

All contain significantly higher $^{87}Sr/^{86}Sr$ than the other samples,, **Figure 2.18a, Table 2.6.** Available Sr could reasonably have been derived from dissolution of detrital feldspars. Certainly silica cementation from well 22/20-3 unequivocally pre-dates concretion precipitation. Pre-cement porosities within these samples are relatively low indicating greater burial before and during precipitation. This allows more time for feldspar dissolution. Texturally later concretions show increasingly radiogenic $^{87}Sr/^{86}Sr$ values up to 0.70964. Enriched $^{87}Sr/^{86}Sr$ waters could also have been introduced from two other sources, i) overlying Tertiary muds could have introduced porewaters during compaction. Present day overpressure gradually increases upwards within the muds, this implies fluid movement into the sandstones (Darby et a1. 1995 in press). ii)

overpressured Jurassic sandstones underlying the Tertiary sandstones may have introduced modified porewaters during pressure-release through major faults and areas affected by salt-diapirism (Burley 1993) see Chapter 6. The small rise in $^{87}Sr/^{86}Sr$ ratios within these wells indicate a definite contribution of silicate strontium but the slight increase can be accomodated by the small amounts of feldspar dissolution within the Montrose Group sediments. This hypothesis is a simpler, and therefore the accepted explanation, than the transfer of ^{87}Sr enriched fluids from underlying pre-Tertiary sediments. Similar trends of calcite cements with higher than depositional $^{87}Sr/^{86}Sr$ ratios are seen within Upper Cretaceous chalk fields within the North Sea, Taylor & Lapre 1987 and Smalley et al. 1992. The rise in Sr ratios are linked to organic acid dissolution of in-situ silicates within the Cretaceous deposits. A rise in $^{87}Sr/^{86}Sr$ ratios of late diagenetic carbonates in the southern North Sea Rotliegendes sandstones was identified by Sullivan et al. (1990). Here the variations in Sr ratios were so large (early dolomite $^{87}Sr/^{86}Sr$~0.7076, and late ankerite $^{87}Sr/^{86}Sr$~0.7112) that they could be confidently interpreted as resulting from the transfer of ^{87}Sr-rich fluids from Carboniferous mudstones into overlying Rotliegendes sandstones.

2.15.3 Coupled carbon and strontium compositions?

In both wells 15/20-4 and 16/28-6 samples were taken from near the centre of the concretions and towards the rim, **Figure 2.19.** There is a weak correlation between carbon and strontium isotopic compositions. This suggests that the processes releasing radiogenic ^{87}Sr may have been linked to the processes affecting ^{13}C.

Carbon isotopes reflect an oxidative source for carbon from degrading hydrocarbons, while strontium values indicate a specific starting source - Palaeocene shell dissolution.

The composition of the concretions moves towards lower ^{13}C and more radiogenic $^{87}Sr/^{86}Sr$ ratios. The decreasing ^{13}C carbon composition indicates an increase in components from oxidation of methane ($\delta^{13}C$~-50‰PDB) and a decreasing component of detrital carbon ($\delta^{13}C$ - 0‰PDB). Oxidation of methane generates organic acids. Such acids have been proposed as being responsible for the dissolution of feldspars (Surdam et al. 1984). Such dissolution would then account for the increase in ^{87}Sr within concretions.

2.16 Size of concretions

Montrose group concretions are between 15cm to 300cm in thickness along core length. Within well 23/16-4 concretions are evident as individual beds are less than 2m thick. All other sampled wells have massive sandstone units at least several metres in thickness. Within well 23/16-4 are cemented horizons equivalent to beds.

According to calculations by Wilkinson & Dampier (1990) the growth of a 1m concretion, a slightly larger than average Palaeocene concretion requires 9My to precipitate in static fluid , and only 5.7 My within fluids moving at 1m a-1 (metre per annum) if sourced only by shell dissolution. Wilkinson & Dampier (1990) assume that the only source for carbonate is the initially even distribution of detrital carbonate within the sandstone body, that solute precipitated as a cement on the concretion surface only and that dissolution of aragonitic shell material is rapid compared to other processes and is therefore considered unimportant in determining concretion growth times.

The times generated by Wilkinson & Dampier (1990) appear unrealistic for concretion growth in these Paleocene sandstones as subsidence is particularly rapid and sediments would compact to lower porosities. Sufficient changes are not recorded isotopically or texturally to permit long precipitation times. Oxygen isotope ratios across individual concretions are consistent with precipitation at fairly constant temperatures. They do not show the textural or chemical changes that may be expected if precipitation took place over a range of temperatures during burial. Therefore the supply of cementing ions must have been very rapid, as might be expected if sourced from migrating fluids.

2.17 Conclusions

Concretionary carbonate is a ubiquitous authigenic cement throughout the Lower Paleocene sands. Calcite cement forms up to 10% of the cored reservoir sandstones. Within the Montrose Group sandstones there is a wide spread of $\delta^{18}O$ and $\delta^{13}C$ values. **Figure 2.20.**

1) In palaeo-nearshore well 14/13-3, calcites precipitated by process of sulfate reduction and dissolution of detrital carbonate within cool (<35°C) predominantly marine pore-fluids.

2) In Witch Ground Graben axis wells 15/20-4 and 16/28-6 unusually strong component of unmodified organic $\delta^{13}C$ suggests that anaerobic oxidation of hydrocarbons occurred during shallow burial (<30°C) within mixed meteoric-marine pore waters. These hydrocarbons may have migrated vertically from the Kimmeridge Clay Formation.

3) In Witch Ground Graben flank wells 15/26-3 and 15/26-4, various reactions occurred. These reactions supplied carbon by detrital calcite dissolution, within cool marine waters, fermentation of detrital organic matter, and sulfate reduction/slight oxidation of methane within mixed meteoric- marine waters at temperatures less than 40°C.

4) In wells 16/29-2, 21/10-1, 22/17-4, 22/20-3, and 23/16-4, low minus-cement porosities suggest deeper and higher temperature reactions sourcing the carbon possibly associated with abiotic degradation of organic material, and dissolution of detrital carbonate, all within pore-waters of a marine composition at temperatures >50°C.

Acknowledgments

Robert Stewart acknowledges a NERC studentship, GT4/90/GS/51. Isotopic analysis was carried out at the Isotope Geoscience Unit at the Scottish Universities Research and Reactor Centre. The SURRC is funded by the Scottish Universities and NERC. Core was supplied by BP (Roger Anderton and Richard Dixon), Amoco UK (Richard King), Chevron UK (Andrew Harding) and Phillips UK (Penny Turner)

References

Atwater G.I. and E.E. Miller 1965 The effect of increase in porosity with depth on future development of oil and gas reserves in South Louisiana. *Bulletin of the American Association of Petroleum Geologists*, **49**, 334.

Baldwin, B. and C.O. Butler 1985 Compaction curves. *Bulletin of the American Association of Petroleum Geologists*, **69**, 622-626.

Barnard, P.C. and M.A. Bastow 1992 Hydrocarbon generation, migration alteration, entrapment and mixing in the Central and Northern North Sea. In: *Petroleum Migration*, W.A. England and A.J. Fleet (eds), *Geol. Soc. Spec. Publ.* **59**, 167-190.

Bjorlykke K. and K. Gran 1994 Salinity variations in North Sea formation waters: implications for large-scale fluid movements. *Marine and Petroleum Geology*, **11**, 5-9.

Bjorkum, P.A. and O. Walderhaug 1990 Lateral extent of calcite-cemented zones in shallow marine sandstones. In: *North Sea Oil and Gas Reservoirs- II*, The Institute of Technology, Graham and Trotman, 331-336.

Boles, J.R. and K.S. Johnson 1983 Influence of mica surfaces on pore-water pH. *Chemical Geology*, **43**, 303-317.

Brennand, T.P., Van Hoorn, B., and K.H. James 1990 Historical Review of North Sea Exploration. In: *Introduction to the Petroleum Geology of the North Sea*, K.W. Glennie (ed), Blackwell Scientific Publications, Oxford, 1- 33.

Brint, J.F. 1989 *Isotope diagenesis and palaeofluid movement: Middle Jurassic Brent sandstones, North Sea.* D. Phil. Thesis, University of Strathclyde, 288pp.

Bryant, I.D., Kantorowicz, J.D., and C.F. Love 1988 The origin and recognition of laterally continuous carbonate-cemented horizons in the Upper Lias sands of southern England. *Marine and Petroleum Geology*, **5**, 108-133.

Burdige D.J. 1993 The biogenchemistry of mangenese and iron reduction in marine sediments. *Earth Science Reviews*, **35**, 249-284.

Burley, S.D., Mullis, J. and A. Matter 1989 Timing diagenesis in the Tartan Reservoir (UK North Sea): constraints from combined cathodoluminescence microscopy and fluid inclusion studies. *Marine and Petroleum Geology*, **6**, 98-120.

Burley, S.D. 1993 Models of burial diagenesis for deep exploration plays in Jurassic fault traps of the Central and Northem North Sea. In: *Petroleum Geology of Northwest Europe: Proceedings of the 4th Conference*, J.R. Parker (ed), Geol. Soc., London, 1353-1375.

Carpenter, S.J., Erickson, J.M., Lohmann, K.C. and M.R. Owen 1988 Diagenesis of fossiliferous concretions within the Upper Cretaceous Fox Hill Formation, North Dakota. *Journal of Sedimentary Petrology*, **55**, 706- 723.

Cayley G.T. 1987 Hydrocarbon migration in the central North Sea. In: *Petroleum Geology of North West Europe*, J. Brooks & K.W. Glennie (eds), Graham & Trotman, London, 549-555

Corfield R.M. 1993 The stable isotope record of the early Palaeogene. In: *Conference Proceedings of Correlation of the Early Paleogene in Northwest Europe*, Geological Society of London, 10.

Crawford R., Littlefair R.W. and L.G. Affleck 1991 The Arbroath and Montrose Fields, Blocks 22/17, 18, North Sea. In: *United Kingdom Oil and Gas Fields, 25 Year Commorative Volume*, I.L. Abbotts (ed) , *Geol. Soc. Mem.* **14**, 211-217.

Curtis, C.D. and M.L. Coleman 1986 Controls on the precipitation of early diagenetic calcite, dolomite and siderite concretions in complex depositional sequences. The Society of Economic Palaeontologists and Mineralogists

Cutts, P.L. 1991 The Maureen Field, Block 16/29a, UK North Sea. In: *United Kingdom Oil and Gas Fields, 25 Years Commemorative Volume.* I.L. Abbotts (ed), *Geol. Soc. Mem.* **14**, 347-352.

Deegan, C.E. and B.J. Scull 1977 A standard lithostratigraphic nomenclature for the central and northern North Sea. *Inst. Geol. Sci. Report* **77/25**.

Den Hartog Jager, D., Giles, M.R., and G.R. Griffiths 1993 Evolution of Paleogene submarine fans of the North Sea in space and time. In: *Petroleum Geology of Northern Europe: Proceedings of the 4th Conference in London*, J.R. Parker (ed), Geol. Soc., London, 59-71.

Dimitrakopolous, R. and R. Muehlenbachs 1987 Biodegradation of petroleum as a source of ^{13}C-enriched carbon dioxide in the formation of carbonate cement. *Chemical Geology (Isotope Geoscience Section*, **65**, 283-291.

Dix, G.R. and H.T. Mullins 1987 Shallow, subsurface growth and burial alteration of Middle Devonian calcite concretions. *Journal of Sedimentary Petrology*, **57**, 140-152.

Donovan, T.J., Friedman, I., and J.D. Gleason 1974 Recognition of petroleum-bearing traps by unusual isotopic compositions of carbonate-cemented surface rocks. *Geology*, 351-354.

Dypvik, H. 1983 Clay mineral transformations in Tertiary and Mesozoic sediments from North Sea. *Bulletin of American Association of Petroleum Geologists*, **67**, 160-165.

Emery, D. and A. Robinson 1993a Porosity and permeability. In: *Inorganic Geochemistry: Applications to Petroleum Geology*, D. Emery and A. Robinson (eds), Blackwell Scientific Publications, Oxford, 129-169.

Emery, D. and A. Robinson 1993b Secondary recovery: Forties Field, offshore UK. In: *Inorganic Geochemistry: Applications to Petroleum Geology*, D. Emery and A. Robinson (eds), Blackwell Scientific Publications, Oxford, 217-220.

Eslinger E. and D. Peaver 1988 *Clay Minerals for Petroleum Geologists and Engineers.* Society of Economic Palaeontologists and Mineralogists: Short Course Notes, **22**.

Folk, R.L. 1974 *Petrology of Sedimentary Rocks.* Hemphill Publishing Company, Austin.

Forester, R.A.W. and H.P. Taylor 1977 $^{18}O/^{16}O$, D/H, and $^{13}C/^{12}C$ studies of Tertiary igneous complex of Skye. *American Journal of Science*, **277**, 136- 177.

Friedman, G.M. 1959 Identification of carbonate minerals by staining methods. *Journal of Sedimentary Petrology*, **29**, 87-97.

Friedman, I. and J.R. O'Neil 1977 Compilation of stable isotope fractionation factors of geochemical interest. In: *Data of Geochemistry* (6th Edn.), M. Fleischer (ed), United States Geological Survey Professional Paper 440-KK.

Galloway, W.E. 1984 Hydrogeological regimes of sandstone diagenesis. In: Clastic Diagenesis, D.A. MacDonald and R.C. Surdam (eds), *American Association of Petroleum Geologists Memoir* **37**, 3-15.

Giles, M.R., Stevenson, S., Martin, S.V., Cannon, S.J.C., Hamilton, P.J., Marshall, J.D., and G.M. Samways 1992 The reservoir properties of the Brent Group: a regional perspective. In: *Geology of the Brent Group*, A.C. Morton, R.S. Haszeldine, M.R. Giles and S. Brown, (eds), *Geol Soc. Spec. Publ.* **61**, 289-327.

Glasmann, J.R. 1992 The fate of feldspar in Brent Group reservoirs, North Sea: a regional synthesis of diagenesis in shallow, intermediate and deep burial environments. In: *Geology of the Brent Group*, R.S. Haszeldine, A.C. Morton, M.R. Giles and S. Brown (eds), *Geol. Soc. Spec. Publ.* **61**, 329-350.

Gould K.W. and J.W. Smith 1978 Isotopic evidence for microbial role in genesis of crude oil from Barrow Island, Western Australia. *Bulletin of American Association of Petroleum Geologists*, **62**, 455-462.

Halliday, A.N., Aftalion, M., Van Breemen, O. and J. Jocelyn 1979 Petrographic significance of Rb-Sr and U-Pb isotopic systems in the 400Ma old British Isles granitoids and their hosts. In: *The Caledonides of the British Isles- Reviewed*, C.H. Holland, B.E. Leake and A.L. Harris (eds) *Geol. Soc. Spec. Publ.* **8**, 653-662.

Hamilton, P.J., Fallick, A.E., MacIntyre, R.M. and S. Elliot 1987 Isotopic tracing of the provenance and diagenesis of Lower Brent Group Sands, North Sea. In: *Petroleum Geology of North West Europe*, Brooks and K. Glennie (eds), Graham and Trotman, London, 936-949.

Haszeldine, R.S., Brint, J.F., Fallick, A.E., Hamilton, P.J. and S. Brown 1992 Open and restricted hydrologies in Brent Group diagenesis: North Sea. In: *Geology of the Brent Group*, R.S. Haszeldine, A.C. Morton, M.R. Giles and S. Brown (eds), *Geol. Soc. Spec. Publ.* **61**, 401-419.

Haughton, P.D.W., Rogers, G. and A.N. Halliday 1991 Provenance of Lower Old Red Sandstone conglomerates in S.E. Kincardinshire; evidence for the relative timing of Caledonian terrane accretion in Central Scotland. *Journ. Geol. Soc London*, **147**, 105-120.

Hower, J., Eslinger, E.V., Hower, M.E. and E.A. Perry 1976 Mechanism of burial metamorphism of argillaceous sediment: 1. Mineralogical and chemical evidence. *Geol. Soc. Amer. Bull.*, **87**, 160-165.

Irwin, H., Curtis, C. and M. Coleman 1977 Isotopic evidence for source of diagenetic carbonates formed during burial of organic-rich sediments. *Nature* **269**, 209-213.

Jacque, M. and J. Thouvenin 1975 Lower Tertiary tuffs and volcanic activity in the North Sea. In: *Petroleum and the continental shelf of north-west Europe*, A.W. Woodland (ed), John Wiley, New York, 455-465.

Jorgensen, N.O. 1989 Holocene methane-derived, dolomite-cemented sandstone pillars from the Kattegat, Denmark. *Marine Geology* **88**, 71-81.

Jones, R.W. and N.J. Milton 1994 Sequence development during uplift: Palaeogene stratigraphy and relative sea-level history of the Outer Moray Firth, UK North Sea. *Marine and Petroleum Geology*, **11**, 157-165.

Knox, R.W.O'B., Morton, A.C. and R. Harland 1993 Stratigraphic relationships of Palaeocene sands in the UK Sector of the central North Sea. In: *Petroleum Geology of the Continental Shelf of North West Europe*, by L.V. Illing and G.D. Hobson (eds), Institute of Petroleum, Heyden and Son, London, 267-281.

Lawrence, J.R. and J.M. Gieskes 1981 Constraints on water transport and alteration in the oceanic crust from isotopic composition of pore-water. *Journal of Geophysical Research*, **86**, 7294-7934.

Longstaffe, F.J. 1989 Stable isotopes as tracers in clastic diagenesis. In: *Short course m Burial Diagenesis*, I.E. Hutcheon (ed), Mineralogical Association of Canada Short Course Series, **15**, 201-277.

Lowe, D.R. 1982 Sediment gravity flows: II. Depositional models with special reference to the deposits of high-density turbidity currents. *Journal of Sedimentary Petrology*, **52**, 279-297.

Macaulay, C.I., Haszeldine, R.S. and A.E. Fallick 1992 Distribution, chemistry, isotopic composition and origin of diagenetic carbonates: Magnus Sandstone, North Sea. *Journal of Sedimentary Petrology*, **63**, 33-43.

MacCrea, J.M, 1950 On the isotope chemistry of carbonates and a palaeotemperature scale. *J. Chem. Phys.* **18**, 837-861.

Maliva R.G., DicksonJ.A.D., Smalley P.C. and N.H. Oxtoby 1995 Diagenesis of the Machar Field (British North Sea) Chalk : evidence for decoupling of diagenesis in fractures and the host rocks. *Journal Sedimentary Research*, **65**, 105-111.

Maxwell J.C. 1964 Influence of depth, temperatureand geologic age on porosity of quartzose sandstone. *Bulletin of the American Association of Petroleum Geologists*, **48**, 697-709.

Milton, N.J., Bertram, G.T. and I.R. Vann 1990 Early Paleogene tectonics and sedimentation in the Central North Sea. In: *Tectonic events responsible for Britain's oil and gas reserves*, R.F.P. Harman and J. Brooks (eds), *Geol Soc. Spec. Publ.* **55**, 339-351

Moore, S.E., Ferrell R.E. and P. Aharon 1992 Diagenetic siderite and other ferroan carbonates in a modem subsiding marsh sequence. *Journal of Sedimentary Petrology*. **62**, 357-366.

Morad, S. and L.F. De Ros. 1994 Discussion: Geochemistry and diagenesis of stratabound calcite cement layers within the Rannoch Formation of the Brent Group, Murchison Field, North Viking Graben (Northern North Sea) - comment. *Sedimentary Geology*, **93**, 135-141.

Morton, A.C., Halsworth, C.R. and G.C. Wilkinson 1993 Stratigraphic evolution of sand provenance during Palaeocene deposition in the Northem North Sea area. In; *Petroleum Geology of Northwest Europe: Proceedings of the 4th Conference*, J.R. Parker (ed), Geol. Soc., London, 73- 84.

Mozley, P.S. and S.J. Burns 1993 Oxygen and carbon isotopic compositions of marine carbonate concretions: an overview. *Journal of Sedimentary Petrology*, **63**, 73-83.

Mudge, D.C. and P. Copestake. 1992 Revised Lower Palaeocene lithostratigraphy for the Outer Moray Firth, North Sea. *Marine and Petroleum Geology*, **9**, 53-69.

O'Brien, W.O. and P. Woods 1994 Vulcan Sub-basin, Timor Sea. Clues to the structural reactivation and migration history from the recognition of hydrocarbon seepage indicators. *Australian Geological Survey Organisation Newsletter*, **21**, 8-11.

Open University 1989 Temperature in the oceans. In: *Seawater: Its composition,properties and behaviour*. Pergammon Press, Oxford, 16-29.

Osborne, M. 1994 *The effect of differing hydrogeological regimes on sandstone diagenesis: Brent Group oilfields, UK North Sea.* PhD Thesis, University of Glasgow

Osborne, M. and R.S. Haszeldine 1993 Evidence for resetting of fluid inclusion temperatures from quartz cements in oilfields. *Marine and Petroleum Geology*, **10**, 271-278.

Pagan, M.C.T. 1980 *Diagenesis of the Forties Field.* M. Phil. Thesis, University of Edinburgh.

Pearson, M.J. and J.S. Small 1988 Illite-smectite diagenesis and palaeotemperatures in Northern North Sea Quaternary to Mesozoic shale sequences. *Clay Minerals*, **23**, 10-132.

Prosser, D.J., Fallick, A.E., Daws, J.A. and B.P.J. Williams 1994 Geochemistry and diagenesis of stratabound calcite cement layers within the Rannoch Formation of the Brent Group, Murchison Field, North Viking Graben (Northern North Sea) - reply. *Sedimentary Geology* **93**, 143-147.

Pryor W.A. 1973 Permeability-porosity patterns and variations in some Holocene sand bodies. *Bulletin of the American Association of Petroleum Geologists*, **57**, 162-189.

Putnis, A. and J.D.C. McConnell 1980 Principles of Mineral Behaviour. Elsevier, New York

Reynolds, T. 1994 Quantitative analysis of submarine fans in the Tertiary of the North Sea Basin. *Marine and Petroleum Geology*. **11**, 202-207.

Saigal G.C. and K. Bjorlykke 1987 Carbonate cements in clastic reservoir rock from offshore Norway - Relationship between isotopic composition, textural development and burial depth. In: *Diagenesis of Sedimentary Sequences*. J.D. Marshall (ed), *Geol. Soc. Spec. Publ.* **36**, 313-324.

Schrag D.P., De Paolo D.J. and F.M. Richter 1995 Reconstructiong past sea surface temperatures: correcting for diagenesis of bulk marine carbonate. *Geochmica et Cosmochimica Acta*, **59**, 2265-2278.

Sclater, J.G. and P.A.F. Christie 1980 Continental stretching; an explanation of the post-mid-Cretaceous subsidence of the central North Sea basin, *Journal of Geophysical Research*, **85**, 3711-3739.

Scmidtz B. and C. Heilmann-Clausen 1993 A stable isotope ($\delta^{18}O$, $\delta^{13}C$) and iridium stratigraphy across the Early Eocene section at Albaek Hoved, Denmark. In: Conference proceedings of 'The Early Paleogene in the Northwest Europ'e, Geological Society of London, 29.

Seley R.C. Porosity gradients in North Sea oil-bearing sandstones, *Geol. Soc. Lond.*, **135**, 119-132.

Shackleton, N.J. and J.P. Kennet 1974 Paleotemperature history of the Cenozoic and the initiation of Antarctic glaciation: oxygen and carbon isotope analysis in DSDP sites 277, 279, 281. In: *Initial Reports of the Deep Sea Drilling Project*, J.P. Kennet et al (eds), Washington: U.S. Government Printing Office, **v29**, 743-755.

Smalley, P.C., Raheim, A., Rundberg, Y. and H. Johansen. 1989 Strontium-isotope stratigraphy: applications in basin modelling and reservoir correlation. In: *Correlation in Hydrocarbon Exploration*, J.D. Collinson (ed), Grahan and Trotman, London, 23-31

Smalley, P.C., Lonoy, A. and A. Raheim 1992 Spatial $^{87}Sr/^{86}Sr$ variations in formation water and calcites from the Ekofisk chalk oil field: implications for reservoir connectivity and fluid composition. *Applied Geochemistry* **7**, 341-350.

Smalley, P.C., Higgins, A.C., Howarth, R.J., Nicholson, H., Jones, C.E., Swinburne, N.M.H. and J. Bessa 1994 Seawater Sr isotope variations through time: A procedure curve to date and correlate marine sedimentary rocks. *Geology*, **22**, 431-434.

Stewart, I.J. 1987 A revised stratigraphic interpretation of the Early Palaeogene of the Central North Sea. In: *Petroleum Geology of North West Europe*, J. Brooks and K.W. Glennie (eds), Graham and Trotman, London, 557-577.

Stewart, R.N.T., Haszeldine, R.S., Fallick, A.E., Anderton, R. and R. Dixon 1993 Shallow calcite cementation in a submarine fan: biodegradation of vertically migrating oil? *American Association of Petroleum Geologists Annual Convention*, 186.

Stewart, R.N.T., Fallick, A.E. and R.S. Haszeldine 1994 Kaolinite growth during pore-water mixing: isotopic data from Palaeocene sands, North Sea, UK. *Clay Minerals*, **29**, 627-636.

Surdam, R.C., Boese, S.W. and L.J. Crossey 1984 The chemistry of secondary porosity. In: Clastic Diagenesis, D. MacDonald and R. Surdam (eds), *American Association of Petroleum Geologists Memoir* **37**, 127-151

Taylor, S.R. and J.F. Lapre 1987 North Sea chalk diagenesis: its effect on reservoir location and properties. In: *Petroleum Geology of North West Europe*, J. Brooks and K. Glennie (eds), Graham and Trotman, London, 483- 495

Timbrell, G 1993 Sandstone architecture of the Balder Formation depositional system, UK Quadrant 9 and adjacent areas. In: *Petroleum Geology of Northwest Europe*, J.R. Parker (ed), Geol Soc., London, 107-121.

Tonkin P.C. and A.R. Fraser 1991 The Balmoral Field, Block 16/21, UK North Sea. In: *United Kingdom Oil and Gas Fields: 25 Years Commemorative Volume*, I.L. Abbotts (ed), *Geol. Soc. Mem.* **14**, 237-243.

Walker, R.G. 1978 Deep-water sandstone facies and ancient submarine fans; models for exploration for stratigraphic traps. *Bulletin of American Association of Petroleum Geologists*, **62**, 932-966.

Watson, R.S. 1993 *The Diagenesis of the Tertiary Sands from the Forth and Balmoral Fields.* PhD Thesis, University of Aberdeen.

Wilkinson M. and M.D. Dampier 1990 The rate of growth of sandstone- hosted concretions. *Geochim. Cosmochim. Acta*, **54**, 3391-3399.

Wilkinson, M. 1991 The concretions of the Bearreraig Sandstone Formation: geometry and geochemistry. *Sedimentology*, **38**, 899-912.

Wills J.M. 1991 The Forties Field, Block 21/10, 22/6a, UK North Sea. In: *United Kingdom Oil and Gas Fields, 25 Year Commemorative Volume*, I.L. Abbotts (ed), *Geol. Soc. Mem.* **14**, 301-308.

Figure Captions

Figure 1 - Structural map of base Cretaceous features showinglocation of wells sampled. A - 14/13-3, B - 15/20-4, C - 15/26-3, D- 15/26-4, E - 16/28-6, F - 16/29-2, G - 21/10-1, H - 22/17-4, J -22/20-3 and K - 23/16-4.

Figure 2a - Tertiary lithostratigraphical nomenclature (after Deegan and Scull 1977).
Figure 2b - Distribution of the Moray and Montrose Groups and their formations in the area south east of the Halibut Horst (after Deegan & Scull 1977)

Figure 2.3 - Concretion from well 16/28-6 (2640.35m), scale bar is 2cm long. Concretion is oblate spheroidally shaped.

Figure 2.4 - Photomicrograph illustrating the presence of small dolomite rhombs within main calcite cementing phase. Outlining dolomite crystals is bituminous-like staining.

Figure 2.5 - Mn(%)-Fe(%) cross plot of authigenic carbonate

Figure 2.6 - Mn(%)-Mg(%) cross plot of authigenic carbonate. Mg rich values of 15/26-3 refer to ankerites. Mg rich values of 16/28-6 carbonates refer to dolomite rhombs.

Figure 2.7 - Mg(%)-Fe(%) cross plot of authigenic carbonate

Figure 2.8 Fe(%),Mn(%),Mg(%) -cored depth plots of authigenic carbonates. Extent of carbonated zone (concretions) is marked by arrow on the left hand side. Figure 2.8g refers to entire well 23/16-4.
a) 15/26-3 1877.8-1873.3m
b) 15/26-3 1894.2-1895.4m
c) 15/26-4 2273.9-2274.9m
d) 16/28.6 2681.4-2683.2m
e) 16/29-2 2642.5-2645.5m
f) 16/29-2 2664.5-2667.0m
g) 23/16-4 2150-2350m
h) 16/28-6 2681.4-2683.2m (dolomite rhombs)

Figure 2.9 - Cathodoluminescence photomicrograph from 16/28-6 (2681.5m) illustrating high minus-cement porosities and no zoning of carbonate

Figure 2.10 - Cathodoluminescence photomicrograph from 16/29-2 (8748'10"). Though not concentrically zoned the concretion has sector zoning a feature associated with initial preciptation.

Figure 2.11 - Minus-cement porosity graph. Compaction curve is from Baldwin & Butler (1985). The growth depth of carbonate concretions can be estimated by assuming that diagenetic cements filled all inter-grain porosity, and that no major replacement of the carbonate has occurred. It is apparent that although the compaction curve is only an approximation, concretions precipitated at different depths during burial. Well labelling A to K as in Figure 2.1.

Figure 2.12 - δ^{18}OSMOW (calcite)-δ^{13}CPDB (calcite) cross-plot of concretion values.
Figure 2.12 - δ^{18}OSMOW (calcite)-δ^{13}CPDB (calcite) cross-plot of data interpreted. Compositions has been grouped according to wells These define palaeo-geographical areas which also relate to distinct organic processes. See text for interpretation.

Figures 2.13 Cored depth - δ^{18}OSMOW (calcite) and δ^{13}CPDB (calcite) for individual concretions

a) 14/13-3 825.4-825.7m
b) 14/13-3 830.3-830.9m
c) 15/20-4 2012.45-2012.6m
d) 15/26-3 1877.6-1878.6m
e) 15/26-3 1894.0-1895.5m
f) 15/26-4 2272.5-2275.0m
g)15/26-4 2300.1-2300.6m
h) 15/26-4 2467.0-2470.5m
i) 16/28-6 2681.0-2683.5m
j) 16/29-2 2641-5-2645.5m
k) 16/29-2 2664.5-2667.5m
l) 16/29-2 2682.6-2683.8m

Figure 2.14- SEM photomicrograph of a rare coccolith within a concretion in well 15/20-4 (2012.5m).

Figure 2.15 Cored depth - δ^{18}OSMOW (calcite) and δ^{13}CPDB (calcite) for core length

a) 15/26-3 1870-1940m
b) 15/26-4 2250-2500m
c) 16/29-2 2630-2690m
d) 23/16-4 2150-2400m

Figure 2.16 - δ^{18}OSMOW (water)-precipitation temperature cross-plot. A range of porewaters and precipitation temperatures are available for each δ^{18}OSMOW (calcite). To constrain temperatures, δ^{13}CPDB (calcite) values and minus-cement porosities can be used to limit precipitation depths.

Figure 2.17 Model for meteoric water influx

Figure 2.18 a) $(^{87}Sr/^{86}Sr)_{45}$-δ^{13}CPDB (calcite) crossplot. Texturally early concretions have $^{87}Sr/^{86}Sr$ ratios close to Palaeocene seawater. Late concretions wells g, h, j and k have a radiogenic component.
1, Range of δ^{13}CPDB values of chalk matrix (Taylor & Lapre 1987)
2, Range of δ^{13}CPDB values of authigenic calcite cements (Taylor & Lapre 1987)
3, Range of $^{87}Sr/^{86}Sr$ of Palaeocene seawater (Smalley et al. 1994)
4, Range of $^{87}Sr/^{86}Sr$ of Zechstein seawater (Smalley et al. 1994)
5, Range of $^{87}Sr/^{86}Sr$ of Upper Cretaceous seawater (Smalley et al. 1994)
6, $^{87}Sr/^{86}Sr$-δ^{13}CPDB field containing Ekofisk Field chalk values (Smalley et a1. 1992)
b) and c) Compared with detrital feldspars (Halliday et al. 1979, Haughton et al. 1991), concretions have little Rubidium and are depleted with respect to Sr. Line a on graph c) refers to concentration of Sr within chalk matrix (Taylor & Lapre 1987)

Figure 2.19 ($^{87}Sr/^{86}Sr$)–$\delta^{13}C_{PDB}$ crossplot contains values from wells 15/20-4 (2012.5m) and 16/28-6 (2681.5m to 2683.2m). Carbon and strontium supply may be linked. As carbonates decrease in' O, strontium ratios increase.

Figure 2.20 Summary processes cartoon. T = Tertiary muds, P =Palaeocene Montrose Group sandstones, K = Cretaceous, J =Jurassic sequence induding Kimmeridge Clay Formation, Tr =Triassic, Z = Zechstein salt dome. Area 1 Interaction of meteoric water and early migrating oil during the late Palaeocene resulted in precipitation of carbonates with extremely low $\delta^{13}C_{PDB}$ values. Area 2 Area away from either migration route of early migrating hydrocarbons or hydrocarbons had become too degraded to have reached this area. Carbonates precipitated with typical positive fermentation $\delta^{13}C_{PDB}$ values. Area 3, late carbonates within this area precipitated as a result of decarboxylation and remobilisation of detrital calcite. Strontium ratios indicate that Montrose Group porewaters may have been mixed with migrating fluids containing radiogenic Sr resulting from the dissolution of silicate minerals. This may have come from the underlying Jurassic sequence. We suggest that fluid movement is associated with salt diapirism.

Tables

Table 2.1 List of cored sample wells

14/13-3	15/20-4	15/26-3	15/26-4	16/28-6
16/29-2	21/10-1	22/17-4	22/20-3	23/16-4

Table 2.2 Grain size of carbonate cement

Well	Crystal grain size
14/13-3, 15/26-3, 15/26-4	10-80μm
15/20-4, 16/28-6, 23/16-4	40-60μm
16/29-2, 21/10-1, 22/17-4, 22/20-3	100-400μm

Table 2.3 Carbonate mineralogy

Well/sample Cored depth (m)	Fe%	Mn%	Ca%	Mg%
14/13-3				
824.9m	2.18	1.80	93.38	2.65
	2.49	1.33	92.16	4.01
	2.55	1.50	92.28	3.67
	2.55	1.61	92.42	3.42
	2.02	1.26	93.34	3.38
830.3m	4.14	0.64	92.50	2.71
	1.60	6.67	90.52	1.21
	1.65	7.52	90.54	0.29
	1.72	9.40	89.07	1.53
	1.87	8.34	88.37	1.42
830.4m	3.36	0.77	92.66	3.21
	3.67	0.88	93.13	2.92
	3.15	0.88	93.18	2.79
	3.48	1.04	92.82	2.66
	3.42	0.83	92.87	2.88
	2.99	1.09	93.04	2.88
15/20-4				
2012.5m	1.93	3.42	90.71	2.75
	1.67	2.50	92.59	3.67
	2.33	2.66	91.51	3.50
	1.78	2.59	91.55	4.08
	1.69	2.63	91.72	3.95
15/26-3				
1874.3m	16.76	0.57	60.92	21.76
	17.20	0.43	60.57	22.21
	19.02	0.21	60.45	20.32
	16.84	0.51	61.33	21.33
	17.46	0.29	60.25	22.01
1877.9m	18.16	0.35	60.00	21.49
	15.81	0.43	60.89	22.87
	15.60	0.57	61.50	22.33
	15.67	0.37	62.15	21.81

	13.72	0.68	62.45	23.24
1878.0m	24.84	0.15	58.89	16.12
	14.70	0.41	61.85	23.04
	14.11	0.40	61.63	23.76
	13.63	0.16	61.32	24.89
	22.88	0.30	58.32	18.49
1894.3m	3.70	0.00	95.70	0.60
	3.78	0.11	95.65	0.46
	2.38	0.12	96.91	0.59
	3.27	0.30	95.63	0.81
	3.47	0.35	95.70	0.48
1895.2m	1.61	1.63	95.89	0.86
	1.10	0.37	97.17	1.36
	1.33	0.78	96.68	1.21
15/26-4				
2724.0m	0.00	0.59	98.47	0.94
	0.27	0.55	98.48	0.71
	1.03	0.23	98.04	0.88
2274.4m	0.23	0.57	98.10	1.10
	0.75	0.30	98.24	1.05
	0.39	0.26	98.37	0.76
	0.44	0.88	98.00	0.48
	0.54	0.39	97.75	1.32
2274.5m	1.38	0.50	96.24	1.88
	1.27	0.34	97.42	0.97
	1.03	0.08	97.55	1.34
2274.6m	0.00	0.62	97.72	1.66
	0.00	0.49	98.44	1.07
	0.98	0.56	98.32	1.03
2274.7m	0.00	0.48	97.99	1.53
	0.26	0.24	98.79	0.71
	0.02	0.27	98.93	0.78
16/28-6				
2681.6m	5.03	0.64	50.78	43.56
	1.44	0.74	93.75	4.074
	4.64	0.62	50.30	44.44
	1.83	0.99	92.41	4.80
	1.58	0.88	93.84	3.70
	1.56	0.95	93.21	4.28
	1.49	0.86	93.08	4.57
	5.06	0.59	49.43	44.92
	1.63	0.90	92.55	4.92
2681.7m	1.00	5.04	92.19	1.78
	5.91	0.74	50.43	42.92
	1.22	1.20	95.76	1.826
	1.59	0.86	92.85	4.703
	3.17	0.54	57.39	38.90

	1.87	0.92	92.12	5.098
	5.59	1.11	49.44	43.86
	1.13	1.69	95.38	1.81
2682.0m	1.22	0.87	96.73	1.19
	0.96	1.05	97.27	0.72
	0.93	1.00	97.82	0.25
	1.11	1.24	96.91	0.74
	1.36	1.54	95.92	1.18
	4.66	0.58	54.18	40.58
	3.33	0.63	53.59	42.45
	3.16	0.43	53.73	42.68
	5.42	0.74	52.82	41.02
2682.3m	1.16	1.21	96.80	0.828
	1.39	1.54	95.49	1.574
	1.21	1.05	96.55	1.19
	1.56	0.97	94.77	2.70
	1.30	1.45	96.02	1.23
	1.40.	1.38	96.06	1.15
	1.54	0.60	48.58	49.27
	4.09	0.43	50.98	44.51
	6.86	0.71	49.61	42.83
	3.12	0.54	52.25	44.10
	5.71	0.65	50.37	43.28
2693.0m	1.08	1.60	96.07	1.26
	1.24	1.62	95.04	2.11
	1.28	1.81	95.49	1.42
	1.36	1.86	95.94	0.84
	1.31	1.52	95.98	1.19
	4.01	0.68	52.51	42.81
	1.76	1.48	44.59	52.18
	3.68	0.76	54.47	41.09
	3.75	0.66	53.47	42.13
	6.54	1.15	46.01	46.30
16/29-2				
2642.6m	1.30	8.39	89.59	0.72
	0.89	6.97	91.76	0.71
	1.31	7.84	90.05	0.79
	1.46	8.29	89.31	0.95
	1.18	9.51	88.49	0.82
2643.5m	0.56	4.93	94.10	0.40
	1.39	8.19	89.38	1.04
	0.68	0.61	98.24	0.47
	0.54	5.44	93.62	0.40
	1.06	5.62	93.06	0.27
2645.1m	0.92	6.61	91.80	0.68
	1.12	7.17	91.23	0.49
	0.65	5.15	93.76	0.45
	0.97	7.36	90.60	1.07
	0.83	7.24	90.68	0.72
2644.7m	0.16	6.67	92.25	0.10
	0.73	7.46	91.29	0.51

	0.40	8.00	91.35	0.26
	0.64	7.00	91.87	0.49
	0.69	7.24	91.66	0.42
2645.2m	0.78	6.68	91.70	0.84
	0.61	4.70	94.27	0.42
	0.44	5.03	93.66	0.88
	0.80	4.88	94.10	0.22
	0.65	6.96	91.65	0.75
2645.4m	1.06	7.00	90.86	1.08
	0.87	7.52	90.59	1.02
	0.63	6.48	92.15	0.74
	1.21	7.81	89.86	1.19
	0.51	6.84	92.08	0.58
2664.9m	0.68	5.08	93.80	0.44
	0.61	4.85	93.98	0.56
	0.79	4.19	93.52	0.67
	0.63	4.57	93.96	0.84
	0.81	3.61	95.57	0.01
2666.4m	0.87	6.89	91.46	0.77
	0.85	7.59	91.29	0.27
	0.92	5.51	92.86	0.70
	0.90	8.10	90.44	0.56
	0.76	5.90	92.62	0.61
	0.86	6.12	92.57	0.45
2666.9m	1.20	7.83	90.36	0.66
	1.11	8.42	89.60	0.87
	0.76	3.26	95.85	0.14
	0.47	2.52	96.06	0.95
	0.63	3.10	96.03	0.25
21/10-1				
2242.4m	4.57	1.55	92.65	1.24
	4.21	0.27	93.60	0.92
	4.36	0.06	93.38	1.19
	4.74	1.32	92.52	1.43
	4.12	1.37	93.19	1.32
2266.2m	4.49	1.23	92.78	1.50
	4.36	1.31	93.10	1.23
	4.56	1.46	92.67	1.31
	4.20	1.54	93.08	1.18
	3.46	0.80	94.62	1.12
22/17-4				
3107.1m	0.93	5.27	93.48	0.33
	0.81	4.91	93.68	0.61
	0.89	5.28	93.44	0.39
	1.31	4.99	93.03	0.67
	0.83	6.12	92.74	0.30
22/20-3				
2689.45m	1.94	4.91	92.57	0.57
	1.72	4.32	93.54	0.42

	2.13	1.18	96.55	0.14
	1.76	4.15	93.82	0.27
	1.75	4.91	92.77	0.57
2689.7m	1.95	6.47	90.81	0.77
	1.77	5.02	92.38	0.84
	1.33	4.60	93.45	0.63
	1.71	4.82	92.82	0.66
	2.16	6.41	91.36	0.07
23/16-4				
21155.9m	1.47	5.65	92.52	0.36
	1.53	6.18	91.37	0.92
	1.35	5.38	92.42	0.85
	1.83	5.14	91.67	1.36
	1.37	5.35	92.33	0.56
2156.6m	0.68	2.13	97.18	0.01
	1.91	6.39	90.78	0.92
	2.18	6.04	90.92	0.86
2202.3m	1.72	4.22	93.55	0.51
	1.77	4.07	93.50	0.73
	1.62	4.54	93.55	0.29
	1.39	3.91	94.71	0.00
	1.89	3.89	93.61	0.61
2310.2m	0.54	0.90	98.40	0.16
	1.73	1.59	95.85	0.83
	1.01	1.61	96.55	0.83
2310.4m	1.09	2.57	96.00	0.33
	1.41	1.11	97.48	0.00
	1.11	2.15	95.78	0.96
	0.65	0.43	98.91	0.00
	0.77	0.63	98.65	0.55
2310.6m	0.23	0.21	98.87	0.70
	0.30	0.30	99.26	0.15
	0.93	0.76	97.32	0.99
	0.69	0.53	97.38	1.23
	0.95	0.72	97.73	0.59
2316.5m	1.37	0.84	97.79	0.19
	0.93	0.57	97.30	1.20
	1.43	0.97	98.16	0.53
	0.94	0.46	97.51	1.09
	1.14	1.36	97.24	0.28

Table 2.4 Point count data of concretions

Well	Cored depth(m)	%carbonate	Well	Cored depth (m)	%carbonate
14/13-3	825.4	46.2	16/28-6	2721.25	39.8
	825.6	46.2		2681.55	47.6
	830.5	37.2		2681.66	49.8
	830.7	40.8		2682.00	51.0
	830.70	41		2682.25	36.8
15/20-4	2012.5	46	16/29-2	2666.66	42.6
15/26-3	1895.18	42.4		2667.00	35.2
	1878.25	42.6	21/10-1	2242.4	30.0
15/26-4	2213.56	67.0	23/16-4	2155.98	35.6
	2221.700	46.4		2156.51	37.2

Table 2.5 Carbon and oxygen composition of concretions

Well	Sample Cored depth (m)	δ^{13}CPDB	δ^{18}OPDB	δ^{18}OSMOW
14/13-3	825.43	-13.5	2.6	28.2
	825.44	-13.6	-3.2	27.6
	825.45	-14.2	-3.1	27.7
	825.58	-4.0	-7.7	23.0
	825.59	-4.0	-7.3	23.4
	830.35	-9.9	-5.6	25.2
	830.36	-8.7	-5.3	25.4
	830.37	-7.5	-6.2	24.5
	830.38	-3.7	-4.2	26.6
	830.31	-3.2	-4.3	26.5
vein	830.32	-3.4	-4.4	26.3
	830.33	-5.1	-4.6	26.2
	830.70	-5.5	-6.7	24.0
	830.71	-9.0	-5.5	25.3
	830.72	-10.5	-5.7	25.0
	830.73	-9.3	-5.2	25.6
	830.82	-10.8	-4.9	25.8
	830.83	-9.8	-4.5	26.3
	830.84	-8.3	-5.4	25.3
	830.85	-5.6	-7.3	23.4
15/20-4	2012.5	-29.0	-10.5	20.5
	2012.5	-26.7	-10.5	20.5
	2012.5	-26.0	-10.4	20.2
	2012.5	-25.2	-10.6	20.0
	2012.6	-24.1	-10.4	20.2
	2012.6	-23.3	-10.3	20.3
15/26-3				
ankerite	1874.3	12.7	-10.3	20.3
ankerite	1875.2	-18.9	-9.5	21.2
ankerite	1877.9	10.3	-7.9	22.8
ankerite	1878.0	11.0	-8.0	22.7
ankerite	1878.3	9.8	-7.9	22.8
	1894.5	12.6	-10.3	20.3
	1894.8	13.5	-10.2	20.4
	1925.9	-6.7	-12.5	18.0
	1929.8	-1.3	-5.9	24.8

15/26-4	2272.9	-18.5	-9.2	21.4
	2274.0	11.1	-9.8	20.9
	2274.3	11.0	-8.0	22.7
	2274.5	11.7	-9.7	20.9
	2274.6	11.5	-9.4	21.2
	2274.7	11.0	-9.7	20.9
	2467.7	0.4	-1.5	29.4
	2468.5	-1.8	-12.6	17.9
	2469.9	-3.6	-15.3	15.2
	2469.9	2.6	-2.7	28.2
	2300.3	-14.0	0.6	31.6
	2300.5	9.0	-9.7	21.0
16/28-6	2681.5	-24.8	-8.5	22.2
	2681.6	-21.9	-8.9	21.7
	2681.7	-20.3	-9.3	21.3
	2682.0	-17.3	-10.6	20.0
	2682.3	-17.0	-10.7	20.0
	2683.0	-18.7	-11.7	18.8
	2683.3	-22.5	-9.0	21.1
16/29-2	2638.0	-4.1	-11.1	23.6
	2638.0	-5.0	-12.5	18.0
	2642.6	-5.4	-12.5	18.1
	2643.5	2.7	-7.1	18.0
	2643.8	-2.3	-12.5	18.5
	2664.9	-1.1	-12.3	18.0
	2666.9	-3.2	-12.5	17.9
	2666.9	-2.9	-12.1	19.5
	2666.9	-3.2	-12.4	18.3
	2666.9	-2.7	-11.4	18.0
vein	2682.8	-0.7	-13.1	17.5
	2683.5	-0.4	-12.6	18.2
	2683.5	-0.7	-12.5	18.0
21/10-1	2155.7	-0.4	-6.3	24.4
siderite	2156.8	2.3	-3.8	27.0
siderite	2156.8	1.7	-3.9	26.9
siderite	2156.8	1.8	-4.6	26.2
siderite	2156.8	-0.5	-3.7	27.1
	2170.2	0.1	-8.6	22.1
	2242.4	-7.4	-11.4	19.2
	2242.4	-15.9	-11.0	19.6
chalk	2242.7	-10.6	-10.6	20.0
22/17-4	3106.8	-11.1	-11.0	19.2
	3107.4	-10.7	-11.2	19.4
	3107.7	-3.7	-10.8	19.8
	3108.0			
22/20-3	2689.4	-4.3	-7.7	23.0
	2689.7	-4.7	-8.0	22.6
23/16-4	2150.2	-2.9	-18.8	11.5
	2156.4	-0.1	-13.0	17.5
	2156.5	-0.3	-12.6	17.9
	2156.8	0.8	-12.9	17.63
	2162.3	-6.3	-9.6	21.1

Table 2.6 Sr data C=centre of concretion, R=rim of concretion

Well	depth (m)	Rb (ppm)	Sr (ppm)	$^{87}Rb/^{86}Sr$	$^{87}Sr/^{86}Sr$	2σ	$(^{87}Sr/^{86}Sr)_{45}$	$\delta^{13}C_{PDB}$	$\delta^{18}O_{SMOW}$
14/13–3	830.5	0.02	1044.5	–	0.70763	2	0.70763	–5.59	23.41
15/20–4	2012.6C	0.85	640.60	0.0038	0.70774	3	0.70774	–23.31	20.26
15/20–4	2012.6R	0.97	868.50	0.0032	0.70789	4	0.70789	–29.03	19.70
15/26–3	1894.8	0.02	663.03	–	0.70790	4	0.70790	13.48	20.41
15/26–4	2469.9	0.02	777.25	–	0.70771	5	0.70771	2.60	28.15
16/28–6	2681.5R	26.51	470.40	0.1634	0.70778	4	0.70768	–24.83	22.15
16/28–6	2682.0C	125.60	1063.0	0.3419	0.70772	4	0.70750	–20.32	20.0
16/28–6	2682.3C	5.73	1183.0	0.0140	0.70774	4	0.70773	–16.99	19.99
16/28–6	2683.2R	1.60	510.00	0.0091	0.70777	4	0.70776	–22.45	21.05
16/29–2	2642.6	0.02	979.81	–	0.70773	4	0.70773	–5.24	18.02
16/29–2	2666.9	0.02	712.72	–	0.70780	4	0.70780	–2.89	18.46
21/10–1	2242.7	0.01	423.48	–	0.70813	3	0.70813	–10.57	19.99
22/17–4	3107.4	11.440	1028.0	0.03216	0.70862	4	0.70860	–10.71	19.50
22/20–3	2689.7	25.63	596.16	0.12442	0.70883	3	0.70875	–4.27	22.63
23/16–4	2156.7	23.11	841.10	0.07951	0.70798	4	0.70793	0.81	17.63
23/16–4	2166.5	34.91	92.710	0.11190	0.70895	4	0.70888	–8.23	20.88
23/16–4	2310.4	22.300	313.78	0.20569	0.70977	3	0.70964	–0.43	20.29

$(^{87}Sr/^{86}Sr)_{45}$ ratios are modern day $^{87}Sr/^{86}Sr$ ratios corrected to 45Ma

	2166.5	-8.2	-9.7	20.9
	2202.9	-5.1	-8.9	21.7
	2263.5	-3.7	-9.7	21.0
	2263.6	-4.0	-9.9	20.7
	2263.6	-3.1	-8.9	21.8
	2310.4	-0.4	-10.3	20.3
	2310.3	-1.3	-9.2	21.4
	2316.5	0.6	-12.4	18.2
vein	2316.6	0.9	-12.4	18.1
	2369.4	1.8	-6.3	24.5

Table 6b $^{87}Sr/^{86}Sr$ ratios of detrital feldspar equivalent.

Sample	Rb	Sr	87Rb/86Sr	87Sr/86Sr	87Sr/86Sr)45
Halliday et al. (1979)					
1282kf	149.50	348.5	1.2420	0.71362	0.71283
1282pl	25.15	309.5	0.2351	0.70738	0.70723
722kf	222.00	263.2	2.4470	0.73353	0.73197
061kf	213.80	1238.0	0.4997	0.70800	0.70768
DBL3kf	163.50	942.2	0.5021	0.70805	0.70773
HH4kf	395.20	290.7	3.9410	0.72880	0.72628
244kf	222.70	1109.0	0.5909	0.70863	0.70825
056Gkf	250.80	416.1	1.7450	0.71587	0.71475
8478kf	294.60	437.0	1.9520	0.71699	0.71574
57/73kf	450.10	226.1	5.7790	0.73985	0.73616
Haughton et al. (1990)					
3134kf	340.50	146.7	6.7490	0.76008	0.75577
3152kf	309.30	322.9	2.7800	0.73089	0.72911
3158kf	169.00	431.2	1.1350	0.71750	0.71677
3503kf	248.10	240.4	2.9940	0.73549	0.73358
3309kf	251.90	440.8	1.6550	0.71584	0.71478
3304pl	30.30	934.4	0.0937	0.70663	0.70657
3304kf	239.80	314.5	2.2080	0.71837	0.71696

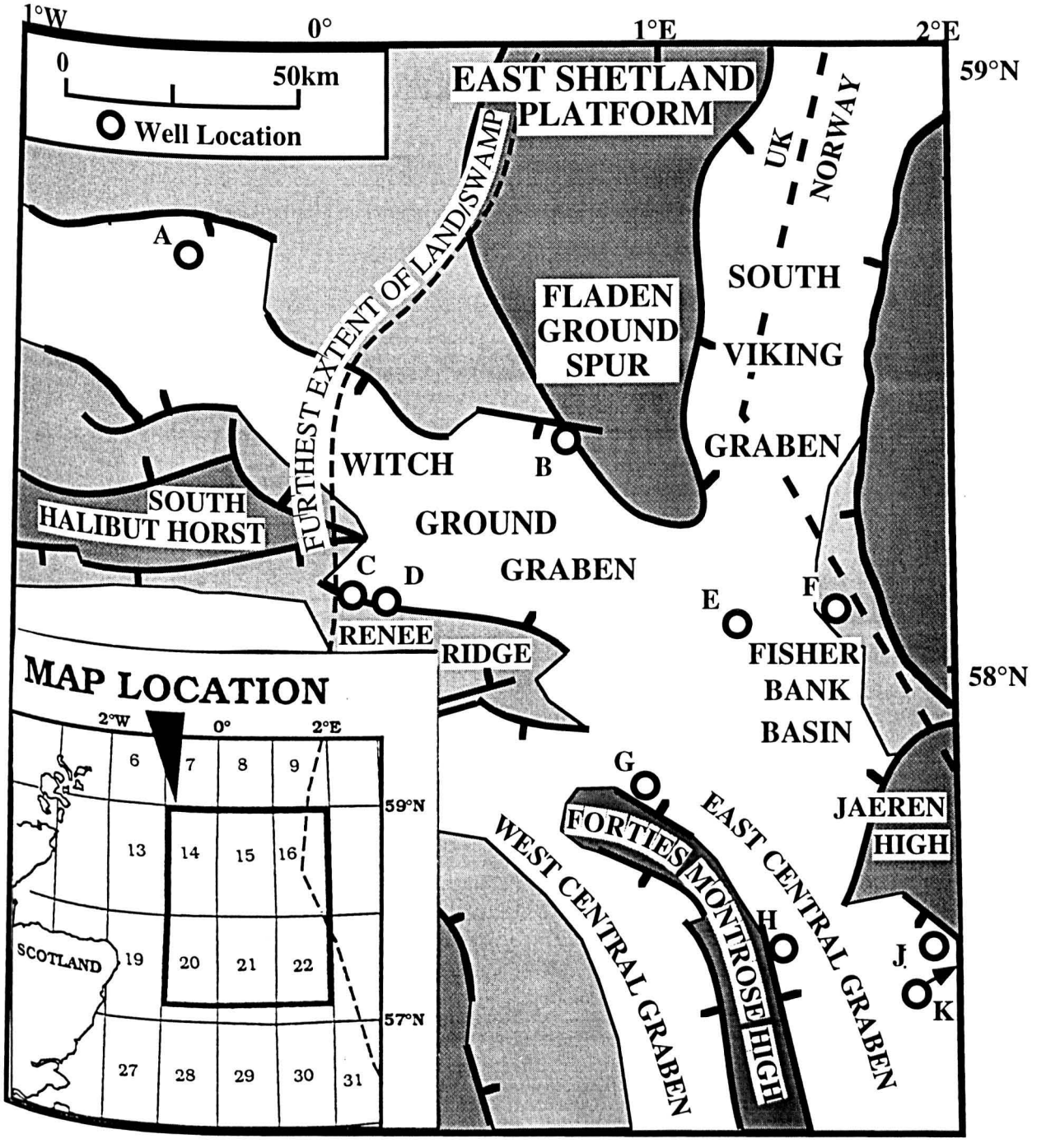

A - 14/13-3	F - 16/29-2
B - 15/20-4	G - 21/10-1
C - 15/26-3	H - 22/17-4
D - 15/26-4	J - 22/20-3
E - 16/28-6	K - 23/16-4

Figure 2.1

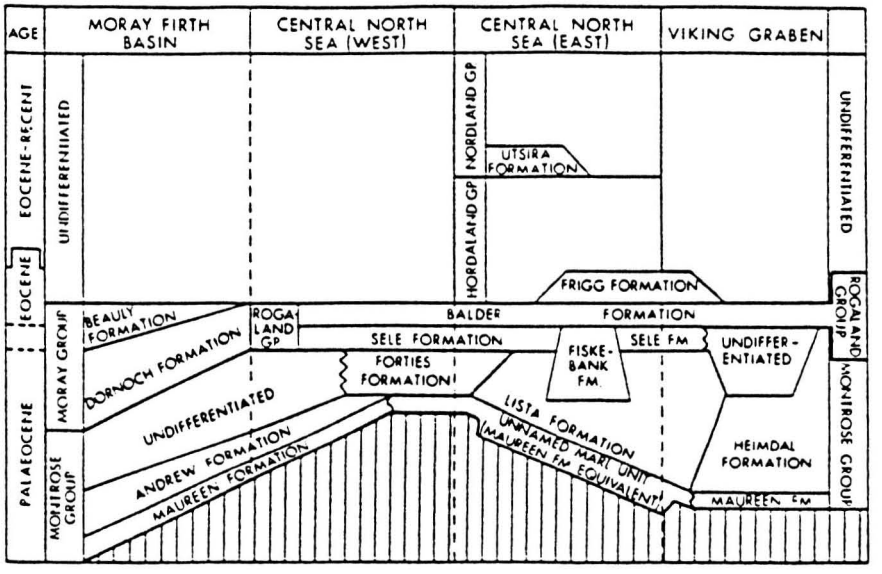
AGE
MORAY FIRTH BASIN
CENTRAL NORTH SEA (WEST)
CENTRAL NORTH SEA (EAST)
VIKING GRABEN
EOCENE-RECENT
UNDIFFERENTIATED
EOCENE
PALAEOCENE
MORAY GROUP
MONTROSE GROUP
BEAULY FORMATION
DORNOCH FORMATION
UNDIFFERENTIATED
ANDREW FORMATION
MAUREEN FORMATION
ROGALAND GP
HORDALAND GP
UTSIRA FORMATION
FRIGG FORMATION
BALDER FORMATION
SELE FORMATION
FORTIES FORMATION
FISKEBANK FM.
SELE FM
UNDIFFERENTIATED
LISTA FORMATION
UNNAMED MARL UNIT (MAUREEN FM EQUIVALENT)
HEIMDAL FORMATION
MAUREEN FM
ROGALAND GROUP
MONTROSE GROUP

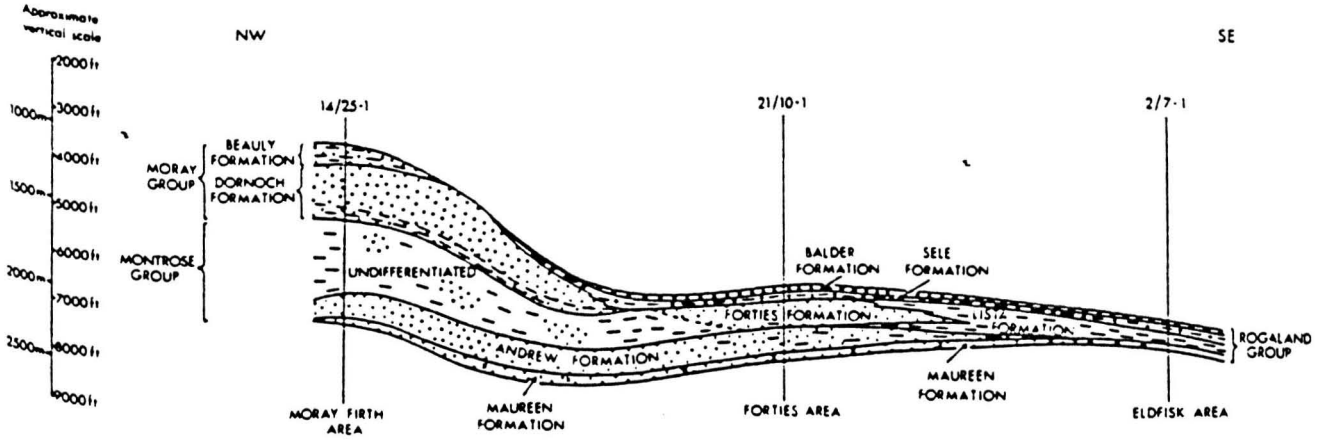
Approximate vertical scale
2000 ft
1000m
3000 ft
4000 ft
1500m
5000 ft
6000 ft
2000m
7000 ft
2500m
8000 ft
9000 ft
NW
SE
14/25-1
21/10-1
2/7-1
MORAY GROUP
BEAULY FORMATION
DORNOCH FORMATION
MONTROSE GROUP
UNDIFFERENTIATED
ANDREW FORMATION
MAUREEN FORMATION
BALDER FORMATION
SELE FORMATION
FORTIES FORMATION
LISTA FORMATION
ROGALAND GROUP
MAUREEN FORMATION
MORAY FIRTH AREA
MAUREEN FORMATION
FORTIES AREA
ELDFISK AREA

Figure 2.2

Figure 2.3

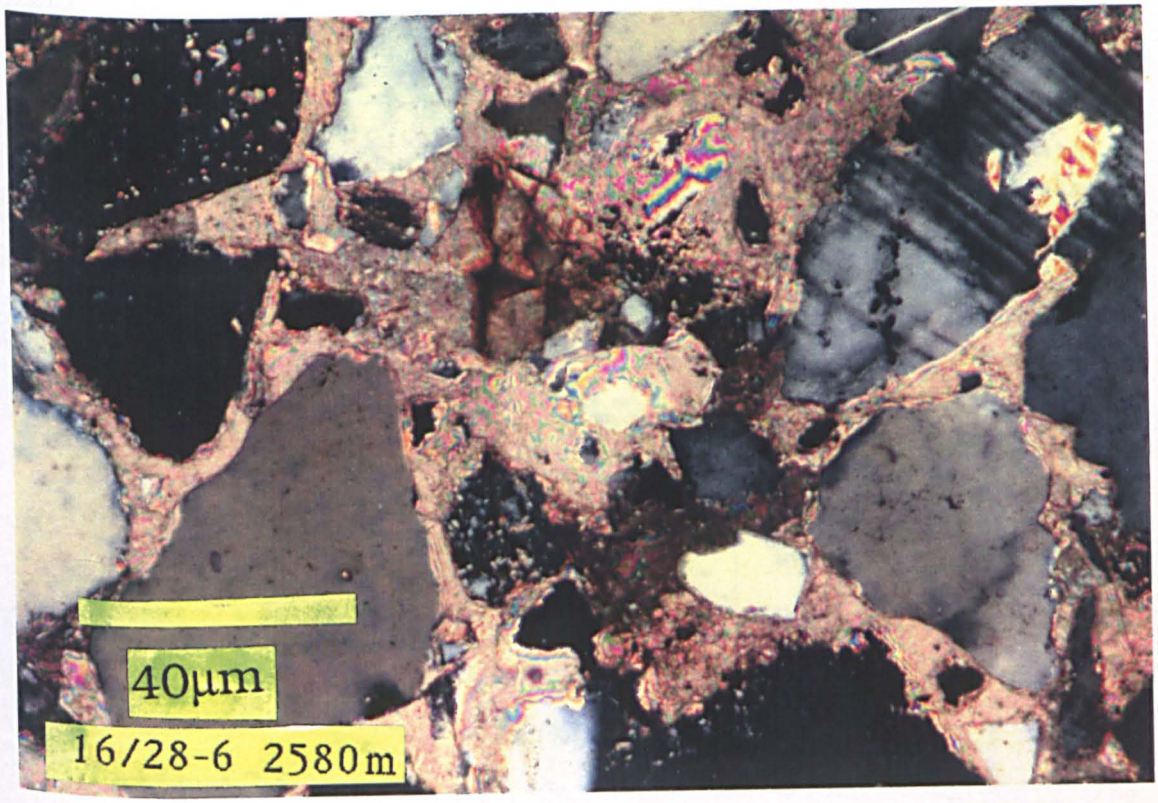

Figure 2.4

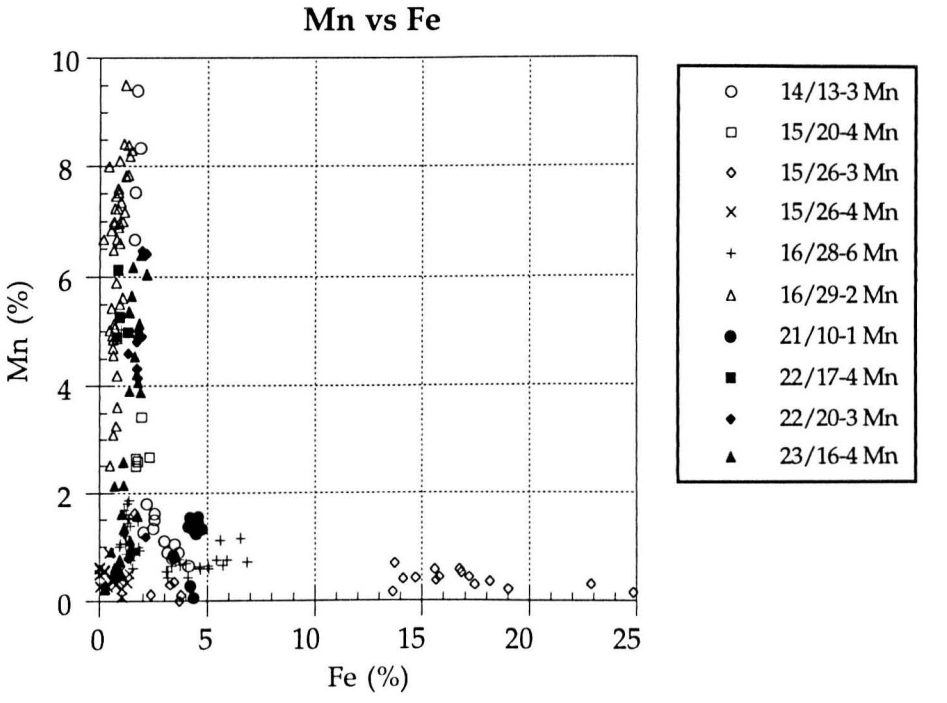
Mn vs Fe
Mn (%)
Fe (%)
0
2
4
6
8
10
0
5
10
15
20
25
14/13-3 Mn
15/20-4 Mn
15/26-3 Mn
15/26-4 Mn
16/28-6 Mn
16/29-2 Mn
21/10-1 Mn
22/17-4 Mn
22/20-3 Mn
23/16-4 Mn

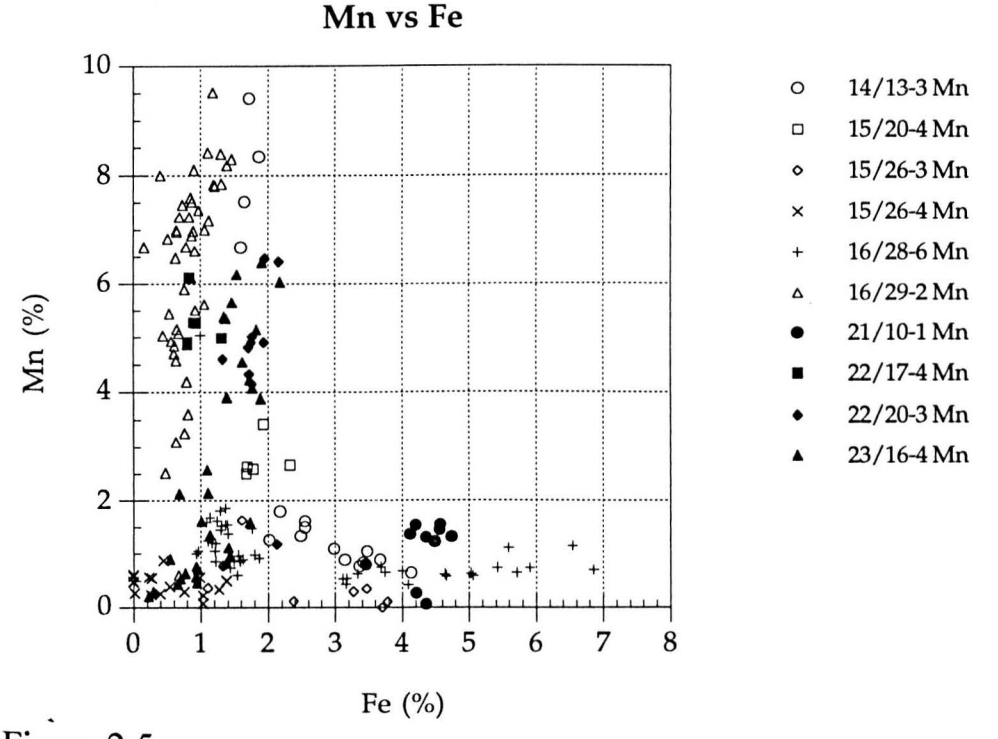
Mn vs Fe
Mn (%)
Fe (%)
0
2
4
6
8
10
0
1
2
3
4
5
6
7
8
14/13-3 Mn
15/20-4 Mn
15/26-3 Mn
15/26-4 Mn
16/28-6 Mn
16/29-2 Mn
21/10-1 Mn
22/17-4 Mn
22/20-3 Mn
23/16-4 Mn

Figure 2.5

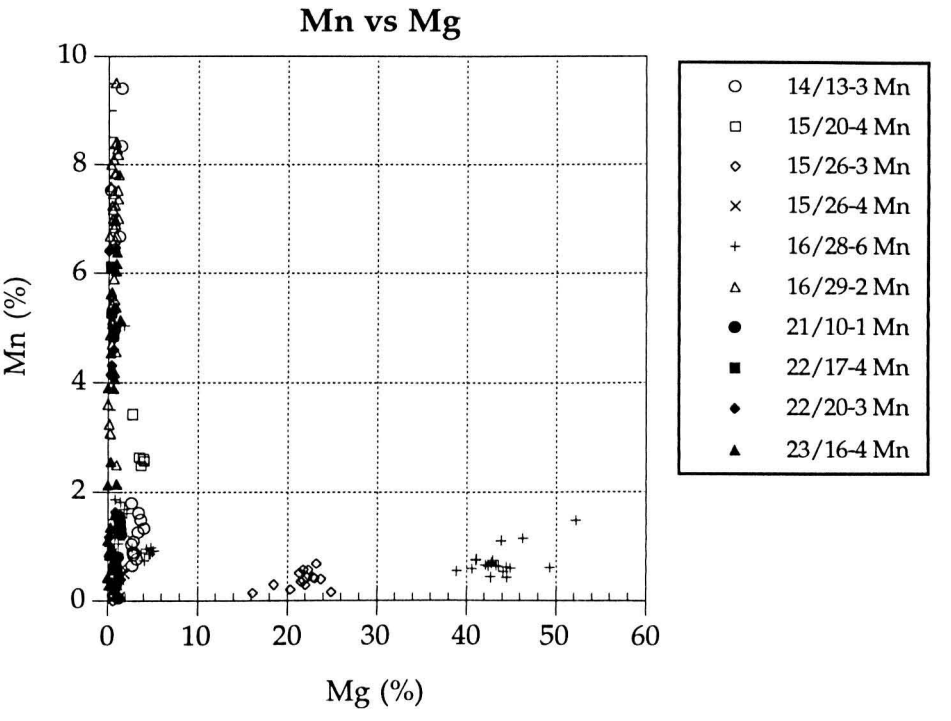
Mn vs Mg
Mn (%)
Mg (%)
0
2
4
6
8
10
0
10
20
30
40
50
60
14/13-3 Mn
15/20-4 Mn
15/26-3 Mn
15/26-4 Mn
16/28-6 Mn
16/29-2 Mn
21/10-1 Mn
22/17-4 Mn
22/20-3 Mn
23/16-4 Mn

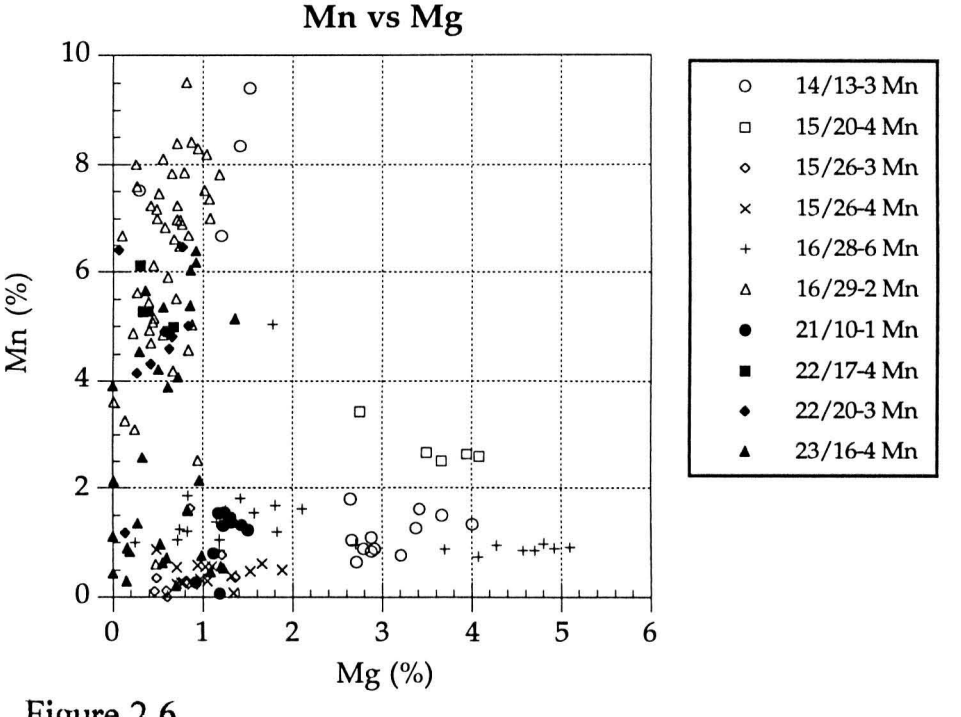
Mn vs Mg
Mn (%)
Mg (%)
0
2
4
6
8
10
0
1
2
3
4
5
6
14/13-3 Mn
15/20-4 Mn
15/26-3 Mn
15/26-4 Mn
16/28-6 Mn
16/29-2 Mn
21/10-1 Mn
22/17-4 Mn
22/20-3 Mn
23/16-4 Mn

Figure 2.6

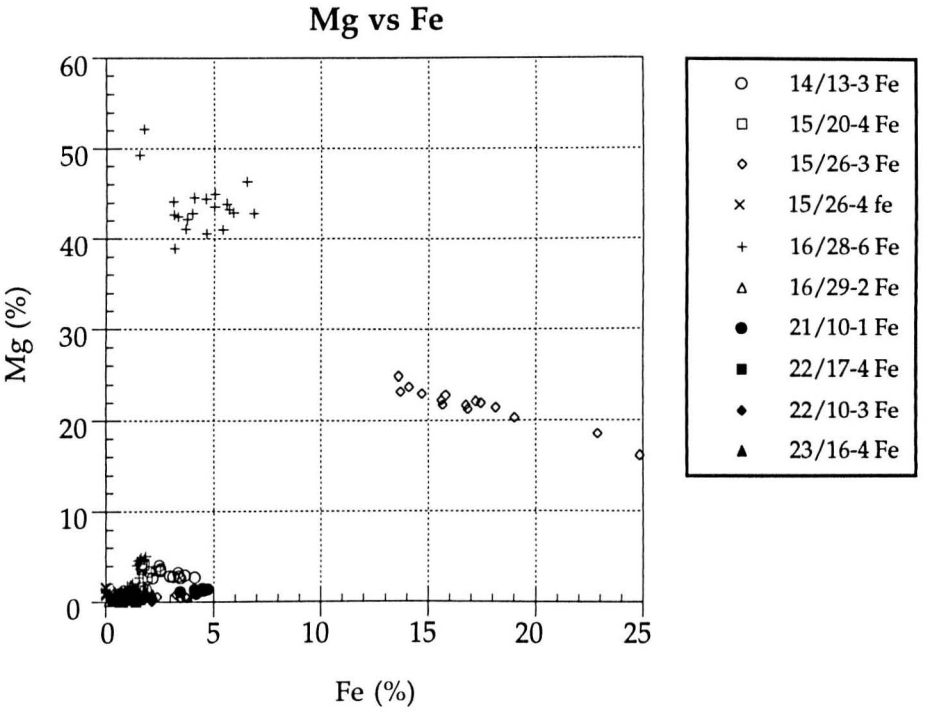
Mg vs Fe
Mg (%)
Fe (%)
0
10
20
30
40
50
60
0
5
10
15
20
25
14/13-3 Fe
15/20-4 Fe
15/26-3 Fe
15/26-4 fe
16/28-6 Fe
16/29-2 Fe
21/10-1 Fe
22/17-4 Fe
22/10-3 Fe
23/16-4 Fe

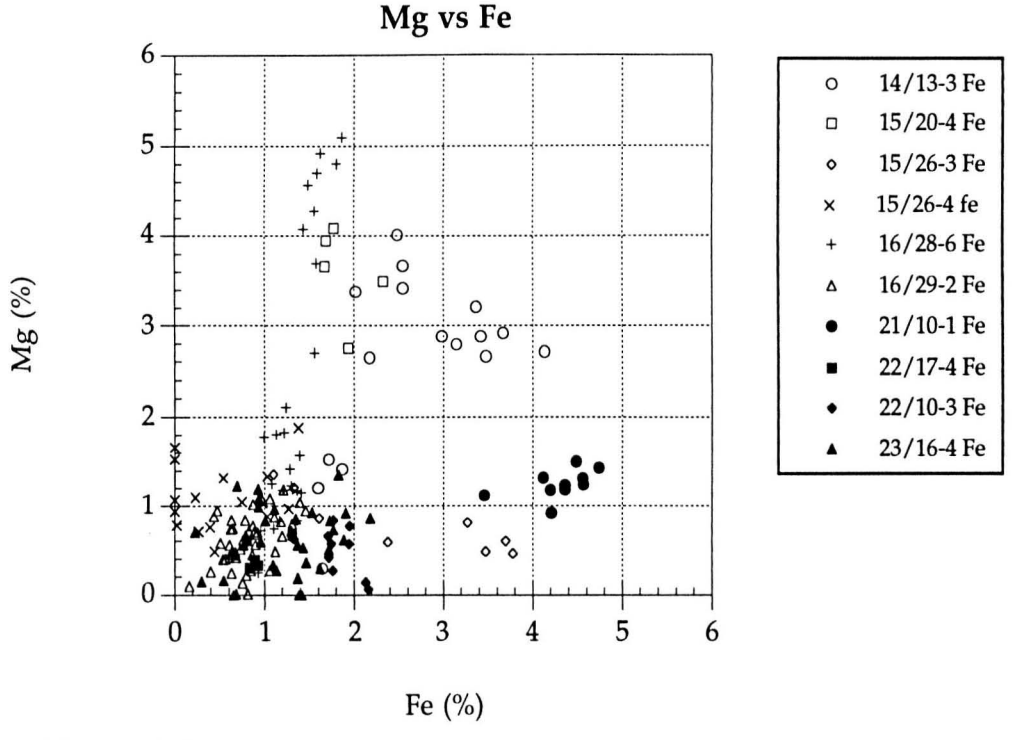
Mg vs Fe
Mg (%)
Fe (%)
0
1
2
3
4
5
6
14/13-3 Fe
15/20-4 Fe
15/26-3 Fe
15/26-4 fe
16/28-6 Fe
16/29-2 Fe
21/10-1 Fe
22/17-4 Fe
22/10-3 Fe
23/16-4 Fe

Figure 2.7

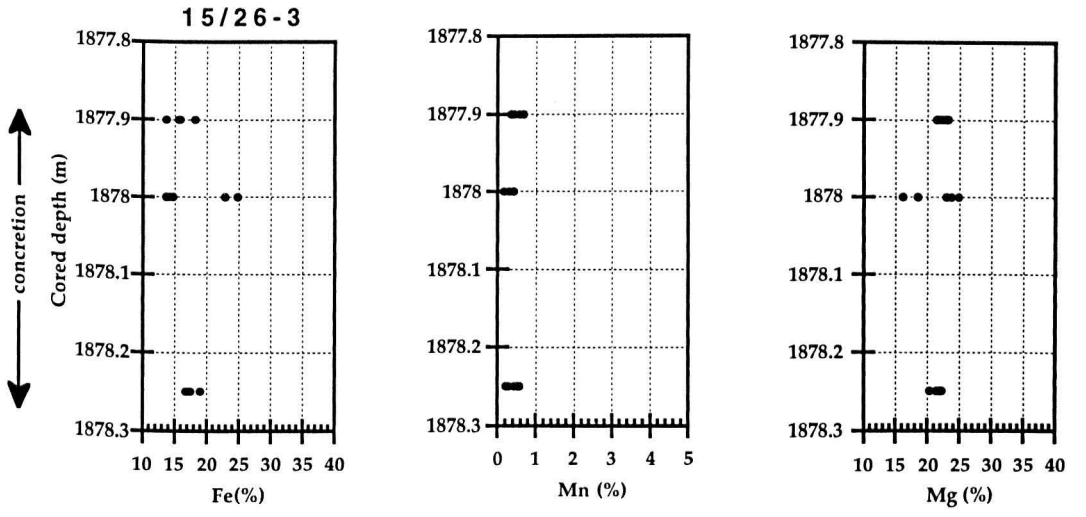

Figure 2.8a

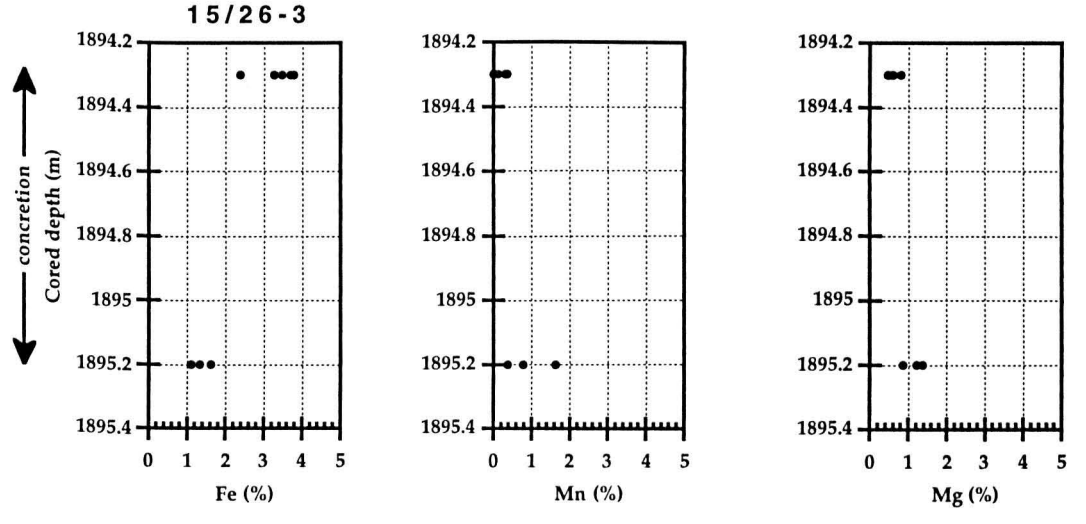

Figure 2.8b

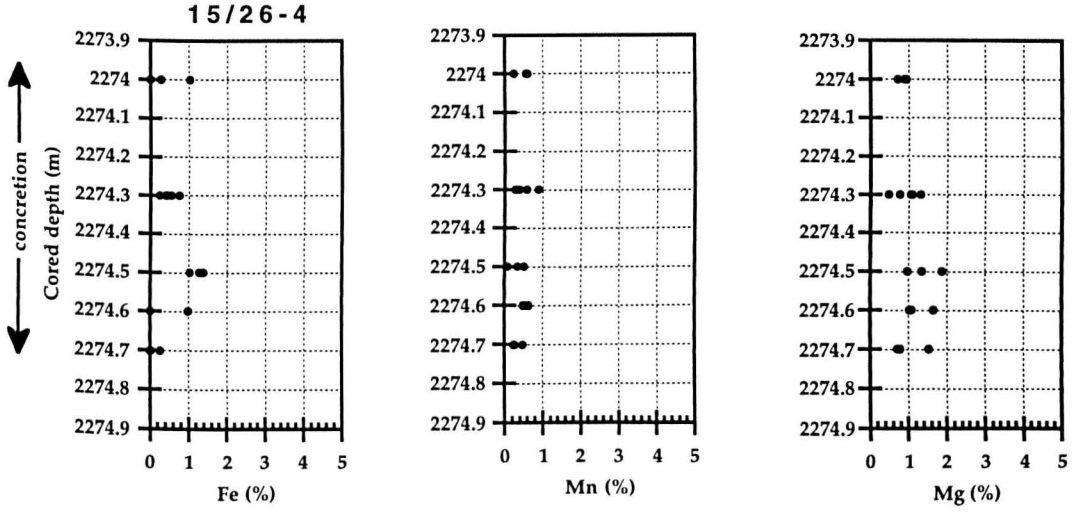

Figure 2.8c

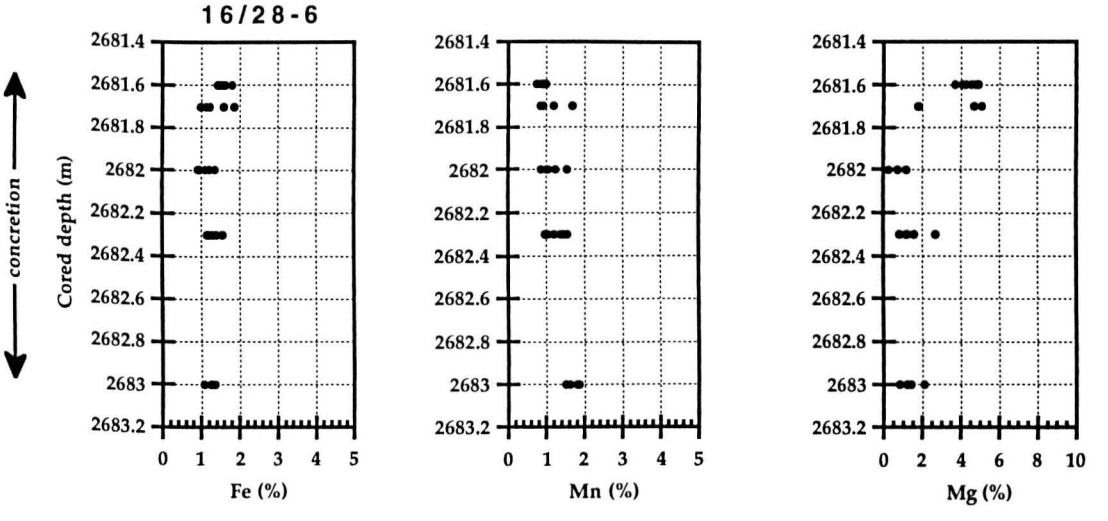

Figure 2.8d

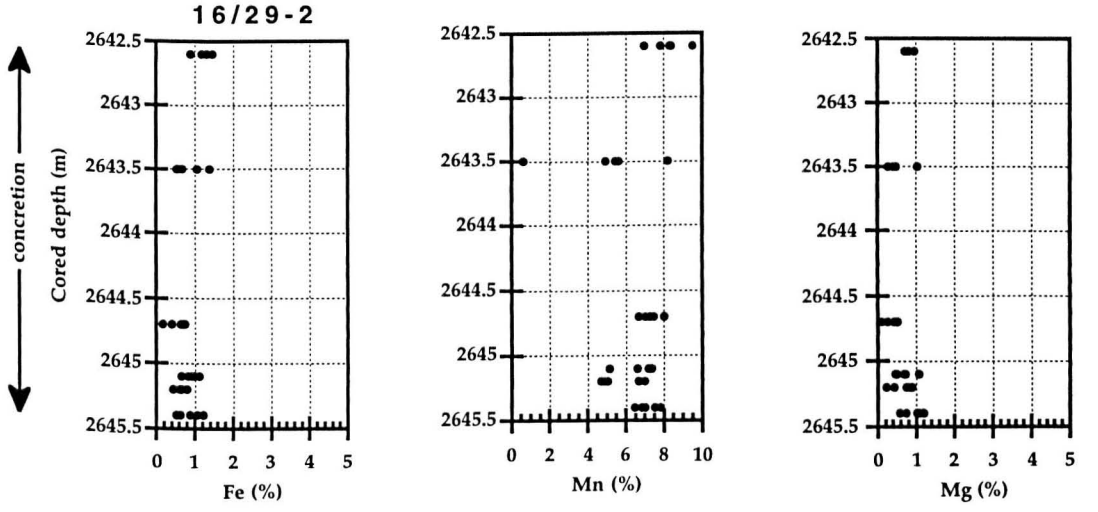

Figure 2.8e

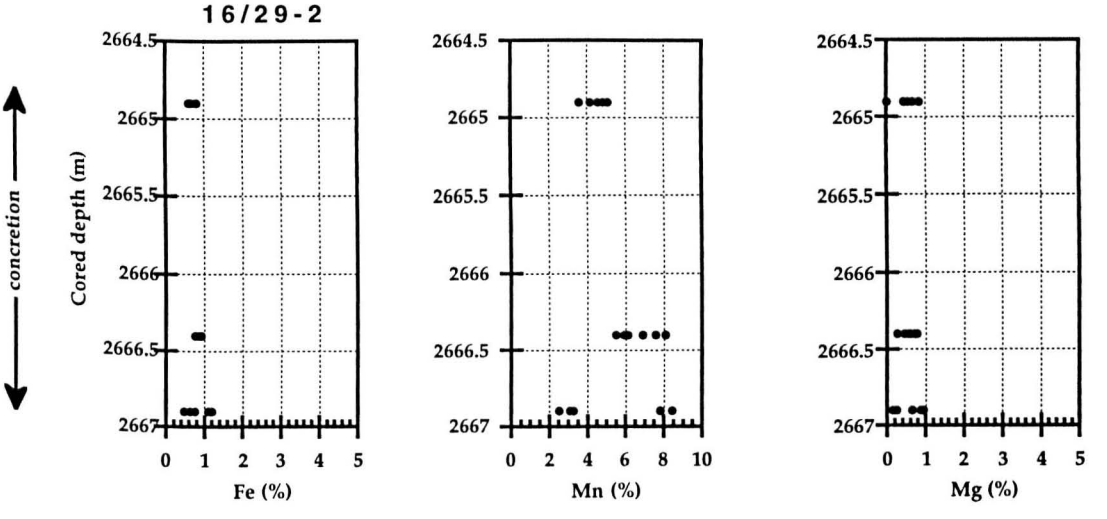

Figure 2.8f

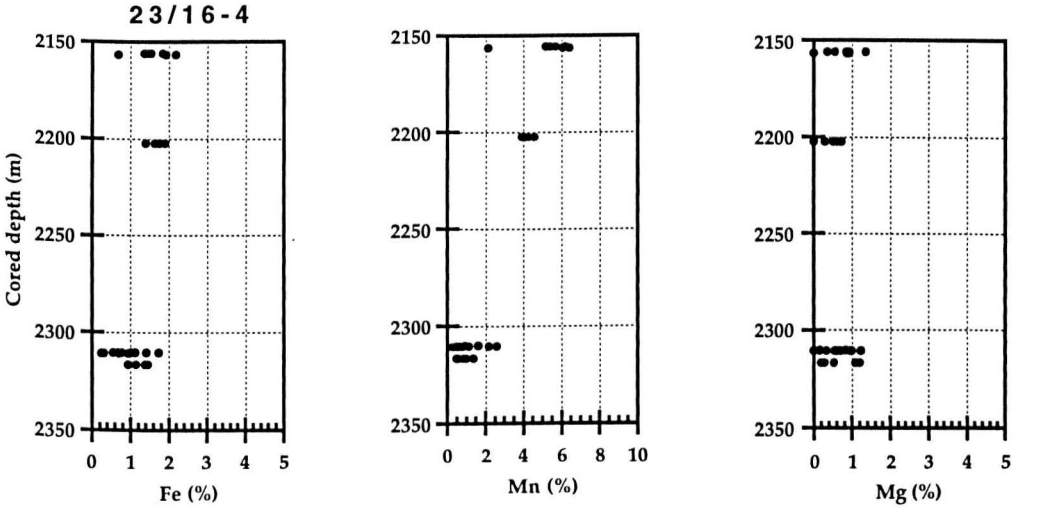

Figure 2.8g

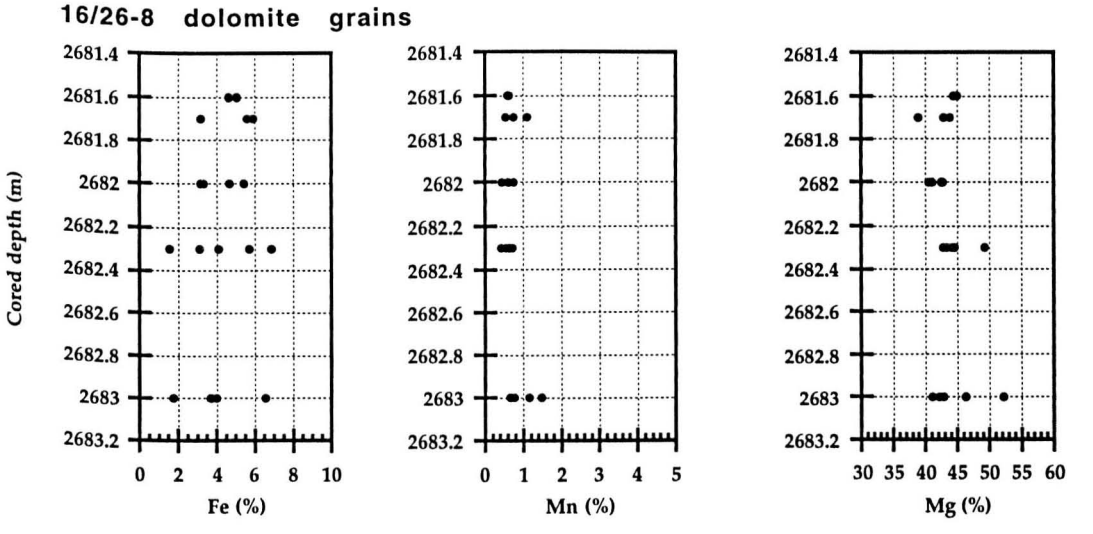

Figure 2.8h

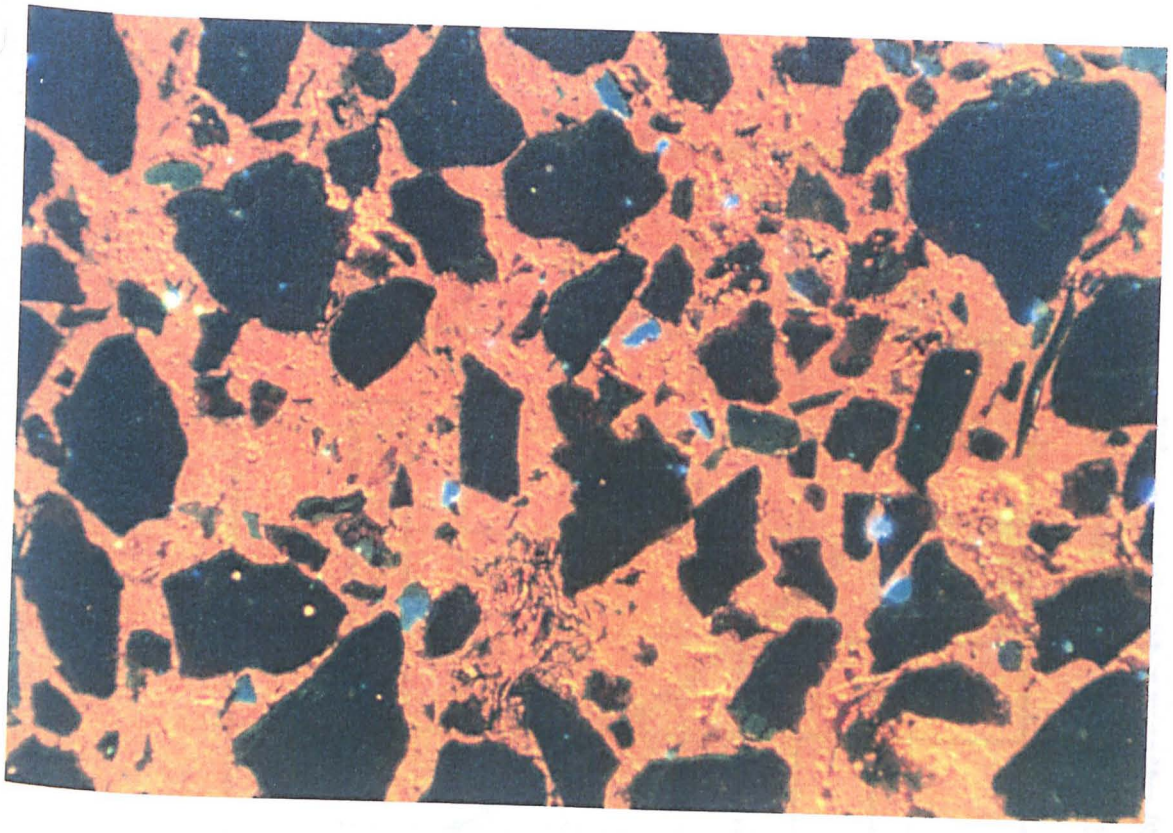

Figure 2.9

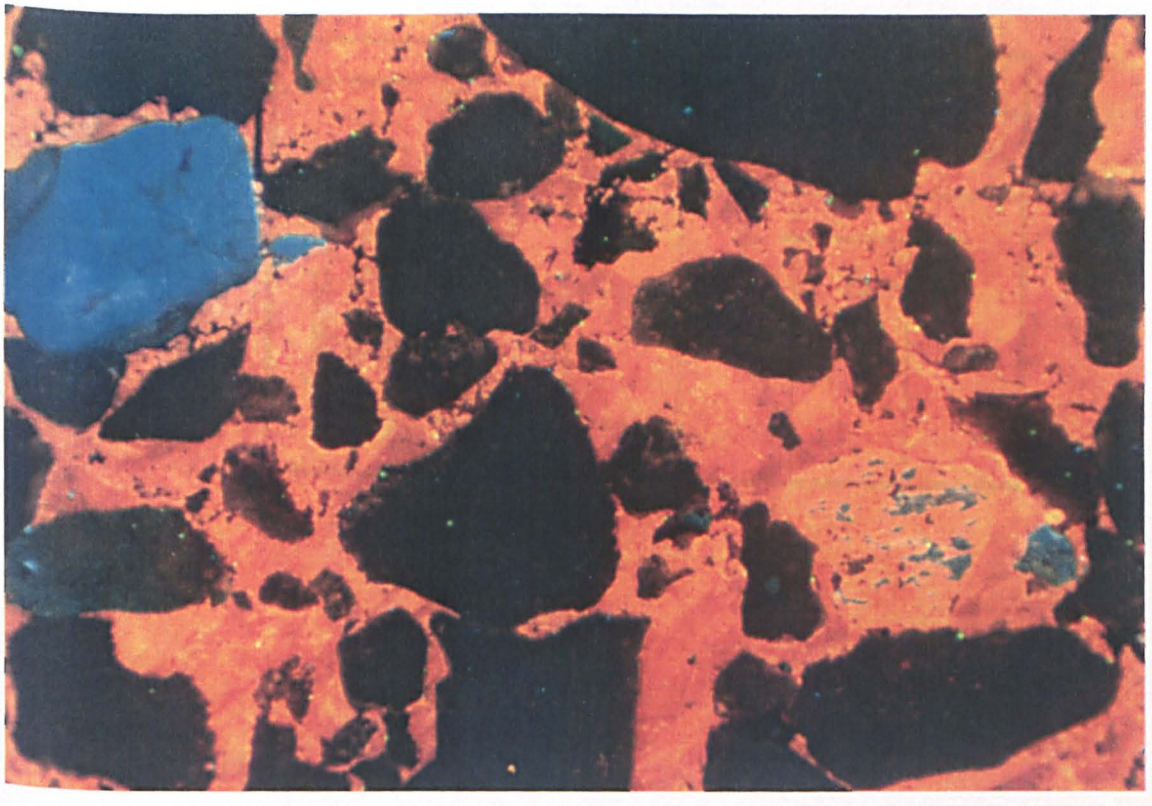

Figure 2.10

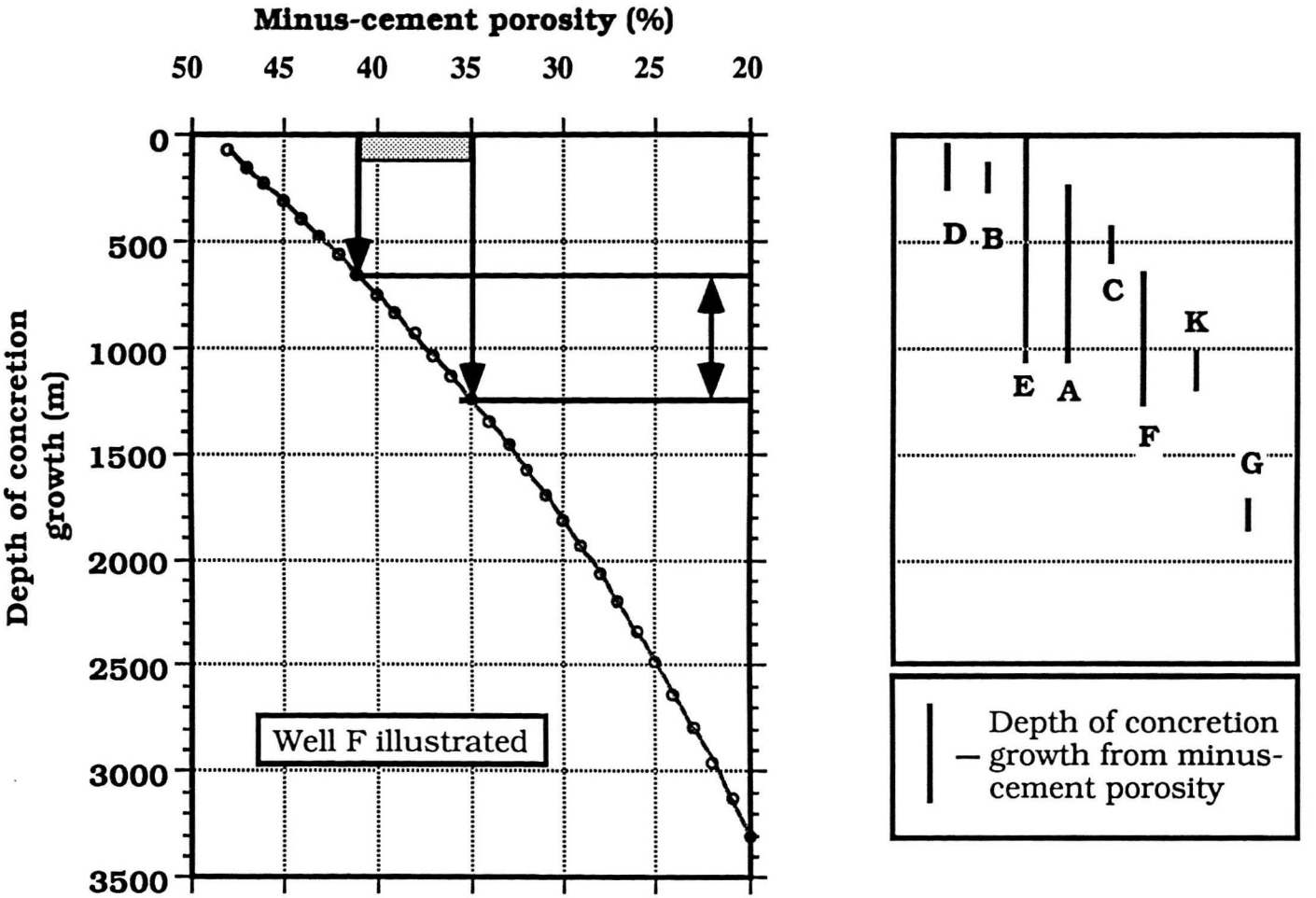
Minus-cement porosity (%)
50
45
40
35
30
25
20
0
500
1000
1500
2000
2500
3000
3500
Depth of concretion growth (m)
Well F illustrated
D
B
C
K
E
A
F
G
Depth of concretion growth from minus-cement porosity

Figure 2.11

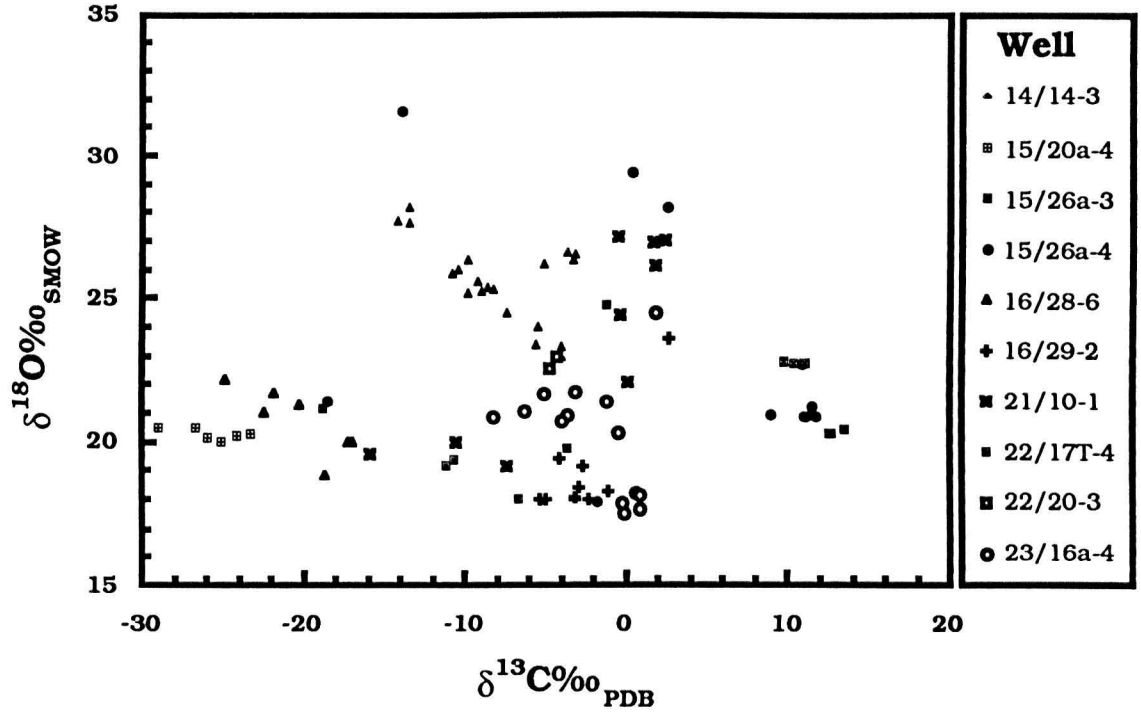

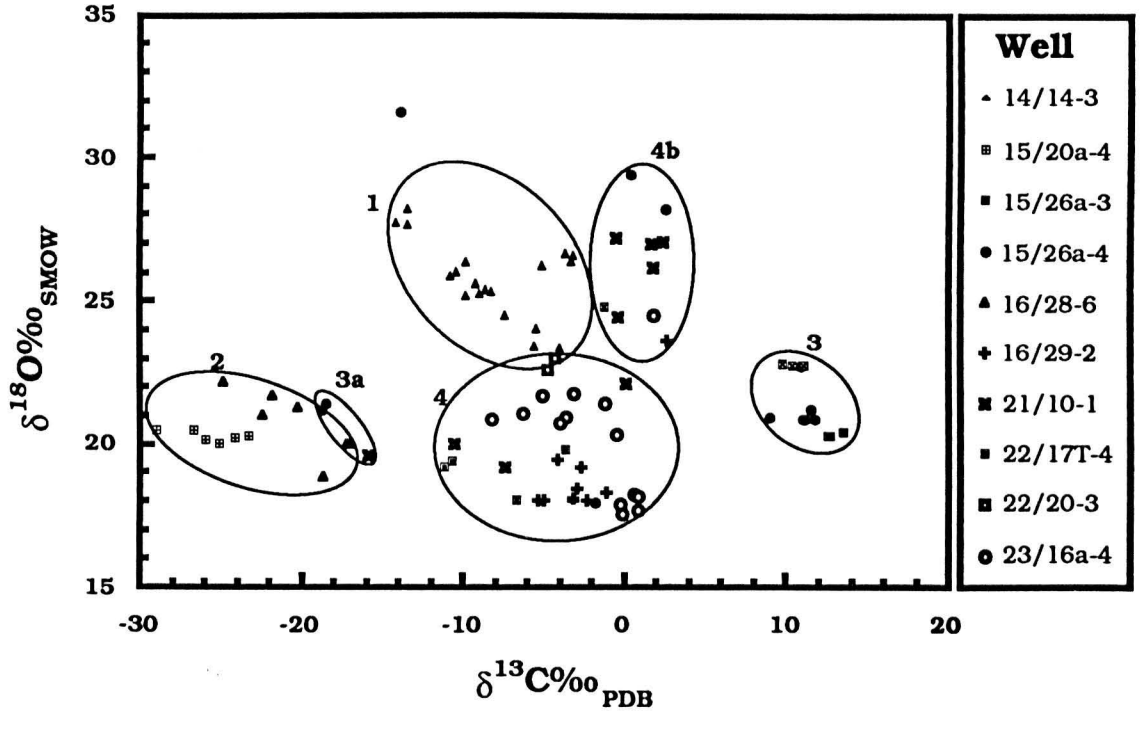

Figure 2.12a,b

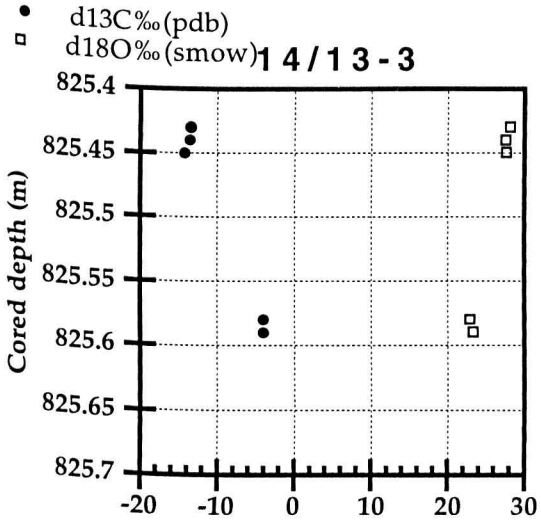

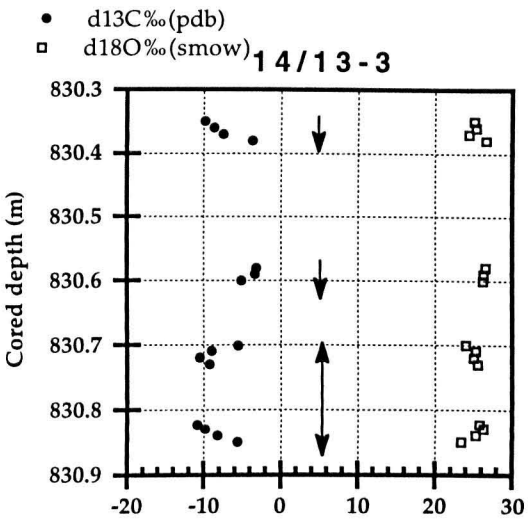

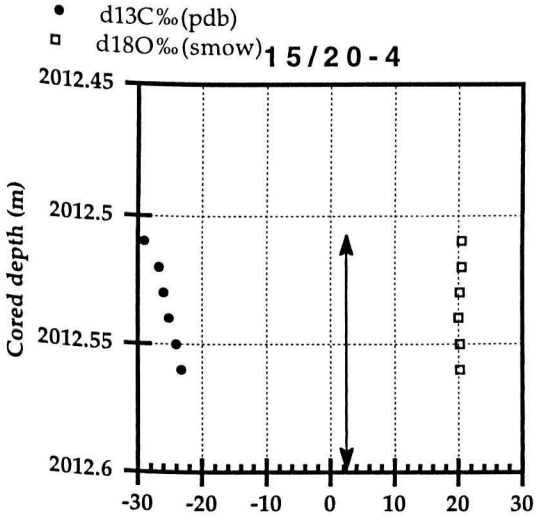

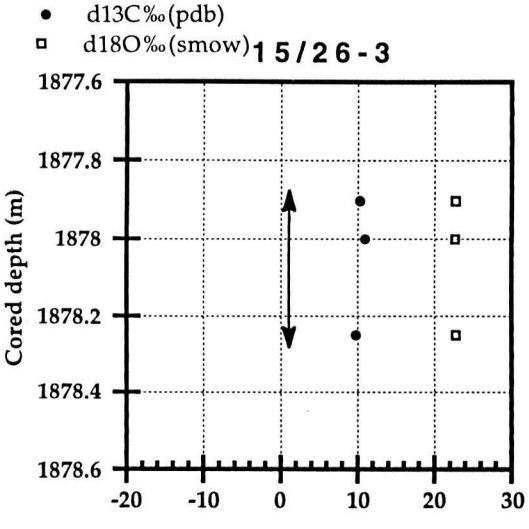

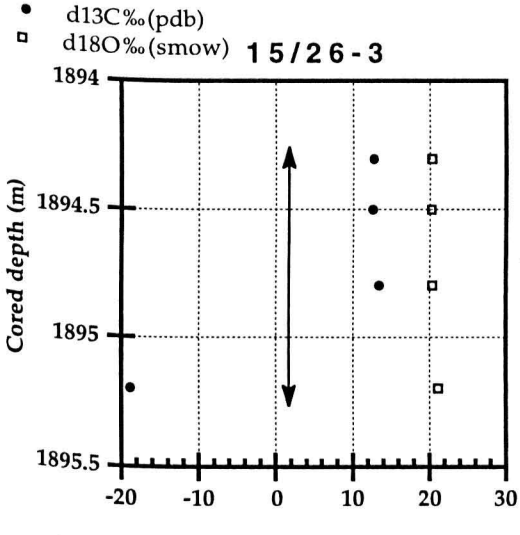

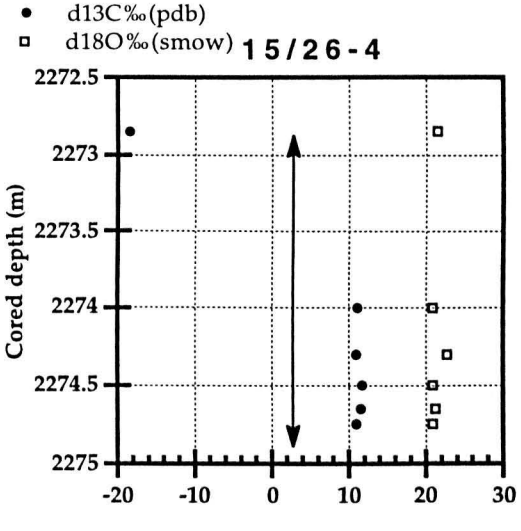

Figure 2.13a-f

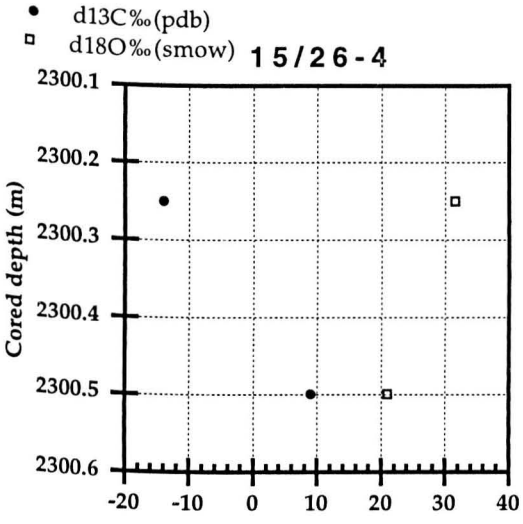

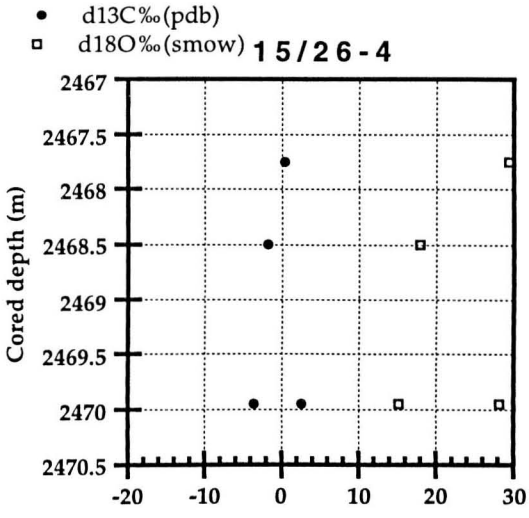

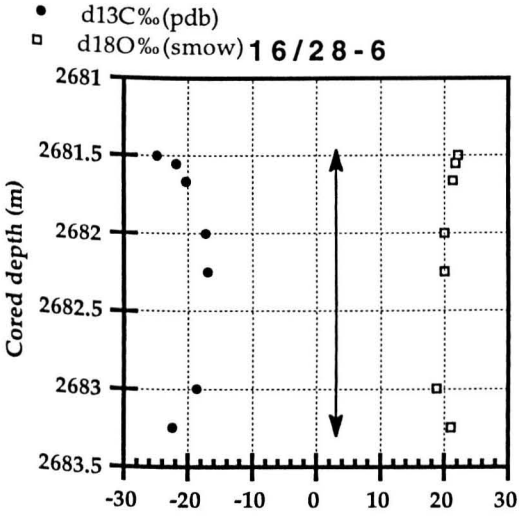

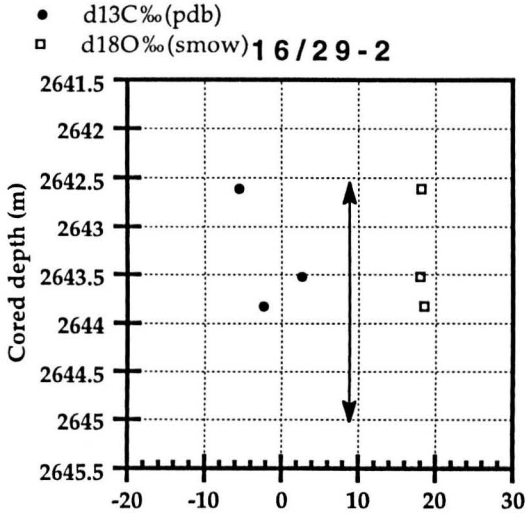

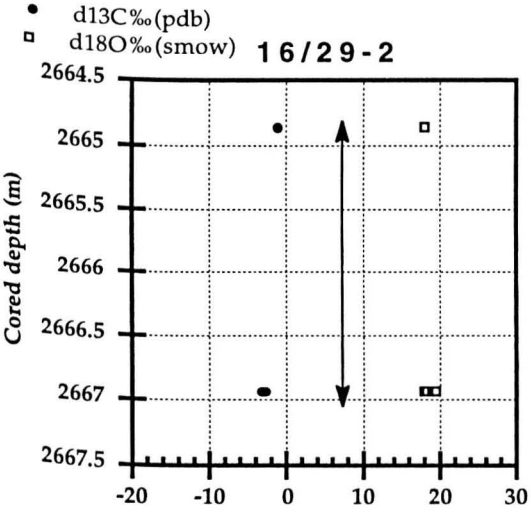

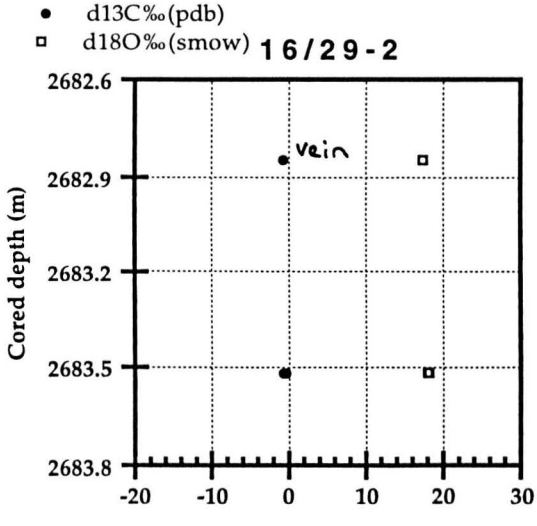

Figure 2.13g-1

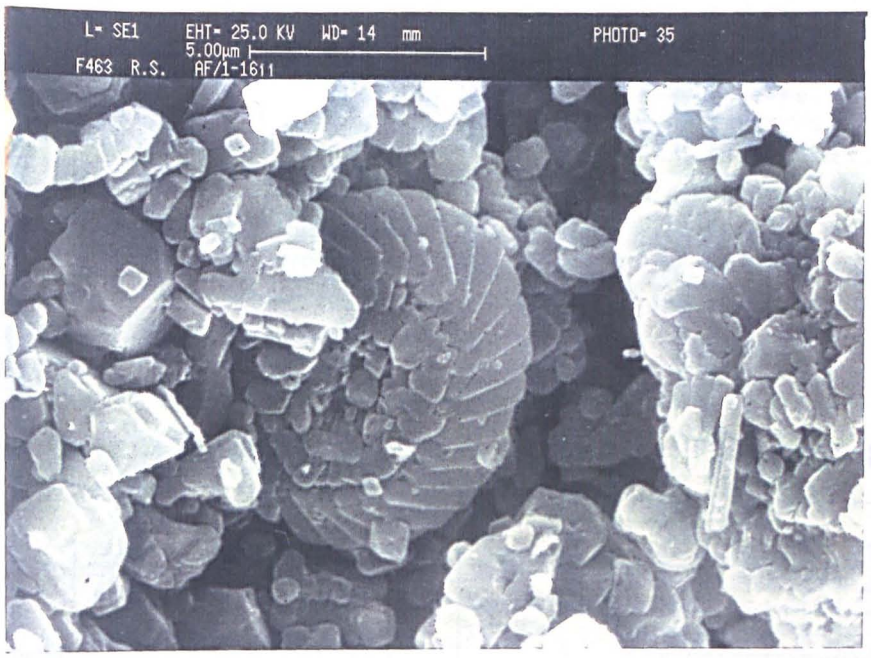

Figure 2.14

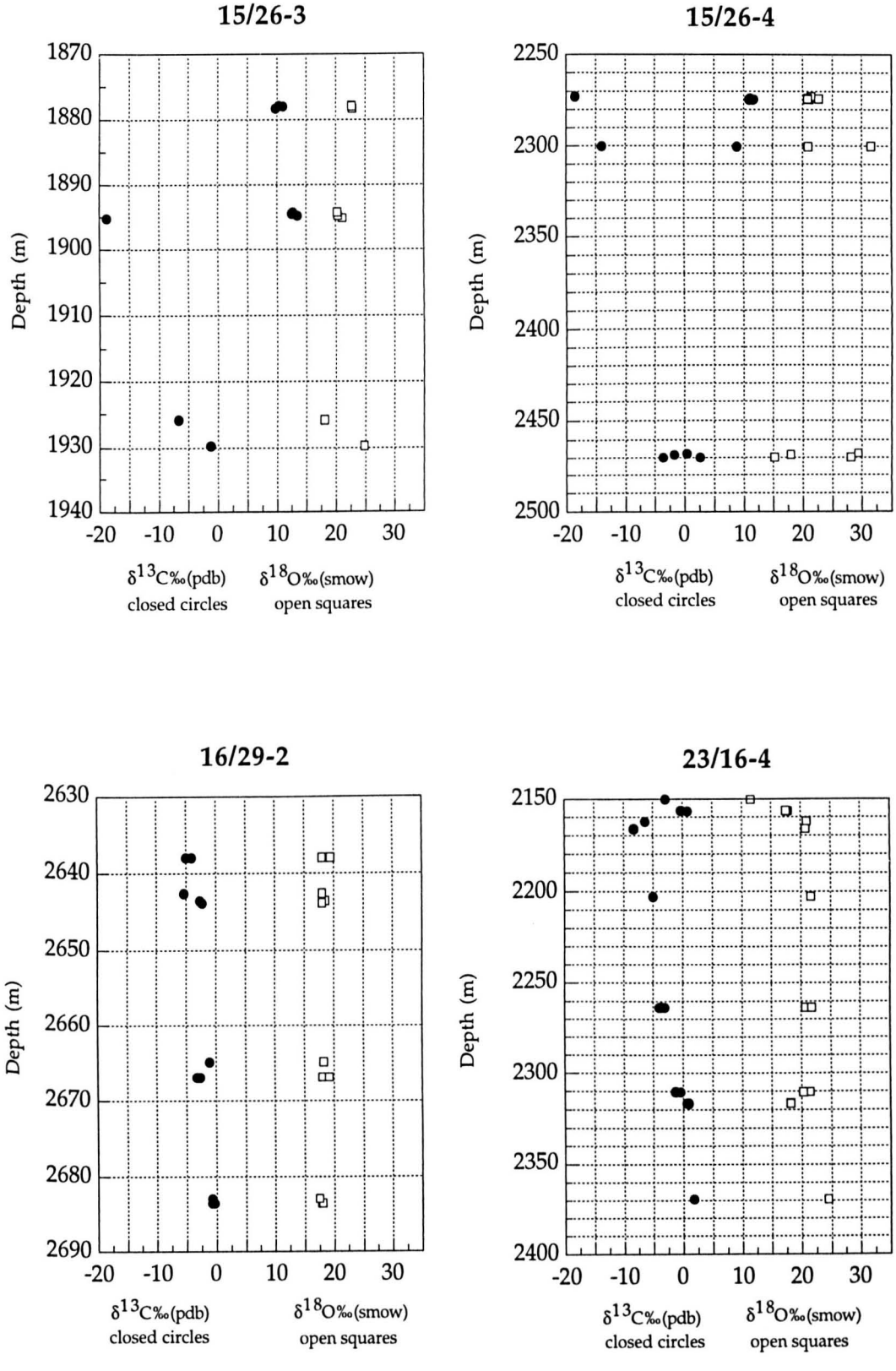

Figure 2.15a-d

Figure 2.16

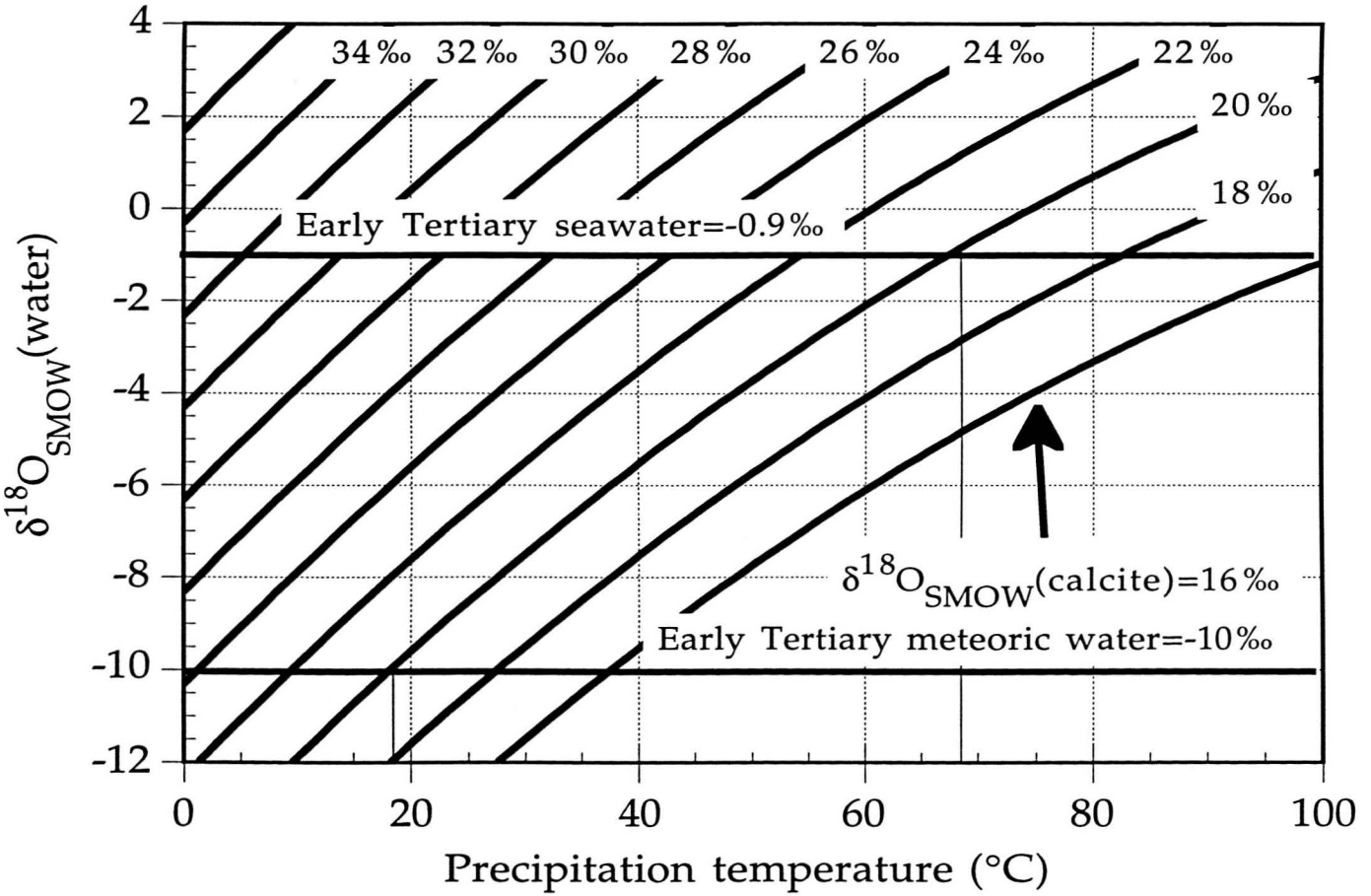
34‰
32‰
30‰
28‰
26‰
24‰
22‰
20‰
18‰
Early Tertiary seawater=-0.9‰
δ18OSMOW(calcite)=16‰
Early Tertiary meteoric water=-10‰
δ18OSMOW(water)
Precipitation temperature (°C)
4
2
0
-2
-4
-6
-8
-10
-12
0
20
40
60
80
100

Figure 2.17 Isotopic data from carbonate separates indicate that pore-waters within Montrose Group submarine sandstones were influenced by a meteoric influx. During late Palaeocene a relative sea-level drop of 900m (Reynolds 1994) resulted in the progradation of a deltaic system (Moray Group) over the Outer Moray Firth. Introduction of meteoric water is inferred to have occurred during this period. Maps illustrate Sequence 3 and 8 (Andrew Formation and Moray Group equivalent) Stewart 1987. Meteoric flushing must have occurred before compaction of overlying Tertiary muds resulting in a regional seal.

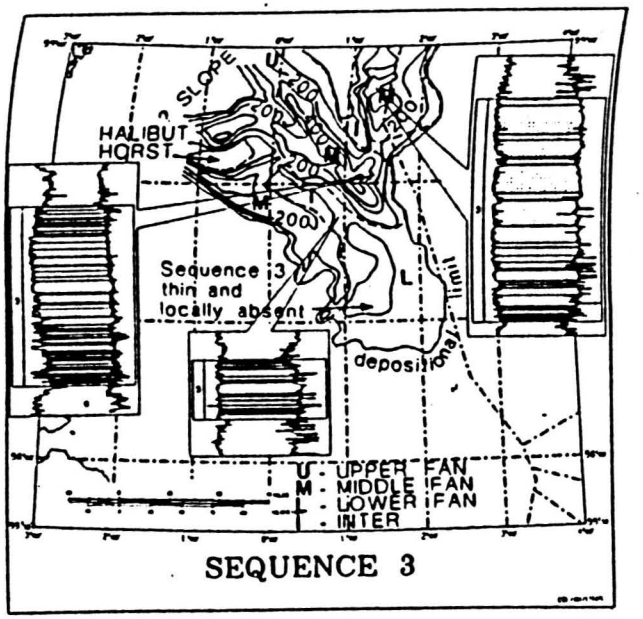

SEQUENCE 3

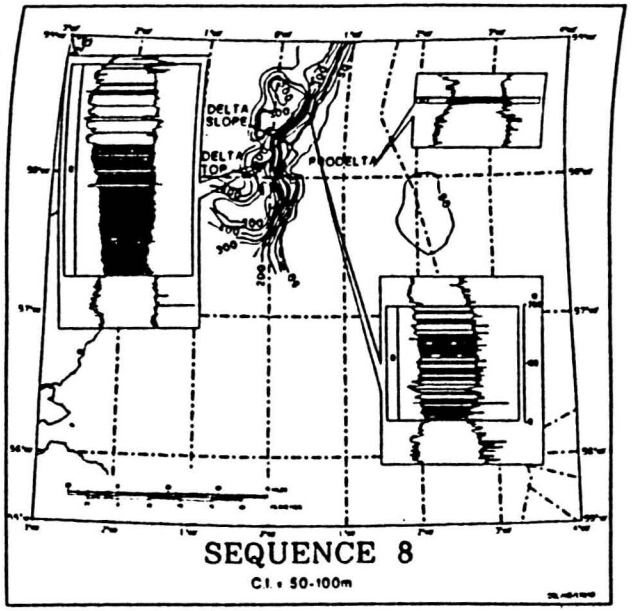

SEQUENCE 8
CI = 50-100m

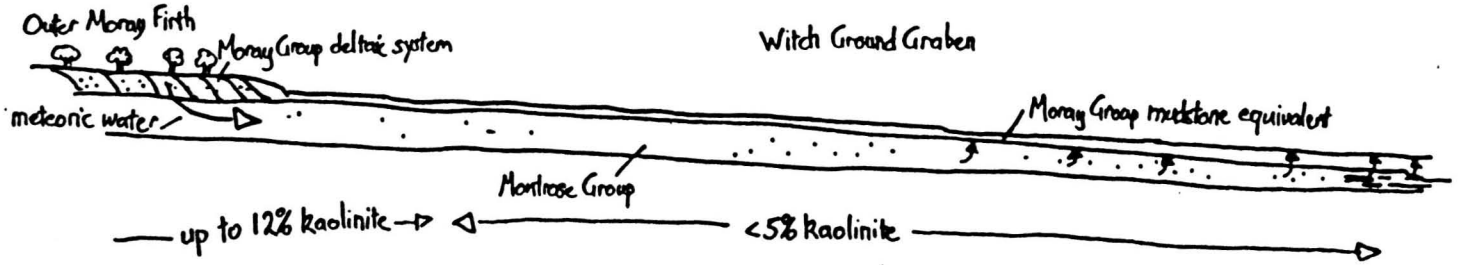

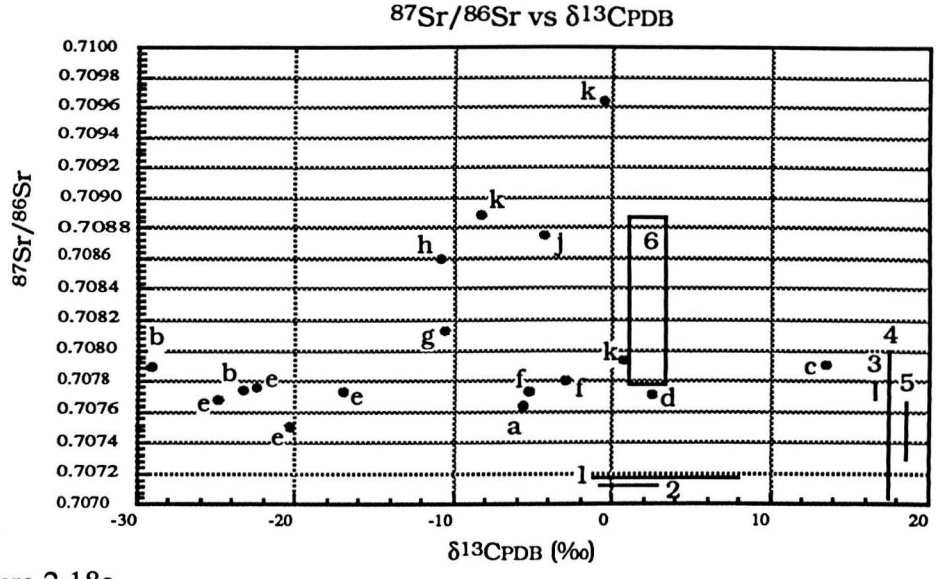

Figure 2.18a

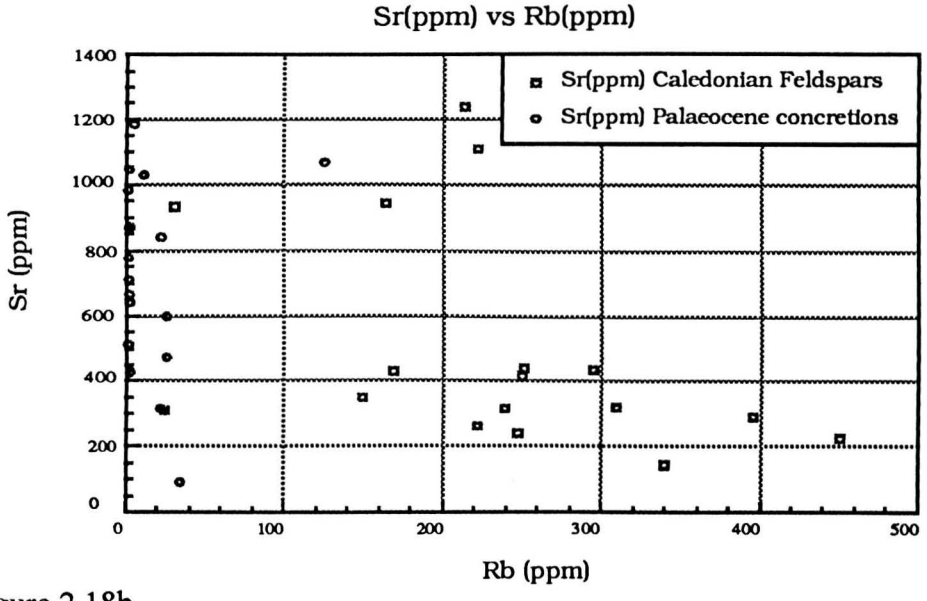

Figure 2.18b

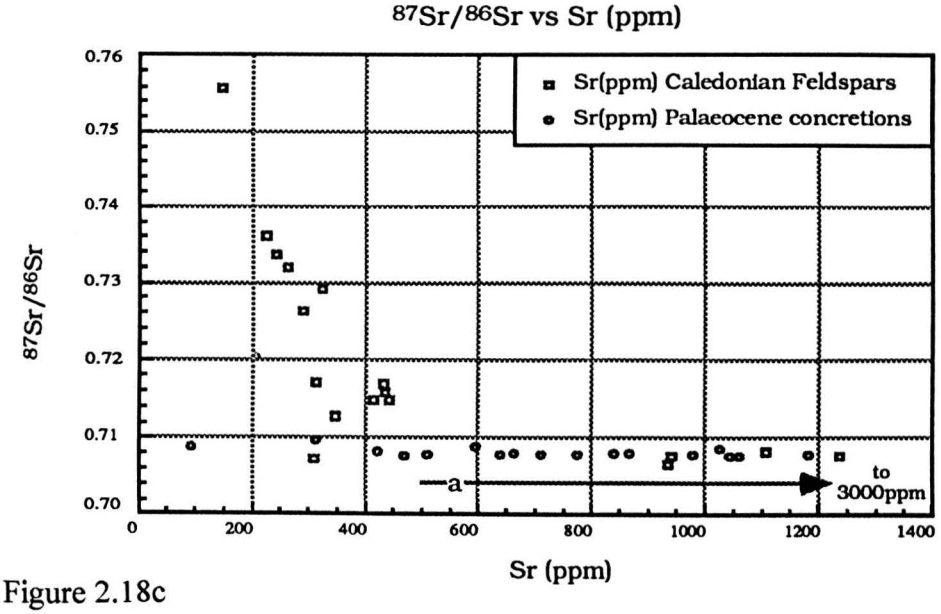

Figure 2.18c

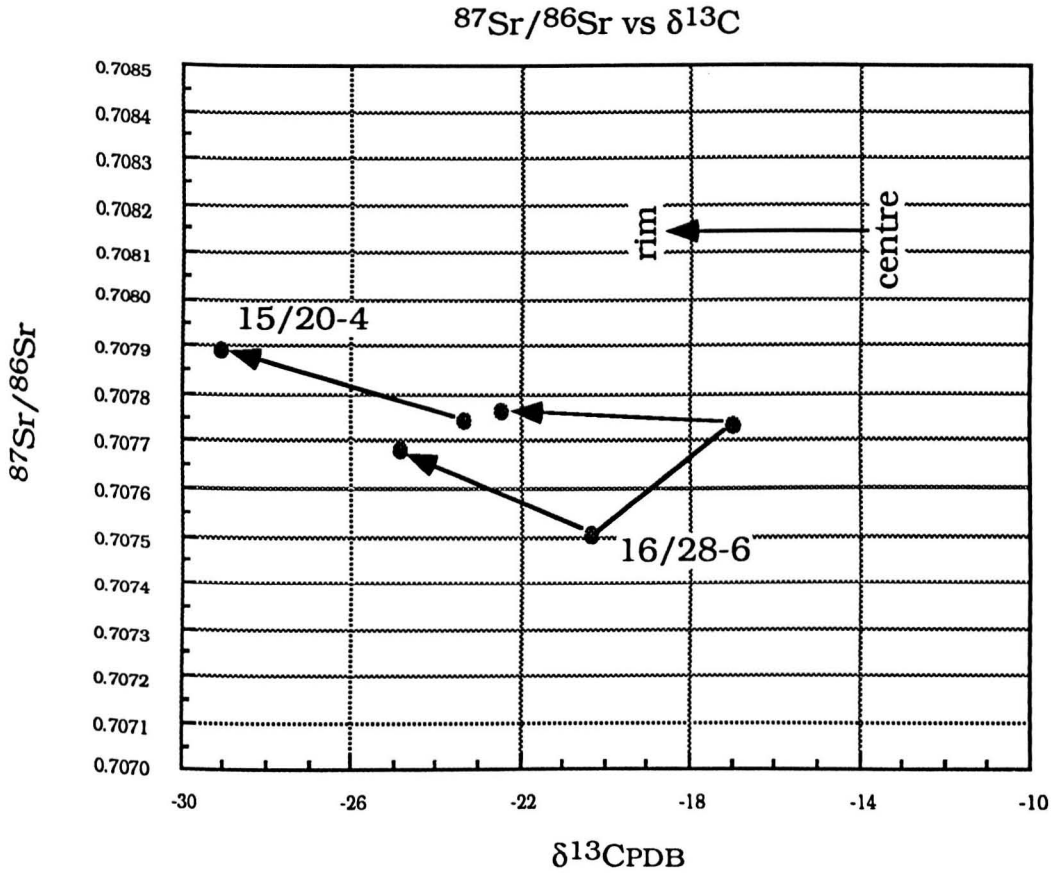
87Sr/86Sr vs δ13C
0.7085
0.7084
0.7083
0.7082
0.7081
0.7080
0.7079
0.7078
0.7077
0.7076
0.7075
0.7074
0.7073
0.7072
0.7071
0.7070
87Sr/86Sr
rim
centre
15/20-4
16/28-6
-30
-26
-22
-18
-14
-10
δ13CPDB

Figure 2.19

Figure 2.20

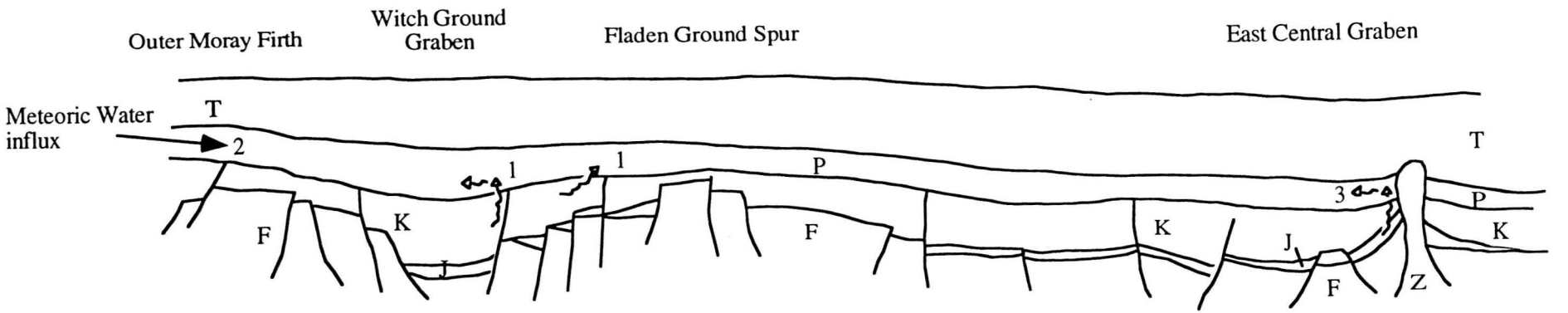
Outer Moray Firth
Witch Ground Graben
Fladen Ground Spur
East Central Graben
Meteoric Water influx
T
2
1
1
P
3
T
P
K
F
K
J
F
K
J
F
Z

CHAPTER 3 DISTRIBUTION OF CARBONATE CONCRETIONS

CHAPTER 3 DISTRIBUTION OF CARBONATE CONCRETIONS RELATED TO FLUID FLOW

3.1 Abstract

Concretions within the Palaeocene Montrose Group form a characteristic feature of the normally thick-bedded and structureless sands. These are identified from composite logs by 'kicks' on the sonic log and aided by well reports. These sonic kick 'concretions' form between 1.6 to 18.0% of core length. 70% of logs indicate that these concretions form 3-7% of the Montrose Group thickness; 50% are between 3.5 and 5.5% of Montrose Group thickness. Carbonate cements are present as concretions and rarely as disseminated grains. Therefore assuming an average minus-cement porosity of 40%, 1.6% to 18.0% of core length equates to bulk rock volumes ranging between 0.6 to 7.2% carbonate within the core. The original bulk volume of detrital carbonate is unknown. Where concretions are not tightly cemented there is likely to be an overestimate of carbonate cement.

Gross thicknesses of concretions for 101 composite logs have been compiled, and plotted in the form of a map. It is clear that concretions are more prevalent in areas along the flank of the Fladen Ground Spur, along the north flank of the Witch Ground Graben and the east flank of the south viking Graben and East Central Graben.

Within the Witch Ground Graben isotopic and petrographic evidence indicates that carbon for concretions within this area may have come from the degradation of early migrating hydrocarbons within cool meteoric waters. This would indicate that the concretions marked out palaeo-leak points or palaeo-migration paths from the underlying Upper Jurassic source-rocks.

Other concretions in the eastern flanks of the Central Graben are petrographically late and precipitated as a result of decarboxylation. The radiogenic strontium and enriched manganese compositions are similar to that found within diagenetic calcites in chalk. The elements required for precipitation can be sourced internally within the Montrose Group. However the precipitation mechanism could have been influenced by of fluid 'leak-off' from the Jurassic through the underlying Cretaceous sequence influenced by salt-tectonics. This remains unresolved. The anomolous increase in concretions in these areas may be due to deposition of carbonate detritus from the eastern flanks from eroding Cretaceous sequence providing carbonate material for remobilisation.

3.2 Introduction

Carbonate cemented horizons are commonly found in oil field cores. Isotopic evidence ($\delta^{13}C$ PDB) from the North Sea indicates that concretions precipitated as a result of organic mediated reactions during shallow burial (Giles et al 1992; Stewart et al. 1993), and by inorganic thermal breakdown of organic material at depths >1.5km burial (Irwin et al. 1977). Within the Brent Group Rannoch Formation, sandstones contain >5% carbonate cement, significantly more than other Formations, (Giles et al. 1992). In the Brent Group higher volumes of cement are associated with shallow marine sandstones

which are thought to have contained detrital carbonate (Bjorlykke et al, 1992; Harris 1992). However $^{87}Sr/^{86}Sr$ ratios of deltaic Ness Formation concretions indicate that cross-formational flow has occurred bringing calcium into the sandstones (Haszeldine et al. 1992).

Within the Montrose Group sandstones, the precipitation of concretions is noted as the volumetrically most important diagenetic reaction (Cutts 1991; O'Connor & Walker 1993). In this study, the percentage of concretions within sandstones has been calculated from composite logs, **Figure 3.1, Table 3.1.** The distribution of 101 wells' concretions is not uniform but enhanced in certain areas. Isotopic compositions of concretions from core samples are combined with the geological history to explain the concretion distribution.

3.3 Geology

The Montrose Group is a composite body composed of three lithostratigraphically similar units; the basal Maureen Formation (up to 100m thick; Stewart's 1987 Maureen Formation equivalent Sequence 2B), the dominant sand-rich Andrew Formation (up to 450m thick; Stewart's (1987) Andrew Formation Equivalent Sequence 3) and the uppermost Forties Formation (up to 250m thick; Stewart (1987) Forties Formation equivalent sequence 7). Sandstones are buried to depths of hundreds of metres within the Moray Firth and up to three thousand metres within the Fisher Bank Basin in the Central North Sea, **Figure 3.2.**

Underlying the Montrose Group are a sequence of Upper Cretaceous marls and chalks up to 1000m thick which thin over Mesozoic highs **Figure 3.2.** Underlying the Cretaceous are Upper Jurassic sandstones and the Kimmeridge Clay. Within the Central Graben, along the east edge of UK Quadrant 22, Zechstein salt domes puncture the overlying sediment and in some cases are brought adjacent to the Montrose Group sandstones (Foster & Rattey 1993). Overlying the Montrose Group in the Outer Moray Firth is the Upper Palaeocene Moray Group, a deltaic complex which prograded eastwards in response to relative sea-level fall. The Moray Group is composed of a thick sandy proximal complex which rapidly declines in thickness and sand:mud ratios away from palaeoshores in the Moray Firth area.

The sandstones were deposited by high-density turbidity flows (Stewart 1987; Knox et al. 1993). Petrographic descriptions of core samples from the Montrose Group indicate that these sandstones predominantly consist of massively-bedded sandstones with sparse de-watering structures; the depositional facies being similar on a regional scale (Thomas et al. 1974; Stewart 1987; Crawford et al 1991; Cutts 1991; Tonkin & Fraser 1991; Den Hartog Jager et al. 1993; Jones & Milton 1994). Sandstones are predominantly sub-arkosic to sub-litharenites (Crawford et al. 1991; Cutts et al. 1991).

Concretions are present within virtually all cores. Concretions are normally on the scale of tens of centimetres but can be up to two metres in diameter (Tonkin & Fraser 1991). The large diameter of concretions make it in impossible to determine whether

concretions are laterally extensive or spherical. However concretions have been noted as to act locally as permeability baffles within the Balmoral Field 16/21 (Tonkin & Fraser 1991). Within this study smaller concretions are oblate spheroids.

The stacked channel sandstones of the Andrew Formation have a high connectivity, particularly within the Witch Ground Graben, which would not hinder any pore-fluid movement. During deposition of the Forties Formation the supply of clastic sediment waned and sand:mud ratios declined. The formation of levee bank during deposition of Andrew Formation sands was hindered due to very high sand:mud ratios. It is thought that the Andrew Formation is derived from shallow buried sandstones on the East Shetland Platform (Den Hartog Jager et al. 1993). There was not sufficient mud to constrain the meandering channels and channels sands end up in multiple stacked systems. The deposition of Forties Formation was centred south of the Halibut Horst and in the East Central Graben. Stable levee banks evolved. Levee systems were previously unstable during deposition of sediments with high sand:mud ratio. Sand-rich channel systems became enclosed in mud levee banks. These sand channels are of the scale of several to tens of km across (Den Hartog Jager et al. 1993). Connectivity within these areas is reduced. Burial of the sediments has been constant with particularly rapid burial within the Witch Ground Graben during the early Eocene (Barnard & Bastow 1992).

3.4 Methodology

Composite logs record physical properties of rocks in-situ; these include transit times, gamma-ray radioactivity and density. The main litho-facies within the Montrose Group is a massively-bedded sandstone with sparse de-watering structures. Amalgamated units of these sandstones can be tens of metres thick. The log traces of this facies are therefore consistently stable. Concretions are identified by a combination of kicks on the sonic and resistivity logs **Figure 3.3.**

To gauge what was recognisable on the composite logs, cored concretions of known thickness were compared with the composite logs available from those particular wells. For well 15/20-4 concretions of diameter as small as 25cm seen in core were identified on the composite log.

For individual wells, gross concretion thickness was recorded. The thickness of individual concretions was measured from the composite logs at the half peak-height width. This was measured manually with a ruler. Measurements were then converted to metres. Peaks within electric logs record the changes in physical parametres in rocks. Kicks or changes in steady traces can be due to a variety of changes in the lithologies. Carbonate concretions are relatively simple to identify within massive-bedded and relatively homogeneous sandstones which make up the bulk of the Montrose Group **Figure 3.3.** Therefore, although the wells were drilled to seek prospects beneath the Tertiary sediments, because of the widespread high sand:mud ratios and the similarity in depositional facies, most drilling encountered Montrose Group sediments which provide stable electric log traces within sandstone beds. Marls

and chalk-rich beds identified on the logs or mentioned in the well reports were not recorded. Only kicks within sandstone units were recorded.

However away from depositional axes and in the areas distal to provenance area, both sand:mud ratios can dramatically rise and bed thickness can drop. 'Ratty' log traces are difficult to measure as the confusing jaggedy trace may relate to sedimentological differences other than concretions **Figure 3.4**. When such wells were encountered, mud-loggers reports, sedimentological reports and notes on the composite log were used to identify whether the sandstones were 'calciferous', 'calcareous', 'carbonate-cemented', or 'hard-cemented', all terms used to describe carbonate cemented horizons. There are likely to be large errors associated with well measurements taken from such composite logs. However although as the measurements are only semi-quantitative the increase in proportion of carbonate cement is likely to be a real phenomenom.

To minimise manual recording errors, the composite logs were sampled in a random selection. Some composite logs were deliberately analysed twice to estimate human errors in estimating 'kick' lengths. This is the largest error within the test. Errors can be up to 30%, most were 10-20%. Larger recording errors were encountered within ratty logs, while recording errors within thick sequences of massive sands were <10%.

Material used was collected at BP's Technical Data Centre, BP Expro, Glasgow and Dyce, courtesy of Dr Roger Anderton.

3.5 Results and discussion

The concretions percentage map for Quadrant 14, 15, 16, 21, 22 and 23 is shown in **Figure 3.5**

Proportions of concretions vary between 1.6 and 18.0% of core length. If the assumption is made that minus-cement porosities average 40% then this represents 0.6% to 7.4% rock volumes. A single vaue for minus-cement porosities was chosen as insufficient point count data is available from the Montrose Group from across the Central North Sea. Actual minus cement porosities vary from between 30-67% (Chapter 2, Table 2.4), the bulk of values between 35-45%. Therefore a potential error exists of ~10% in predicted carbonate volumes. Concretions in wells in the East Central Graben have lower minus cement porosities than Witch Ground Graben wells indicating precipitation at greater depths. The actual range of concretion volume is quite small, 70% of the wells have concretions of between 3-7% of core length and 50% are between 3.5 and 5.5% of core length **Table 3.2.** This range of concretion percentage is remarkable similar over most of the Central North Sea.

The amount of detrital carbonate is unknown within sandstones as detrital carbonate is rarely seen outwith cemented horizons. This is a key measurement which could explain the volume and distribution of the carbonate concretions. Unaltered detrital carbonate is rarely found within the Montrose Group, above Danian marly and

carbonate-rich horizons at the base of the Montrose Group. It is known that erosion of chalks situated at the west Central North Sea basin margins during deposition of the Montrose Group contributed to the sediments at the base of the Maureen Formation (Stewart 1987). Most Maureen Formation sediments have a marly/chalky rich base of Danian age. Isotopic chemistry goes someway to determining the origin of concretions. Isotopic analysis indicates that precipitation of concretion have been influenced by the presence of organic/inorganic reaction taking place during burial.

There are distinct areas where concretion percentage increases to volumes above this background level. These are generally along the north flank of the Witch Ground Graben, along the axes of the Witch Ground Graben and East Central Graben, and at points deeper into the graben system.

3.5.1 Witch Ground Graben concretions

Montrose Group is dominated by the Andrew Formation in this area. Composite logs and cores examined indicate that the sequence is dominated by massively bedded thick bedded sandstone layers. 'Kick' lengths are real and represent enhanced concretion precipitation.

Concretions from wells 15/20-4 and 16/28-6, within the Witch Ground Graben and Fisher Bank Basin, have been isotopically analysed, see Chapter 2. They have $\delta^{13}C$ PDB compositions similar to that of carbonates which have precipitated as a result of degradation of hydrocarbons (Dimitrakopolous and Muehlenbachs 1987; O'Brien and Woods 1994). Tar stains were seen within concretions from wells 16/28-6 and 15/20-4. Oxygen isotopic compositions of the concretions indicate that because the concretions are texturally early, then concretions precipitated within meteoric influenced waters with negative $\delta^{18}O$ SMOW compositions.

The predominance of diagenetic carbonate in this area may therefore be due to the mixing of migrating hydrocarbons with meteoric water, **Figure 3.6**. Meteoric water is only likely to have flowed through the Montrose Group during the late Palaeocene during a period of extreme sea-level fall. This was likely to have taken place concurrently during the deposition of Montrose Group and during the progradation of the Moray Group when a 800m relative sea level fall occurred (Jones & Milton 1994). This has implications for oil migration into the Palaeocene. The Witch Ground Graben underwent particularly rapid burial during the Palaeocene accommodating up to 600m of clastic sediments. Maturation of Kimmeridge Clays began during the Maastrichtian (Barnard & Bastow 1992), and migration of this oil began during the Lower Eocene. If the diagenetic carbonate marked out palaeo-migration paths in this area, then, timing of migration can be given a minimum date. Other authors put migration timing to Oligocene (Mason et al. 1995). Later early Miocene sea-level fall is thought to have introduced meteoric water into these sandbodies in the outer Witch Ground Graben. The degradation of migrating hydrocarbons within Eocene reservoirs in the Witch Ground Graben has been indicated to have occurred within this period as reservoir conditions were right for organic biodegradation. These authors also suggest that

Palaocene reservoirs in this area have also been affected but not so substantially as reservoir temperatures were higher, however field temperatures within these Montrose Groups reservoirs would have been low enough to sustain degredation (Mason et al. 1995) and there remains the possiblity of concretion formation during this period. Watson et al. (1995) found concretions of isotopic composition ($\delta^{13}C$=-25 to -5‰PDB) within the Montrose Group hosted Balmoral Field,Block 16/21. These authors suggest that oxygenated meteoric water flowing into the sands shortly after burial oxidised organic matter ($\delta^{13}C$=-25‰PDB) within the sediments. Oil stains within concretions were not seen within cores in this study and the possibility of oil migration concurrent with meteoric influx was rejected.

3.5.2 Concretions in the eastern flanks of the East Central Graben and South Viking Graben

Montrose Group sediments in this area are thin-bedded and can form ratty composite log traces. These areas are on the fringe of Montrose Group depositional area. The percentage values of carbonate concretions within this area are probably relative rather than absolute.

The late concretions within East Central Graben sandstones have carbon isotopic values which indicate that they formed during decarboxylation reactions (Chapter 2). Compositions of these concretions also indicate that they are Mn-calcites. Mn enrichment has been noted to occur during diagenesis within the underlying chalk sequence (Taylor & Lapre 1987). These cements are related to reactions occurring within the chalks during movement of pore-fluids from the underlying Jurassic. Strontium ratios from late concretions in the Montrose Group (Chapter 2) are also slightly more radiogenic than depositional calcite. This indicates that radiogenic ^{87}Sr had entered the porewaters during precipitation. Such an increase in ^{87}Sr could result from dissolution of silicate minerals (Emery & Robinson 1993). Calcite cements within the underlying chalks are also noted to be slightly more radiogenic than matrix chalk and becoming more radiogenic in ^{87}Sr with depth (Taylor & Lapre 1987; Smalley et al. 1992) **Figure 2.15.** This was related by Smalley et al. (1992) to have resulted from waters from underlying Jurassic sediments (and Zechstein salt) moving upwards into the Cretaceous **Figure 3.7.** Though there is a possibility of organic acids from the underlying Jurassic remobilising detrital carbonate, the late diagenetic nature of the carbonates would suggest that remobilisation of the detrital carbonate was influenced by decarboxylation reactions taking place at higher burial temperatures. The enrichment of diagenetic carbonates in depositionally distal areas appears to be related to areas where salt tectonics are important in Blocks 22/9, 23/11. **Figure 3.7.**

Anomolous rise in concretion thickness may be due partly to depositional reasons. The geographical locations of the rise of concretion is against the eastern flanks of the graben system in the Central North Sea. These flanks although not subarially exposed during the Palaeogene may have contributed carbonate detritus during deposition of the Montrose Group, gradually decreasing during the late Palaeocene as scarp slopes were filled (O'Connor and Walker 1993). Thus in the Montrose Group within this area there

may have been a greater contribution of detrital carbonate than within graben axes where clastic sediment from the west of Scotland was the sole sediment source. This detrital carbonate appears to have been mobilised during decarboxylation and reprecipitated as concretionary cements. The mixing between decarboxylation carbon and detrital carbonate can be seen in isotopic profiles of concretions in single wells although detrital carbonate can no longer be seen petrographically (Chapter 2).

3.6 Conclusions

1) Concretions mapped out by composite log analysis indicates that concretions comprise between 1.6 to 18.0% of sandstone length. The majority of wells have 3-7% of composite log length.

2) If 40% original porosity is chosen then this relates to 0.6-7.4% carbonate within the Montrose Group. 70% are between 3-7% which is 1.2 to 2.8% carbonate.

2) Mapping out of concretions has identified areas which have high concentrations of carbonate concretions. These are along axis and north flank of the Witch Ground Graben, along the axis of the East Central Graben and flank of the Jaeren High.

3) Combining the map with isotopic compositions of concretions indicates that concretions precipitated i) during early subsidence when early migrating oil mixed with meteoric water. The meteoric water entered the Montrose Group during a period of relative sea-level fall. ii) detrital carbonate content was greater within areas adjacent to Cretaceous scarps on the east side of the graben system in the Central North Sea which was remobilised during decarboxylation reactions.

Acknowledgements - Robert Stewart acknowledges NERC grant GT4/90/GS/51. Dr Roger Anderton is thanked for useful discussions and access to the Technical Data Centre in BP Expro, Glasgow and Dyce, Aberdeen

References

Barnard, P.C. and M.A. Bastow 1992 Hydrocarbon generation, migration alteration, entrapment and mixing in the Central and Northern North Sea. In: *Petroleum Migration*, W.A. England and A.J. Fleet (eds), *Geol. Soc. Spec. Publ.* **59**, 167-190.

Bjorlykke, K., Nedkvitne, T., Ramm, M. and G.C. Saigal 1992 Diagenetic processes in the Brent Group. In: *The Geology of the Brent Group*, A.C. Morton, R.S. Haszeldine, M.R. Giles, and S. Brown (eds), *Geol. Soc. Spec. Publ.* **61**, 263-289.

Crawford, R., Littlefair, R.W. and L.G. Affleck 1991 the Arbroath and Montrose Fields, Block 22/17, 18, UK North Sea. In: *United Kingdom Oil and Gas Fields: 25 Years Commemorative Volume*, I.L. Affleck (eds) *Geol. Soc. Mem.* **14**, 211-218.

Cutts, P.L. 1991 The Maureen Field, Block 16/29a, UK North Sea. In: *United Kingdom Oil and Gas Fields, 25 Years Commemorative Volume*, I.L. Abbotts (ed), *Geol. Soc. Mem.* **14**, 347-352.

Den Hartog Jager, D., Giles, M.R., and G.R. Griffiths 1993 Evolution of Paleogene submarine fans of the North Sea in space and time. In: *Petroleum Geology of Northern Europe: Proceedings of the 4th Conference in London*, J.R. Parker (ed), Geol. Soc., London, 59-71.

Dimitrakopolous, R. and L. Muehlenbachs 1987 Biodegradation of petroleum as a source of ^{13}C-enriched carbon dioxide in the formation of carbonate cement. *Chemical Geology, Isotope Geoscience*, Section **65**, 283-291.

Emery, D. and A. Robinson 1993 History of fracturing in a Chalk reservoir: Machar Field, Central North Sea. In: *Inorganic Geochemistry: Applications to Petroleum Geology*. D. Emery and A. Robinson (eds), Blackwell Scientific Publications, Oxford, 156-165.

Foster, P.T. and P.R. Rattey 1993 The evolution of a fractured chalk reservoir: Machair Oilfield, UK North Sea. In: *Petroleum Geology of Northwest Europe*. J.R. Parker (ed), Geol. Soc. Lond., 1445-1452.

Giles, M.R., Stevenson, S., Martin, S.V., Cannon, S.J.C., Hamilton, P.J., Marshall, J.D. and G.M. Samways 1992 The reservoir properties of the Brent Group: a regional perspective. In: *Geology of the Brent Group*, . A.C. Morton, R.S. Haszeldine, M.R. Giles and S. Brown (eds), *Geol. Soc. Spec. Publ.* **61**, 289-327.

Harris, N.B. 1992 Burial diagenesis of Brent sandstones: a study of Statfjord, Hutton and Lyell fields. In: *Geology of the Brent Group*, . A.C. Morton, R.S. Haszeldine, M.R. Giles and S. Brown (eds), *Geol. Soc. Spec. Publ.* **61**, 351-357.

Haszeldine, R.S., Brint, J.F., Fallick, A.E., Hamilton, P.J. and S. Brown. 1992 Open and restricted hydrologies in Brent Group diagenesis: North Sea. In: *Geology of the Brent Group*, A.C. Morton, R.S. Haszeldine, M.R. Giles and S. Brown (eds), *Geol. Soc. Spec. Publ.* **61**, 401- 419.

Irwin, H., Curtis, C. and M. Coleman. 1977 Isotopic evidence for source of diagenetic carbonates formed during burial of organic-rich sediments. *Nature*, **269**, 209-213.

Jones, R.W. and N.J. Milton. 1994 Sequence development during uplift: Paleogene stratigraphy and relative sea-level history of the Outer Moray Firth, UK North Sea. *Marine and Petroleum Geology*, **11**, 157-165.

Knox R.W.O'B., Morton A.C. and R. Harland 1993 Stratigraphic relatiohsips of Palaeocene sands in the UK Sector of the central North Sea. In: *Petroleum Geology of the Continental Shelf of North West Euope*, L.V. Illing & G.D. Hobson (eds), Institute of Petrokeum, Heyden & Son, London, 267-281

Mason P.C., Burwood R. and B. Mycke 1995 The reservoir geochemistry and petroleum charging histories of Palaeogene reservoired fields in the Outer Witch Ground Graben. In: *The Geochemistry of Reservoirs*, J.M.Cubitt and W.A. England (eds), *Geol Soc. Spec. Publ.*, **86**, 281-302.

O'Brien, W.O. and P. Woods. 1994 Vulcan Sub-basin, Timor Sea. Clues to the structural reactivation and migration history from the recognition of hydrocarbon seepage indicators. *Australian Geological Survey Organisation Newsletter*, **21**, 8-11.

O'Connor, S.J. and D. Walker. 1993 Palaeocene reservoirs of the Everest trend. In: *Petroleum Geology of Northwest Europe: Proceedings of the 4th Conference in London*, J.R, Parker (ed), Geol. Soc., London, 1455-160.

Smalley, P.C., Lonoy, A. and A. Raheim 1992 Spatial $^{87}Sr/^{86}Sr$ variations in formation water and calcites from the Ekofisk chalk oil field: implications for reservoir connectivity and fluid composition. *Applied Geochemistry*, **7**, 341-350.

Stewart, I.J. 1987 A revised stratigraphic interpretation of the Early Palaeogene of the central North Sea. In: *Petroleum Geology of North West Europe*, J. Brooks and K. Glennie (eds), Graham and Trotman, London, 557-576.

Stewart, R.N.T., Haszeldine, R.S., Fallick, A.E., Anderton,R. and R. Dixon 1993 Shallow calcite cementation in a submarine fan: biodegradation of vertically migrating oil? *American Association of Petroleum Geologists Annual Convention*, 186.

Taylor, S.R. and J.F. Lapre 1987 North Sea chalk diagenesis: its effect on reservoir location and properties. In: *Petroleum Geology of North West Europe*,. J. Brooks and K. Glennie (eds), Graham and Trotman, London, 483-495.

Thomas A.N., Walmsley P.J. and D.A.L. Jenkins 1974 Forties Field, North Sea. Bulletin of the American Association of Petroleum Geologists, **58**, 396-406.

Den Hartog Jager D., Giles M.R. and G.R. Griffiths 1993 Evolution of Palaegene submarine fans in time and space. In: *Petroleum Geology of Northwest Europe*, J.R. Parker (ed), Geol. Soc. London, 59-71.

Tonkin, P.C. and A.R. Fraser 1991 The Balmoral Field, Block 16/21, UK North Sea. In: *United Kingdom Oil and Gas Fields, 25 Years Commemorative Volume*, I.L. Abbotts (ed), *Geol. Soc. Mem.* **14**, 237-243.

Watson R.S., Trewin N.H. and A.E. Fallick 1995 The formation of carbonate cements in the forth and Balmoral Fields, northern North Sea: a case for biodegredation, carbonate cementation and oil leakage during early burial. In: *Characterisation of Deep Marine Clastic systems*. A.J. Hartley & D.J. Prosser (eds) *Geol. Soc. Spec. Publ.* **94**, 177-200.

Figure captions

Figure 3.1 Location map of the Central North Sea showing base Cretaceous structural elements. Wells sampled in the study are illustrated.

Figure 3.2 Cartoon cross-section across the Central North Sea

Figure 3.3 Composite log of 22/8-3. A type example of distinct concretions within monotonous Montrose Group sandstones. In wells similar to this concretion thicknesses are simple to measure. Concretion thickness is measured at half peak height width of sonic kick.

Figure 3.4 Composite log of 22/10-5. This well illustrates nature of Montrose Group lateral to depositional axes. Measuring concretions within wells like this requires mudloggers and geological reports to aid identification of cemented horizons.

Figure 3.5 Map of concretion percentage for Montrose Group sandstones. For the bulk of sandstones concretions generally make from 3-7% of thickness of Montrose Group. There are areas which have anomalously high amounts of concretions. These are i) axis of Witch Ground Graben, north flank of Witch Ground Graben and around the southern tip of the Fladen Ground Spur, ii) along the axis of the East Central Graben, iii) around the east side of Quadrant 22, and iv) within blocks 16/28and 16/29.
Values greater than 2.5%. shaded.

Figure 3.6 Cartoon illustrating possible scenario within the Witch Ground Graben during the late Palaeocene. Meteoric water entering from the Outer Moray Firth mixed with early migrating hydrocarbons. The hydrocarbons were biodegraded and concretions were precipated within this area.

Figure 3.7 Seismic section illustrating the effect of salt-diapirsm on overlying sediments (Platt & Phillip 1993). Late concretions have strontium ratios which indicate introdution of Sr into the sandstones. Diagenetic calcites from the underlying Cretaceous chalks, also have radiogenic component introduced into the sands which increases downwards (Smalley et al 1992). The anomalous amounts of concretions may be related to vertical fluid transfer from overpressured underlying turassic sediments during fluid leak-off.

Table 3.1

Well	Carbonate % assuming 40% minus-cement porosity	'Concretion' thickness
14/14-2	1.38	3.45
14/14-3	2.00	5.00
14/15-1	1.93	4.83
14/17-1	1.66	4.15
14/18-7	1.88	4.70
14/19-17	2.74	6.85
14/19-18	1.43	3.58
14/20-8	0.61	1.62
14/24-2	2.69	6.73
15/6-1	0.88	2.20
15/7-1	1.55	3.88
15/8-1	1.45	3.63
15/11-2	2.22	5.55
15/11-3	2.16	5.40
15/13-4	1.73	4.35
15/14-3	1.64	4.10
15/15-1	5.63	14.10
15/17-3	1.94	4.85
15/17-8	2.18	5.45
15/18-2	2.86	7.15
15/20-1	7.21	18.03
15/20-3	4.78	11.95
15/21-15	1.76	4.40
15/22-6	1.54	3.85
15/23-2	2.26	5.15
15/23-3	2.00	5.00
15/23-6	1.89	4.73
15/24-1	2.58	6.45
15/24-2	1.98	4.95
15/27-1	1.46	3.65
15/28-2	4.80	12.00
15/29-4	1.58	3.95
15/30-6	2.10	5.25
16/6-1	1.79	4.48
16/11-1	2.32	5.80
16/11-4	1.39	3.48
16/12-4	1.26	3.15
16/12-9	2.49	6.23
16/12-10	2.34	5.85
16/13-2	1.97	4.93
16/13-3	2.15	5.38
16/16-2	1.05	2.63
16/17-5	1.56	3.9
16/17-7	1.54	3.85
16/17-12	2.09	5.23
16/18-1	4.38	10.95
16/18-2	1.79	4.48

16/21-5	5.16	12.90
16/22-3	2.44	6.10
16/22-5	2.42	6.05
16/23-3	3.37	8.43
16/23-4	3.67	9.18
16/26-19	1.91	4.78
16/27-2	2.00	5.00
16/27-3	1.57	3.93
16/28-3	2.73	6.83
16/28-6	3.31	8.28
16/28-7	3.11	7.78
16/28-8	4.57	11.43
21/1-14	2.51	6.28
21/1-16	1.91	4.78
21/2-7	0.84	2.10
21/2-8	1.29	3.23
21/3-3	1.66	4.15
21/4-4	1.97	4.93
21/9-10	2.15	5.38
21/10-7	1.24	3.10
21/15-2	2.12	5.30
21/18-2	4.37	10.93
22/1-7	1.40	3.50
22/2-1	1.62	4.05
22/2-2	2.45	6.13
22/2-3	2.89	7.23
22/3-1	1.57	3.93
22/4-1	1.03	2.58
22/4-3	1.53	3.83
22/6-13	1.38	3.45
22/7/-1	2.73	6.83
22/7-2	2.76	6.90
22/8-2	2.22	5.55
22/8-3	2.32	5.80
22/9-3	5.99	14.98
22/9-4	1.87	4.68
22/10-5	6.56	16.40
22/11-9	2.15	5.38
22/12-3	2.00	5.00
22/12-4	1.78	4.45
22/13-4	3.77	9.43
22/14	4.26	10.65
22/15-2	2.53	6.33
22/16/2	1.16	2.90
22/18-3	0.98	2.45
22/18-4	1.54	3.85
22/19-1	2.46	6.15
22/20-1	3.08	7.70
22/20-3	3.75	9.35
22/21-3	2.61	6.53

22/22-1	3.63	9.08
22/26-2	2.88	7.20
22/30-1	1.72	4.30
23/11-2	3.91	9.78

Table 3.2

Concretion length	No. of wells
0.5	0
1.0	0
1.5	0
2.0	1
2.5	3
3.0	3
3.5	6
4.0	13
4.5	10
5.0	10
5.5	13
6.0	5
6.5	8
7.0	6
7.5	3
8.0	2
8.5	2
9.0	0
9.5	4
10.0	1
10.5	0
11.0	3
11.5	1
12.0	1
12.5	1
13.0	1
13.5	0
14.0	0
14.5	1
15.0	1
15.5	0
16.0	0
16.5	1
17.0	0
17.5	0
18.0	0
18.5	1

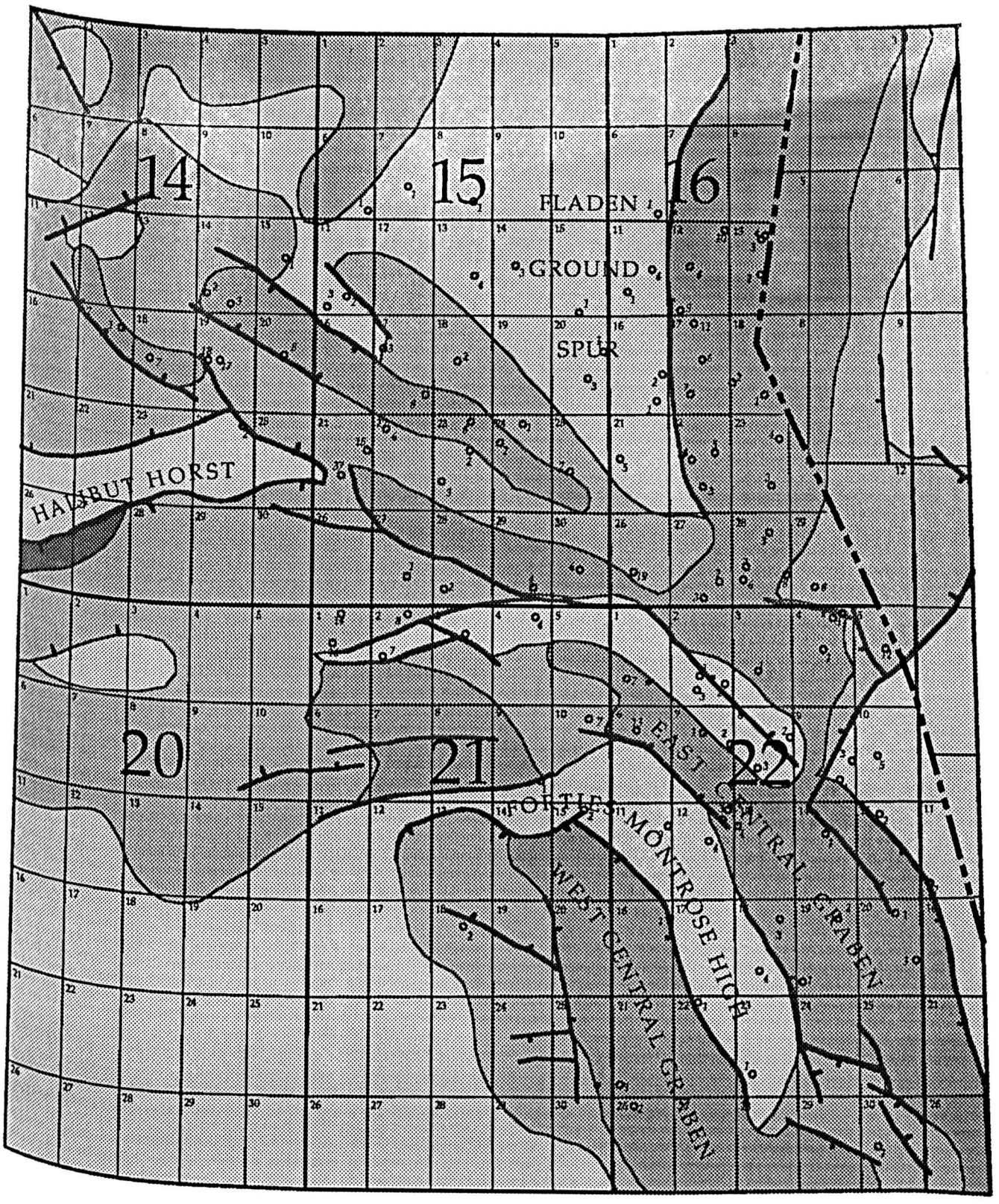
14
15
16
FLADEN
GROUND
SPUR
HALIBUT HORST
20
21
22
EAST CENTRAL GRABEN
MONTROSE HIGH
WEST CENTRAL GRABEN

Figure 3.1

Figure 3.2

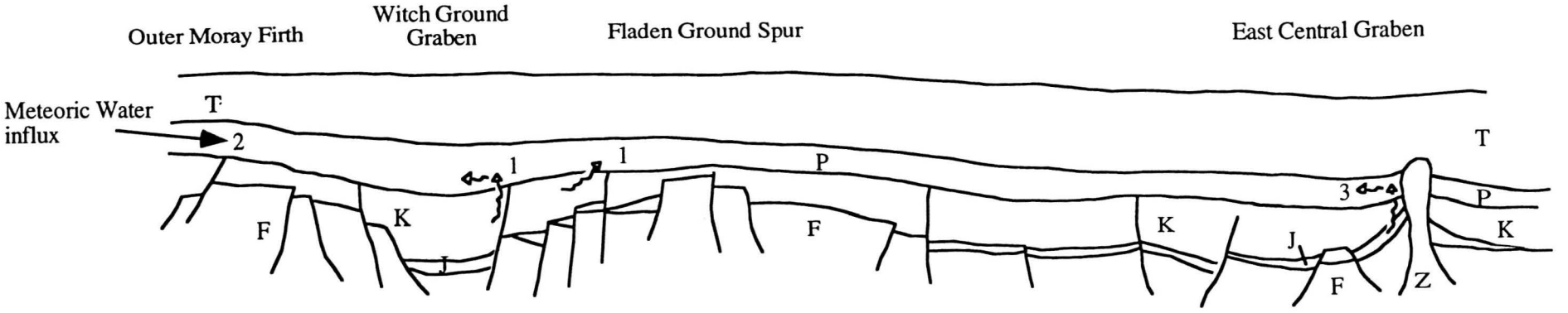
Outer Moray Firth
Witch Ground Graben
Fladen Ground Spur
East Central Graben
Meteoric Water influx
T
2
1
1
P
3
T
P
K
F
K
J
F
K
J
F
Z

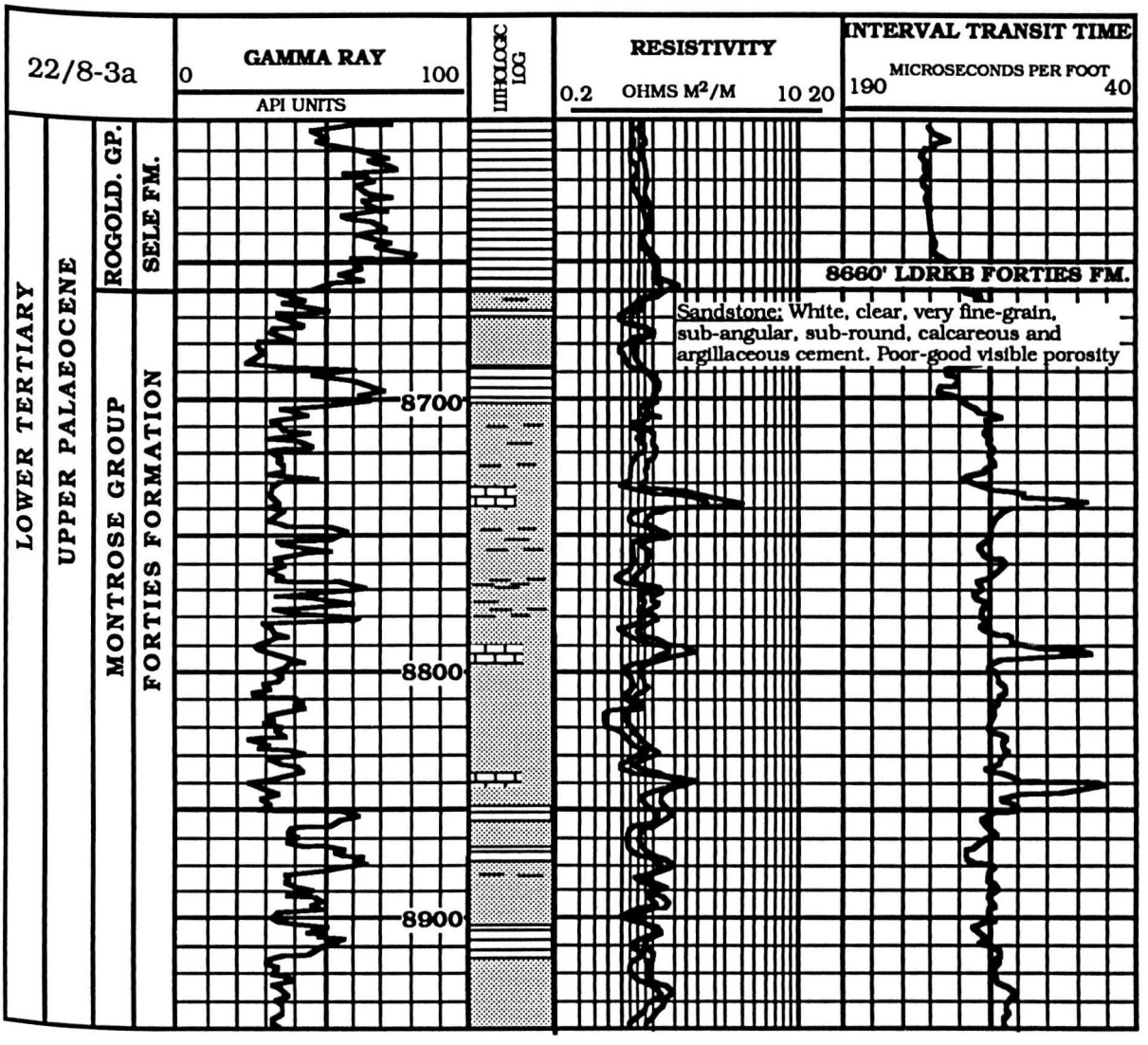
22/8-3a
GAMMA RAY
0
100
API UNITS
LITHOLOGIC LOG
RESISTIVITY
0.2
OHMS M²/M
10 20
INTERVAL TRANSIT TIME
MICROSECONDS PER FOOT
190
40
LOWER TERTIARY
UPPER PALAEOCENE
MONTROSE GROUP
ROGOLD. GP.
SELE FM.
FORTIES FORMATION
8660' LDRKB FORTIES FM.
Sandstone: White, clear, very fine-grain, sub-angular, sub-round, calcareous and argillaceous cement. Poor-good visible porosity
8700
8800
8900

Figure 3.3

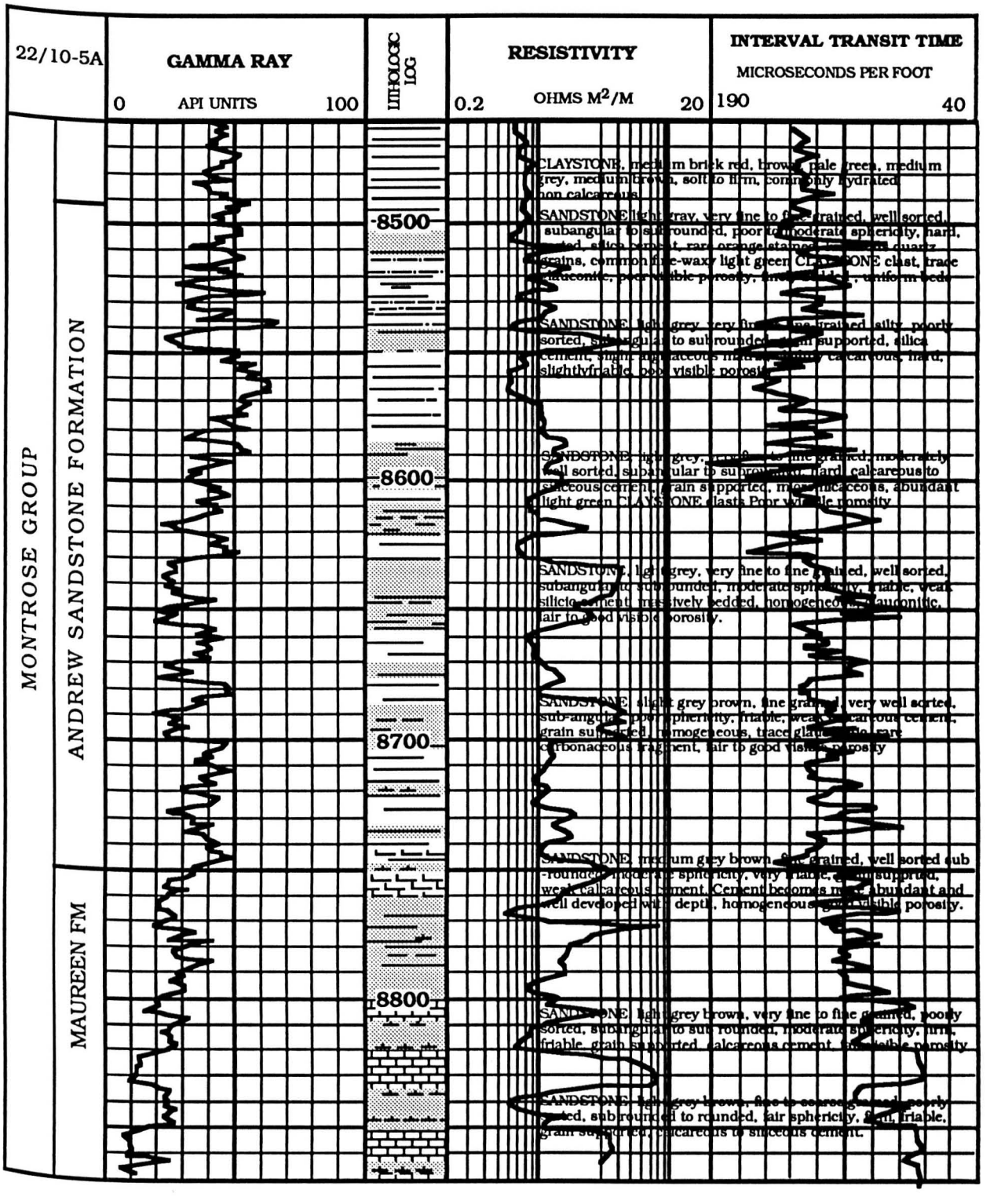
22/10-5A
GAMMA RAY
0 API UNITS 100
LITHOLOGIC LOG
RESISTIVITY
0.2 OHMS M²/M 20
INTERVAL TRANSIT TIME
MICROSECONDS PER FOOT
190 40
MONTROSE GROUP
ANDREW SANDSTONE FORMATION
MAUREEN FM
8500
8600
8700
8800
CLAYSTONE, medium brick red, brown, pale green, medium grey, medium brown, soft to firm, commonly hydrated non calcareous.
SANDSTONE light grey, very fine to fine grained, well sorted, subangular to subrounded, poor to moderate sphericity, hard, silica cement, rare orange stained quartz grains, common fine waxy light green CLAYSTONE clast, trace glauconite, poor visible porosity, fine laminated, uniform bedd
SANDSTONE light grey, very fine to fine grained, silty, poorly sorted, subangular to subrounded, grain supported, silica cement, slightly argillaceous matrix, locally calcareous, hard, slightly friable, poor visible porosity
SANDSTONE, light grey, very fine to fine grained, moderately well sorted, subangular to subrounded, hard, calcareous to siliceous cement, grain supported, micaceous, abundant light green CLAYSTONE clasts Poor visible porosity
SANDSTONE, light grey, very fine to fine grained, well sorted, subangular to subrounded, moderate sphericity, friable, weak siliceous cement, massively bedded, homogeneous, glauconitic, fair to good visible porosity.
SANDSTONE, light grey brown, fine grained, very well sorted, sub-angular, poor sphericity, friable, weak calcareous cement, grain supported, homogeneous, trace glauconite, rare carbonaceous fragment, fair to good visible porosity
SANDSTONE, medium grey brown, fine grained, well sorted sub-rounded, moderate sphericity, very friable, grain supported, weak calcareous cement. Cement becomes more abundant and well developed with depth, homogeneous, good visible porosity.
SANDSTONE light grey brown, very fine to fine grained, poorly sorted, subangular to sub rounded, moderate sphericity, firm, friable, grain supported, calcareous cement, fair visible porosity
SANDSTONE, light grey brown, fine to coarse grained, poorly sorted, subrounded to rounded, fair sphericity, firm, friable, grain supported, calcareous to siliceous cement.

Figure 3.4

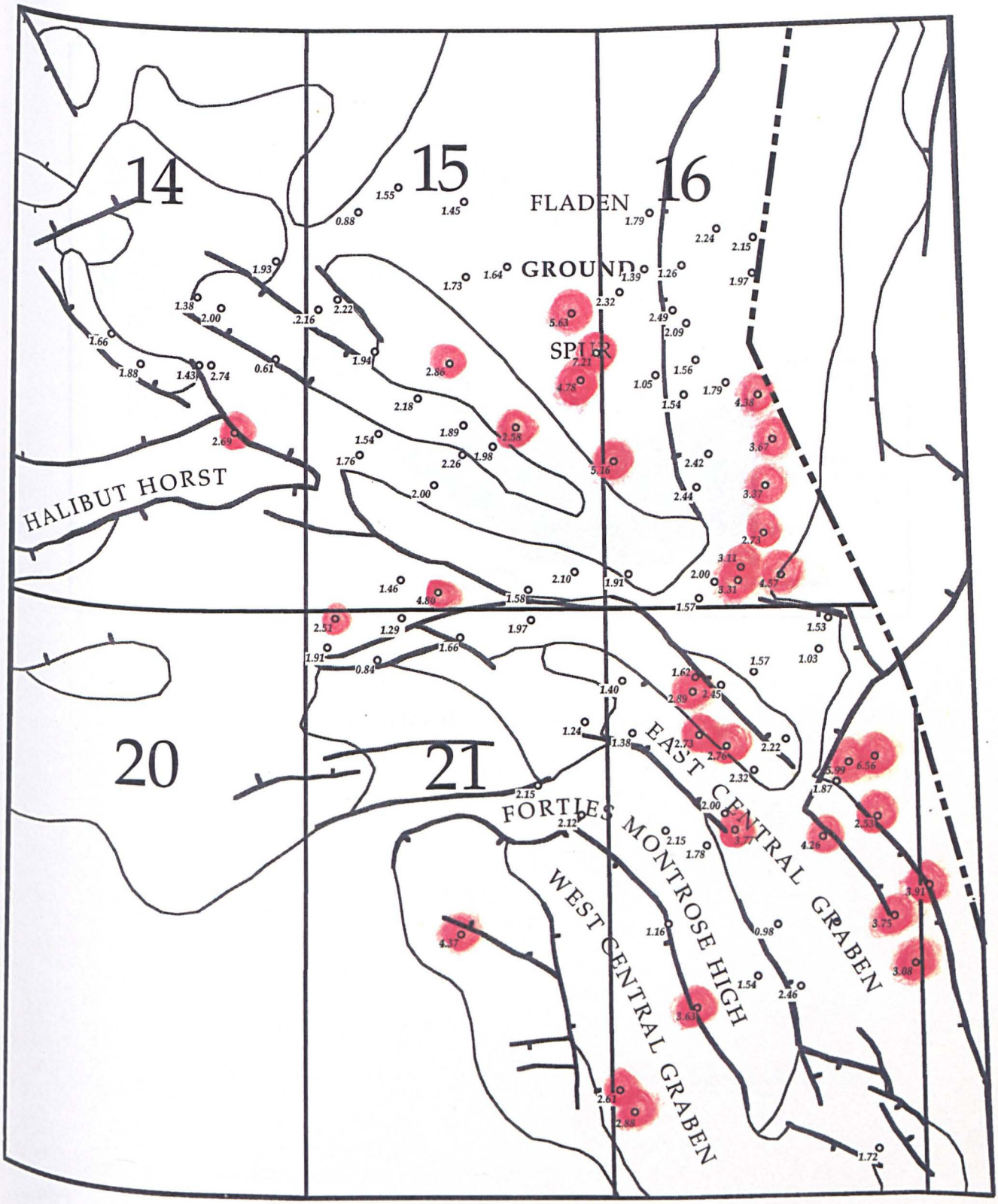
14
15
16
FLADEN
GROUND
SPUR
HALIBUT HORST
20
21
EAST CENTRAL GRABEN
FORTIES MONTROSE HIGH
WEST CENTRAL GRABEN

Figure 3.5

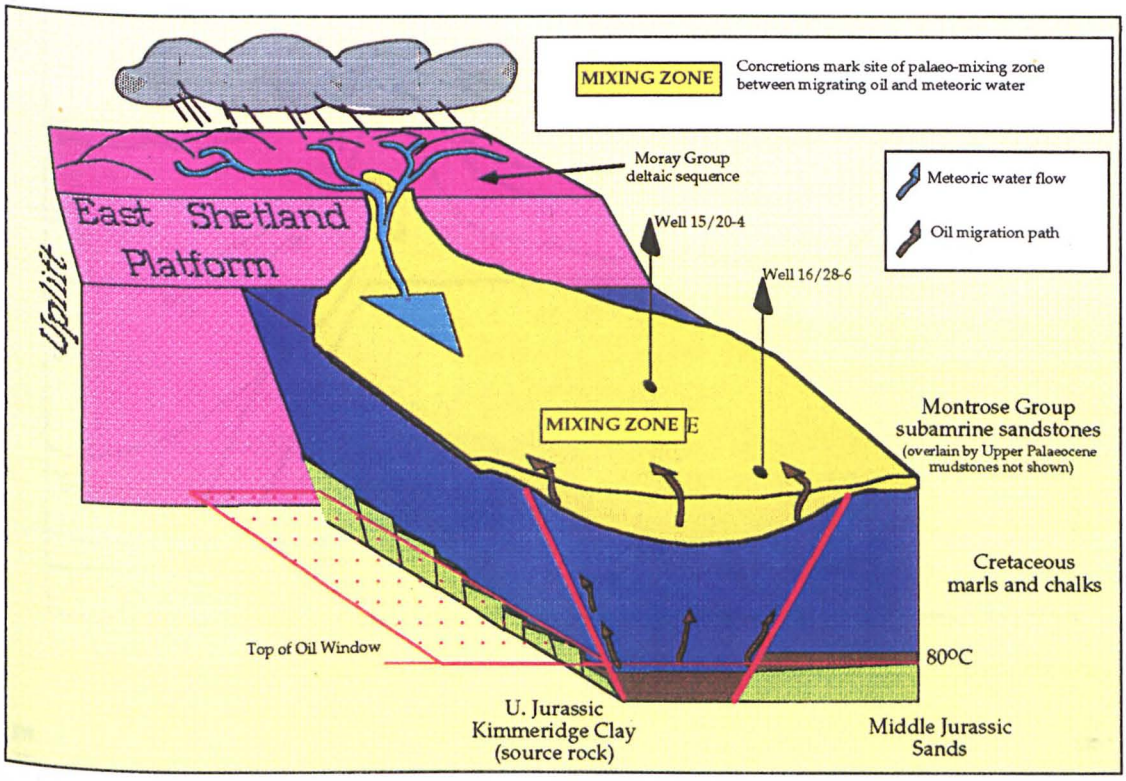

Figure 3.6 Oil migration

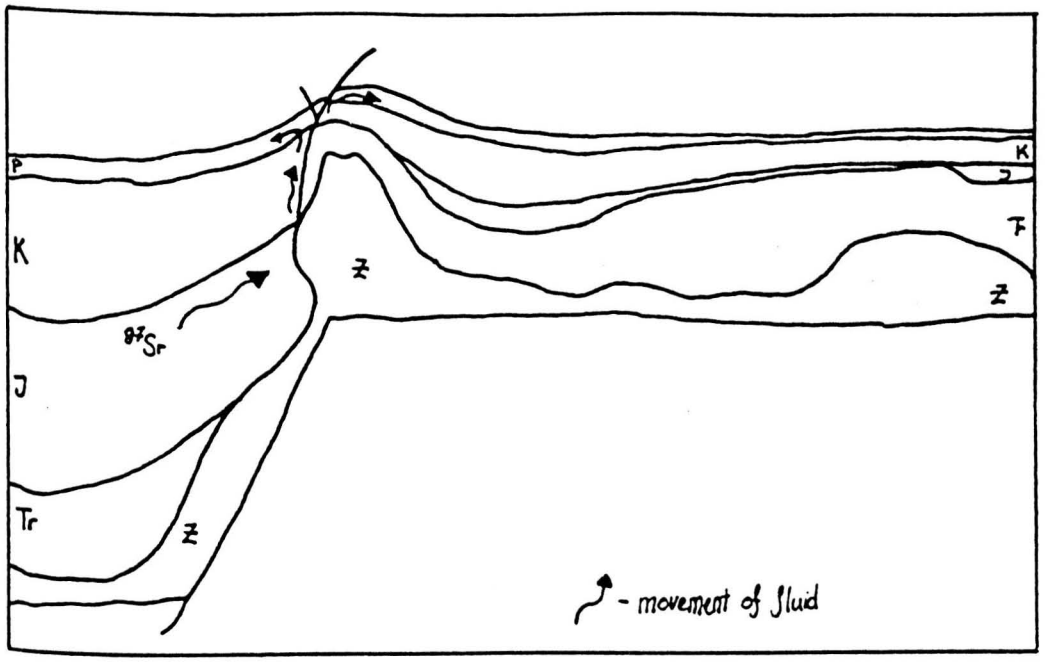
P
K
J
Tr
Z
^{87}Sr
- movement of fluid

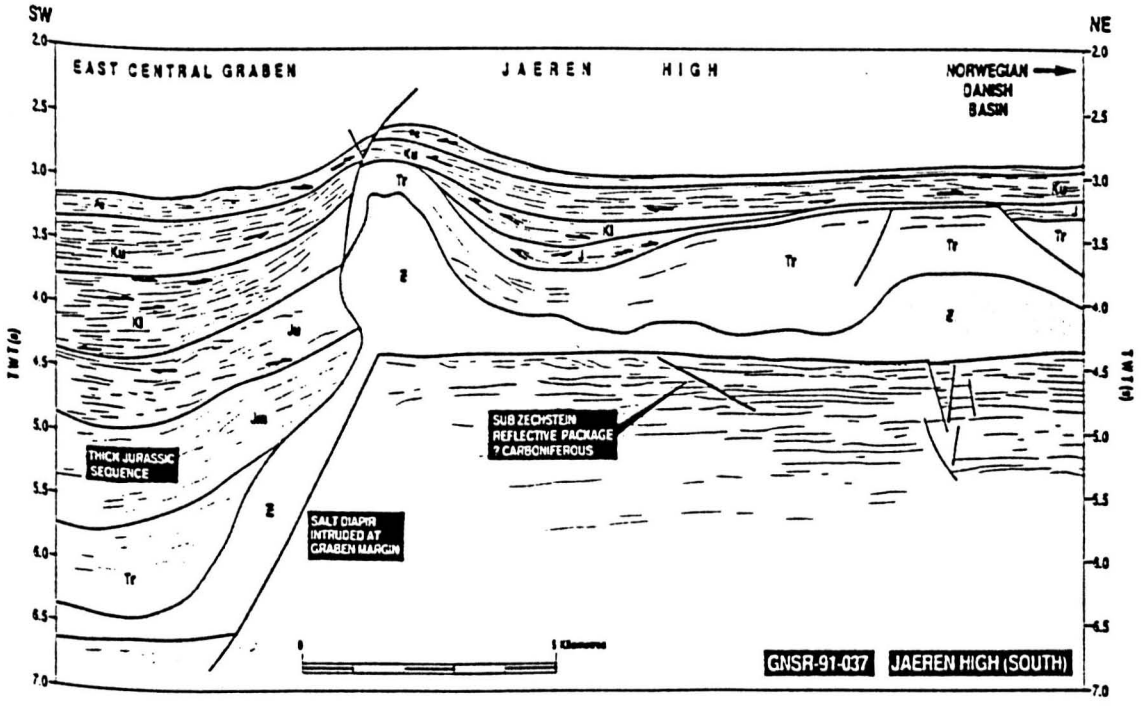
SW
NE
EAST CENTRAL GRABEN
JAEREN HIGH
NORWEGIAN DANISH BASIN
THICK JURASSIC SEQUENCE
SALT DIAPIR INTRUDED AT GRABEN MARGIN
SUB ZECHSTEIN REFLECTIVE PACKAGE ? CARBONIFEROUS
GNSR-91-037
JAEREN HIGH (SOUTH)
TWT(s)

Figure 3.7

CHAPTER 4 KAOLINITE GROWTH DURING PORE-WATER MIXING: ISOTOPIC DATA FROM PALAEOCENE SANDS, NORTH SEA UK.

CHAPTER 4 KAOLINITE GROWTH DURING POREWATER MIXING: ISOTOPIC DATA FROM PALAEOCENE SANDS. NORTH SEA. UK.

4.1 Abstract

Stable isotopic and petrographic data are used to interpret conditions for the formation of authigenic kaolinite within Palaeocene sands, Central North Sea. Ten wells within the Central North Sea were sampled. Texturally early calcite concretions have isotopic compositions ($\delta^{18}O$ = 18.0 to 22.8‰SMOW) which indicate that they were precipitated in predominantly meteoric waters. The isotopic composition of later kaolinite (av. $\delta^{18}O$ =13.8 to 16.7‰SMOW and δD = -53.0 to -76.8‰SMOW) indicates that kaolinite precipitated at around 35 to 80°C, from a mixed meteoric-marine pore water ($\delta^{18}O$ = -6.5 to -4‰SMOW). These modelled precipitation temperatures are consistent with the paragenetic sequence and consequently post-precipitation hydrogen isotope exchange between kaolinite and the pore-waters is presumed not to have occurred. We infer that the original depositional marine pore-waters were flushed out by a head of meteoric water from the East Shetland Platform during deposition of Palaeocene Montrose Group sandstones and progradation of the Palaeocene/early Eocene Moray Group deltaic system. The Palaeocene aquifer became closed to meteoric influx after marine transgression during the Eocene. The remaining meteoric pore-waters in the sandstones became mixed with water from compacting marine muds surrounding the hydrostatically pressured sandstones.

4.2 Introduction

The Palaeocene reservoir sands of the Central North Sea contain almost one half of the recoverable oil reserves within this region, ($476x10^6m^3$, 2.99Bbbbl: Brennand et al. 1990) estimated to be approximately $956x10^6m^3$, 6.01Bbbl (Brennand et al. 1990). The larger fields such as Forties, (Block 21/10), and Maureen, (Block 16/29), have been in production since the 1970s (Abbotts 1991). Surprisingly little has been published concerning the diagenesis of these sands (Pagan 1980; Tonkin & Fraser 1991; Watson 1993a). The diagenesis of Lower Palaeocene volcanic-rich shale layers within the Central North Sea have been studied by Huggett (1992) and Pearson (1990). Authigenic kaolinites from Montrose Group sandstones are described and isotopic data has been measured from authigenic kaolinite separates. This is integrated with petrographic data to interpret pore-fluid evolution in the Palaoecene sandstones

The Palaeocene Montrose Group, (Deegan & Scull 1977), is a sequence of submarine fan systems which form extensive sand-rich basin-floor aprons (Stewart 1987). The sands are similar to braided channel deposits laid down in mid-fan suprafan lobes as described by Walker (1978). The three formations, Maureen, Andrew and Forties, are similar lithostratigraphic stacked composite sandbodies. The dominant Andrew Formation is the uppermost sandstone unit within the Witch Ground Graben overlain by a thin sequence of Forties Formation mudstones and siltstones. The Andrew Formation is made up of amalgamated submarine channels of high connectivity (Den Hartog Jager et al. 1993). This makes it an ideal aquifer to transport fluids. It was selected in this study in the expectation that the hydrology of this formation would be influenced by open connection to the proximal areas in the Outer Moray Firth. After deposition of the Montrose Group, the Moray Group delta system prograded over the Montrose Group within the Outer Moray Firth (Rochow 1981). Provenance and

palaeogeographical studies indicate that the sources for detrital grains were Palaeozoic or Mesozoic sediments from the southern part of the East Shetland Platform (Morton et al. 1993), and possibly eroded Dalradian schists from the Scottish Highlands (Morton 1987), both areas experienced uplift during the early Tertiary. Sediments were transported eastwards to be deposited in the subsiding Central North Sea along basins overlying pre-existing Mesozoic grabens (Knox et al. 1981). An intermittent supply of volcanic debris (clasts and wind-blown ashes) was carried over the Scottish Highland watershed from the West of Scotland igneous centres (Jacque & Thouvenin 1975).

After deposition the sediments experienced a relatively simple sag pattern of subsidence, with particularly rapid burial during the Palaeocene-Eocene (Barnard & Bastow 1992). Interpretation of seismic reflection data suggests that no major faults cut the Palaeocene sequence (Milton et al. 1990). Thus the original depositional aquifer connections are intact without tectonically induced fluid barriers or conduits.

4.3 Methodology

Core samples from the Montrose Group, were taken from ten wells located in the Central North Sea **Table 4.1, Figure 4.1.**
Samples have been examined by standard petrographic techniques including point count analyses (500 points) of resin-impregnated thin-sections to quantify detrital mineralogy, authigenic cements and porosity. In addition point count data from wells 16/28-4, 16/28-5, 21/10-FB55, 22,12-5 and 22/12-7 from BP reports were available. Rock stubs were examined using a scanning electron microscope (SEM) to determine the morphology, composition and distribution of the authigenic minerals. Kaolinite separates were extracted from wells 14/13-3, 15/20-4, 16/28-6, 16/29-2, 22/17-4, 22/20-3 and 23/16-4. Kaolinite extraction follows the method of Jackson (1979); disaggregation of the rock, separation of the clay fraction, oxidation of organic material, deflocculation of the clays and separation into size fractions by settling and centrifugation. Size fractions refer to theoretical settling times of perfect spheres through pure water at 20°C so the 0.1μm size fraction does not necessarily refer to clay grains 0.1μm across. The 0.1μm to 10μm size fractions were selected for isotope analyses on the basis of a high kaolinite percentage estimated from SEM analysis and X-ray Diffraction (XRD) analyses. XRD traces of kaolinite standards were used to test for the presence of dickite. XRD traces indicated that most samples had less than 5% silicate contaminant. As proportions of the silicate impurities are unreliable, at <10% volume total from XRD analysis and no isotopic information is known about these fractions, no corrections were made. Oxygen isotopic analysis follows the method of Clayton and Mayeda (1963), and hydrogen analysis follows the method of Biegelman et al. (1952). All isotopic data are presented in per mil values with respect to Standard Mean Ocean Water (SMOW). The analytical error of laboratory standard δD and $\delta^{18}O$ values was +5‰ and +0.3‰ respectively.

4.4 Petrography

Sandstone units are dominated by a thick-bedded structureless facies. The sandstones are generally fine-medium grained, poor-moderately sorted, uncompacted and sub-arkosic to sub-lithic in composition. In all wells monocrystalline quartz is the most abundant detrital grain type. Lithic fragments include: granitic clasts, polycrystalline quartz grains, and altered igneous clasts and volcanic glass with opaque mineral rims.

Feldspars show some degree of dissolution, the amount of secondary porosity is not significant being generally less than 4% of rock volume, **Figure 4.2.** Secondary porosity was identified from intergranular porosity within feldspars. Textural relationship of dissolution with respect to paragenetic sequence is unclear. Texturally early diagenetic smectite is seen within the intergranular voids as is diagenetically late calcite and texturally blocky kaolinite. There is also the possibility that detrital feldspars may have been deposited with secondary porosity. Secondary porosity is consistently slightly higher within wells 15/26-3, 15/26-4 21/10-1 and 22/15-2 being around 3 to 3.5% rock volume. Detrital illite-smectite clays coating grains are now partly recrystallised to a box-framework morphology. A characteristic of the thick-bedded and interconnected sand bodies is their regionally high porosities and permeabilities, see Chapter 5.

4.4.1 Diagenesis

A general paragenetic sequence is shown in **Figure 4.3.** The volumetrically dominant authigenic phases are quartz overgrowths and kaolinite and locally, calcite concretion 'doggers' (less than 2m thick), and strata-bound grain-coating chlorite. The paragenetic sequence can be divided into three stages

1. Early burial diagenesis; precipitation of disseminated dolomite, pyrite, chlorite, K-feldspar overgrowths, and microquartz precipitation.

2. Moderate burial diagenesis; petrographically early calcite 'doggers' with high minus-cement porosity (36.8-50.1%) within wells 14/13-3, 15/20-4, 15/26-3, 15/26-4 and 16/28-6 indicate that concretion growth began within a few hundred metres of burial (Sclater & Christie 1980; Stewart et al. 1993). Traces of etched vermiform kaolinite exist within these concretions but volumetrically more kaolinite is found within the sands. Vermiform kaolinite (**Figures 4.4, 4.5, 4.6**), growth therefore had begun by commencement of concretion precipitation and continued after calcite precipitation stopped. Kaolinite has a more developed blocky crystal shape within deeper-distal wells (**Figure 4.7, 4.8**). The proportions of vermiform to blocky kaolinite is not known within wells .

3. Late burial diagenesis consisted of continued quartz overgrowths and late carbonate concretions within wells 16/29-2, 21/10-1, 22/17-4, 22/20-3 and 23/16-4. Both blocky and vermiform kaolinite are seen intergrown and overgrown by thin and irregular quartz overgrowths (**Figure 4.8**). Quartz overgrowths engulfing kaolinite can be seen within shallower wells, though it is more apparent in the deeper wells. It is not known what proportion, if any, of the quartz overgrowths are inherited from the source area. Pitted quartz overgrowths indicative of sediment transport are seen which have no textural relationship to Lower Palaeocene authigenic phases. Within deep buried wells 16/28-6, 21/10-1, 22/17-4, 22/20-3 and 23/16-4, hairy illite precipitated upon the edges of frayed vermiform kaolinites, **Figure 4.9.**

Authigenic kaolinite is a ubiquitous but minor (generally less than 4%) mineral phase throughout cored sections, **Figure 4.10.** It forms ragged verms made up of pseudo-hexagonal plates (5-20 μm) which fill primary pores (**Figures 4.4 & 4.5**), or coarser flakes (50-100μm) between expanded detrital mica flakes (**Figure 4.6**). Within the deeper study wells, later kaolinite precipitation exhibits a blocky nature (**Figure 4.7**).

On the basis of XRD analysis there is no evidence for the formation of dickite with depth.

Two sampled wells (15/26-3 and 15/26-4) contain anomalously high percentages of kaolinite (up to 12% rock volume). Here kaolinite habit is predominantly ragged and vermiform. Verms are large, up to 100μm, and fill primary pore-spaces.

4.4.2 Mass balance

Using the equation from Osborne (1994), which can be written as
2V Feldspar = V Kaolinite + 4V Quartz,

$$2KAlSi_3O_8 + 2H^+(aq) + H_2O = 2K^+ + Al_2Si_2O_5(OH)_4 + 4SiO_2$$
$$2NaAlSi_3O_8 + 2H^+(aq) + H_2O = 2Na^+ + Al_2Si_2O_5(OH)_4 + 4SiO_2$$

$$2 \times 104.7 = 99.5 + 4 \times 22.7$$
$$209.4 = 99.5 + 90.8$$

from Osborne (1994) where V Feldspar, V Kaolinite, and V Quartz represent molar volumes of feldspar, kaolinite and quartz respectively, it is possible to determine whether the amount of kaolinite present within the sandstone can be generated by the amount of feldspar assumed to have dissolved out during burial. From SEM analysis of core stubs microporosity between kaolinite flakes from visual estimates will be 10's of percent. Nadeau & Hurst (1991) assume a 40% microporosity between kaolinite flakes. Point count estimates of kaolinite is also likely to be exaggerated due to the fine grained nature of the kaolinite. Point counts of secondary porosity are likely to be underestimated as oversized pores are likely to be crushed during mechanical compaction (Wilkinson et al. In prep). Average point count percentages for both secondary porosity and kaolinite is sligthly less than 2%. Consequently from the dissolution of feldspar, 0.9% kaolinite and 0.8% quartz overgrowth are expected to precipitate. Assuming a 40 % microporosity between kaolinite flakes (Nadeau & Hurst 1991) means that point-counted kaolinites should be ~1.2% rock volume. Actual point-counts from Palaeocene wells indicate an average of 2% kaolinite. These low values are well within point-counting errors and it is assumed that silica and aluminium are preserved within a thin-section scale. For wells 15/26-3 and 15/26-4 it is clear that values up to 12% kaolinite cannot be precipitated from the small volumes of secondary porosity point-counted within the sands. Point counts of secondary porosity are likely to be underestimated as oversized pores are likely to be crushed during mechanical compaction (Wilkinson et al. in prep).

Secondary porosity and kaolinite

It is currently accepted that authigenic kaolinite within sandstones precipitates during the dissolution of feldspars (Giles 1987; Macaulay et al. 1993). It would be expected that low secondary porosities are matched with low percentages of kaolinite. However a straightforward relationship between kaolinite and secondary porosity has rarely been shown petrographically. There are problems associated with showing a relationship;

1) The volume of secondary porosity within the sand grains during deposition is unknown. The Palaeocene sandstones are known to have been partly derived from

shallow buried Mesozoic sandstones on the East Shetland Platform and may have been deposited with initial secondary porosity.
2) Grains with extensive secondary porosity are crushed during burial.
3) The true volume of kaolinite is notoriously unreliable. Point-counted volumes of kaolinite are likely to overestimate the true volume of kaolinite present (Nadeau & Hurst 1991). Using an SEM, kaolinite clearly has microporosity between flakes which is not visible for the point-counter using standard petrographic microscopes.
4) Ions in porewater may be transported as a result of fluid-flow within the sandstones precipitating at a distance from initial feldspar dissolution. This movement of ions clearly takes place on a thin-section scale as kaolinite preferentially precipitates within intergranular porespaces and not in direct contact with secondary porosity

For Montrose Group sandstones as volumes of secondary porosity and kaolinite are low, no clear trends can be seen. Most values cluster around the origin, **Figure 4.11, 4.12.**

Assuming that no secondary porosity existed during deposition of the sands and 50% porosity between kaolinite plate indicates that overall more kaolinite exists that can be accounted for by secondary porosity in wells 15/26-3 and 15/26-4 (and possibly 23/16/-4 though point counted volumes are generally low). This discrepancy within these wells may relate to either the input of aluminium into the sands from an unknown source or the complete dissolution or crushing of skeletal feldspar grains reducing the amount of recognisable secondary porosity.

4.5 Isotopic data

4.5.1 Stable isotope principles

Assuming; 1) precipitation at a given temperature, 2) conditions of isotopic equilibrium, and 3) no post-precipitation isotope exchange has occurred, then the stable isotope composition of a mineral phase (δm) can be related to the isotopic composition of the fluid (δw), and the temperature of precipitation (T°K) by an equation of the form:

$$\delta m - \delta w = a/T^2 + b$$

where a and b are numerical constants (see e.g. Savin & Lee, 1988). For $\delta^{18}O$, a=2.5 and b=-2.87; Land & Dutton (1978). For δD, a=-4.53 and b=19.4; Lambert & Epstein (1980).

For any measured value of δ m, we can construct a plot of δw versus temperature which shows the locus of permissible values of δ w, T, **Figure 4.13.** For clay minerals, $\delta^{18}O$ and δD calibration curves of this type have been recently reviewed by Savin & Lee (1988).

The assumption must be made that the mineral has not undergone isotopic exchange after precipitation. Experimental work by O'Neil & Kharaka (1976) found that oxygen isotopic exchange for kaolinite is insignificant below 350°C. However, hydrogen isotope exchange from kaolinite with present day pore waters has been recorded by Bird & Chivas (1988), and Longstaffe & Ayalon (1990) at temperatures <80°C, and <40°C respectively. Hence oxygen isotopic ratios are indicative of the

temperature and porewater conditions of precipitation while hydrogen ratios may not be reliable.

4.5.2 Oxygen and hydrogen isotopes; results and discussion.

Isotopic analyses of kaolinites gave a range of $\delta^{18}O$= 8.9 to 23.1‰SMOW and δ D= -53.0 to -76.8‰SMOW (**Table 4.2, Figures 4.14 and 4.15**).

The range of $\delta^{18}O$ composition is broad within each well **Figure 4.14, 4.16**. Overall the 5th percentile is 11‰, 25th percentile is 13.2‰, 75th percentile is 16.8‰ and the 95th percentile is 20.1‰. The median value is 15.2‰. **Figure 4.17**

Assuming kaolinite precipitation from Palaeocene marine depositional pore-water ($\delta^{18}O$ = -0.9‰SMOW, δD = -7‰SMOW; Shackleton and Kennet, 1974) yields formation temperatures of between 52°C (95th percentile) and >100°C (5th percentile). Precipitation temperatures generated between the 25th percentile and the 75th percentile are between 74°C and 111°C **Figure 4.13**. Kaolinite separates are from burial depths between 7000 and 9000feet and such precipitation temperatures, near to current well temperatures, would indicate that kaolinites are a late diagenetic phase unless there was an anomolous rise in temperature during burial. As kaolinite is not petrographically the last diagenetic phase to form (**Figures 4.8, 4.9**) these temperatures are deemed unlikely. On a δD-$\delta^{18}O$ cross-plot (**Figure 4.15**), the values lie below theoretical compositions for kaolinites which could have precipitated from marine water, at any temperature. To suggest that original Palaeocene marine pore-fluids were present during kaolinite precipitation, would also require exchange with an isotopically depleted hydrogen source of at least -40‰SMOW with respect to depositional marine water. Therefore it is considered that marine water was an unlikely pore-fluid during kaolinite precipitation.

Texturally early (36.8-50.1% minus-cement porosity) calcite concretions from wells 15/20-4, 15/26-3, 15/26-4 and 16/28-6, which pre-date kaolinite have $\delta^{18}O$ compositions of 18.0 to 22.7‰SMOW, Chapter 2. Precipitation at shallow burial (i.e. at temperatures <25°C) would necessitate a pore-water composition similar to that of early Tertiary meteoric water, $\delta^{18}O$ = -10‰SMOW, δD = -85‰SMOW; Forester and Taylor 1977; Stewart et al 1993). Since the bulk of kaolinite post-dates early concretion growth, Palaeocene meteoric water could therefore have been a possible pore-fluid during kaolinite growth. This would indicate kaolinite precipitation at 17°C (75th percentile) to 38°C (25th percentile). Such temperatures would suggest a syn-depositional origin for the kaolinites which contradicts petrographic evidence for growth during moderate to late burial diagenesis Hydrogen isotope values are also incompatible with kaolinite precipitation from meteoric water. On the δD–$\delta^{18}O$ cross-plot (**Figure 4.15**), isotopic compositions lie well above theoretical compositions calculated for kaolinite precipitated from Tertiary meteoric water. δD compositions lie above the -85‰SMOW value estimated for early Tertiary meteoric water (Forester and Taylor, 1977). Post-precipitation exchange with isotopically enriched hydrogen with respect to meteoric water of +40‰SMOW is required if kaolinite precipitated from meteoric water. We therefore consider a meteoric formation water to be unlikely.

A mixed water of a marine dominated composition is hence the most likely pore-water during kaolinite precipitation. From the δD-$\delta^{18}O$ cross-plot kaolinite could have precipitated from pore-waters with $\delta^{18}O$ between -6.5 and -4‰SMOW (**Figure 4.15**) generated by simple mixing of Palaeocene marine and meteoric waters. The proportion of early Tertiary meteoric water required would be at most 65%. Resulting precipitation temperatures of between 35 and 80°C are compatible with the paragenetic sequence

Precipitation depths - It would be wrong for geologists to interpret kaolinite precipitation temperatures in terms of burial depth without taking account variation in paleao-thermocline and palaeo-surface water temperatures. The actual temperature of the bottom of the Tertiary North Sea is unknown (see Chapter 2). However there is strong evidence that surface water temperatures were elevated during the late Palaeocene to mid Eocene. Oxygen isotopic data from fossil shallow living molluscs can be interpreted as a rise in the surface temperature of seawater from 10-13°C to 22-28°C reaching a maximum art around 47Ma (Burchardt 1978). Geologists should be wary of applying thermoclines where bottom waters reach 5°C at the seafloor during this warming period. The spread of isotopic values of kaolinite separates is likely to point to precipitation over a period of time during burial history and not to one specific time where the chemical system was altered resulting in kaolinite precipitation.

4.5.3 Hydrogen isotope exchange?

Macaulay et al. (1993) have raised the possibility that during precipitation of kaolinites within the North Sea Upper Jurassic Magnus Sands, the presence of 'organic-water' ($-90 > \delta D > -250$‰, Sheppard and Charef, 1986) may have been responsible for remarkably low δD values. Abnormally depleted $\delta^{13}C$ values (up to -30‰PDB) in the Lower Palaeocene early calcite concretions, in wells 15/20-4 and 16/28-6, that predated the bulk of kaolinite precipitation provide evidence that hydrocarbon were present within the Palaeogene sands during the early Tertiary within the Fisher Bank Basin and Frigg Basin area (Stewart et al. 1993, Watson 1993b). These hydrocarbons may have been early oil migrating into the sands or methane produced in-situ within the Montrose sands during early burial. Abnormally depleted hydrogen isotope compositions have not been observed in the kaolinites in this study, though from the $\delta^{13}C$ values of the concretionary calcites in wells 15/20-4 and 16/28-6, hydrocarbons had already been present in the sands at this time. Any involvement of isotopically depleted organic hydrogen would result in kaolinite being interpreted as precipitating at lower temperatures (within increasingly meteoric water) than the 35 to 80°C already indicated. It is therefore concluded that measured kaolinite δD values have not been influenced by hydrogen (of low δD) associated with organic matter. Further, there is no evidence for post-precipitation hydrogen isotope exchange leading to uniform δD values as observed by Longstaffe and Ayalon (1990).

4.5.4 Timing of meteoric ingress

The introduction of meteoric water into these marine sandstones could have occurred during the Palaeocene/early Eocene. This was a period of widespread regression within the North Sea (Milton et al. 1990) during the deposition of the Montrose and Moray Groups (63 to 54Ma, Milton et al. 1990; 61 to ~56Ma, Jones & Milton 1994)

when there was a 800m relative sea- level (Jones & and Milton 1994). This sea-level fall has previously been suggested by Barnard & Bastow (1992) to have caused the degradation of hydrocarbons within the Northern North Sea. From the distribution of early Eocene lignite beds within the overlying Beauly Formation (Milton et al. 1990; Mudge & Copestake 1992), the presence of a wide coastal plain extending eastwards at least to Quads 14 and 15 (Milton et al 1990, Timbrell 1993) has been deduced. This lies directly over the thickest and shallowest section of the Lower Palaeocene sands, indicating that there was a large body of fresh water in the proximal part of the Lower Palaeocene aquifer. The introduction of meteoric water into the sands would have been aided by the meteoric head from the adjacent elevated East Shetland Platform which supplied sediment throughout the early Tertiary (Knox et al. 1981). A second-order marine transgression across the East Shetland Platform (Milton et al. 1990) took place in the Eocene. This would have cut off the supply of meteoric water into the sands. De-watering of the marine mudrocks overlying the hydrostatically pressured sands could have supplied basinal pore-water into the sands resulting in the mixing of isotopically different waters during kaolinite growth. A later significant period of relative sea-level fall also took place during the late Eocene (Jones and Milton 1994) where a sub- arial erosion surface is present over the Outer Moray Firth. A further period of meteoric recharge is proposed to have occurred during the Miocene by Mason et al. (1995). This is used to explain the occurrence of degraded oils within Palaeogene oilfields in the Outer Witch Ground Graben. Meteoric water could also have entered the Montrose Group sands at this time. However a thick blanket of muds over the Montrose Group at these times may have acted as an aquiclude during this period. It is possible that kaolinite growth may have been triggered by the changes of hydrogeological states, i.e. during meteoric incursion in the late Palaeocene/early Eocene and late Eocene.

4.6 Conclusions

1. Combined oxygen and hydrogen stable isotopic data suggest that kaolinite was precipitated from mixed meteoric- marine water, ($\delta^{18}O$ = -6.5 to -4‰SMOW, δD= -52 to -28‰SMOW at temperatures between 35 to 80°C. This is compatible with petrographic and isotopic data from early calcite concretions.

2. Pore water evolution can be tentatively related to Palaeogene sea-level changes. Depositional marine pore-waters were displaced during deposition of the Palaeocene sandstones by meteoric water flushing as a result of eastward progradation of deltaic deposits which reached a maximum extent during the latest Palaeocene/early Eocene (54.8 to 54.0 Ma). Meteoric influx was cut off by a marine transgression (54.0 Ma) and westwards migration of the coastline within the North Sea Basin. Meteoric ingress may have been renewed at 37Ma, during the late Eocene.

Acknowledgements Robert Stewart acknowledges NERC award no. GT4/90/GS/51. We would also like to thank Dr Mark Wilkinson for useful discussions, and the technical support at S.U.R.R.C.. The Isotope Geosciences Unit at S.U.R.R.C. is funded by NERC and the Scottish Universities.

References

ABBOTTS I.L.(ed.) (1991) 565 Pp. *United kingdom Oil and Gas Fields, 20 Years Commemorative Volume. Geol. Soc. Memoir* **No. 14,** London.

BARNARD P.C. & BASTOW, M. A. (1992) Hydrocarbon generation, migration, alteration, entrapment and mixing in the Central and Northern North Sea. Pp. 167- 190 in: *Petroleum Migration* (W.A. England & A.J. Fleet, editors). *Geol. Soc. Spec. Publ.* **No. 59**, London.

BIEGELMAN J., PERLMAN, M. L. & PROSSER H, C, (1952) Conversion of hydrogenic materials to hydrogen for isotopic analysis. *Anal. Chem.* **24**, 1356.

BIRD M.I. & CHIVAS A.R. (1988) Stable isotope evidence for low temperature kaolinitic weathering and post-formational hydrogen exchange in Permian kaolinites. *Chem. Geol.* **72**, 249-265.

BRENNAND T.P., VAN HOORN B. & JAMES K.H. (1990) Historical Review of North Sea Exploration. Pp. 1-33 in: *Introduction to the Petroleum Geology of the North Sea* (K.W. Glennie, editor) Blackwell Scientific Publications, London.

BURCHARDT B. (1978) Oxygen isotopes palaeotemperatures from the Tertiary period in the North Sea area. *Nature*, **275**, 121-123.

CARMAN G.J. & YOUNG R. 1981 Reservoir geology of the Forties Oilfield. Pp. 371-379 in: *Petroleum Geology of North West Europe* (J. Brooks K.W. Glennie, editors. Graham & Trotman, London.

CLAYTON R.N. & MAYEDA T.K. (1963) The use of bromine pentafluoride in the extraction of oxygen from oxides and silicates for oxygen analysis. *Geochim. Cosmochim.* Acta. **27**, 43-52.

DEEGAN C.E. & SCULL. B.J. (1977) A standard lithostratigraphic nomenclature for the central and northern North Sea, *Inst. Geol. Sci. Bull. Norwegian Petrol Direct .Report.* **77/25**, 36pp.

DEN HARTOG JAGER D., GILES M.R. & GRFFITHS G.R. (1993) Evolution of Paleogene submarine fans of the North Sea in time and space. Pp. 59-71 in: *Petroleum Geology of Northwest Europe* (J.R. Parker, editor). Geol. Soc., London.

FOLK R.L. (1974) 182pp. *Petrology of Sedimentary Rocks*, Hemphill Publishing Company, Austin.

FORESTER R.A.W. & TAYLOR H.P. (1977) $^{18}O/^{16}O$, D/H, and $^{13}C/^{12}C$ studies of the Tertiary igneous complex of Skye, Scotland. *American Journal of Science* **277**, 136-177.

GILES M.R. (1987) Mass transfer and problems of secondary porosity creation in deeply buried hydrocarbon reservoir. *Marine and Petroleum Geology*, **4**, 188-204.

GILES M.R., STEVENSON S., MARTIN S.V., CANNON S.J.C., HAMILTON P.J., MARSHALL J.D. & SAMWAYS G.M. (1992) The reservoir properties and diagenesis of the Brent Group: a regional perspective. Pp. 289-327 in: *Geology of the Brent Group* (A.C. Morton, R.S. Haszeldine, M.R. Giles S. Brown, editors). *Geol. Soc. Spec. Publ.* **No. 61**, London.

HASZELDINE R. S., BRINT J.F., FALLICK A.E., HAMILTON P.J. & BROWN S. (1992) Open and restricted hydrologies in Brent Group diagenesis: North Sea. Pp. 401-419 in*: Geology of the Brent Group* (A.C. Morton, R.S. Haszeldine, M.R. Giles S. Brown, editors). *Geol. Soc. Spec. Publ.* **No. 61**, London.

HUGGETT J.M. (1992) Petrography, Mineralogy, and Diagenesis of overpressured Tertiary and Late Cretaceous mudrocks from the East Shetland Basin. *Clay Miner.* **27**, 487-506.

JACKSON M. L. (1979) 895 pp *Soil Chemical Analyses advanced course* 2nd edition: Published by the author, Madison, Wisconsin 53705.

JACQUE M. & THOUVENIN J. (1975) Lower Tertiary tuffs and volcanic activity in the North Sea. Pp. 455-465 in: *Petroleum and the continental shelf of north-west Europe* (A.W. Woodland, editor). New York, John Wiley.

JONES R.W. & N.J. MILTON (1994) Sequence development during uplift: Palaeogene stratigraphy and relative sea-level history of the Outer Moray Firth, UK North Sea. *Marine and Petroleum Geology*, **11**, 157-165.

KNOX, R.W.O'B., MORTON, A.C. & R. HARLAND (1993) Stratigraphic relationships of Palaeocene sands in the UK Sector of the central North Sea. In: *Petroleum Geology of the Continental Shelf of North West Europe*, by L.V. Illing and G.D. Hobson (eds), Institute of Petroleum, Heyden and Son, London, 267-281.

LAMBERT S.J. & EPSTEIN S. (1980) Stable isotope investigations of an active geothermal system in Valles Caldera, Jemez Mountains, New Mexico. *J. Volcan. Geotherm. Res.*, **8**, p111-1129.

LAND L.S. & DUTTON S.P. (1978) Cementation of a Pennsylvanian deltaic sandstone: Isotopic data. *J. Sed. Pet.* **48**, 1167-1176

LONGSTAFFE F.J. & AYALON A. (1990) Hydrogen-isotope geochemistry of diagenetic clay minerals from Cretaceous sandstones, Alberta, Canada: evidence for exchange. *App. Geochem.* **5**, 657-668.

MACAULAY C.I., FALLICK A.E. & HASZELDINE R.S. (1993) Textural and isotopic variations in diagenetic kaolinite from the Magnus Oilfield Sandstones. *Clay Miner.* **28**, 625-639.

MASON P.C., BURWOOD R. & MYCKE B. (1995) The reservoir geochemistry and petroleum charging histories of Palaeogene-reservoired fields in the Outer Witch Ground Graben. Pp.281-302 in: *The Geochemistry of Reservoirs* (J.M. Cubitt & W.A. England, editors). *Geol. Soc. Spec. Publ.* **No 86**, London.

MILTON N.J., BERTRAM G.T. & VANN I.R. (1990) Early Palaeogene tectonics and sedimentation in the Central North Sea. Pp. 339-351 in: *Tectonic Events Responsible for Britain's Oil and Gas Reserves* (R.F.P. Hardman & J. Brooks, editors). *Geol. Soc. Spec. Publ.* **No. 55**, London.

MORTON A.C., HALSWORTH C.R. & WILKINSON G.C. (1993) Stratigraphic evolution of sand provenance during Palaeocene deposition in the Northern North Sea Area. Pp. 73-84 in: *Petroleum Geology of Northwest Europe* (J.R. Parker, editor). Geol. Soc., London.

MORTON A.C. (1987) Influences of provenance and diagenesis on detrital garnet suites in the Paleocene Forties Sandstone, Central North Sea. *Journal of Sedimentary Petrology* **57**, 1027-1032.

MUDGE D.C. & COPESTAKE P. (1992) Revised Lower Palaeocene lithostratigraphy for the Outer Moray Firth, North Sea. *Marine and Petroleum Geology* **9**, 53-69.

NADEAU P.H. & HURST A. (1991) Application of back-scattered electron microscopy to the quantification of clay mineral microporosity in sandstone. *Journal of Sedimentary Petrology*, **61**, 921-925.

O'NEIL J.R. & KHARAKA Y.K. (1976) Hydrogen and oxygen isotope exchange reactions between clay minerals and water. *Geochim. Cosmochim. Acta* **40**, 241- 246.

OSBORNE M. (1994) *The effect of differing hydrogeological regimes on sandstone diagenesis: Brent Group oilfields, U.K. North Sea.*Ph.D. Thesis, Glasgow University.

PAGAN M.C.T. (1980) *Diagenesis of the Forties Field sandstone.* M. Phil. Thesis, University of Edinburgh.

PEARSON M.J. (1990) Clay mineral distribution and provenance in Mesozoic and Tertiary mudrocks of the Moray Firth and Northern North Sea. *Clay Miner.* **25**, 519-541.

ROCHOW K.A. (1981) Seismic stratigraphy of the North Sea 'Palaeogene' deposits. In*: Petroleum Geology of the Continental Shelf of North- West Europe*, I.V. Illing and G.D. Hobson (eds), Heyden, London, 225-266.

SAVIN S.M. & LEE M. (1988) Isotopic studies of phyllosilicates. in*: Hydrous Phyllosilicates (exclusive of micas)* (S.W. Bailey, editor) Miner. Soc. Am., *Reviews in Mineralogy* **16**, 188-233.

SCLATER J.G. & CHRISTIE P.A.F. (1980) Continental stretching: an explanation of the post-mid Cretaceous subsidence of the Central North Sea. *Journal of Geophysical Research* **85**, 3711-3739.

SHACKLETON N.J. & KENNET J.P. (1974) Paleotemperature history of the Cenozoic and the initiation of Antarctic glaciation: oxygen and carbon isotope analysis in DSDP sites 277, 279, 281. Pp 743-755 in: (J.P. Kennet, R.E. Houtz et al., editors) *Initial Reports of the Deep Sea Drilling Project* **29**, Washington (U. S. Government Printing Office).

SHEPPARD S.M.F. & CHAREF A. (1986) Eau organique: characterisation isotopique et evidence de son role dans le gisement Pb-Zn de Fedj-el-Adoum, Tunisie. *C. R. Acad. Sci. Paris.* t. 302, serie II, **19**, 1189-1192.

SCHMITZ B. & HEILMAN-CLAUSEN C. (1993) A stable isotope ($\delta^{18}O$, $\delta^{13}C$) and iridium stratigraphy across the Early Eocene section at Albaek Hoved, Denmark. Conference *abstracts Correlation of the Early Palaeogene in Northwest Europe*, Geol. Soc. London, December, 30.

STEWART I.J. (1987) A revised stratigraphic interpretation of the Early Palaeogene of the Central North Sea. Pp. 557-577 in *Petroleum Geology of North West Europe* (J. Brooks & K.W. Glennie, editors) Graham & Trotman, London.

STEWART R.N T., HASZELDINE R.S., FALLICK A.E., ANDERTON R. & DIXON R. (1993) Shallow Calcite Cementation in a Submarine Fan; Biodegradation of Vertically Migrating Oil? Abstract in: *A.A.P.G Annual Convention Am. Assoc. Petrol. Geol.*p. 186

TONKIN P.C. & FRASER A.R. (1991) The Balmoral Field. Pp. 237-243 in*: United Kingdom Oil and Gas fields, 25 Years Commemorative Volume.* (I.L. Abbots, editor). *Geol. Soc. Memoir* **No. 14**, London.

TIMBRELL G. (1993) Sandstone architecture of the Balder Formation depositional system, UK Quadrant 9 and adjacent areas. Pp. 107-121 in: *Petroleum Geology of Northwest Europe* (J. R. Parker, editor). Geol. Soc., London.

WALKER R.G. (1978) Deep-water sandstone facies and ancient submarine fans; models for exploration for stratigraphic traps. *Bull Am. Assoc. Pet. Geol.* **62**, 932-966.

WATSON R.S. (1993)(a*) The Diagenesis of the Tertiary Sands from the Forth and Balmoral Fields, Northern North Sea.* PhD Thesis, University of Aberdeen, pp 315.

WATSON R. (1993)(b) The Forth Field, British Sector, North Sea: evidence of palaeo-oil leakage in a near surface reservoir. Abstract in: *A.A.P.G Annual Convention, Am. Assoc. Petrol. Geol.* p. 198

WILKINSON M., DARBY D., & R.S. HASZELDINE 1995 Late secondary porosity associated with overpressure leak-off: evidence from the Fulmar Formation, UK Central North Sea. in prep.

Figure captions

Figure 4.1 Central North Sea showing location of sample wells and base Cretaceous structural elements

Figure 4.2 Secondary porosity with depth, supplemented with BP point-counted data from wells 16/28-4, 21/10-FB55, 22/12-7. Secondary porosity generally makes less than 4% of rock volume. Wells 15/26-3, 15/26-4, 22/12-7 and 22/17-4 contain more secondary porosity than other sample wells.

Figure 4.3 Paragenetic sequence for Montrose Group sandstones. Kaolinite post-dates eo-genetic mineral cements, but pre-dates petrographically late quartz overgrowths and fibrous illite.

Figure 4.4 SEM photomicrograph. Cluster of pore-filling vermiform kaolinite maintains pore-space. Well 15/20-4, 1981m.

Figure 4.5 SEM photomicrograph. Pore-filling vermiform kaolinite from well 15/26-4, cored depth 2070.2m. Kaolinite forms up to 12% rock volume within this well.

Figure 4.6 SEM photomicrograph. Larger vermiform kaolinite up to 100μm across fill spaces created by expanded mica flakes. Well 16/28-6, 2631.0m.

Figure 4.7 SEM photomicrograph. With greater burial a more blocky habit of kaolinite predominates. Blocky habit kaolinites often appear to overgrow kaolinite verms Well 23/16-4, 2309.63m.

Figure 4.8 SEM photomicrograph. Blocky kaolinite within well 15/26-3 overgrown by later quartz overgrowths. Cored depth 1876.5m.

Figure 4.9 SEM photomicrograph. At depth greater than 2500m, fibrous illite precipitates upon the edge of fraying kaolinite flakes. Well 16/28-6, 2734m.

Figure 4.10 Kaolinite percentage versus depth. Within wells 15/26-3 and 15/26-4 substantially more kaolinite (up to 12% rock volume) is seen compared with other wells.

Figure 4.11 Secondary porosity (% - horizontal axis) vs kaolinite (% - vertical axis) plots for individual wells. No wells show a linear relationship between secondary porosity and kaolinite that would be expected if kaolinite and authigenic quartz were derived simply from the dissolution of feldspar.

Figure 4.12 Secondary porosity (%) vs kaolinite (%) plots for all well . The line 2Vfeldspar=Vkaolinite refers to the relationship if kaolinite is derived from the disolution of feldspar. The line Vfeldspar=Vkaolinite adjusts the former relatioship assuming 50% porosity between kaolinite flakes. Most volumes are low, less that 3% secondary porosity, and kaolinite cluster at the origin. Wells 15/26-3 and 15/26-4 show a distinct excess of kaolinite than can be acounted for by point-counted seconary porosity.

Figure 4.13 Precipitation temperature vs δ^{18}OSMOW (kaolinite) plot. Two possible porewaters are marked, Tertiary meteoric water and marine water ($\delta^{18}O$ = -10‰SMOW and -0.9‰SMOW respectivley; Forester & Taylor 1977 and Shackleton & Kennet 1974). Two kaolinite composition of 13 and 17‰SMOW, close to 25th and 75th percentiles 13.2 and 16.8‰SMOW (all wells), are marked as thick curved lines. Intersection of kaolinite and porewater values are carried over horizontally to the vertical axis where precipitation temperatures can be read off.

Figure 4.14 Oxygen isotope histograms of kaolinite values from individual wells. Values range from 8.9‰SMOW in well 15/20-4 to 23.1‰SMOW in well 23/16-4.

Figure 4.15 Cross-plot of diagenetic kaolinite isotopic composition ($\delta^{18}O$ vs. δD). Solid lines represents compositions of kaolinites which theoretically would precipitate out of waters of differing compositions. Porewaters -9, -7, -5, and -3‰ lie on a simple mixing line between Tertiary meteoric (-10‰SMOW, Forester & Taylor 1977) and marine waters (-0.9 ‰SMOW, Shackleton & Kennet 1974). Dashed lines represent isotherms in °C. Simple interpretation of kaolinite compositions indicates that kaolinite precipitated out of mixed meteoric -marine porewaters of between $\delta^{18}O$=-6.5 and -4.0‰SMOW at temperatures of between 35-80°C.

Figure 4.16 Box plots of kaolinite oxygen isotope values, n=4, 14/13-3; n=23 15/20-4; n=3 15/28-5; n=16 16/28-6; n=8 16/29-2; n=4 22/17-4; n=11 23/16-4. Each box has a line inside, this line shows the median value. The top and bottom of the box marks the limits of 25% of the variable population; each box contains 50% of the data.

Figure 4.17 Percentile plot of kaolinite oxygen isotopvalues from all wells. Vertical line in box shows the median value. The dashed vertical line represents 25% and 75% of the data. The edge of the box represents 5% and 95% of the data. The 25th and 75th percentiles are 13.2 and 16.7‰SMOW respectively.

Tables

Table 4.1 Sampled wells

14/13-3	15/26-3	16/28-6	21/10-1	22/20-3
15/20-4	15/26-4	16/29-2	22/17-4	23/16-4

Table 4.2 Isotopic compositions of kaolinite

Well	cored depth (m)	size (μm)	δ^{18}OSMOW	δDSMOW
14/13-3	826.90	2	15.6	
	826.90	0.5	14.2	
	829.60	2	11.5	
	829.60	0.5	17.5	
15/18-5	1679.00	2	17.6	
	1686.00	2	11.8	
	1686.00	0.1	17.7	
15/20-4	1975.00	10	14.9	-52.9
	1975.00	10	19.4	
	1975.00	5	15.3	-54.2
	1975.00	2	15.4	
	1975.00	2	13.8	
	1975.00	0.5	15.3	
	1975.00	0.1	15.1	
	1975.00	0.1	20.1	
	1975.00	0.1	11.2	
	1981.00	5	15.0	
	1981.00	0.5	14.1	
	1986.85	5	15.6	
	2002.60	5	21.0	
	2013.55	5	15.1	
	2013.55	5	10.7	
	2019.40	10	16.2	-70.1
	2019.40	2	15.8	
	2019.40	2	11.0	-63.9
	2019.40	0.1	13.6	
	2019.40	0.1	10.8	
	2019.40	0.1	15.0	
16/28-6	2585.50	10	11.5	
	2585.50	2	14.0	
	2585.80	5	15.1	
	2598.75	10	15.0	-55.6
	2598.75	5	15.2	-70.5
	2598.75	2	16.2	
	2598.75	2	14.5	
	2660.25	5	20.0	
	2660.25	5	16.7	
	2689.75	5	17.1	
	2675.70	2	13.2	
	2705.75	2	11.0	
	2734.50	2	13.4	
	2734.50	2	10.6	
16/29-2	2638.16	2	13.5	

	2638.16	0.5	15.2	
	2638.16	0.1	13.4	
	2654.80	2	14.1	-71.3
	2654.80	0.1	12.6	
	2683.51	2	12.7	
	2683.51	2	15.5	-55.1
	2683.51	1	14.5	-53.0
22/17-4	2580.43	2	15.4	
	2580.43	0.5	12.8	-55.5
	2644.44	5	13.2	
	2644.44	2	12.1	-58.0
22/20-3	2689.70	2	17.3	
23/16-4	2150.19	2	17.6	
	2155.82	2	18.6	
	2161.65	2	16.7	
	2161.65	1	15.6	
	2161.65	0.5	15.8	-76.8
	2180.25	1	19.8	-58.6
	2180.25	0.1	16.8	-76.8
	2180.25	0.1	12.9	
	2180.95	2	17.4	
	2309.65	1	23.1	
	2309.65	0.5	15.5	

Well	Depth (m)	Grain size (μm)	δ^{18}OSMOW	δD
Brint (1989) mixed habit				
211/18-A45	2628.0	2-5	16.9	-48
211/18-A45	2630.0	2-5	16.0	-66
211/18-A45	2631	2-5	16.0	-66
211/18-A45	2634	2-5	16.9	-54
211/18-A45	2800	2-5	17.7	-68
211/18-A30	2741	2-5	16.1	-54
211/18-A31	2756	2-5	15.8	-59
211/18-A31	2768	2-5	17.2	-49
211/18-A31	3012	2-5	15.1	-55
211/19-4	3048	2-5	17.1	-61
211/19-4	3056	2-5	17.0	-58
211/19-4	3187	2-5	16.7	-55
211/19-6	2875	2-5	15.6	-57
211/23-2	2875	2-5	15.6	-57
211/23-2	2880	2-5	16.1	-54
211/23-3	2711	2-5	15.8	-67
211/23-4	2765	2-5	16.7	-67
211/23-4	2831	2-5	18.3	-58
211/23-4	1838	2-5	17.2	-66
Glasmann et al. (1989) blocky habit				
2/5-3	3353.1	2-10	13.5	-52
2/5-4	2962.7	2-15	13.9	-52
2/5-9	3325.9	2-15	14.6	-34
2/5-9	3325.9	10-20	14.5	-44
2/5-12A	3569.6	2-15	13.6	-44
2/5-12A	3581.9	2-15	13.1	-60
2/5-12A	3590.0	2-15	13.6	-54
2/5-H4	3619.8	2-15	13.7	-54
2/5-H4	3625.4	2-15	13.6	-53
2/5-H4	3654.6	2-15	14.3	-56
2/5-H4	4323.9	2-15	14.3	-58
MacAulay et al (1994) Dickite/blocky habit				
211/27-c12	11530ft	2-5	13.4	-47
211/27-A8	11607ft	2-5	13.3	-44
211/27-A22	11806ft	8-15	12.8	-50
211/27-A22	11806ft	5-8	11.3	-47
211/27-A22	12031ft	8-15	12.9	-42
211/27-A22	12058ft	8-15	12.6	-50
211/27-A22	12058ft	5-8	11.0	-47
211/27-A22	12058ft	2-5	13.4	-49
211/27-A17	11956ft	2-5	13.8	-48
211/27-A22	12084ft	8-15	14.4	-36

211/27-A28	12779ft	8-15	13.3	-38
211/27-A28	13064ft	8-15	13.0	-33
MacAulay et al. (1994) vermiform				
211/27-2	10541ft	2-5	14.3	-49
211/27-2	10562ft	0.2-0.5	14.5	-48
Osborne et al. (1994) vermifrom habit				
2/10-a6	1672.8	0.5-2	16.7	-55
2/10-a6	1672.8	2-10	17.7	-53
2/10-a6	1672.8	53-64	18.3	-47
2/10-a7	1638.6	<0.5	16.9	-54
2/10-a7	1648.7	2-10	17.0	-68
2/10-a7	1679.5	2-10	16.1	-54
2/10-a7	1679.5	0.5-2	16.3	-54
3/11-b3	1681.0	0.5-2	16.4	-58
3/11-b3	1681.6	2-10	17.2	-56
3/11-b3	1681.6	2-10	18.5	-67
3/11-b3	1682.8	2-10	17.2	-49

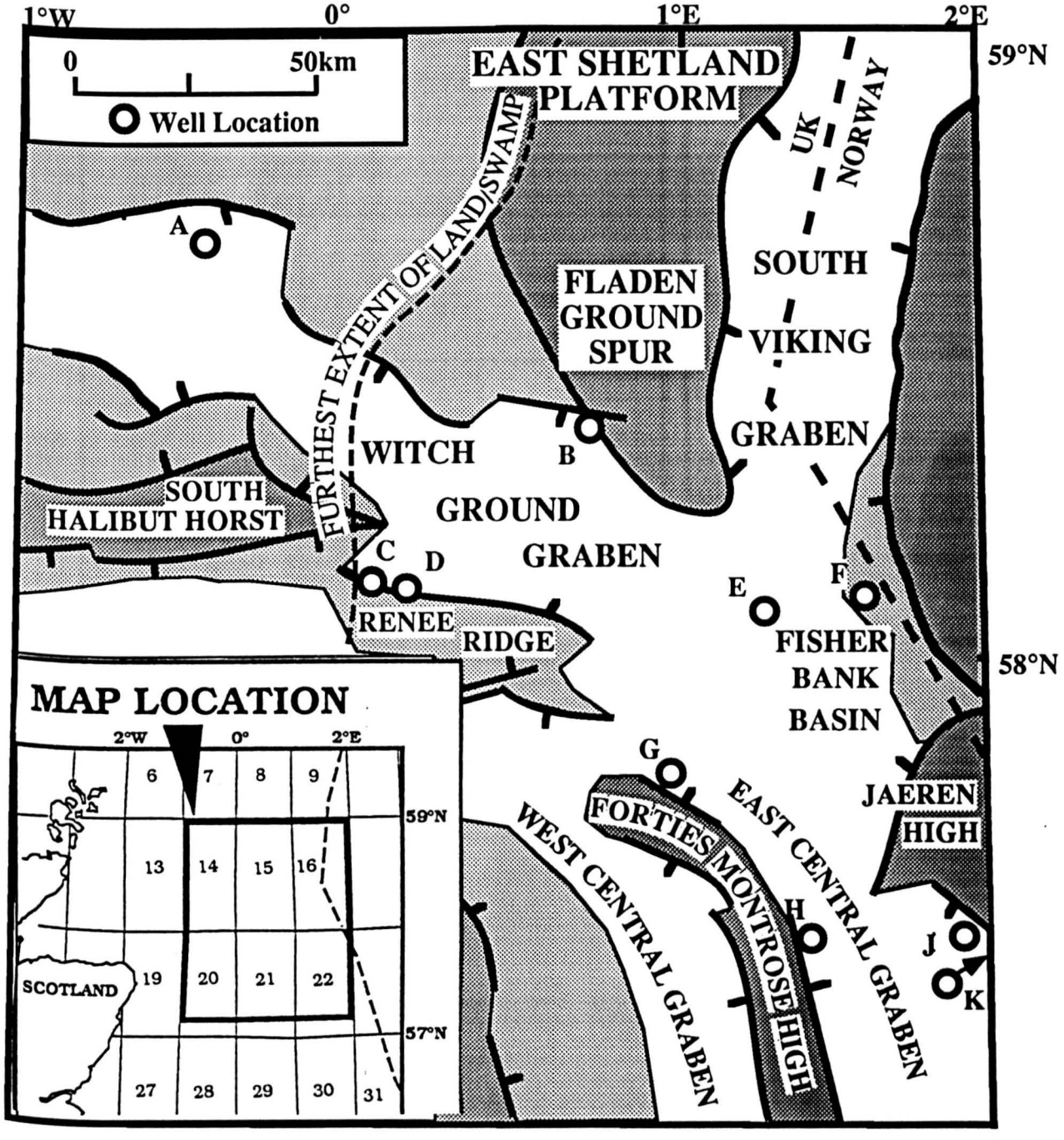

Figure 4.1 Location Map

A - 14/13-3	F - 16/29-2
B - 15/20-4	G - 21/10-1
C - 15/26-3	H - 22/17-4
D - 15/26-4	J - 22/20-3
E - 16/28-6	K - 23/16-4

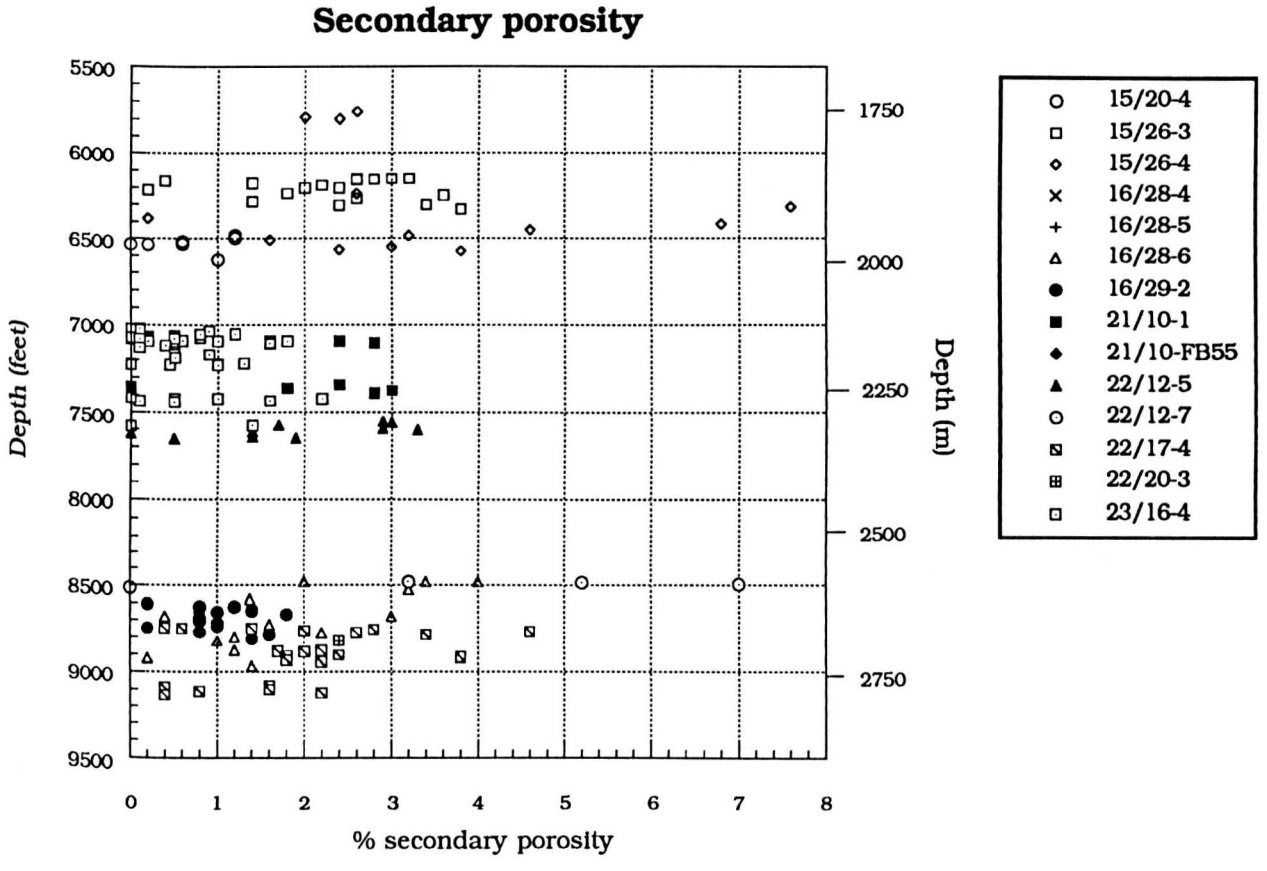
Secondary porosity
Depth (feet)
5500
6000
6500
7000
7500
8000
8500
9000
9500
1750
2000
2250
2500
2750
Depth (m)
0
1
2
3
4
5
6
7
8
% secondary porosity
15/20-4
15/26-3
15/26-4
16/28-4
16/28-5
16/28-6
16/29-2
21/10-1
21/10-FB55
22/12-5
22/12-7
22/17-4
22/20-3
23/16-4

Figure 4.2

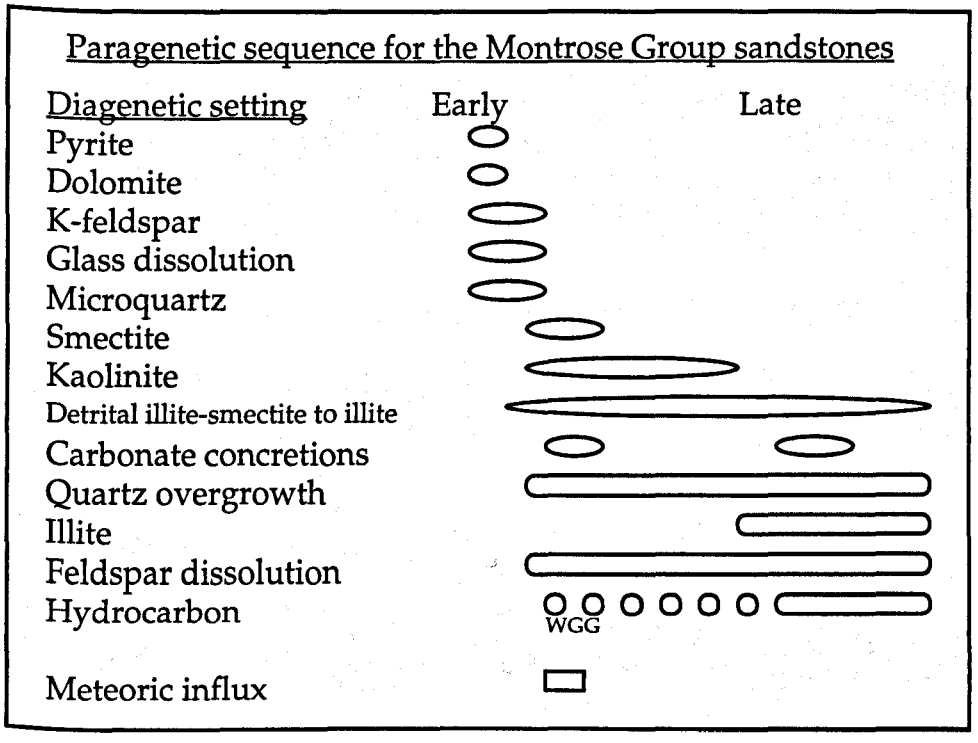
Paragenetic sequence for the Montrose Group sandstones
Diagenetic setting
Early
Late
Pyrite
Dolomite
K-feldspar
Glass dissolution
Microquartz
Smectite
Kaolinite
Detrital illite-smectite to illite
Carbonate concretions
Quartz overgrowth
Illite
Feldspar dissolution
Hydrocarbon
WGG
Meteoric influx

Figure 4.3

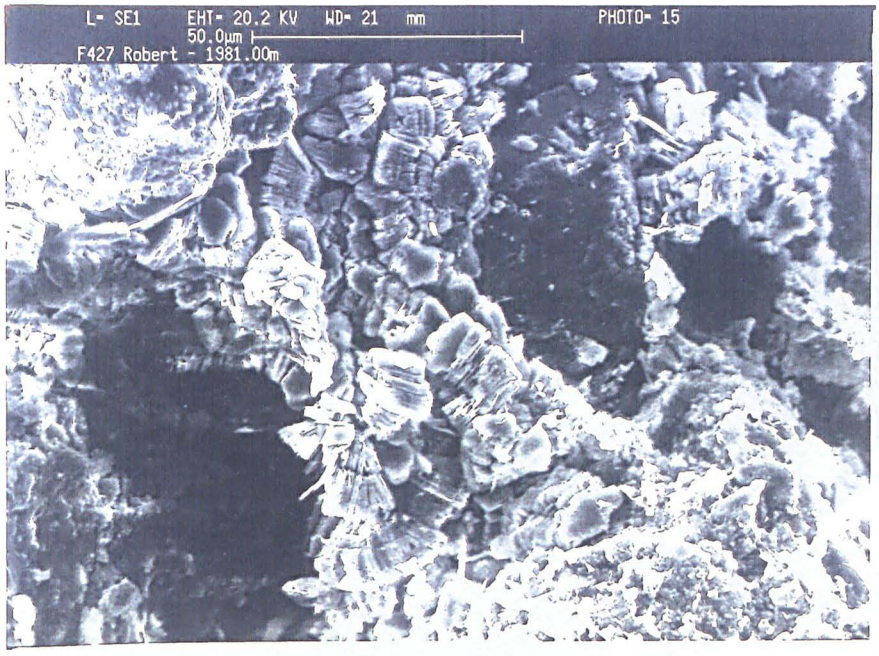

Figure 4.4

Figure 4.5

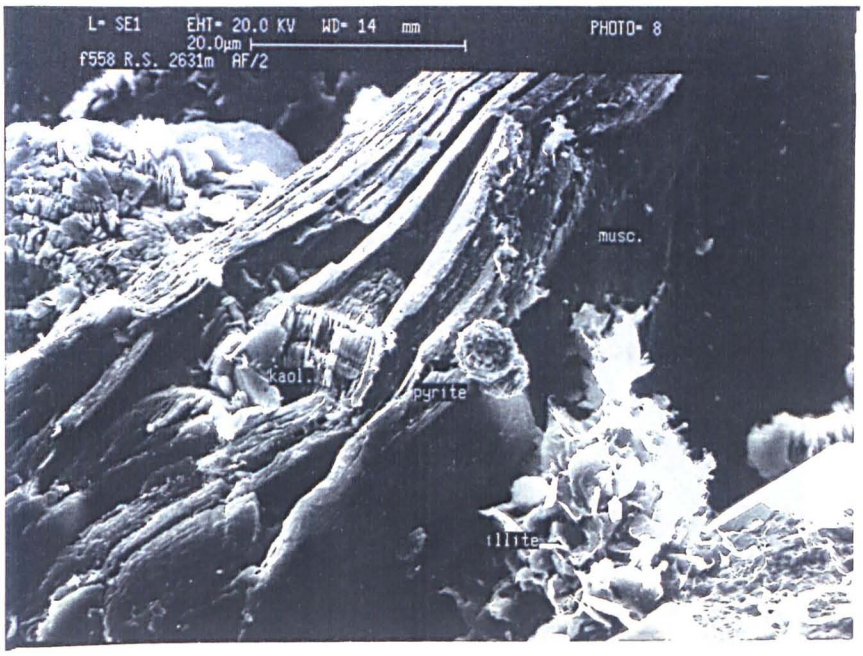

Figure 4.6

Figure 4.7

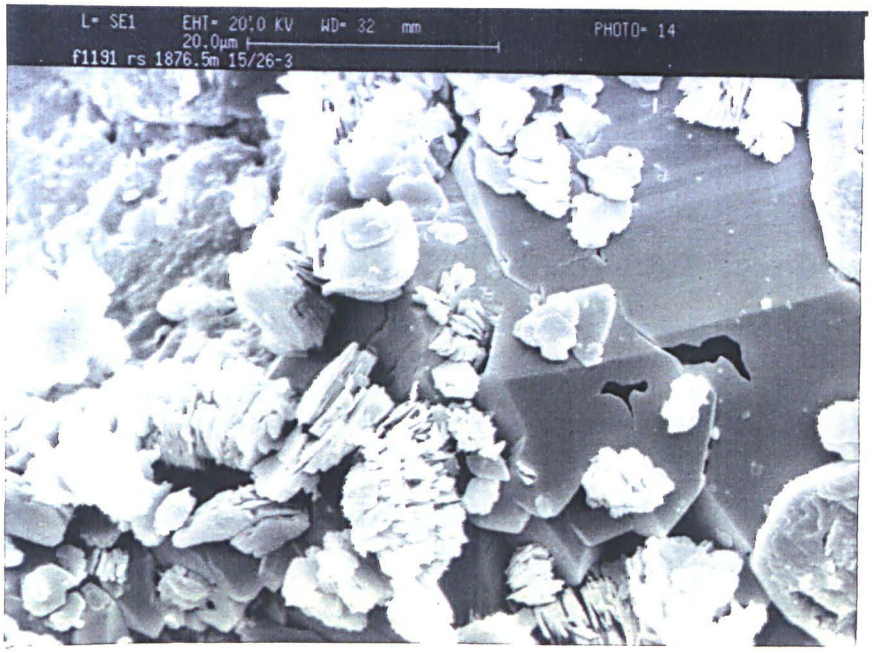

Figure 4.8

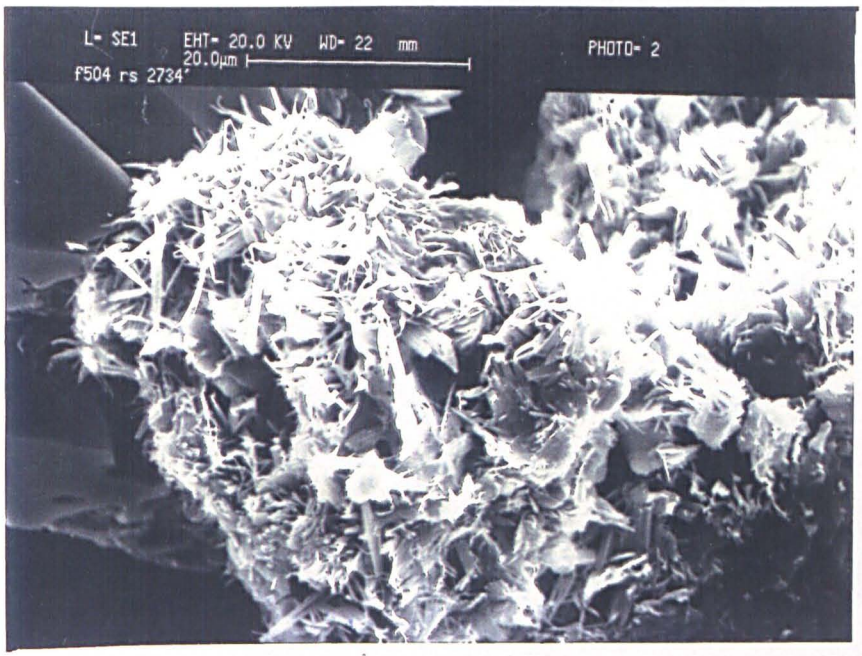

Figure 4.9

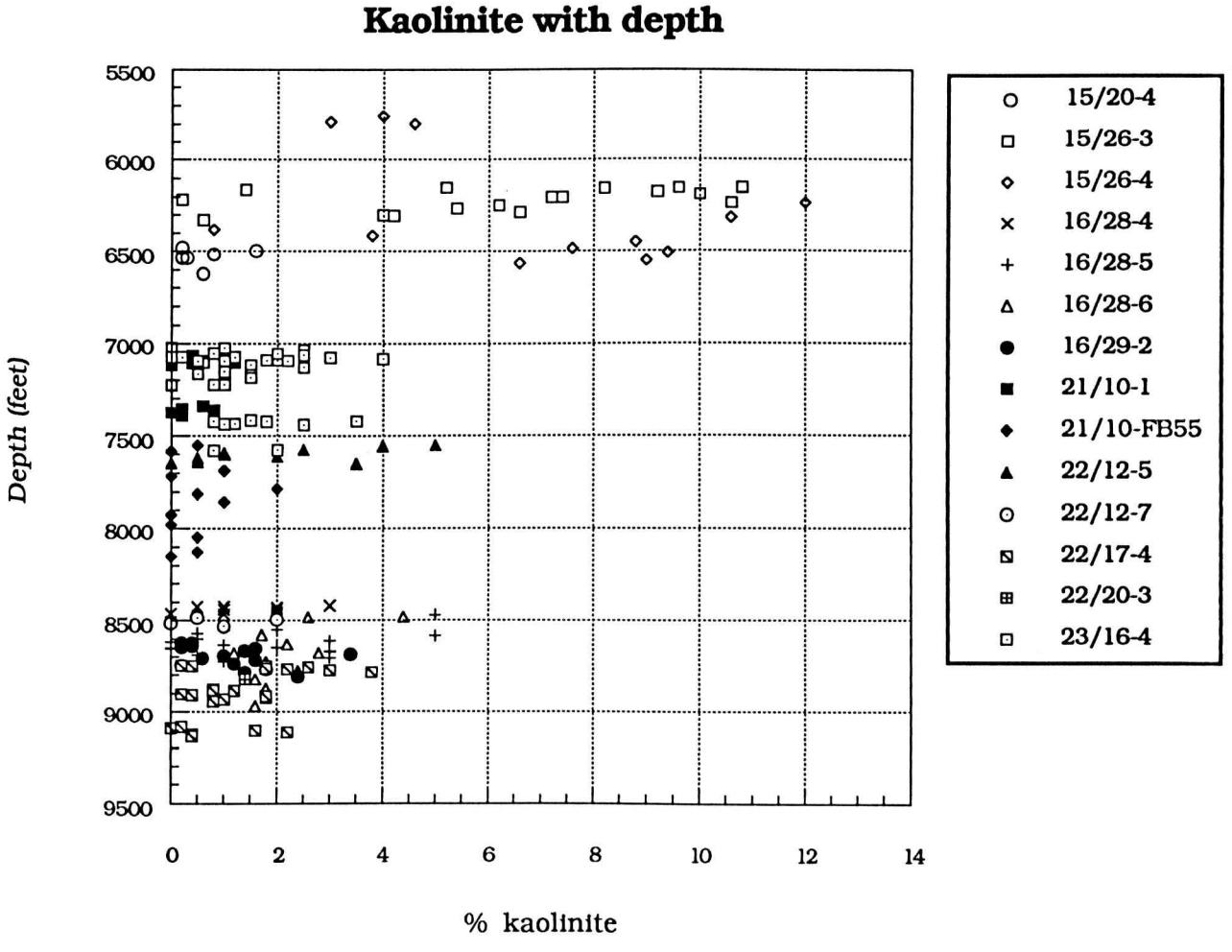
Kaolinite with depth
Depth (feet)
5500
6000
6500
7000
7500
8000
8500
9000
9500
0
2
4
6
8
10
12
14
% kaolinite
15/20-4
15/26-3
15/26-4
16/28-4
16/28-5
16/28-6
16/29-2
21/10-1
21/10-FB55
22/12-5
22/12-7
22/17-4
22/20-3
23/16-4

Figure 4.10

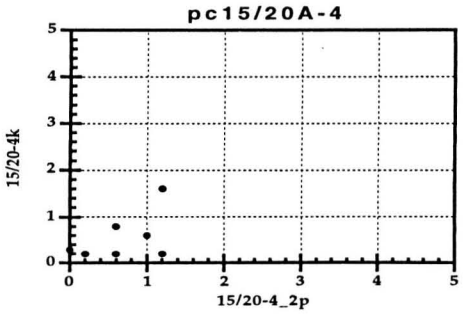

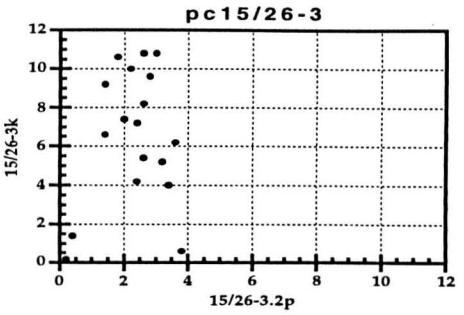

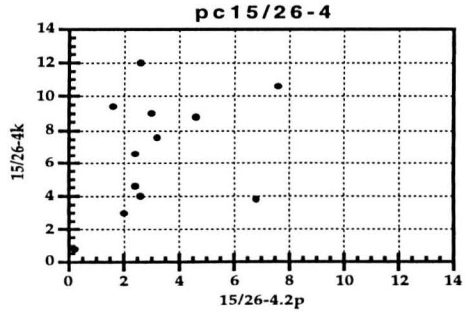

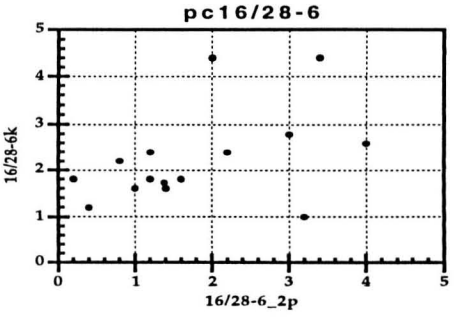

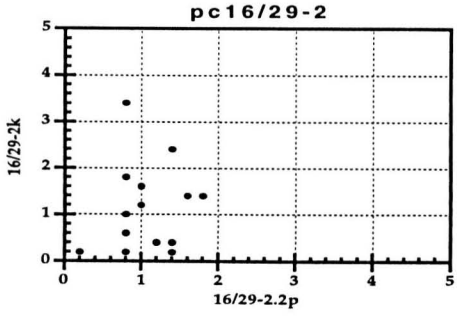

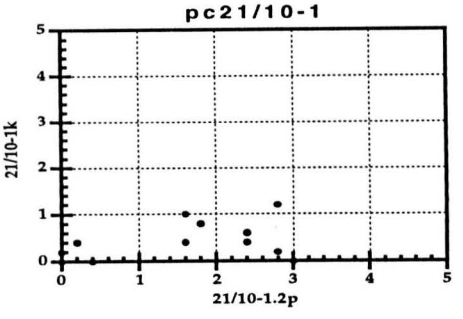

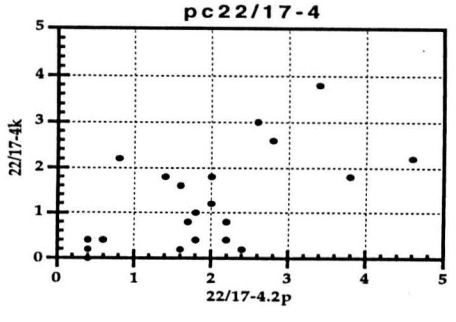

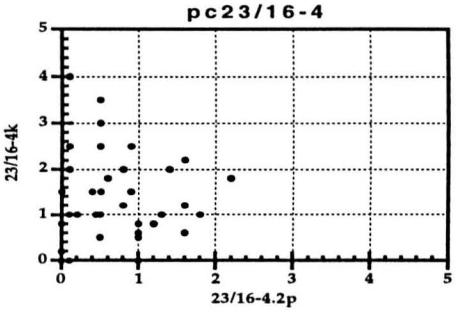

Figure 4. 11a-h

Figure 4.12

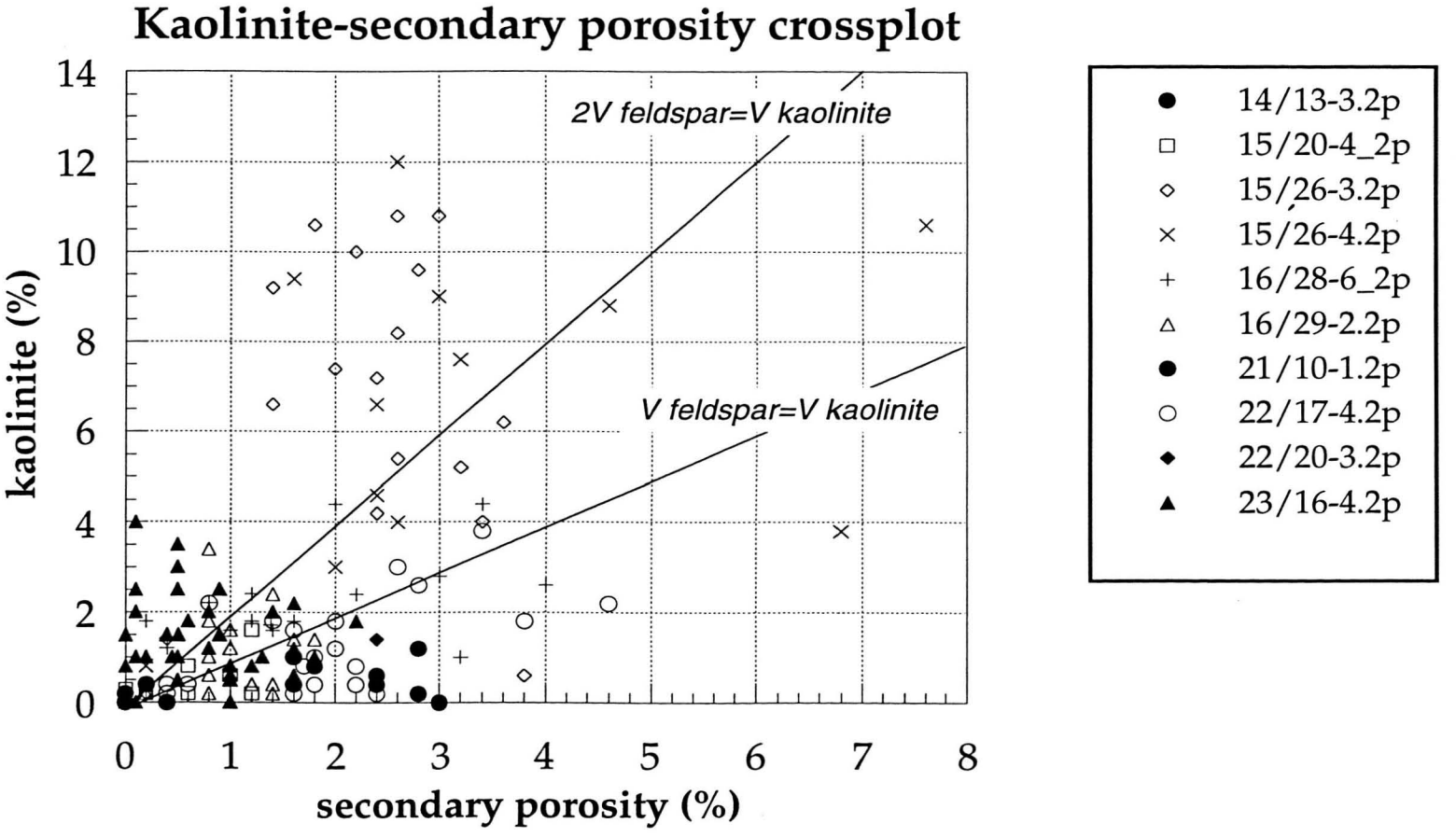
Kaolinite-secondary porosity crossplot
kaolinite (%)
secondary porosity (%)
2V feldspar=V kaolinite
V feldspar=V kaolinite
0
2
4
6
8
10
12
14
0
1
2
3
4
5
6
7
8
14/13-3.2p
15/20-4_2p
15/26-3.2p
15/26-4.2p
16/28-6_2p
16/29-2.2p
21/10-1.2p
22/17-4.2p
22/20-3.2p
23/16-4.2p

Temperature of precipitation (°C)
0
10
20
30
40
50
60
70
80
90
100
110
120
Pore-water composition (δ^{18}Osmow)
-12 -11 -10 -9 -8 -7 -6 -5 -4 -3 -2 -1 0 1 2 3 4
δ^{18}Osmow(kaolinite) = 22 ‰
20‰
18‰
17‰
16‰
14‰
13‰
12‰
10‰

Figure 4.13

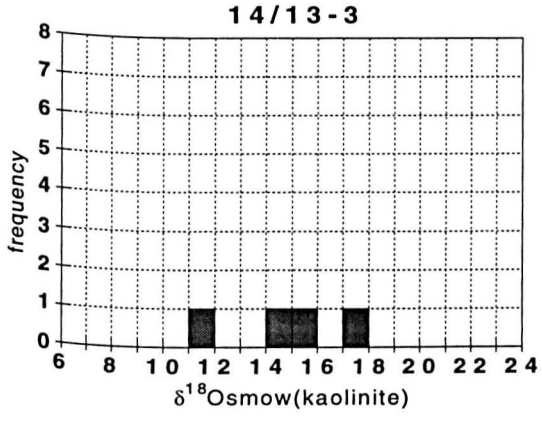

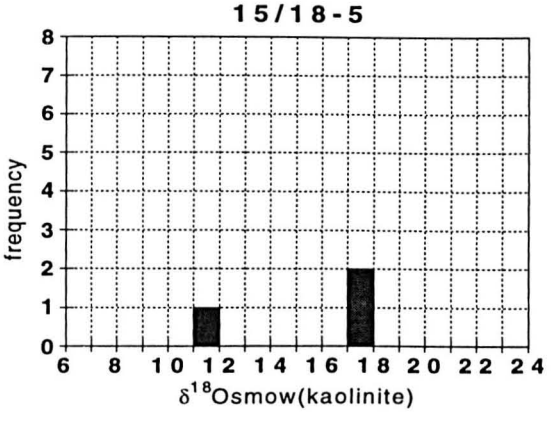

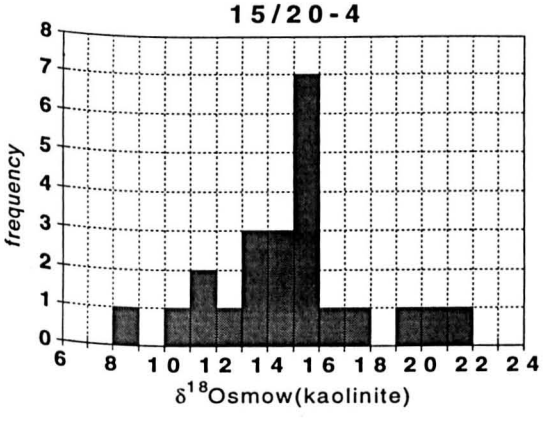

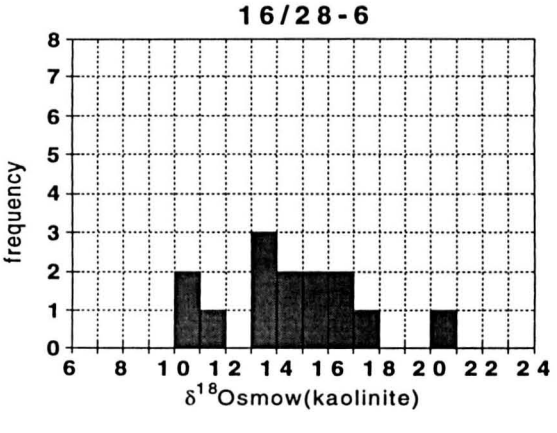

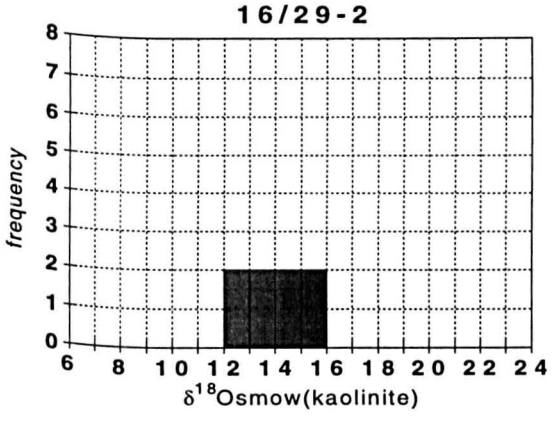

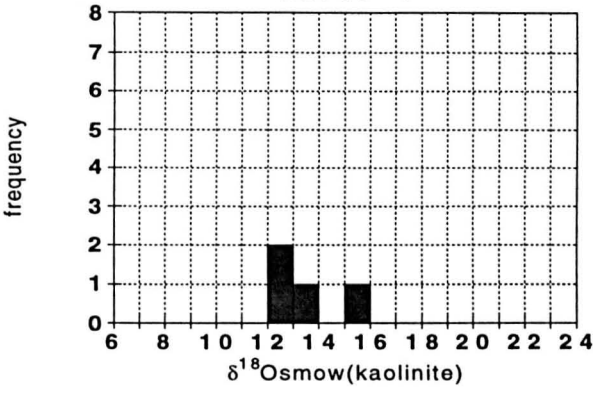

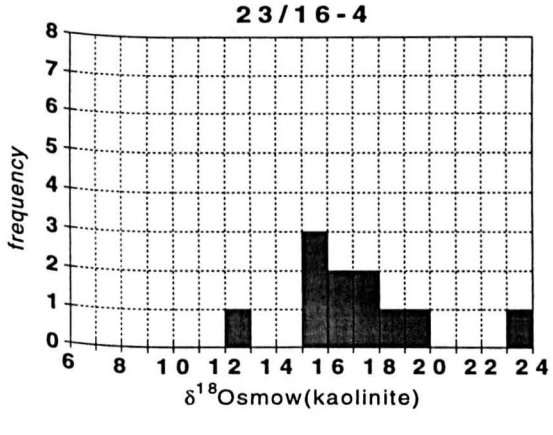

Figure 4. 14a-g

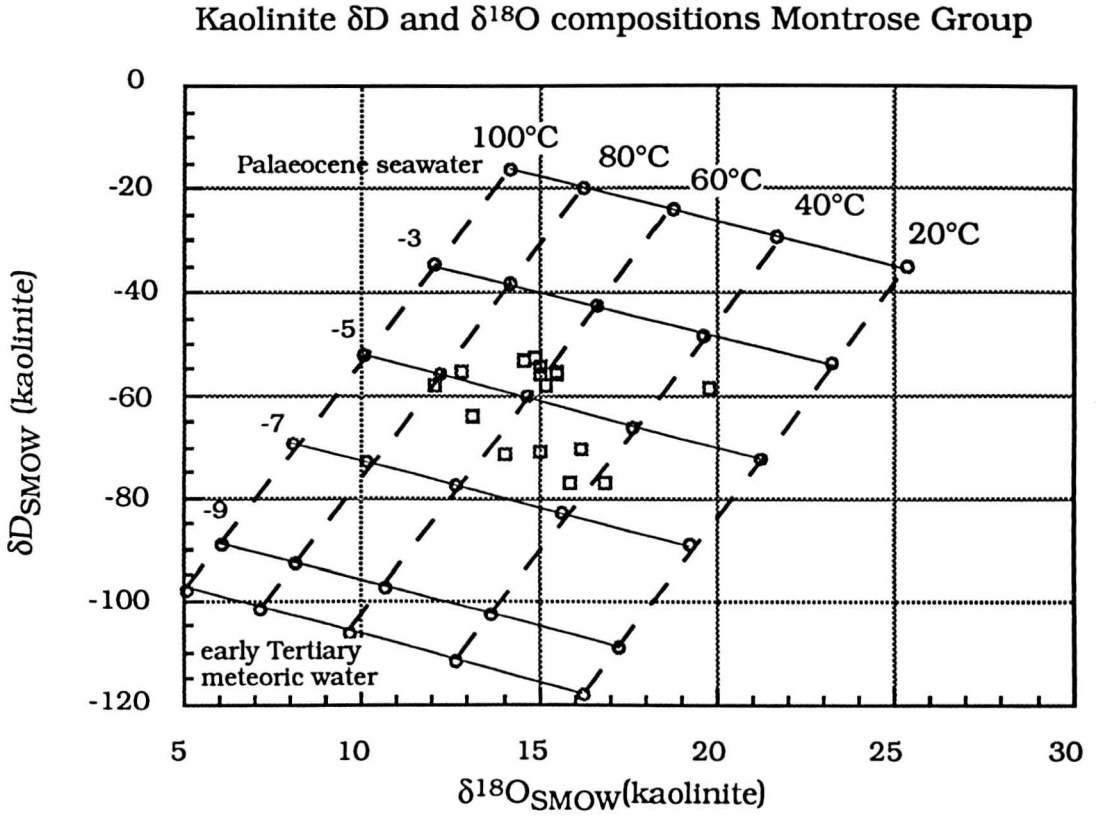
Kaolinite δD and δ18O compositions Montrose Group
0
-20
-40
-60
-80
-100
-120
100°C
80°C
60°C
40°C
20°C
Palaeocene seawater
-3
-5
-7
-9
early Tertiary
meteoric water
5
10
15
20
25
30
δDSMOW (kaolinite)
δ18OSMOW(kaolinite)

Figure 4.15

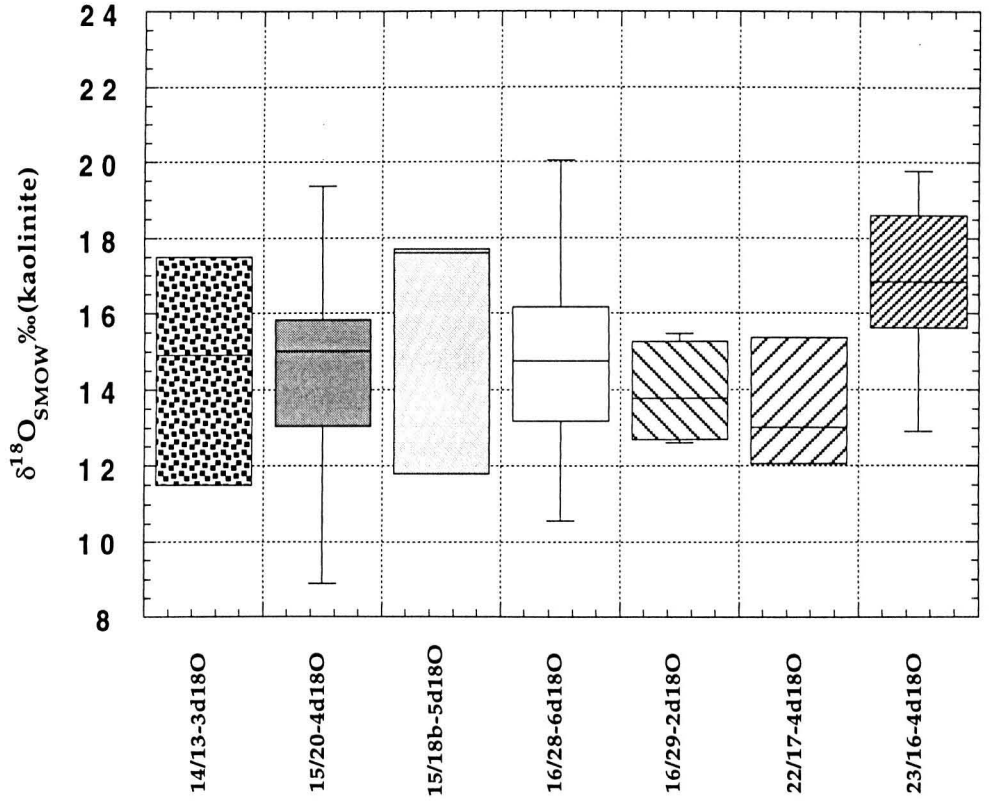

Figure 4.16

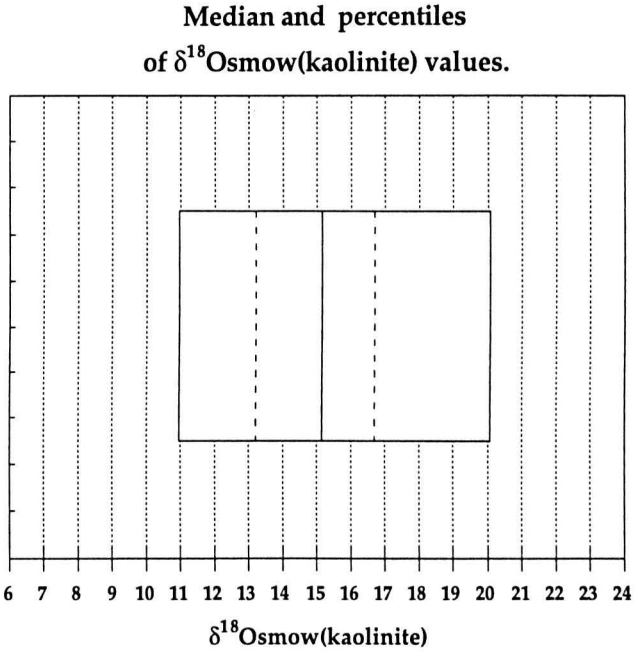

Figure 4.17

CHAPTER 5 POROSITY AND PERMEABILITY CHARACTERISTICS OF THE PALAEOCENE CLASTIC SEQUENCE, CENTRAL NORTH SEA, UK SECTOR

Figures

Tables

CHAPTER 5 POROSITY AND PERMEABILITY CHARACTERISTICS OF THE LOWER PALAEOCENE CLASTIC SEQUENCE, CENTRAL NORTH SEA, UK SECTOR.

5.1 Abstract

A regional study has been undertaken to determine the main controls on porosity and permeability within the Montrose Group sandstones, the most productive reservoir interval in the Central North Sea.

Poroperm data have been collated from Lower Palaeocene Montrose Group submarine fan sandstones encountered in forty-two wells in the Central North Sea at depths ranging from 5800ft to 9400ft (1.8 to 2.9km). Well-logs indicate that massive sands with sharp bases and tops occur within thick mudrock sequences. Within cored wells, lithofacies are dominated by amalgamated sequences of massively- bedded sandstones (>75% of core length) with infrequent dish-and-pillar sedimentary structures. These are interpreted as vertical amalgamation of channel deposits. Petrography indicates that the sands form a fine-to-medium grained, poorly-to-moderately sorted sublitharenite, mud content <5%. The distribution of cored Palaeocene wells reflects the underlying Mesozoic structures that create traps and as a consequence wells have been subdivided into four areas: Fladen Ground Spur (FGS), Fisher Bank Basin (FBB), Forties Montrose High (FMH) and the East Central Graben (ECG).

Within each area poroperm crossplots from the massive-bedded lithofacies show tightly constrained clusters of values; FGS 22-33% 150-3000mD, FBB 17-32% 40-1050mD, FMH 22-36% 80-1050mD, ECG 15-30% 1-400mD. Where there was a tuffaceous component in massive-bedded sandstones, diagenetic chloritic grain coatings maintain high porosities, but permeabilities drop by a factor of ten. In wells located lateral to submarine fan depositional centres, porosities of massive sandstone remain high but permeabilities can drop to <1mD. Tight carbonate cemented zones, 10's cm to 1.5m in length, with negligible porosities and permeabilities, are present within the sands, generally making up to a few percent of core length.

Poroperm variations in individual wells are controlled by depositional sub-facies. These include poorer sorted or muddy matrix sediment at the bases of sandstones, and the presence of fluid escape structures. In sandstone intervals >10m thick, 'poroperm bows' 5-9m in length, are apparent (porosities vary by up to several percent, permeabilities vary by up to a factor of four). Dish-and-pillar structures which are prevalent towards the top of individual sand depositional units coincide with lower poroperm values. Carbonate cemented zones are also associated with these dish-and-pillar structures. We infer that carbonate fines were present in the depositional sand matrix. Dewatering concentrated these into 'dishes' which later acted as nucleation surfaces for diagenetic cements.

The diagenesis of the Montrose Group has been slight with sandstones containing less than 5% volume authigenic minerals. Volumetrically the most important minerals are concretionary carbonate, quartz overgrowths and vermiform kaolinite. Porosity/depth relationships are similar to those reported from the Brent Group and Norwegian Shelf sandstones, until depths of 8000ft (2.4km), where Montrose Group porosities decline at a higher rate. For each area porosity-declines per thousand feet are; FGS 1.69,

FBB 2.68, FMH 4.04 and ECG 12.27. The reason for the rapid decline in porosities in the ECG is unclear. It could result from a combination of a) depositional variation or b) diagenetic processes.

The lack of volumetrically important authigenic minerals within the FBB, FMH and FGS indicates that porosity decline in these areas has resulted from mechanical compaction and not chemical alteration/compaction. By contrast rapid decline in the ECG implies different processes. Similar porosity trends have been noted in the M. Jurassic and U. Jurassic sands in the Northern North Sea e.g. (Magnus Field), (Emery et al. 1993).

5.2 Introduction

Porosity and permeability relationships with facies and depth are of prime importance during regional evaluation of new prospects. Such relationships are normally based on empirical porosity- depth curves, (Sclater & Christie 1980; Baldwin & Butler 1985) and later modified by integration with existing core data, paragenetic sequences and burial history curves (Giles et al. 1992; Ramm 1992; Emery et al. 1993; Ramm & Bjorlykke 1994). Within the Northern North Sea published data and interpretations of poroperm trends of the Brent province (Giles et al. 1992; Harris 1992; Kantorowicz et al. 1992) and the Norwegian Shelf (Ramm 1992; Ramm & Bjorlykke 1994) are widely available. These generally show on a regional scale that although major diagenetic alterations have had a strong influence in modifying porosity type and permeability, particularly with regards to feldspar dissolution, no apparent deviation from linear porosity-depth trends can be seen. Similarly Texas Gulf Coast Tertiary sandstones show no rapid alteration in porosity at any depth although feldspar dissolution (up to 15%BV) takes place at 6000ft to 9000ft (1.8 to 2.7km) burial (Loucks et al. 1984). MacBride et al (1991) in a study of Texas Gulf Coast sandstones found that rate of porosity decline by mechanical compaction was high until burial depths of 1200m. At depths greater than 1200m the porosity decline continued at a slower rate with intergranular porosity reaching single figures at depths >3500m. These authors also found that diagenetic quartz overgrowths consistently formed over 10% of thin-section volume at depth greater than 2500m. Emery et al. (1993) concluded that trends of rapid porosity decline within Northern North Sea Mesozoic fields could be explained by the interaction of oil migration and quartz cementation. The importance of time of compaction has been demonstrated for uncemented sands of Jurassic to Holocene age (Palmer & Barton 1987) and the importance of time-temperature index of thermal maturity to porosity loss by compaction for several formations has been demonstrated by Schmoker & Gautier (1988)

During the initial exploration of the North Sea, simple porosity- depth trends were determined shortly after porosity data was recovered from Palaeocene sandstones (Selley 1978). Sclater & Christie's widely used (Sclater & Christie 1980) empirical porosity depth curves also included data from North Sea Tertiary sandstones. Sufficient core data have now been released from the Palaeocene Montrose Group to create porosity-depth plots and examine any regional variation. The Palaeocene sandstones are cored to 9000ft (2.7km) and provide a useful comparison with mid-Jurassic sands cored to 9000ft (2.7km) and deeper in the northern North Sea. In this study the effects of chemical versus mechanical compaction in destroying porosity are contrasted. It has generally been established that porosity declines in way of

sandstones by way of mechanical compaction at depth to 0.5-3km (Kurkjy et al. 1987; Ramm & Bjorlykke 1994) and deeper than 2.5km, processes of chemical compaction become more dominant (Giles et al. 1992). However McBride et al. (1991) in their substantial study of Palaeogene sandstones (Wilcox and Claiborne Groups) find that compaction is rapid to approximately 1200m. Below this depth compaction is more variable and slower but is still the main cause of porosity reduction, though quartz cements may have retarded compaction.

5.3 Location

The Montrose Group sandstones (Deegan & Scull 1977) subcrop within the Central North Sea: the study area covers Quads 14, 15, 16, 21, 22 and 23, **Figure 5.1.** The Montrose Group has been separated into the generally accepted lithostratigraphic three-fold partition of submarine fan sequences, **Figure 5.2** (Maureen, Andrew and Forties Formations (Deegan & Scull 1977): They are identified on a coarse scale by large gamma-ray bows aided by the colour of interbedded muds (Carman & Young 1981). Much confusion occurs regarding the precise stratigraphy of the Montrose Group (Knox et al. 1981; Milton et al. 1990; Mudge & Copestake 1992). This results from the high sand/shale ratio of the sands which reduces the diversity and preservation potential of microfossils. These stratigraphic problems do not affect this study as clastic depositional processes did not vary throughout the early Tertiary, though there is a general decrease of sand/shale ratios during the Palaeocene (Den Hartog Jager et al. 1993)

Deposition was generally from the north-west through the Witch Ground Graben with a sandy fan of increasing importance sourced from the west, south of the Halibut Horst (Rochow 1981; Reynolds 1994). Subsidence was particularly rapid in the Witch Ground Graben area during Palaeocene-Eocene, and in the East Central Graben during the Pliocene onwards (Sclater & Christie 1980) **Figure 5.3.** Burial history curves for the Tertiary-Quaternary are generally poorly constrained.

5.4 Sedimentology

The dominant lithofacies throughout the clastic sequence is a massively bedded sandstone (Crawford et al. 1991; Cutts 1991; Mound et al. 1991; Tonkin & Fraser 1991; Wills 1991; O'Connor & Walker 1993). Regionally these massive sandstones are petrographically fine (to medium) grained and moderately (to poorly) sorted, sublitharenites. The sands are dominated by simple strained quartz grains, with lithic grains suggesting an input from a metamorphic hinterland (Morton et al. 1993). Minor facies are sandstone with dish structures, sandstone with mud clasts, ripple and planar laminated sandstone, muddy siltstone, mudstone and bioturbated sandstone (Carman & Young 1981; O'Connor & Walker 1993)

5.5 Methodology

5.5.1 Sampling

He-porosity and permeability data from Palaeocene cores have been compiled from 42 wells, **Table 5.1.** The original data is available for public access in BP, Dyce, Aberdeen; or at the BGS core store in Edinburgh. Readings are in most cases taken every foot if Imperial measurements are used and every 25cm if metric. Copies of composite logs of cored intervals were also taken to compare log traces with poroperm variations. Data was entered into graphics/spreadsheet program

(Kaleidagraph). All well data was examined courtesy of R. Anderton and R. Dixon, BP, Aberdeen.

Montrose Group sandstones are often uncemented due to both shallow burial and lack of volumetrically important authigenic cementing minerals. "Loose", "crumbly", "poorly cemented", or "friable" are terms commonly found on composite logs describing these sands. Some core samples themselves, particularly tuffaceous-rich sands, are bagged to prevent the sands simply spilling into sample boxes. This may result in either a lack of poroperm data where no measurements could have been taken, or misleading high permeability streaks resulting from fracturing during handling if the sands had some consolidation (Emery & Robinson 1993)

5.5.2 Log facies

Sands with an homogenoeus character were isolated to compile porosity-depth trends. This was carried out in two ways, a) by defining log facies and b) from porosity-permeability cross-plots.

a) Log facies - Carman & Young (1981), used gamma-ray patterns to define five log facies of Forties Field sandstone. These were correlated with cored intervals in order to build up a three- dimensional model of the field where wells were logged but not cored. These 'log-facies' are limited by the resolution of the gamma-ray logging tool and cannot identify small scale, approximately <50cm sized sedimentary units (Geel 1993). The pattern, recognised by Carman & Young (1981) as 'constant low gamma-ray', with uniformly low gamma, density and sonic but high resistivity electric logs, corresponded to amalgamated successions (10-60m thick) of massive sandstone with individual beds <1.5m thick, with minor pebbly sandstones and sparse 'proximal-turbidites'.

In this study, blocky gamma-ray signature is defined as intervals where gamma-ray readings are low (<35 API units with +5 API units variation), and where possible sandstone thickness is greater than 5m (15ft) thick. Comparison with core samples reveals that the actual lithofacies of these blocky zones range from pebbly sandstones, massive sandstones to massive sandstone with dish structures. The density and sonic logs closely match the lack of variation within these intervals with the exception of sudden and isolated kicks where tightly cemented zones are encountered within the sandstone.

b) Poroperm crossplots; where blocky facies are greater than 5m/15ft thick the above system works very well, such as in the Fladen Ground Spur area. Towards distal areas, areas lateral to channel systems or nearing the very top of formations where overall sand/shale ratios decline, the massive sandstones/amalgamated units become too thin for blocky gamma-ray identification. Therefore in these cases an assumption was made, on the basis of available BP sedimentological reports, that the dominant facies within the core is massive sandstones. Hence tightly grouped values on porosity-permeability cross-plot represent this facies. These groupings were visually estimated and separated from other well values by isolating them on spreadsheets.

Montrose Group cored wells are not uniformly distributed, but reflect the underlying Mesozoic structures that create trapping structures. Four-way closure drape traps

resulting from compaction over Jurassic tilted fault blocks and Zechstein salt domes are the most common trapping method. Wells have therefore been consigned to four regional groups; Fladen Ground Spur, Fisher Bank Basin, East Central Graben and the Forties Montrose High, **Table 5.1.**

Ten wells, chosen to represent the different regions were core sampled, **Table 5.2.** Epoxy-resin impregnated thin-sections from these wells were used to compare porosity variations with sedimentological and diagenetic properties. Rock stubs were used to identify diagenetic alterations using a scanning electron microscope. BP in-house sedimentological reports were also available.

5.6.1 Porosity/permeability-depth variations in single wells

Where cored intervals are long enough, poorly defined 'bows' of porosity and permeability values are a common feature particularly in 'blocky' intervals. The bows start and end with low porosity/permeability and have higher values within the middle. **Table 5.3.** These 'bows' are often but not always recorded by subtle changes in the gamma-ray log. Examples of this include **Figures 5.4, 5.5, 5.6, 5.7, and 5.8.** These poroperm variations are of interest to petroleum geologists as they illustrate the range in poroperm characteristics and give the vertical scale of poroperm variations within a seemingly homogeneous sandstone as suggested by electric logs.

a) Within well 16/21-20, **Figure 5.4,** (7328ft to 7355ft) poroperm variations are mapped by subtle changes in the gamma-ray log.

b) In well 15/25-2, **Figure 5.5,** distinct 'bows' in permeability at depths 7180ft to 7240ft are not clearly mirrored by the relatively constant trace of the gamma or sonic log. Well 16/29-8, **Figure 5.6,** has two distinct bows of 15ft (4.6m) in length with a wide range in porosity and permeability (k=20-500mD, ϕ=15-25%) which occur within the Andrew Formation. They are not identified on gamma-ray traces.

Of note is the fact that cemented horizons as picked out on the sonic/density logs are often found in the vicinity of bow tips **Figures 5.5 and 5.7** (15/25-2 and 15/26-3). These kicks, described as 'calcite-cemented horizons', 'hard-cemented' or 'arenaceous limestone', on the composite logs are of the scale 10's of cm and up to 1.5m.

5.6.2 Explanation

There are two possibilities to explain the occurrence of bows within the amalgamated massive sands;
a) diagenetic and/or b) sedimentological

a) Diagenetic alteration - The changes in porosity and permeability could be diagenetic in origin and represent the dissolution of material preferentially along certain layers perhaps following beds which originally had higher permeability (Haszeldine et al. 1984). In the case of the calcite concretions this represents transfer of homogeneously distributed detrital calcite to a precipitation surface thus leaving a 'leached zone' of higher porosity around the vicinity of concretions. Wilkinson & Dampier (1990) illustrate a radius of influence where an homogeneous sandstone with a previously even distribution of detrital carbonate has a zone of depleted carbonate surrounding authigenic calcite concretions.

Well 15/26a-3, **Figure 5.7, 5.9, Table 5.4**, illustrates one of the bows present. Across the tip of the bow at core depth 1890.6 to 1904.7m a series of five core samples were taken. Petrographical analysis by thin-section indicated that the depositional grain size of the samples do not vary significantly. Neither authigenic nor detrital calcite is present outside the concretion. Rock volumes suggested by porosity change implies a noticeable dissolution of detrital carbonate (Wilkinson & Dampier 1990). However the high porosity bows are much wider than expected by dissolution. Authigenic calcite does not extend further than the edge of the concretions. This suggests that the diagenetic alterations do not explain the presence of the bows.

However although no substantial calcite substrate can be found outside concretions, $^{87}Sr/^{86}Sr$ analysis of concretions indicates that detrital Palaeocene carbonate and resedimented chalk are the predominant sources for calcite (Chapter 2). It is hypothesised that:- either detrital calcite, probably a very small percentage of the rock, at one time evenly distributed has later been dissolved and then reprecipitated to form concretions. Or, that calcite had been introduced into the sands from adjacent mudrocks; small calcite veins within sandstones would support an input of carbonate into sands.

b) Sedimentological

The changes in porosity and permeability recorded by 'bows' may also identify amalgamated channels of similar composition and grain size. In some well's composite logs (wells 15/25-2 **Figure 5.5**, 16/29-8 **Figure 5.6**), individual channel beds in a stacked sequence cannot be distinguished from the gamma-ray log. It is likely that many amalgamation planes between different massive sandstones (log facies B, Carman & Young 1981) are impossible to see visually and on electric logs because of insufficient compositional or grain size contrasts between consecutive sandstones. (Roger Anderton BP, Dyce, pers. comm 1992; Prosser et al. 1993). This possibility remains unresolved.

The only sedimentological structures that are commonly present within massive sands are fluid escape 'dish-and-pillar structures' outlined by detrital fines (Wentworth 1967; Lowe 1975). These fluid escape structures result from liquefaction of resedimented sands during the sudden breakdown of a meta-stable loosely packed grain framework. The grains become temporarily suspended in the pore-fluid and settle rapidly through the fluid until a grain supported structure is re-established. To form dish-and-pillar structures sufficient fines have to be carried in suspension during submarine flows. Such conditions exist for mixed grain-mud flows during abandonment stages of individual fan channels (Wentworth 1967, Low 1975, Tonkin & Fraser 1991). Dish and pillar structures are also more frequent towards the top of formations where there is an overall decrease in sand/mud ratios. This was a consequence of the lowering sand deposition rates on the East Shetland Platform edge prior to resedimentation within North Sea depocentres. High permeability sands tend to dewater without disturbance of the grain framework which implies that structureless sands were originally deposited without traction structures.

Observationally dish structures are prevalent towards the top of individual flow deposits, suggesting that such tops contain sediments together with finer sediment.

The concentration of these fines during dewatering enables visual identification of such structures. Detrital fines outlining dish-and-pillar structures comprise clays, carbonate mud and fine-grained micaeceous fragments.

Results

Plots of poroperm obtained from conventional core analysis were compared in depth with detailed sedimentological reports from wells 16/28-6, **Figure 5.8** and 15/20a-4. In both wells several tens of metres thickness of massively-bedded sandstones (described in SediMentological Reports as 'channel sands') have been cored. Porosity and permeability declines as dish structures are approached and the gamma-ray log shows a concordant and subtle increase in radioactivity (**Table 5.5**).

It therefore appears that dish-structures control poroperm variations within massive sands which frequently make up to 90% of core length. The difference in porosity is small (<5% variation) but the permeability drops by a power of 10 over a distance of a metre. Control over the siting of concretions is also apparent. The detrital composition of the fines was presumably rich in micaceous particles and carbonate as the agglutinated benthic forams were the predominant forams during this period (Berggren & Gradstein 1981). Thin-sections were not taken across these 'dishes', however visual analysis of cores indicates that muddy beds within the Montrose Group are calcitic. Bjorkum & Walderhaug (1990) showed that layers where detrital carbonate was concentrated were also the places where concretions would precipitate out. The nucleation points of calcite precipitation were more likely to be found within these layers. Also fracturing of muscovites provides nucleation points for calcite precipitation (Boles & Johnson 1983). Concretions are more prevalent within dish-and-pillar areas, **Figures 5.5, 5.7.** As a consequence of this, on composite logs, without the benefit of poroperm information, concretions would appear to be randomly situated.

5.7 Porosity-permeability cross plots by structural region (Figures 5.10 and 5.11)

In this section, poroperm data are compiled for different regions of the study area. These regions are based on the underlying Jurassic structural provinces which controlled deposition of these Palaeocene sediments, and also controlled the post-depositional subsidence of the Palaeocene sediments. The objective was to ascertain if the variations in calcite cement (Ch 2) also controlled general poroperm. In all regions, with the exception of the East Central Graben, 'blocky data' refers to data isolated from analysis of composite logs. Porosities and permeabilities were only taken from these blocky units where gamma-ray readings were low and sonic transit times were uniformly high. For the East Central Graben, because sand units are often too thin for 'blocky' identification, data was isolated from poroperm cross-plots. On the basis of sedimentological reports, the dominant facies was massive sandstones and hence grouped values represented this facies.

5.7.1 Fladen Ground Spur,

The groups are defined on Figure **5.10a**

ai) Blocky sands, **Figure 5.11a** high poroperm values (ϕ-k group = 22 to 33%, 150 to 3000mD) are consistently high throughout the area probably reflecting little regional variation in grain-size and a low mud content. Values are tightly constrained representing distinct differences in lithologies with no merging of lithofacies.

aii) Blocky sands, **Figure 5.11a**, similar high porosities but with lower permeabilities (ϕ-k group = 24 to 32%, 40 to 150mD). In well 15/20-4, 15/20-7 authigenic chlorite coating on grains although less than 2% can reduce permeabilities by a factor of ten.
b) Broad range of poroperms representing minor lithofacies - ripple-laminated sandstones and muddy siltstones (ϕ-k group = 5 to 25%, 0.02 to 100mD)
c) Carbonate cemented sandstones (ϕ-k group = <10%, <1mD). Although calcite cemented zones have no visible porosity in thin- sections, they have porosities up to 10%. This may represent fractured samples.

5.7.2 Fisher Bank Basin, The groups are defined on Figure 5.10b
ai) Blocky data **Figure 5.11b** (ϕ-k group = 17 to 32%, 40 to 1050mD) There is a drop in poroperm values with respect to the Fladen Ground Spur probably representing a decrease in depositional sorting in the basin compared to the palaeo-horst. Well 16/29-2 has better sorting resulting in higher porosities.
aii) Blocky data, **Figure 5.11b**, (ϕ-k group = 15 to 27%, 0.2 to 100mD). Wells lateral to major depositional axis in the Fisher Bank Basin, 22/3-2, 22/3-3 porosities remain high but permeabilities drop by a factor of ten, The elongate stretch of values may represent increasing mud content within massive sandstones.
b) Broad range of values with lower porosities and permeabilities than the massive sandstones representing silty-sandstones and other minor facies (ϕ-k group = 2 to 20%, 0.02 to 50mD)
c) Carbonate cemented sandstones (ϕ-k group = <10%, <0.05mD)

5.7.3 Forties Montrose High,
The groups are defined on **Figure 5.10c**
ai) Blocky data **Figure 5.11c** (ϕ-k group = 22 to 36%, 80 to 1050mD) High values for core samples around the Forties Field area represent clay-free sandstones deposited on structural horst.
aii) Blocky data **Figure 5.11c**, (ϕ-k group = 15 to 30%, 0.1 to 800mD) Large range of values containing data from depositionally distal wells. 22/17T-4 data is concentrated (ϕ-k group = 20 to 30%, 6 to 800mD) while 22/18-3 contains muddy sandstones.
b) Broad range of low values representing other facies (2 to 20%, 0.02 to 10mD)
c) Carbonate cemented sandstones (ϕ-k group = <10%, <0.02mD)

5.7.4 East Central Graben,
The groups are defined on **Figure 5.10d**
a) Blocky data **Figure 5.11d**, (ϕ-k group = 15 to 30%, 0.05 to 400mD) Artificially tight grouping as most points have been sorted visually from individual well poroperm cross-plots and not from blocky facies.
b) A substantial percentage of values taken are low, reflecting greater proportion of other lithofacies (ϕ-k group = 2 to 20%, 0.02 to 1mD).
c) Carbonate cemented sandstones (ϕ-k group = <10%, <0.02mD).

5.8 Poroperm trends with depth.
Blocky log facies values have been isolated to construct porosity depth trends as outlined in the methodology.

Curve fitting was calculated by 'least squares' method, on Kaleidagraph data analysis computer application. This calculates a set of coefficients to the specified function, that minimises the square of the difference between the original data and the predicted function. This is relatively simple in terms of computing power but has a major weakness in its sensitivity to outliers from bulk populations. r_{test} values were compared with table of test values for correlation coefficients.

Comparison between trends was done according to Student's *t* test to calculate confidence limits (Cheeney 1983). Critical region was 0.01.

A simple statistical test was carried out to determine the minimum length of core to determine regional porosity decline using the standard sample spacing of 25cm. Sampled core lengths varied from 7.5m (24ft) in well 15/19-2 to 130m (420ft) in 16/28-6. The number of sample points varied between 11 in 22/5-10 to 236 points in well 16/28-6 where log facies were present. Within individual wells , where construction of porosity decline gradients were possible, porosity decline with depth varies from 181.25 to -86.39%/1000ft (594%/km to -283%/km) **Table 5.6** cumulative proportion curves for porosity gradients and sampled core lengths are shown in **Figures 5.12a , 5.12b.** It is obvious that such rapid trends cannot be sustained over core length and this range of porosity declines could be due to
a) Sampling artifacts
b) Sedimentological features
c) Diagenentic alterations
These are discussed below.

5.8.1 Sampling effects

a) To determine whether sampling artifacts had an effect upon trends, it was decided to;
i) see if trends are distributed in a significant manner
ii) compare core lengths with porosity declines
iii) see if trends are statistically significant

i) Disregarding outlying porosity declines (>30 and <-15%/1000ft, 98%/km to 49.21%/km), statistical analysis, using students-t test, indicates that porosity declines have a normal distribution with a mean of 4.51%/1000ft (σ = 14.262, n=28), **Figure 5,12c.** Two sub- peaks have means of 2.575%/1000ft (σ=1.15, n=10) and 17.36%/1000ft (σ=18.2, n=10) **Figure 5.12d.** The first peak has a non-Gaussian distribution and is negatively skewed.

ii) When porosity decline is plotted against sampled core length it is apparent that as the length of core sampled increases, values of porosity decline gradient move towards 0%/1000ft, **Figure 5.13a, 5.13b.** Indeed 6 out of 9 cores over 100ft have porosity declines from 0 to 6%/1000ft (0 to 19.7%/km).

iii) Of the 28 trends calculated only 13 are >80% significant, the majority being <80% significant when tested with the students-t test, **Table 5.6.** No relationship was found between sampled core length and significance of porosity gradient trends. Neither was a relationship between regional area and trends found to be >80% significant.

This indicates that sampled core length strongly influences porosity decline. Longer cores give values closer to established declines of regional porosity declines (0-6%/1000ft, 0 to 19.7%/km). Shorter cores (<100ft) have a spread of values (-15% to 42%/1000', -49.2 to 137.8%/km) but with generally higher gradients of decline. This factor of core length possibly relates to the sediments of the depositional units, here channel fills may individually produce fining-up grain-size trends. These have increasing porosities down-wards for depositional reasons over scales of 100ft. The low proportion of significant trends may be the result of blind choice of what constitutes massive facies i.e. gamma-ray 'blocky facies'. This probably results in sands of a different lithofacies being identified as massive facies resulting in an unnecessarily wide range in porosities eg. the spread of values for well 16/29-2 at 8800ft (2680m) is 8%. Future sampling strategies must target cored intervals longer than depositional units. Sampling should be conducted with sedimentological and electric log facies if possible.

5.8.2 Sedimentological effects

To determine if sedimentological effects were influencing porosity gradients it was decided to investigate;
i) sampling spacing
ii) core length relative to sedimentological features

i) Sampling spacing. Bows in poroperm trends for individual wells are easily identified from core analysis of massive sandstones where blocky facies units are >10m thick. This is an artifact of the spacing interval (25cm, 1 foot) of core-plug measurements of poroperm. As the thickness of amalgamated units declines 'bows' cannot be identified. It is simply scale of preserved units that changes, this does not necessarily represent a change in depositional lithofacies, for example stacked 'bouma' sequences or rapid decline in the overall sand/mud ratio, eg **Figure 5.14**. The representativeness of core plug measurements must always be seen in the light of plug measurements being point data from a continuous core. (Hurst 1987; Prosser et al. 1993). It is important to vary sampling lengths to quantify internal permeability heterogeneity.

ii) Scale comparable to sedimentological features.
Sedimentological features have several scales. Lower Palaeocene formations identified by broad gamma-ray bow signatures are composite bodies constructed of several channel sandstones, partly eroded and stacked vertically. Superimposed upon these are individual channel complexes identified by parasitical bows or blocky traces. A finer scale amalgamated sandstones are picked out by subtle gamma-ray variations or by sedimentological logging of core. Upon consideration of these facies the conclusion can be drawn that long cores have low porosity declines similar to statistically valid values of regional porosity decline (**Table 5.6**) and that high rates of porosity declines represent lithological variations; they have no large scale significance.

5.8.3 Diagenetic effects

Porosity declines with depth and could be due to compaction, or to pore-filling cementation. These two effects can be distinguished, using thin-section point-counting technique to generate cross-plots showing: cement, porosity and intergranular volume (Housnecht 1984). These plots enable us to investigate two effects:-

i) Comparison between diagenesis and compaction using Housnecht intergranular volume plots.
ii) Long cores (16/28-6, 16/29-2, 21/10-1 and 22/17-4) diagenetic mineral volumes

i) **Figure 5.15** illustrates four representative wells' point count data plotted on a Housenecht Intergranular-Volume-Plot (Housnecht 1984) **Table 5.7.** Porosities are point counted not He-porosities; point counting carries large systematic errors and porosities are likely to be underestimated. The plot illustrates the relatively minor effect that diagenesis has had on the decline in porosity. There is generally less than 5%BV authigenic minerals (kaolinite, quartz overgrowth, disseminated carbonates, pyrite and barytes). Compaction has been the process dominating porosity reduction.

ii) Cement percentage with depth Four sampled long wells (>100ft, 30.5m) were examined. For each sample the percentage cement was recorded, these cement %BV are plotted against core depth, **Figure 5.16.** They indicate that there is no systematic increase in cement percentage with depth.

In conclusion, compaction has had an overwhelmingly large contribution to porosity decline compared to diagenesis. This is in keeping with Ramm (1992) and Ramm & Bjorlykke (1994) in studies of Norwegian North Sea Sector sandstones of Triassic to Palaeocene age. These authors indicated that at depths 0-2.5 to 3km, porosity trends are controlled by the stability of the grain framework and effective stress, empirically implying that at these depths it would be unusual to find quantitatively significant authigenic cementing phases. The minimum sampling length to approach regional porosity gradients begin at 50m (150ft). Sampling lengths smaller than this can give varying gradients, both positive and negative, which relate to the large natural variation in porosity encountered even when identical facies are sampled throughout a core.

In Jurassic Brent Group sandstones, the depth at which diagenesis assumes a major control on reservoir quality is around 9000ft, 2.7km (present day depth), (Giles et al. 1992). Volumetrically the most important phases are quartz overgrowth and creation of secondary porosity resulting from feldspar dissolution with resultant kaolinite precipitation. None of these effects are peculiar to the Brent, all are seen in the Palaeocene but with substantially lesser volumes. These same processes of diagenesis have affected the Palaeocene sands at 1.5 to 2.7km (6200ft to 9000ft) but with much less effect.

5.9 Regional trends: comparison with published porosity depth trends.

These trends of porosity decline with depth for the Palaeocene are compared to published values derived from electric log and core information
i) comparison with empirical curves (Baldwin & Butler 1985; Sclater & Christie 1980; Scherer 1987)
ii) comparison with Brent Group and North Sea data

5.9.1 Comparison with empirical compaction curves

Individual wells are superimposed upon Sclater & Christie (1980) and Scherer (1987) empirical porosity depth curves **Figure 5.17.**

The well known empirical sandstone compaction curve by Sclater & Christie (1980) is based upon decompaction curves from 8 wells from the Central Graben, North Sea (Sclater & Christie 1980), and porosities from early exploration wells (Selley 1978). Selley (1978) appeared to generate a Palaeocene porosity gradient from two data points, namely Forties and Montrose. (The Baldwin & Butler (1985) curve is the logarithmic equivalent of Sclater & Christie's (1980) exponential curve).

Wells closely match the Sclater & Christie curve within 2.5% porosity error bars until 8000ft (2.4km) where predicted porosities are up to 5% higher than actual values. As litho-facies do not change this must be a real compactional effect. Therefore the Sclater & Christie curve does not hold and does not provide an accurate template for porosity prediction for Central North Sea Palaeocene sandstones.

Scherer's (1987) model is based on analysis of 428 Shell oilfields. A series of predicted porosities for sandstones of different ages (Mid Ordovician to Pliocene) and burial depths (1000m to 5000m) was produced using computer modeling programs. The model predicts the opposite from Sclater & Christie (1980), lower than real values for shallow wells but more accurate values for wells >8000ft (2.4km). Scherer indicated that porosity decline is linear from 500 to 5000m(1650ft to 16500ft) burial. McBride et al. (1991) study of Texas Gulf Coast sandstones showed that porosity declined rapidly until around 1200m burial. From burial depths deeper than 1200m there is a smaller but steady decline in porosity. Palmer & Barton (1987) indicate that rapid porosity decline from grain rearrangement takes place up to 500m burial (47.2% to 35.6%). An experiment by Kurkjy (1987) indicated a linear porosity decline by mechanical deformation as pressure increased from 1500 to 5000psi (equivalent to 3,000ft-10,000ft, 900m to 3.03km burial). It is interesting to note the subparallel trends of FGS, FMH and FBB **Figure 5.18**, are not coincident with each other but maintain porosity differences between them. The cause for the rapid decline of porosities within the ECG is uncertain and could be due to a) decrease in sorting but same facies or b) diagenetic effects.

5.9.2 Comparison with North Sea compaction curves

Regional trends for FGS, FBB and FMH are close to established porosity declines. ECG rate of decline is particularly rapid.

In the most comprehensive Brent Group study, Giles et al. (1992) found that there is a smooth decrease of porosity (on a macroscopic scale) with burial depth, and implies that exponential porosity declines are 'straightened out' by diagenetic effects and maintained by continuing diagenesis. Although major changes in porosity take place (quartz cementation >5% at depths >9000ft (2.7km), and gradual dissolution of feldspars) no apparent discrepancy between Brent and Palaeocene porosity declines (except for ECG) is seen, **Figure 5.18**. Most porosity decline rates (Loucks et al. 1984; Giles et al. 1992; Harris 1992) do not show any distinct change with depth although major mineralogical and cementation changes are known to occur around 9000ft, 2.7km depth.

Emery et al. (1993), found that there is wide variation between individual Mesozoic oilfield porosity trends from the Northern North Sea. Some follow standard trends 6-9%/km (1.8- 2.7%/1000ft) while in others porosities decline at a higher rate 20%/km

(6.1%/1000ft). Porosity values on structural crests correspond closely to porosities that would be predicted from sandstone compaction curves (Sclater & Christie 1980). In the Magnus field, the decline in porosity was matched to result of enhanced quartz cementation within deeper sands. This happened because quartz diagenesis was co-genetic with oil migration. Oil filled the trap and gradually slowed down cementation. Ramm & Bjorlykke (1994) produced linear declines for the Central North Sea, North and South Viking Graben and the Haltenbanken Basin. Sandstones in their study ranged from deep marine Tertiary Heimdal Formation, to fluvial and marine sandstones of the Jurassic to Triassic Skagerak Formation. They chose 75th percentile values porosities and permeabilities of 260 lithostratigraphic units/members greater than 10m thick. These closely match Palaeocene curves except for ECG. When their data (Ramm & Bjorlykke 1994) from regions are combined it is apparent that at depths greater than 2500m (8200ft) actual values for depth intervals less than 1km thick decline at higher rates than gross trends. This is explained as pressure-solution and quartz cementation processes becoming important at 2.5km. Overpressuring was important for preserving high porosities where pressure approached lithostatic gradients. Both Emery et al. (1993) and Ramm & Bjorlykke (1994) indicate that 2.5km burial depth represents a significant depth where quartz cementation resulting from pressure solution starts to become significant and form significant volumes. Although no samples for thin-sectioning from the deep ECG were taken within this study it is apparent from point-count data from Palaeocene well reports that quartz overgrowths begins to take up to 5% volume at depths 8500ft (2.6km) present day burial depth **Figure 5.19**. It is concluded that it is likely that the ECG porosity decline is high as a result of local pressure solution. These sample ECG wells are also directly associated with salt diapirism and enhanced quartz cementation and decline in porosity may be related to enhanced heat transfer from conductive salt diapirs accelerating the process of pressure solution. An insufficient range of depths has been sampled to ascertain if this ECG trend continues deeper.

5.10 Conclusions

1) Porosity and permeability within massively-bedded sandstones are influenced by fluid escape dish-and-pillar structures. These form distinctive bows of poroperm representing channels on a 5- 30m scale. From visual analysis of many composite logs, carbonate concretions preferentially precipitated within dish-and-pillar structure zones.

2) Porosity trends match the Sclater & Christie (1980) empirical compaction curve until 8000ft, 2.4km where actual porosities are up to 5% lower.

3) Porosity trends for the Fladen Ground Spur, Fisher Bank Basin and Forties Montrose High are similar to general Brent Group and Norwegian Sector sandstones porosity declines.

4) The porosity trend for East Central Graben is similar to published fields specific high declines in Mesozoic Northern North Sea sandstones resulting from quartz cementation. Further petrographic analysis of deep East Central Graben cores would need to be undertaken to confirm that individual rapid porosity declines in Montrose Group sandstones in this region result from similar processes.

5) Porosity decline measurements from a single well to be representative of regional porosity declines must be sampled from uniform facies, over core lengths greater than the thickness of depositional units. For the Montrose Group such cores would be greater than 150feet.

6) Palaeocene quartz overgrowths volumes form less than 5%BV at depths 1.9 to 3.1km; this is within the range of Brent Group cements at similar depths.

Acknowledgements - Roger Anderton BP, Dyce is thanked for allowing sampling at BP Expro Technical Data Centre, Dyce.

References

Baldwin, B. and C.O. Butler 1985 Compaction curves. *Bulletin of the American Association of Petroleum Geologists*, **69**, 622-626.

Berggren, W.A. and F.M. Gradstein 1981 Agglutinated benthonic foraminiferal assemblages in the Palaeocene of the Central North Sea: their biostratigraphic and depositional significance. In: *Petroleum Geology of the Continental Shelf of North- West Europe*, I.V. Illing and G.D. Hobson (eds), Institute of Petroleum, Heyden and Son, London, 282-285.

Bjorkum P.A. and O. Walderhaug 1990 Lateral extent of calcite-cemented zones in shallow marine sandstones. In: *North Sea Oil and Gas Reservoirs-II*, The Norwegian Institute of Technology, Graham and Trotman, 331-336.

Boles J.R. and K.S. Johnson 1983 Inlfuence of mica surfaces on pore-water pH. *Chemical Geology*, **43**, 303-317.

Carman R.N. and R. Young 1981 Reservoir Geology of the Forties Oilfield. In: *Petroleum Geology of North West Europe*, J. Brooks and K. Glennie (eds), Graham and Trotman, London, 371-379.

Cheeney R. Theoretical distributions and confidence intervals. In: *Statistical Methods in Geology*, George Allen and Unwin, London, 58-71.

Crawford, R., Littlefair R.W. and L.G. Affleck 1991 The Arbroath and Montrose Fields, Block 22/17,18 UK North Sea. In: *United Kingdom Oil and Gas Fields, 25 Years Commemorative Volume*, I.L. Abbotts (ed), *Geol. Soc. Lond. Mem.* **14**, 211-217.

Cutts P.L. 1991 The Maureen Field, Block 16/29a, UK North Sea. In: *United Kingdom Oil and Gas Fields, 25 Years Commemorative Volume*, I.L. Abbotts (ed), *Geol. Soc. Lond. Mem.* **14**, 347-352.

Deegan C.E. and B.J. Scull 1977 A standard lithostratigraphic nomenclature for the central and northern North Sea. *Inst. Geol. Sci. Report* **77/25**

Den Hartog Jager D., Giles M.R. and G.R. Griffiths 1993 Evolution of Paleogene submarine fans of the North Sea in space and time. In: *Petroleum Geology of Northwest Europe: Proceedings of the 4th Conference*, J.R. Parker (ed), Geol. Soc., London, 59-71.

Emery D. and A. Robinson 1993 Porosity and permeability. In: *Inorganic Geochemistry: Applications to Petroleum Geology*, D. Emery and A. Robinson (eds), Blackwell Scientific Publications, London, 129-169.

Emery, D., Smalley, P.C. and N.H. Oxtoby 1993 Synchronous oil migration and cementation in sandstone reservoirs demonstrated by quantitative description of diagenesis. *Phil. Trans. R. Soc. Lond.*. **344**, 115-125.

Geel, C.R. 1993 Recognition of thin-bedded turbidites from gamma-ray logs using forward modelling and simulated annealing. In: *Reservoir characterisation of deep marine clastic systems*, A. Hartley and J. Prosser (eds), University of Aberdeen, 12.

Giles, M.R., Stevenson, S., Martin, S.V., Cannon, S.J.C., Hamilton, P.J., Marshall, J.D. and G.M. Samways 1992 The reservoir properties of the Brent Group: a regional perspective. In: *Geology of the Brent Group*, A.C. Morton, R.S. Haszeldine, M.R.Giles and S. Brown (eds), *Geol. Soc. Spec. Publ.* **61**, 289-327

Harris, N.B. 1992 Burial diagenesis of Brent sandstones: a study of Statfjord, Hutton and Lyell fields. In: *Geology of the Brent Group*, A.C. Morton, R.S. Haszeldine, M.R.Giles and S. Brown (eds), *Geol. Soc. Spec. Publ.* **61**, 351-357.

Haszeldine, R.S., Samson, I.M. and C. Cornford 1984 Quartz diagenesis and convective fluid movement: Beatrice Oilfield, UK North Sea. *Clay Minerals*, **19**, 391-402.

Housnecht, D.W. 1984 Influence of grain size and temperature on intergranular pressure solution, quartz cementation, and porosity in a quartzose sandstone. *Journal of Sedimentary Petrology*, **54**, 348-361.

Hurst, A. 1987 Problems of reservoir characterization in some North Sea sandstones reservoirs solved by the application of microscale geological data. In: *North Sea Oil and Gas Reservoirs:II*, The Norwegian Institute of Technology, Graham and Trotman, 153-167.

Kantorowicz, J.D., Eigner, M.R.P., Livera, S.E., Van Schijndel-Goester, F.S. and P.J. Hamilton 1992 Integration of petroleum engineering studies of producing Brent Group fields to predict reservoir properties in the Pelican Field, UK North Sea. In: *Geology of the Brent Group*, A.C. Morton, R.S. Haszeldine, M.R.Giles and S. Brown (eds), *Geol. Soc. Spec. Publ.* **61**, 452-471.

Knox, R.W.O'B., Morton, A.C. and R. Harland. Stratigraphic relationships of Palaeocene sands in the UK Sector of the central North Sea. In: *Petroleum Geology of the Continental Shelf of North West Europe* in London, L.V. Illing and G.D. Hobson (eds), Institute of Petroleum, Heyden and Son, 267-281.

Kurkjy, K.A., Smith, J.C. and A.S. Trevena 1987 Losses of porosity and permeability in lithic sands assessed with compaction experiments. *Bulletin of American Association of Petroleum Geologists*, **71**, 579.

Loucks, R.G., Dodge, M.M. and W.E. Galloway 1984 Regional controls on diagenesis and reservoir quality in Lower Tertiary sandstones along the Texas Gulf Coast, In: *Clastic Diagenesis*, D.A. MacDonald and R.C. Surdam (eds), *American Association of Petroleum Geologists Memoir* **37**, 15-46.

Lowe, D.R. 1975 Water escape structures in coarse-grained sediments. *Sedimentology*, **22**, 57-204.

McBride E.F., Diggs T.N. and J.C. Wilson 1991 Compaction of Wilcox and Carizzo Sandstones (Palaeocene-Eocene) to 4420m, Texas Gulf Coast. *Journal of Sedimentary Petrology*, **61**, 73-86.

Milton, N.J., Bertram, G.T. and I.R. Vann 1990 Early Paleogene tectonics and sedimentation in the Central North Sea. In: *Tectonic events responsible for Britain's oil and gas reserves*, R.F.P. Harman and J. Brooks (eds), *Geol. Soc. Spec. Publ.*, **55**, 339-351.

Morton, A.C., Halsworth, C.R. and G.C. Wilkinson 1993 Stratigraphic evolution of sand provenance during Palaeocene deposition in the Northern North Sea area. In: *Petroleum Geology of Northwest Europe: Proceedings of the 4th Conference*, J.R. Parker (ed), Geol. Soc., London, 73-84.

Mound, D.G., Robertson, I.D. and R.J. Wallis 1991 The Cyrus Field, block 16/28, UK North Sea. In: *United Kingdom Oil and Gas Fields, 25 Years Commemorative Volume*, I.L. Abbotts (ed), *Geol. Soc. Mem.* **14**, 295-300

Mudge, D.C. and P. Copestake 1992 Revised Lower Palaeocene lithostratigraphy for the Outer Moray Firth, North Sea. *Marine and Petroleum Geology*, **9**, 53-69.

O'Connor, S.J. and D. Walker 1993 Paleocene reservoirs of the Everest trend. In: *Petroleum Geology of Northwest Europe: Proceedings of the 4th Conference,* J.R. Parker (ed),Geol. Soc., London, 145-160.

Palmer, S.N. and M.E. Barton 1988 Porosity reduction, microfabric and resultant lithification in UK uncemented sands. In: *Diagenesis of Sedimentary Sequences*, J.D. Marshall (ed), *Geol. Soc. Spec. Publ.* **36**, 29-40.

Prosser D.J., McKeever M., Hogg, A.J.C. and A. Hurst 1993 Permeability heterogeneity within Jurassic submarine fan sandstones from the Miller Field, UK Northern North Sea. In*: Reservoir characterisation of deep marine clastic systems*, A. Hartley and J. Prosser (eds), University of Aberdeen, 25.

Ramm, M. 1992 Porosity-depth trends in reservoir sandstones: theoretical models related to Jurassic sandstones offshore Norway. *Marine and Petroleum Geology*, **9**, 553.

Ramm, M. and K. Bjorlykke 1994 Porosity/depth trends in reservoir sandstones: assessing the quantitative effects of varying pore-pressure, temperature history and mineralogy, Norwegian Shelf data. *Clay Minerals*, **29**, 475-490.

Reynolds, T. 1994 Quantitative analysis of submarine fans in the Tertiary of the North Sea Basin. *Marine and Petroleum Geology,* **11**, 202-207.

Rochow, K.A. 1981 Seismic stratigraphy of the North Sea "Palaeocene" deposits. In*: Petroleum Geology of the Continental Shelf of North-West Europe*, I.V. Illing and G.D. Hobson (eds), Heyden, London, 225-266.

Scherer, M. 1987 Parameters influencing porosity in sandstones: a model for sandstone porosity prediction. *Bulletin of American Association of Petroleum Geologists*, **71**, 485-491.

Sclater, J.G. and P.A.F. Christie 1980 Continental stretching; an explanation of the post-mid-Cretaceous subsidence of the central North Sea basin. *Journal of Geophysical Research*, **85**, 3711-3739.

Selley R.C. 1978 Porosity gradients in the North Sea oil-bearing sandstones. *J. Geol. Soc. London*, **135**, 119-132.

Schmoker J.W. and D.L. Gaultier 1988 Sandstone porosity as a function of thermal maturity. *Geology*, **16**, 1007-1010.

Tonkin, P.C. and A.R. Fraser 1991 The Balmoral Field, Block 16/21, UK North Sea. In: *United Kingdom Oil and Gas Fields, 25 Years Commemorative Volume,* I.L. Abbotts (ed), *Geol. Soc. Mem.* **14**, 237-243.

Wentworth, C.M. 1967 Dish structures, a primary sedimentary structure in coarse turbidites. *Bull. Am. Ass. Petrol. Geol.*, **51**, 485.

Wilkinson, M. and M.D. Dampier. 1990 The rate of growth of sandstone-hosted calcite concretions. *Geochimica et Cosmochimica Acta*, **54**, 3391-3399.

Wills, J.M. 1991 The Forties Field, Block 21/10, 22/6a, UK North Sea. In: *United Kingdom Oil and Gas Fields, 25 Years Commemorative Volume,* I.L. Abbotts (ed), *Geol. Soc. Mem.* **14**, 301-308.

Figure captions

Figure 5.1 Location map of Central North Sea sample wells with base Cretaceous structural elements.

Figure 5.2 Lithostratigraphy from Deegan & Scull (1977)

Figure 5.3 Burial history curves for regions based on Barnard & Bastow (1991)

Figure 5.4 Composite log, porosity and permeability logs of well 16/21-20. Illustrates bows apparent in poroperm with depth, subtly reflected in gamma-ray trace. 'Bows' are illustrated with arrows.

Figure 5.5 Composite log, permeability and porosity logs of well 15/25-2. 'Bows' apparent on permeability and porosity logs are not identified on the gamma-ray log. 'Bows' are illustrated by arrows on the right.

Figure 5.6 Composite porosity and permeability logs of well 16/29-8. Illustrates two distinct bows within the Andrew Formation not identified on the gamma-ray log. 'Bows' are illustrated on the right by arrows

Figure 5.7 Composite, porosity and permeability logs of well 15/26-3. Cemented horizons as picked out on sonic logs are more prevalent at the tips of poroperm 'bows'. 'Bows' are illustrated by arrows on the left.

Figure 5.8 Well 16/28-6 illustrating massive sands and the relationship between dish structures and poroperm variations.

Figure 5.9 Graph of porosity and carbonate cements across a concretion. Variation in porosity where there is no carbonate must relate to other factors than calcite precipitation.

Figure 5.10 Porosity-permeability cross-plots of regional areas. Areas a, represent data defined by 'blocky' facies, areas b, represent subordinate facies, and areas c, represent carbonate cemented horizons.

Figure 5.11 Porosity-permeability cross-plots of regional areas. Data selected is 'blocky' facies identified from composite logs.

Figure 5.12 Statistical data plots concerning porosity decline variations.

Figure 5.13 Cross plots illustrating relationships between sampled core length and porosity decline. Longer cores (>100ft, 30.5m) porosity decline rates are more likely to move towards zero than short cores which have a broad range of porosity decline rates.

Figure 5.14 Cartoon sedimentary logs illustrating relationship between thickness of amalgamated units and uniform-spaced sampling strategy. Sedimentary units are more likely to be identified if sampling spacing considers unit thickness.

Figure 5.15 Housnecht diagram. Four wells data plotted onto intergranular volume cross-plot illustrates that mechanical compaction has had an overwhelming contribution to porosity loss within Montrose Group sandstones.

Figure 5.16 Point-count data of authigenic cements plotted against depth show that volumes do not increase down well. Authigenic cements do not affect single wells porosity decline rates.

Figure 5.17 Porosity depth trends for individual wells compared with Sclater & Christie (1980) and Scherer's (1987) empirical porosity-depth curves.

Figure 5.18 Regional porosity declines for Montrose Group sandstones compared with Norwegian Shelf sandstones (Ramm & Bjorlykke 1994), Brent Group sandstones (Giles et al, 1992; Harris 1992) and Texas Gulf Coast Tertiary sandstones (Loucks et al. 1984).

Fig 5.19 Plot of quartz overgrowth v. depth, from point count data. Generally less than 4%, except near salt.

Tables

Table 5.1 Sample wells included in poroperm study.

Fladen Ground Spur				
15/19-2	15/20-4	15/2-5	15/20-7	15/25-2
16/16-1	16/21-1	16/21-6	16/21-20	16/22-4
Fisher Bank Basin				
16/27-1	16/28-6	16/29-2	16/29-4	16/29-8
22/3-2	22/3-3	22/5-10		
East Central Graben				
21/9-1	21/9-2	21/10-1	21/10-4	21/10-5
22/6-2	22/12-6	22/17-4	22/18-3	
Forties Montrose High				
22/9-3	22/9-4	22/10-3	22/14-1	22/14-2
22/15-2	22/20-3	23/11-2	23/16-4	
The wells below are outwith these areas				
14/13-3	15/26-3	15/26-4	16/23-4	21/1-15
21/16-6				

Table 5.2 Wells sampled for thin-section petrography

14/13-3	15/20-4	15/26-3	15/26-4	16/28-6
16/29-2	21/10-1	22/20-3	22/17T-4	

Table 5.3 Poroperm 'bows' within sample wells. Permeability variations are more sensitive to reservoir quality.

Wells	Length of bow	δHelium Porosity (%)	δPermeability (mD)
15/20-4	5m	26-30	500-1000
	5m	20-25	400-3000
	6m	20-25	350-2000
	5m	26-30	500-600
	2.5m	25-28	350-1000
15/25-2	10m	no variation	400-1050
	4m	no variation	400-1000
	4m	no variation	800-1000
	4m	25-27	700-1050
15/26-3	2m	23-28	50-250
	2m	24-26	15-100
	10m	24-28	15-30
16/21-1	4m	24-29	700-3000
16/21-20	3m	23-26	500-1000
	3m	23-26	450-800
16/28-6	6m	15-20	50-400
	6m	22-26	200-650
16/29-2	6m	22-28	350-1050
	2	no variation	300-600
	3m	28-32	350-1000
	7.5m	20-26	70-600
	4.5m	22-28	60-300

16/29-8	9m	15-27	45-1050
	8.5m	15-27	28-350
21/10-5	6m	no variation	400-1050
	6m	26-33	400-1050
22/3-2	6m	22-25	0.4-10
22/9-3	10.5m	20-27	11-150
22/10-3	8.5m	1.5-35	15-21
22/17-4	3m	22-24	40-100
	6m	19-27	1-800

Table 5.4 Point count data from well 15/26-3

Sample	carbonate	porosity	Q:F:L
1890.6m	0%	27%	88:8:3
1891m	0%	21.6%	93:5:2
1895.18m	42.4%	0%	83:11:6
1900.75m	0%	18.2%	91:5:4
1904.7m	0%	25%	90:9.5:1.5

Table 5.5 Poroperm variations relating to the presence of fluid escape dish-and-pillar structures

Well	Cored depth (m)	Permeability (mD)	Helium Porosity (%)
15/20-4	1983-1992	400-3000	20-25
	2002-2011	350-2000	20-25
16/28-6	2705-2735	50-400	15-20
no dish structures	2627-2639	200-300	18-19

Table 5.6

FGG	Well	Cored Length (feet)	Data points	ϕ-loss/1000'	% significant
	15/19-2	5924-5948	18	85.51	95-99
	15/20-4	6475-6620	78	0.82	<80
	15/20-5	6375-6410	30	-6.34	<80
		6500-6552			
	15/20-7	6455-6490	27	13.35	<80
	15/25-2	7150-7350	102	0.61	<80
	16/16-1	7385-7425	30	24.97	<80
	16/21-6	7020-7048	26	-86.39	<80
	16/21-20	7270-7370	68	20.02	99-99.9
	16/23-4	8265-8309	33	-51.03	99-99.9
FBB	16/28-6	8560-8980	236	5.61	99.9
	16/29-2	8645-8825	108	0.34	<80
	16/29-4	9110-9142	32	0.65	<80
	22/3-2	8400-8465	72	16.2	90-95
	22/3-3	8412-8494	41	-4.76	<80
	22/5-10	9160-9185	11	13.14	99-99.9
		9242-9267			
ECG	22/8-3	8686-8718	27	48.80	90-95
	22/9-3	8545-8680	67	1.13	<80
	22/9-4	8550-8830	25	1.25	<80
	22/10-3	8959-9008	49	4.97	<80
	22/14-2	8710-8752	20	5.59	<80
	22/20-3	8845-8930	47	-36.40	99-99.9

FMH	21/9-1	7296-7336	24	181.25	99.9
	21/9-2	6984-7009	17	90.29	90-95
	21/9-4	7420-7447	26		<80
	21/10-1	7085-7123	31	12.60	<80
	21/10-5	7262-7395	116	22.25	99-99.9
	22/17-4	10065-10280	149	11.22	99.9
	22/18-3	8785-8845	47	38.23	95-99

Table 5.7 Point count volumes of cement and porosity

Well	Depth (m)	Cement (%)	Porosity (%)
16/28-6	2585.8	6.6000	19.400
	2585.9	6.0000	18.800
	2586.0	6.4000	20.000
	2598.7	4.0000	16.200
	2615.1	3.4400	16.700
	2631.2	4.0000	11.200
	2645.4	6.0000	15.400
	2645.5	3.2000	16.400
	2660.2	3.0000	13.600
	2675.7	5.8000	16.800
	2683.3	5.2000	16.800
	2689.7	2.2000	14.400
	2705.7	5.4000	14.000
	2720.5	3.4000	15.600
	2721.2	1.4000	0.0000
	2734.5	4.2000	12.400
16/29-2	2628.9	1.4000	16.400
	2629.4	1.8000	24.400
	2634.1	1.8000	27.400
	2636.5	1.4000	21.200
	2638.1	2.0000	20.200
	2642.0	2.0000	16.200
	2648.4	5.6000	18.200
	2650.8	1.8000	20.880
	2654.8	1.6000	19.000
	2657.9	2.6000	13.200
	2663.9	2.2000	11.400
	2666.4	0.60000	1.2000
	2673.7	2.6000	21.400
	2678.3	2.0000	15.200
	2685.4	9.2000	12.400
21/10-1	2153.4	6.0000	11.800
	2155.7	2.8000	7.4000
	2158.2	4.4000	7.6000
	2161.9	1.4000	23.600
	2165.3	3.2000	23.400
	2165.4	3.4000	17.800
	2166.5	1.2000	19.000
	2169.0	7.4000	5.0000
	2238.1	2.4000	24.200
	2242.4	1.2000	0.20000
	2244.8	2.2000	22.200
	2248.5	3.4000	23.000

	2253.1	3.4000	21.600
22/17-4	2667.0	9.4000	6.6000
	2667.3	5.8000	2.2000
	2667.6	5.6000	12.400
	2669.8	6.6000	16.600
	2671.6	5.0000	15.000
	2673.4	5.0000	18.800
	2675.0	7.6000	15.800
	2678.3	6.2000	22.600
	2707.0	2.6000	20.200
	2708.2	2.6000	22.700
	2709.1	2.8000	12.000
	2714.9	2.6000	21.000
	2716.1	1.4000	23.600
	2718.5	3.2000	20.400
	2726.4	2.0000	21.400
	2723.4	2.6000	23.400
	2768.6	1.6000	27.800
	2771.3	14.200	8.2000
	2775.2	2.8000	23.400
	2777.9	3.4000	20.400
	2781.3	1.2000	20.200
	2784.1	4.8000	20.400

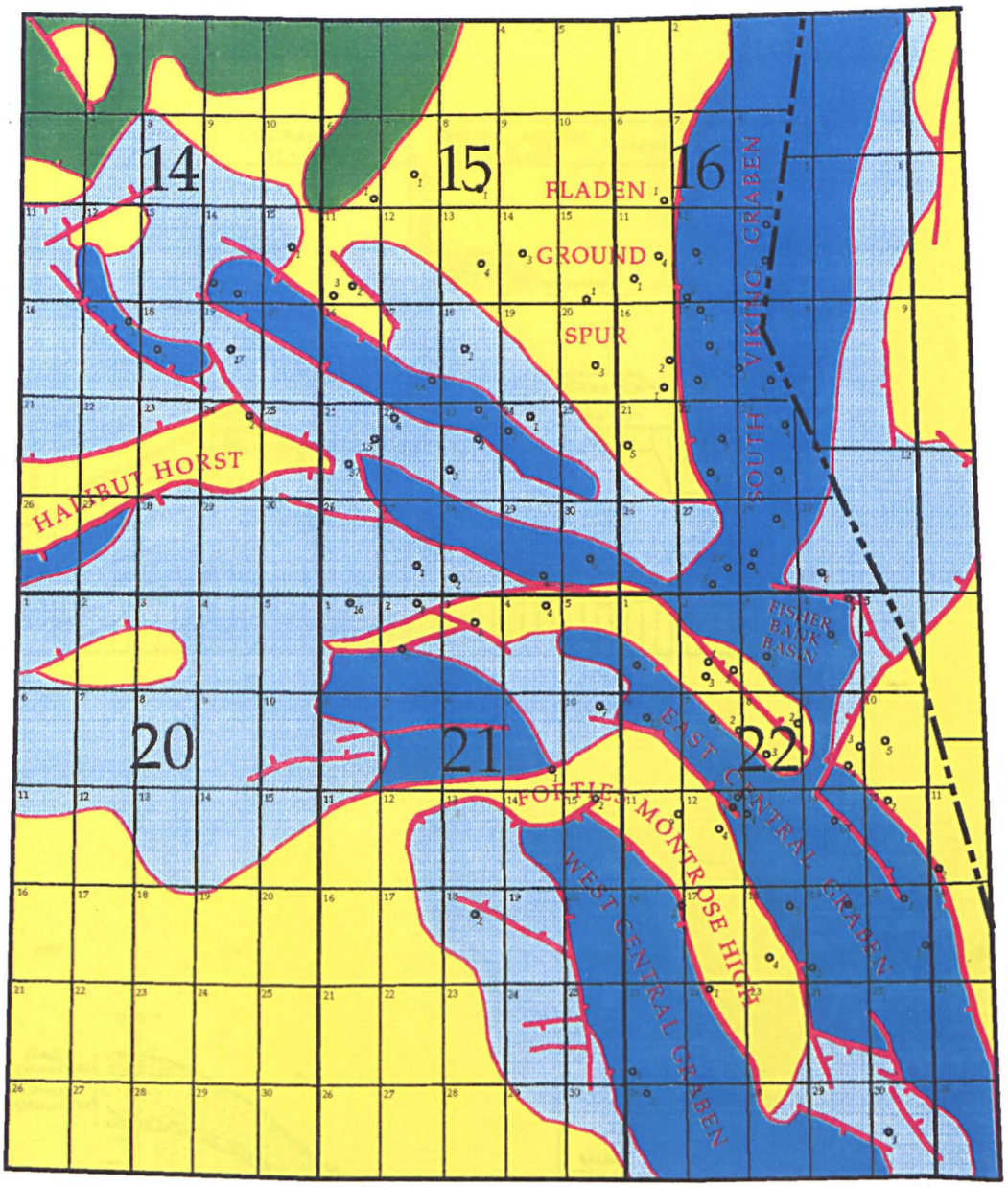

Figure 5.1 Central North Sea location map for sample wells with base-Cretaceous structural elements

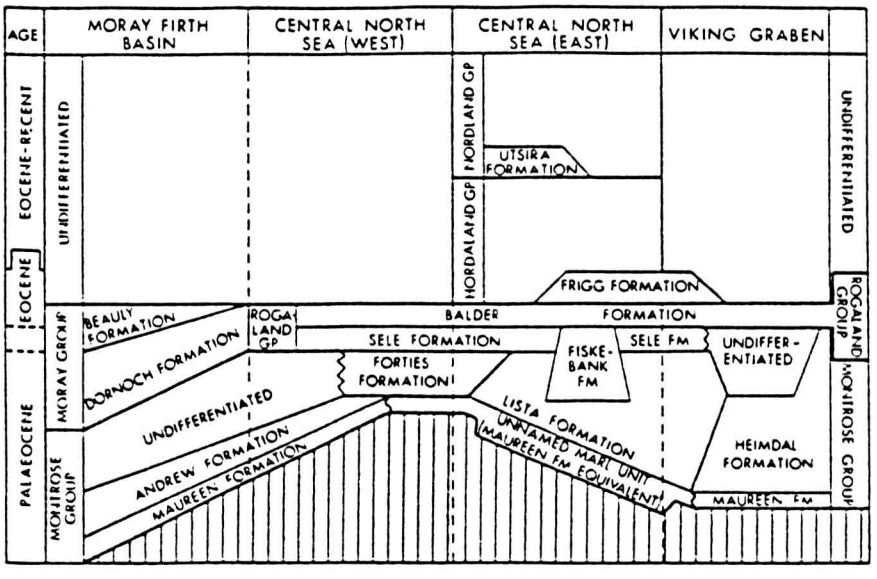
AGE
MORAY FIRTH BASIN
CENTRAL NORTH SEA (WEST)
CENTRAL NORTH SEA (EAST)
VIKING GRABEN
EOCENE-RECENT
UNDIFFERENTIATED
NORDLAND GP
UTSIRA FORMATION
HORDALAND GP
UNDIFFERENTIATED
EOCENE
FRIGG FORMATION
ROGALAND GROUP
BEAULY FORMATION
DORNOCH FORMATION
MORAY GROUP
ROGALAND GP
BALDER FORMATION
SELE FORMATION
SELE FM
UNDIFFER-ENTIATED
FISKE-BANK FM
FORTIES FORMATION
UNDIFFERENTIATED
ANDREW FORMATION
MAUREEN FORMATION
PALAEOCENE
MONTROSE GROUP
LISTA FORMATION
UNNAMED MARL UNIT (MAUREEN FM EQUIVALENT)
HEIMDAL FORMATION
MAUREEN FM
MONTROSE GROUP

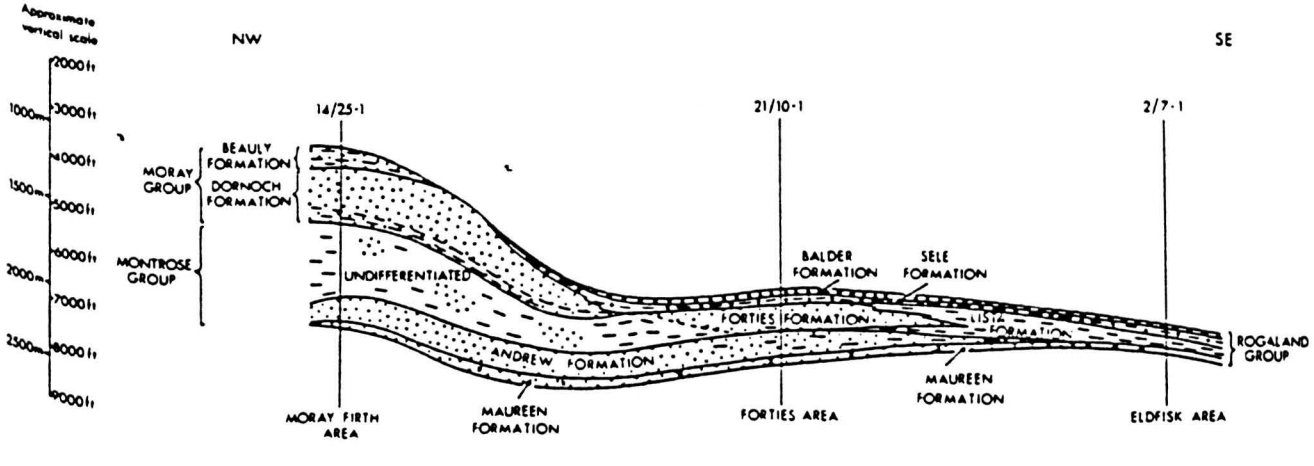
Approximate vertical scale
2000 ft
1000m
3000 ft
4000 ft
1500m
5000 ft
6000 ft
2000m
7000 ft
2500m
8000 ft
9000 ft
NW
SE
14/25-1
21/10-1
2/7-1
MORAY GROUP
BEAULY FORMATION
DORNOCH FORMATION
MONTROSE GROUP
UNDIFFERENTIATED
BALDER FORMATION
SELE FORMATION
FORTIES FORMATION
LISTA FORMATION
ANDREW FORMATION
MAUREEN FORMATION
ROGALAND GROUP
MORAY FIRTH AREA
MAUREEN FORMATION
FORTIES AREA
ELDFISK AREA

Figure 5.2

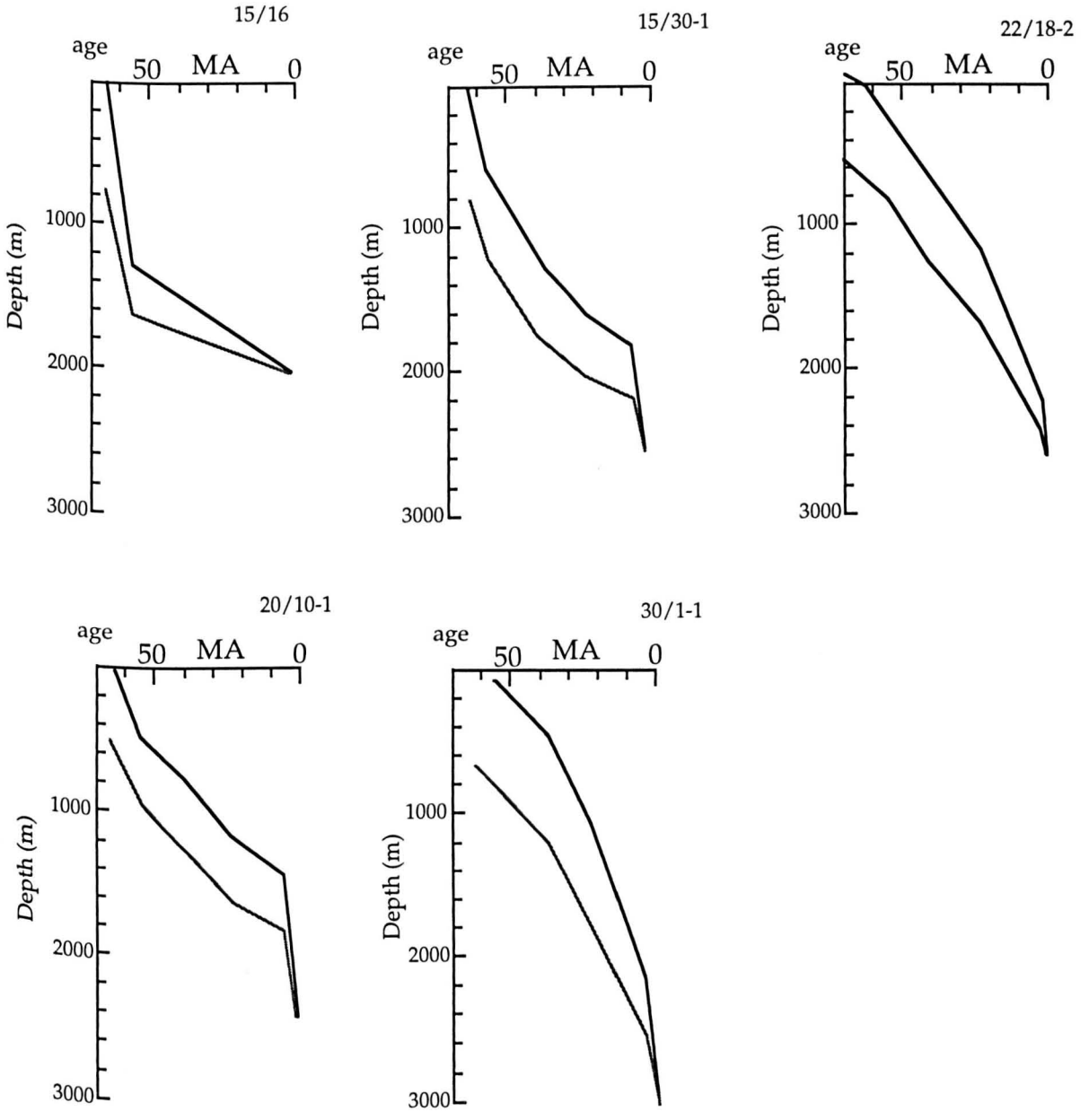
15/16
age
50
MA
0
Depth (m)
1000
2000
3000
15/30-1
age
50
MA
0
Depth (m)
1000
2000
3000
22/18-2
age
50
MA
0
Depth (m)
1000
2000
3000
20/10-1
age
50
MA
0
Depth (m)
1000
2000
3000
30/1-1
age
50
MA
0
Depth (m)
1000
2000
3000

Figure 5.3

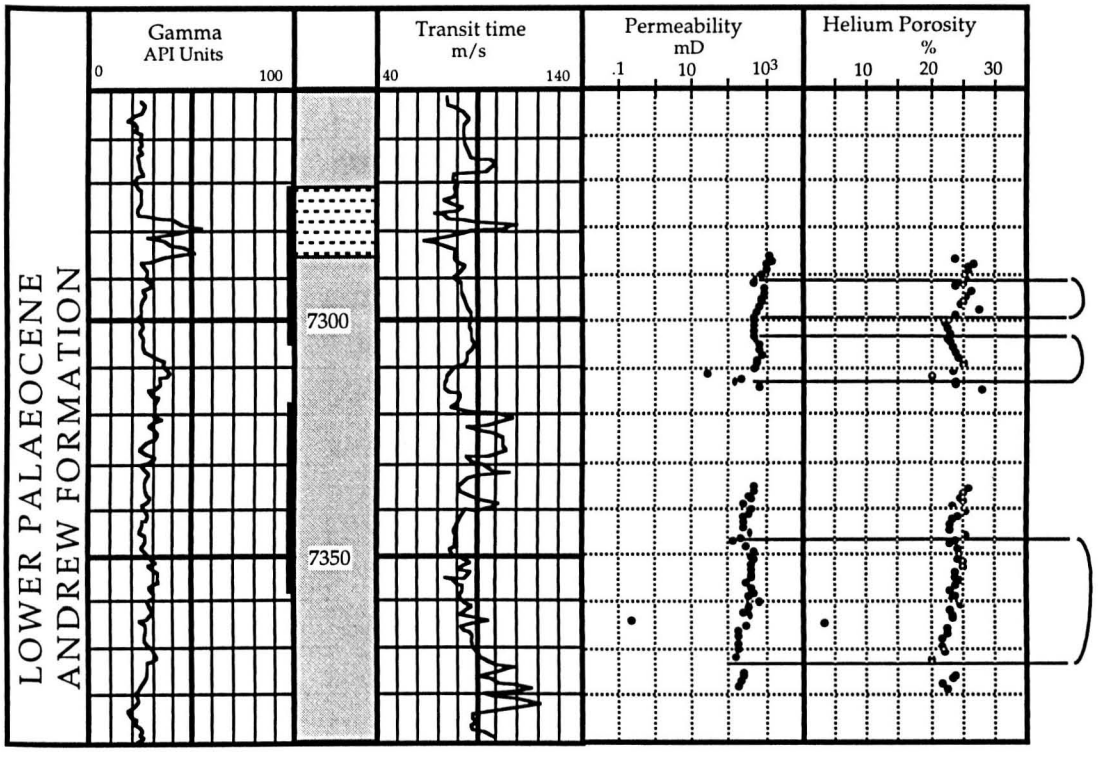

Figure 5.4 Composite log, porosity and permeability logs of well 16/21-20. Illustrates bows apparent in poroperm with depth, subtly reflected in gamma-ray log trace. 'Bows' are illustrated on the right.

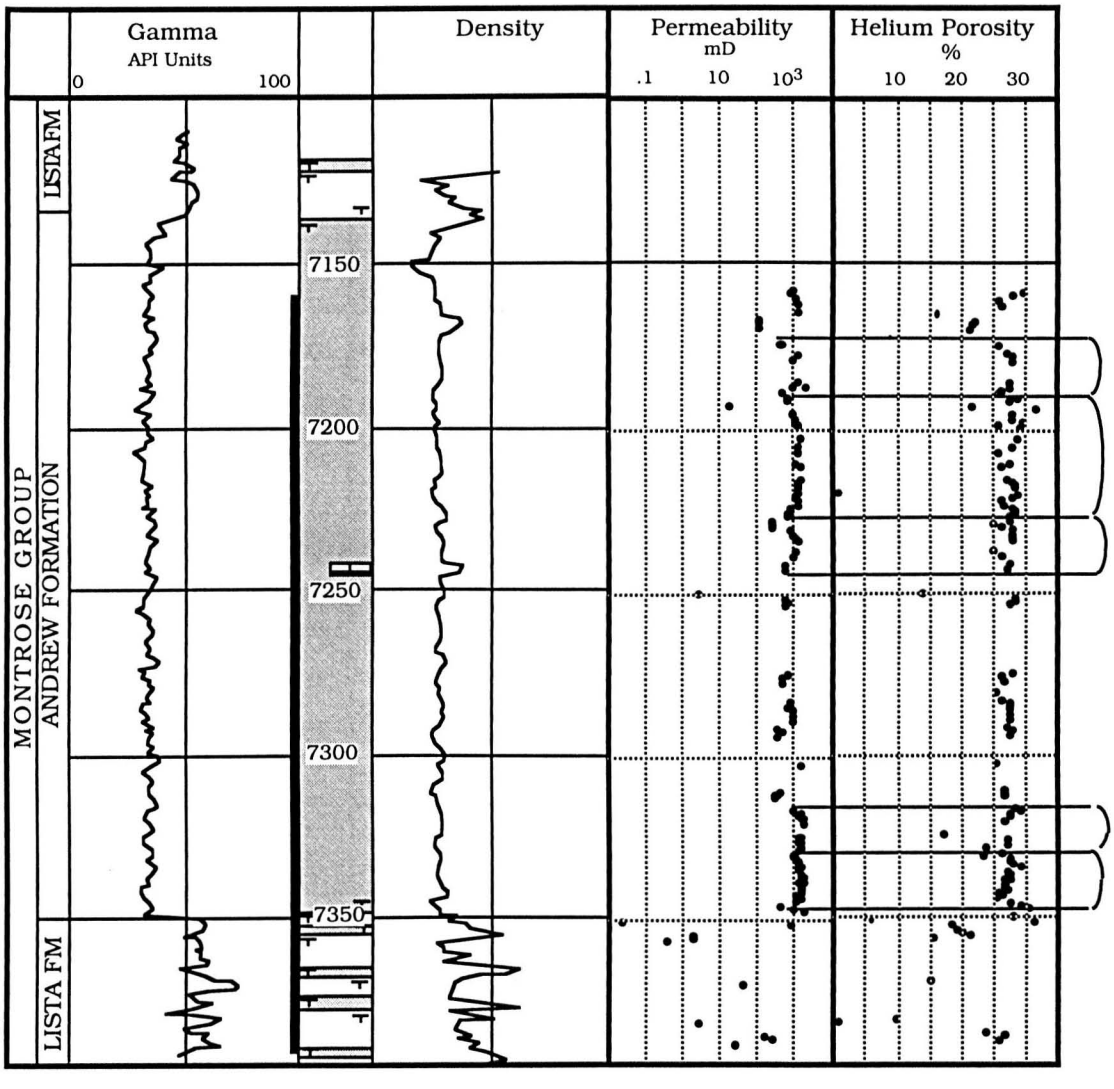

Figure 5.5 Composite, permeability and porosity logs of well 15/25-2. 'Bows' apparent on permeability and porosity logs are not identified on the gamma-ray log. 'Bows' are illustrated on the right.

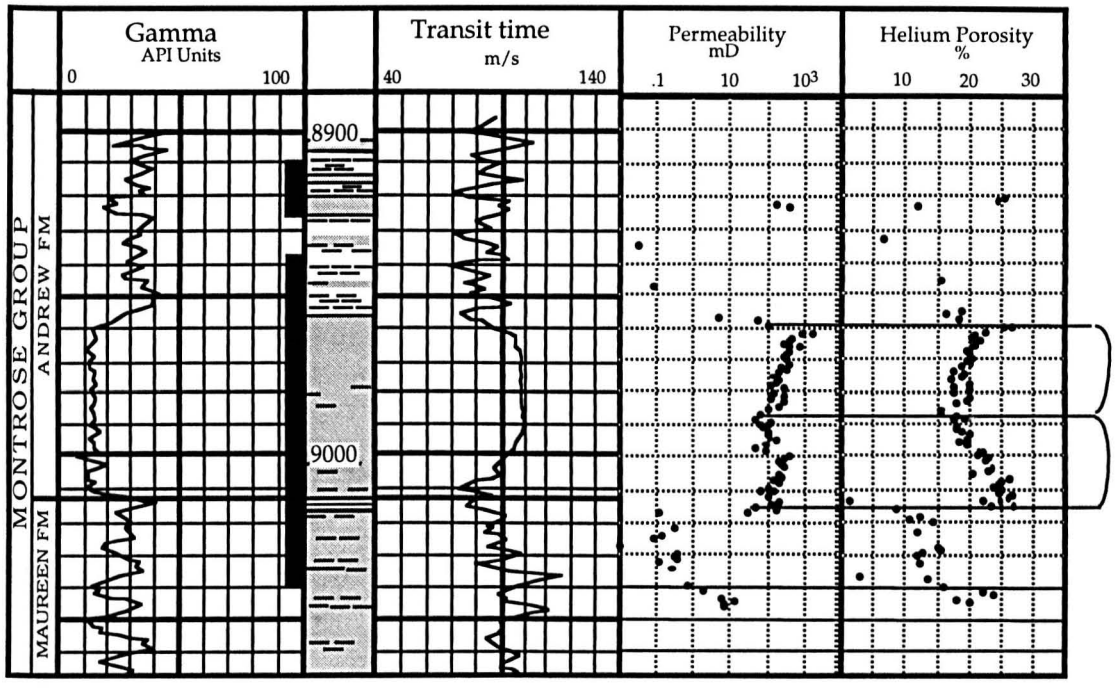

Figure 5.6 Composite, porosity and permeability logs of well 16/29-8. Illustrates two distinct 'bows' within the Andrew Formation not identified on the gamma-ray log.
'Bows' are illustrated on the right.

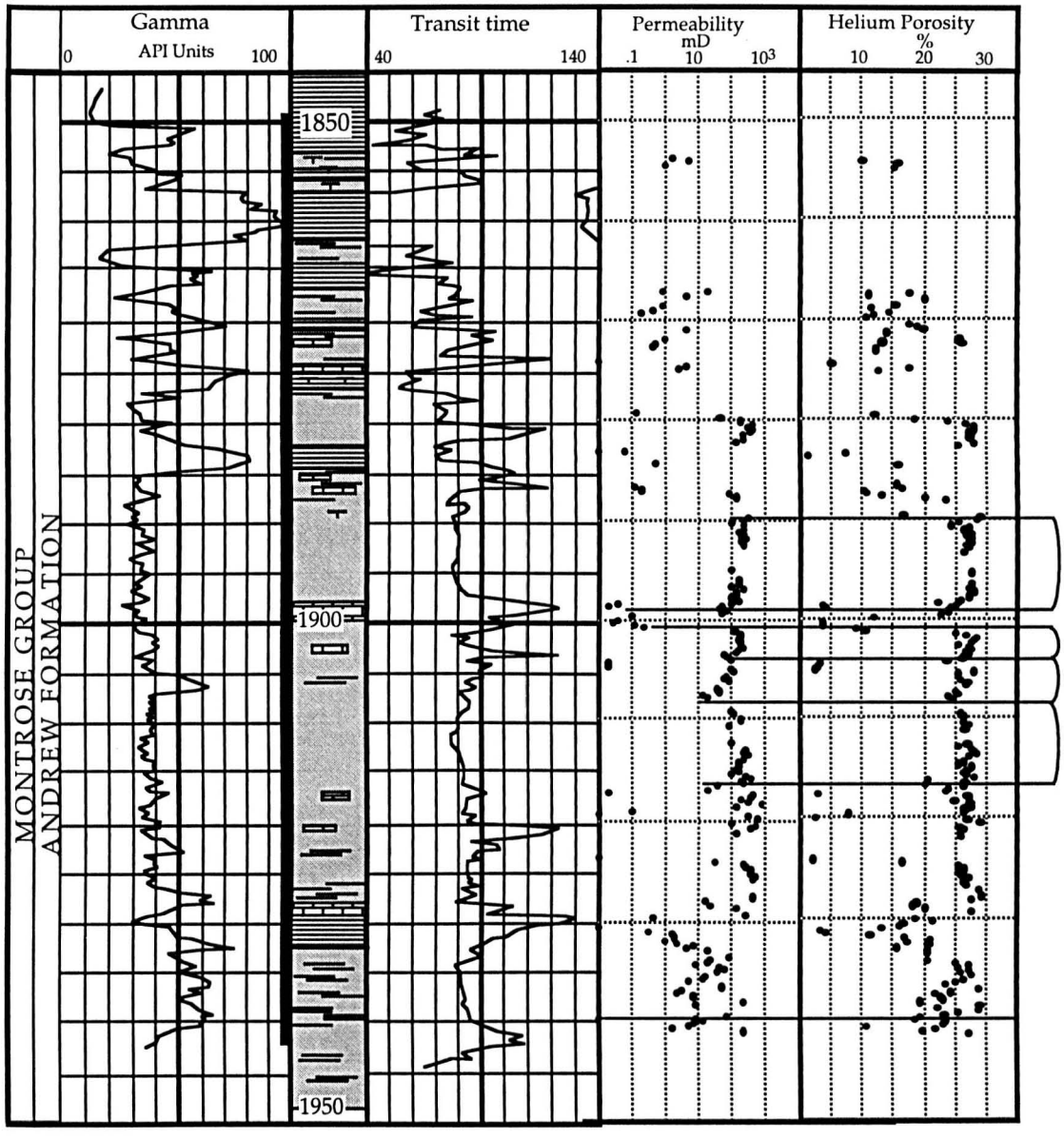

Figure 5.7 Composite, porosity and permeability logs of well 15/26-3. Cemented horizons as picked out on sonic logs are more prevalent at the tips of poroperm 'bows'. 'Bows' are illustrated on right.

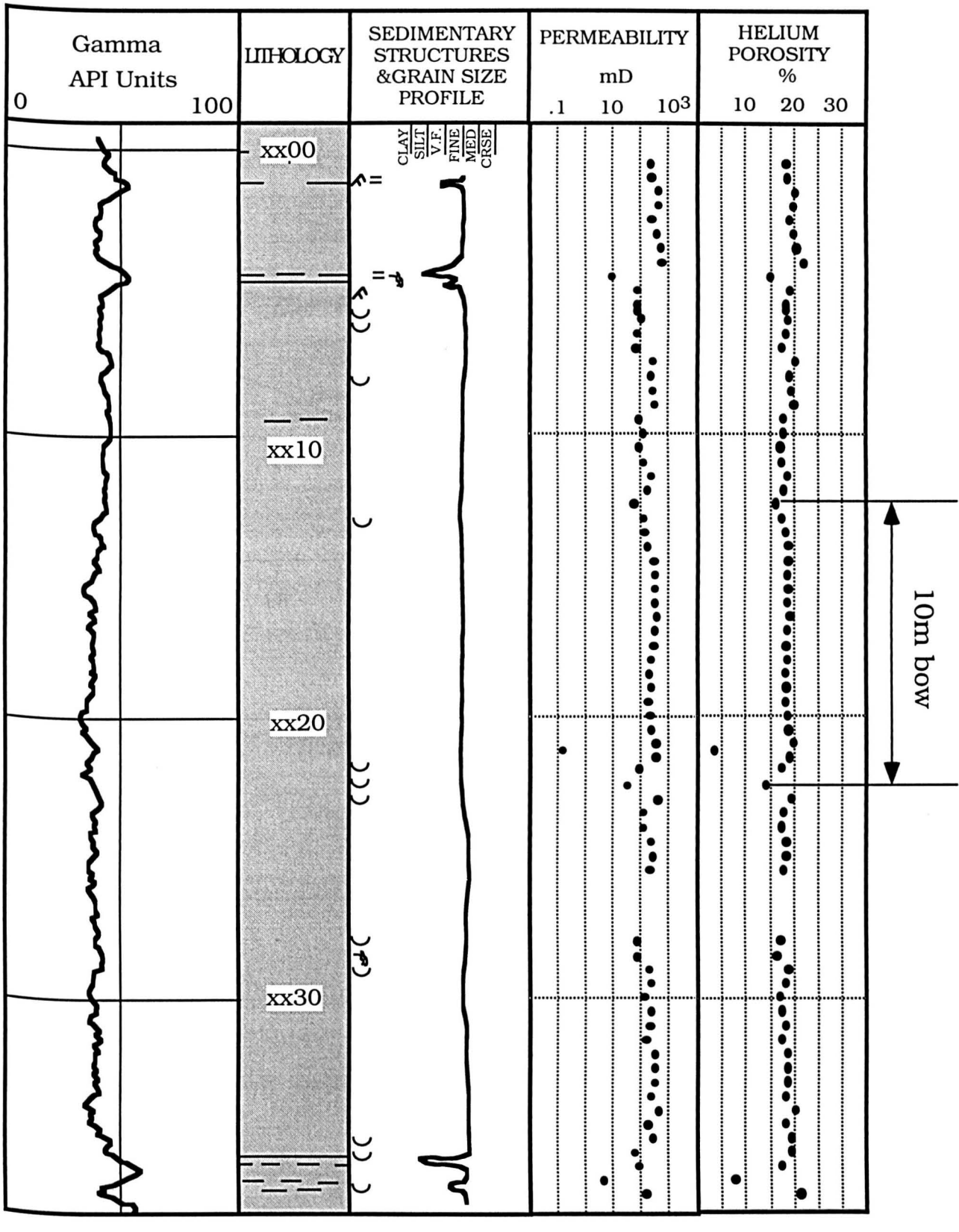

Figure 5.8 Well 16/28-6 illustrating massive sands and the relationship between dish structures and poroperm variations

Figure 5.9 Graph of porosity and carbonate across a concretion. Variation in porosity where there is no carbonate must relate to other factors than calcite dissolution.

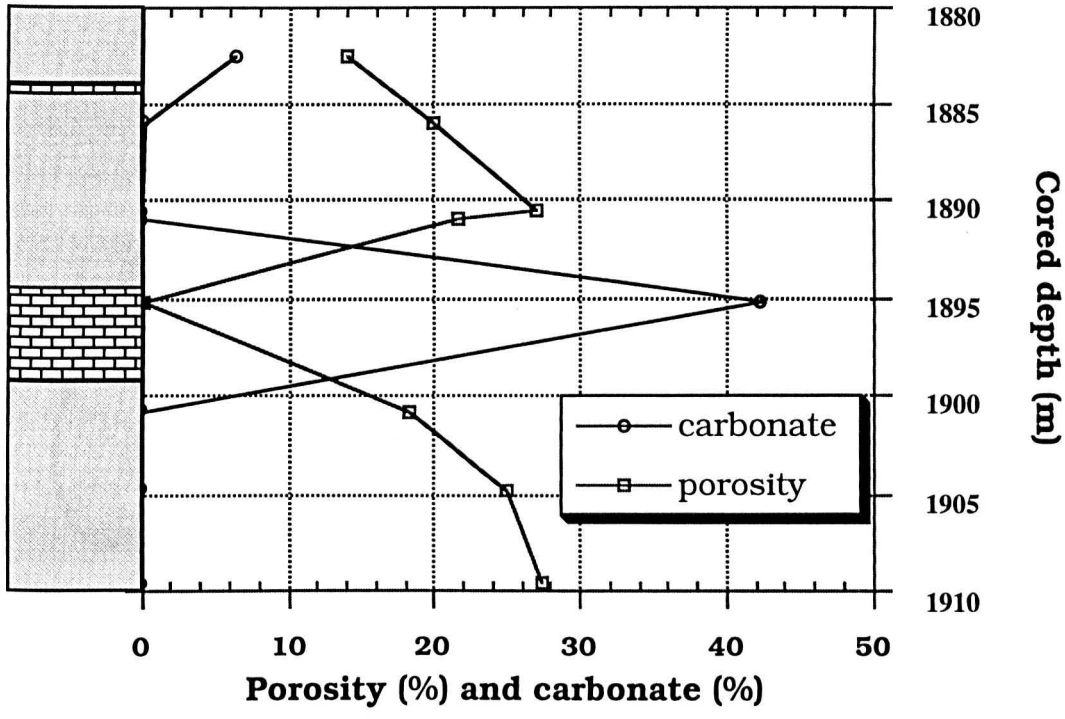

Fig5.10a Fladen Ground Spur_all data

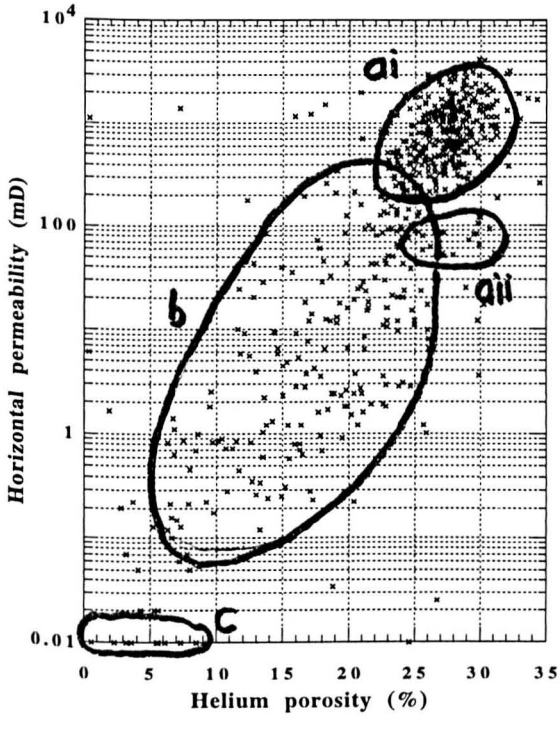

Figure 5.10b Fisher Bank Basin_all data

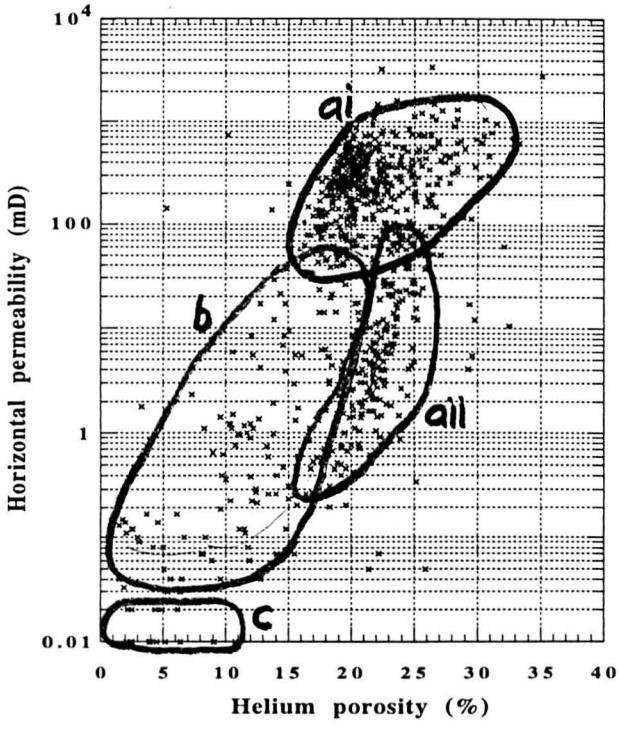

Fig5.10c Forties Montrose High_all data

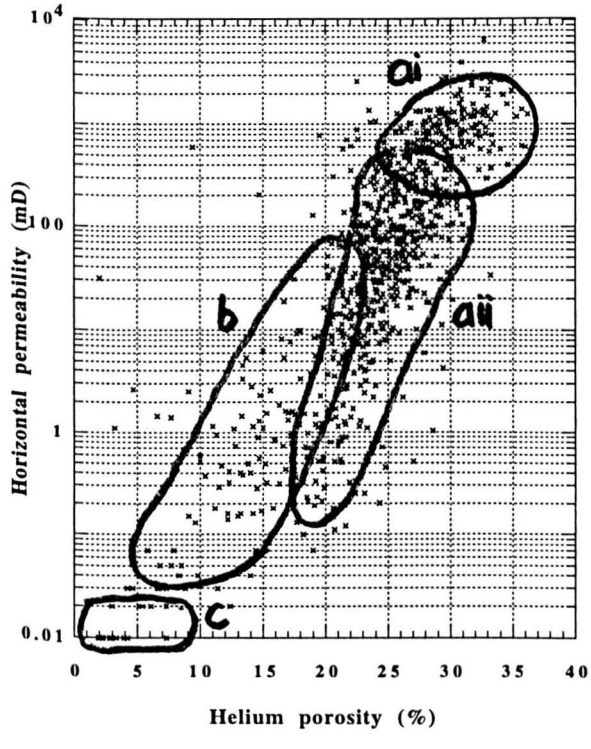

Fig5.10d East Central Graben_all data

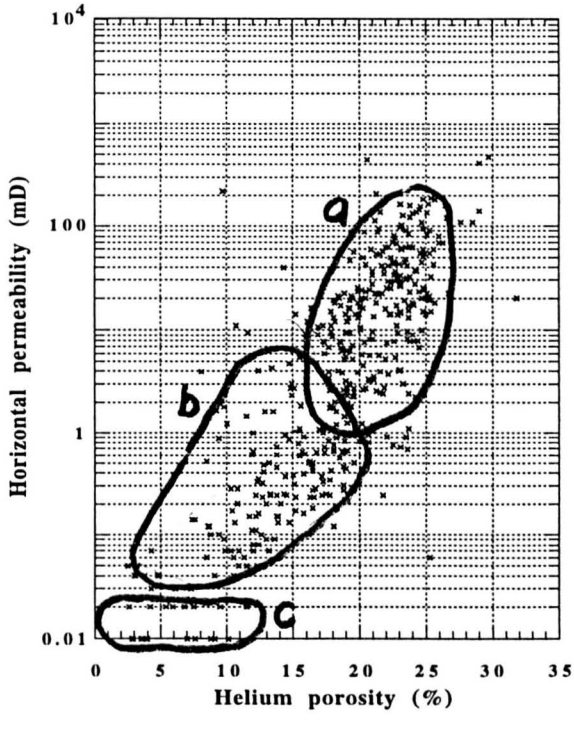

Figure 5.11a Fladen Ground Spur_blocky facies

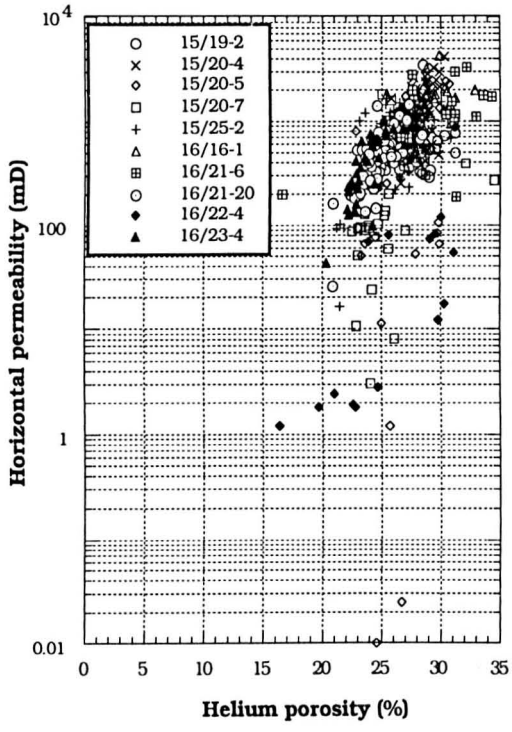

Figure 5.11b Fisher Bank Basin_blocky facies

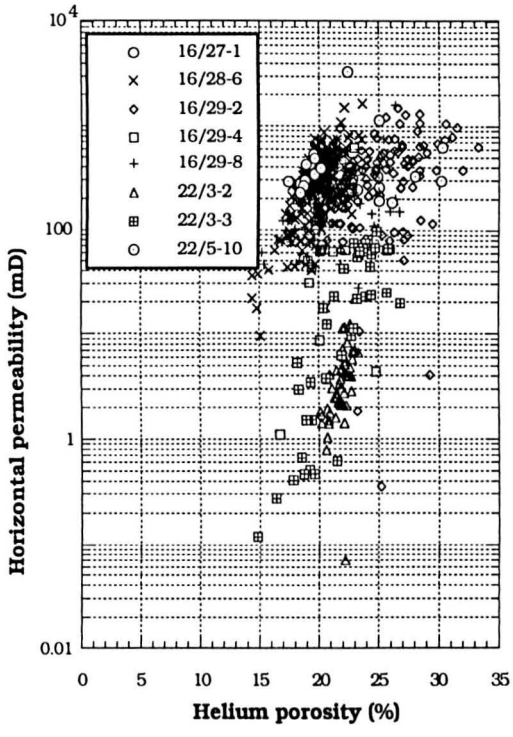

Figure 5.11c Forties Montrose High_blocky facies

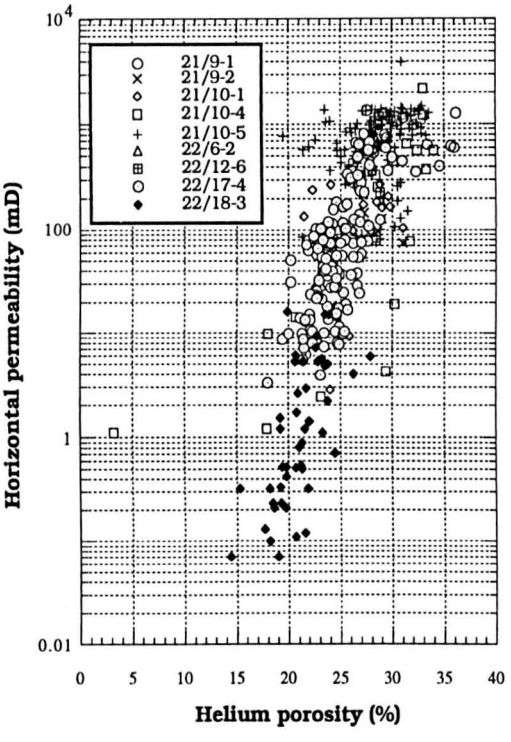

Figure 5.11d East Central Graben_blocky facies

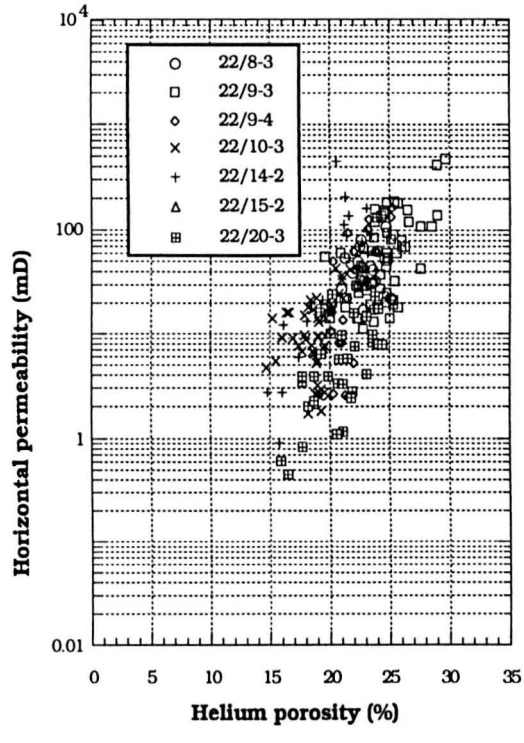

Figure 5.12a Porosity gradient CDF

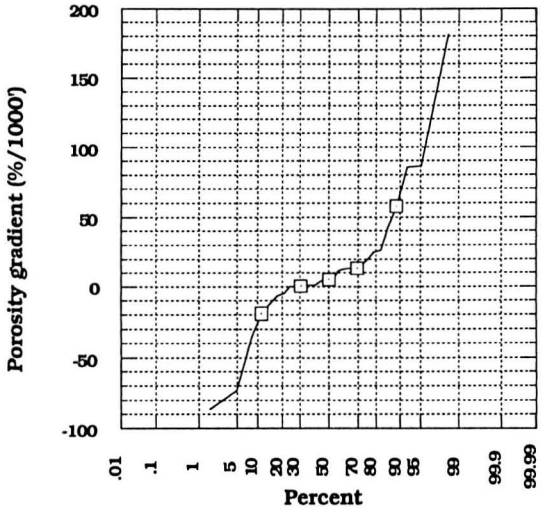

Figure 5.12b Sampled core length CDF

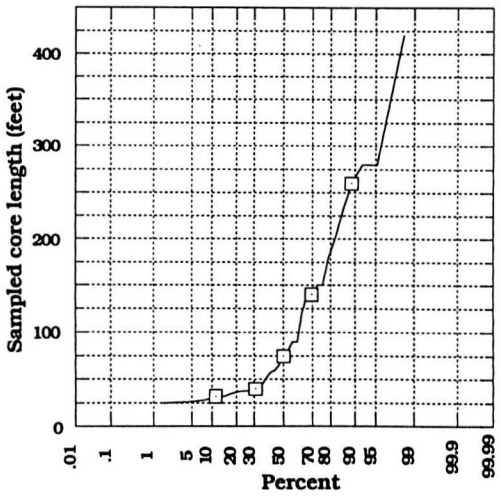

Figure 5.12c Porosity gradient histogram

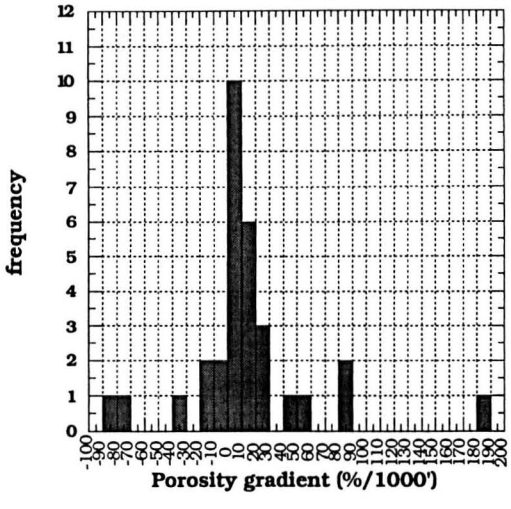

Figure 5.12d Porosity gradient histogram

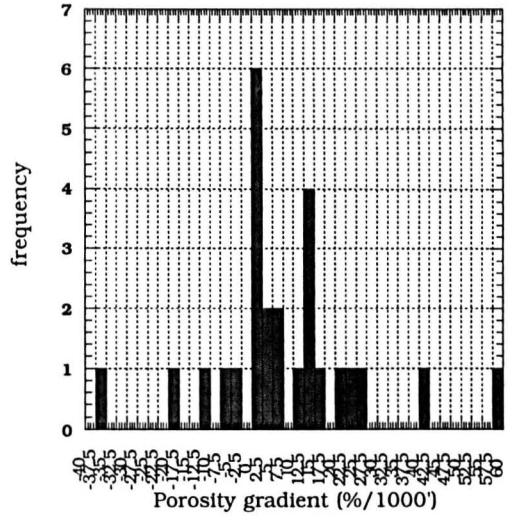

Figure 5.13 Sampled core length vs porosity loss

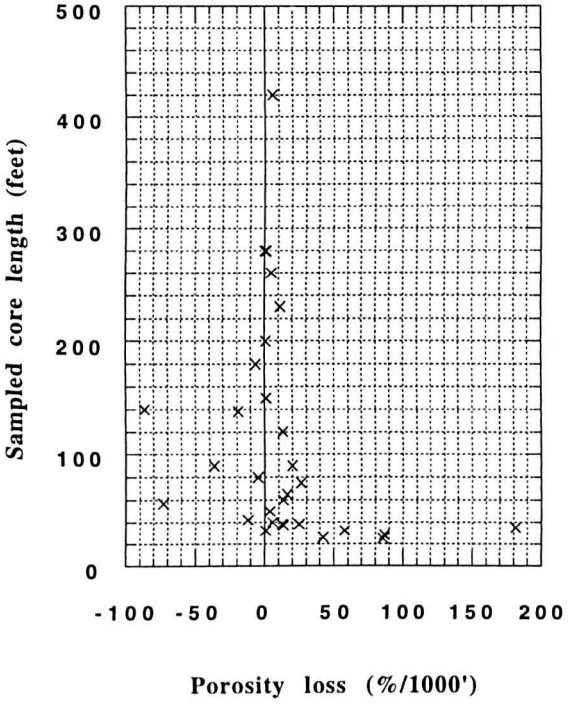

Figure 5.13 Sampled core length vs porosity loss

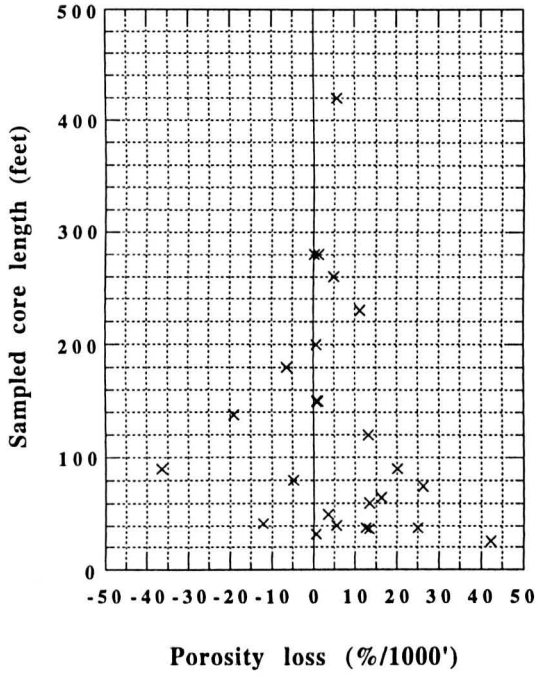

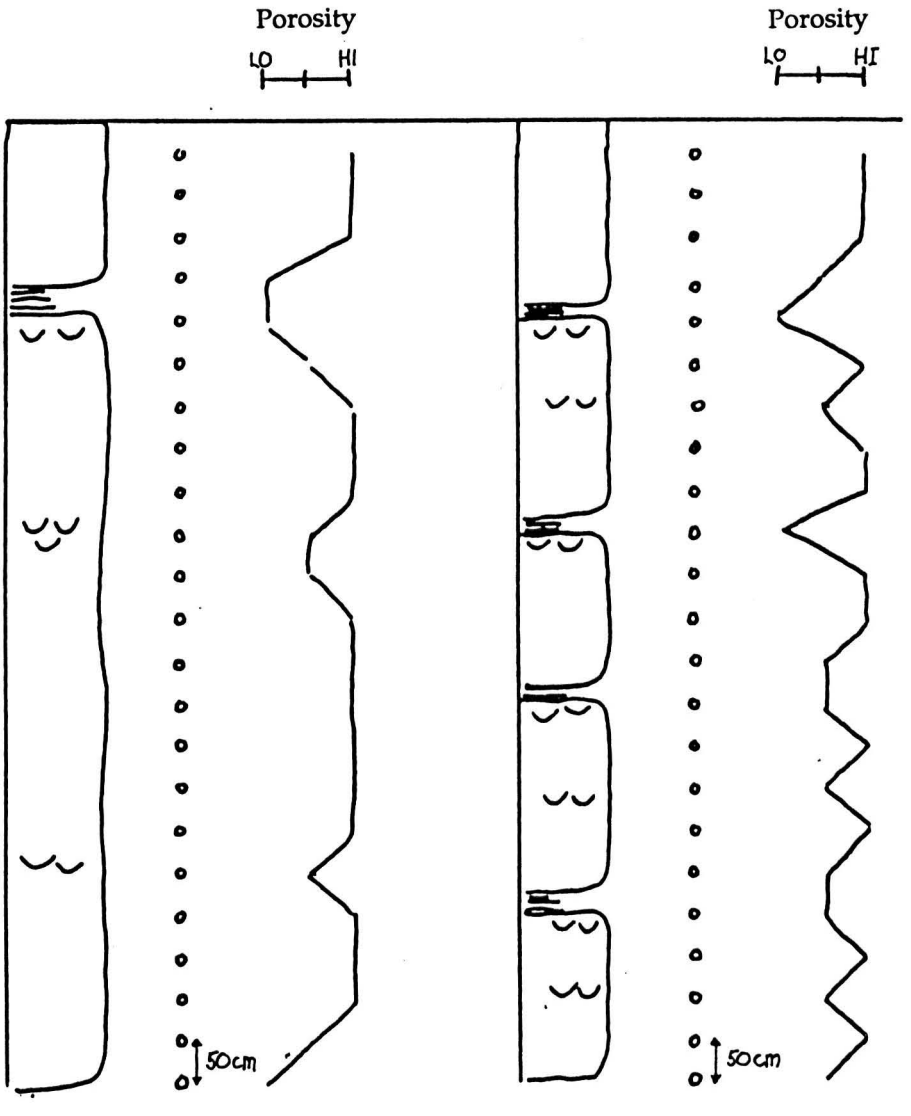

Figure 5.14

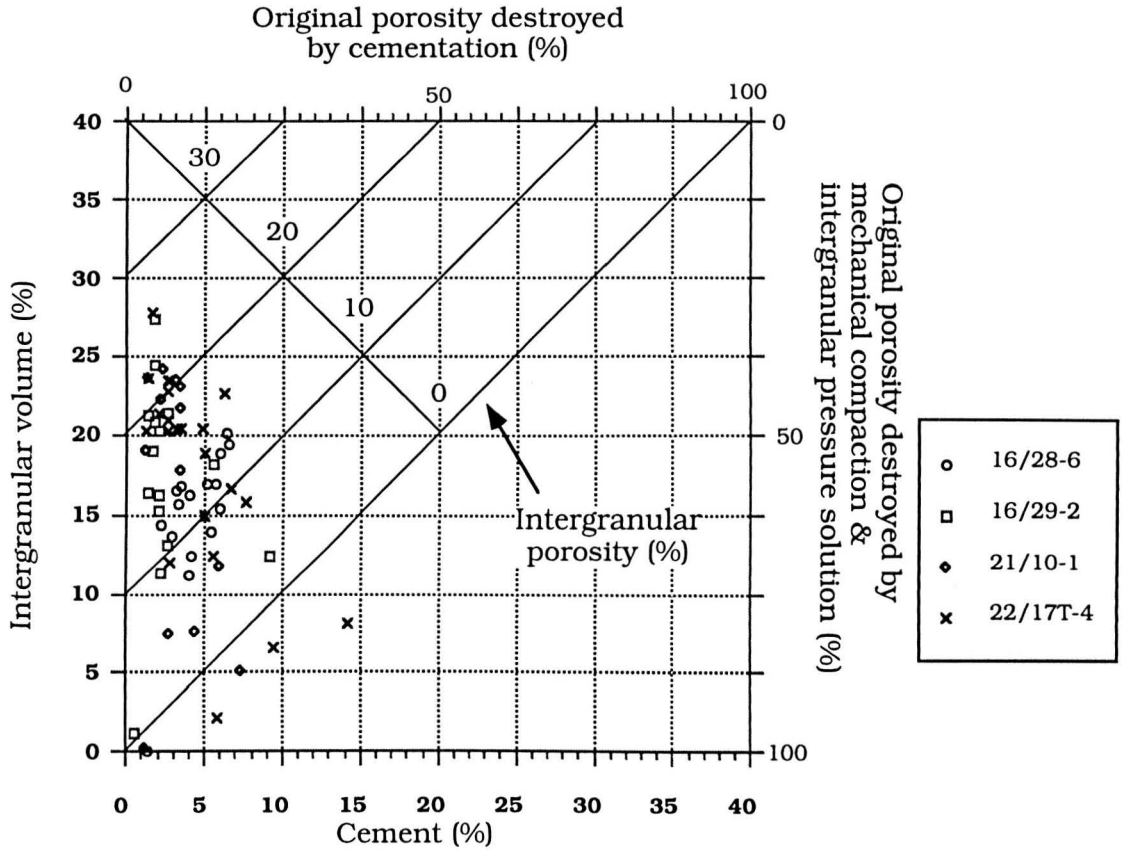

Figure 5.15 Housenecht diagram

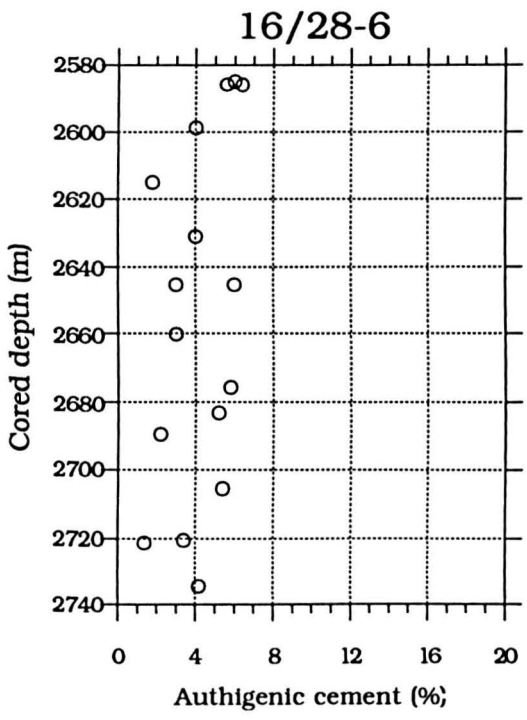

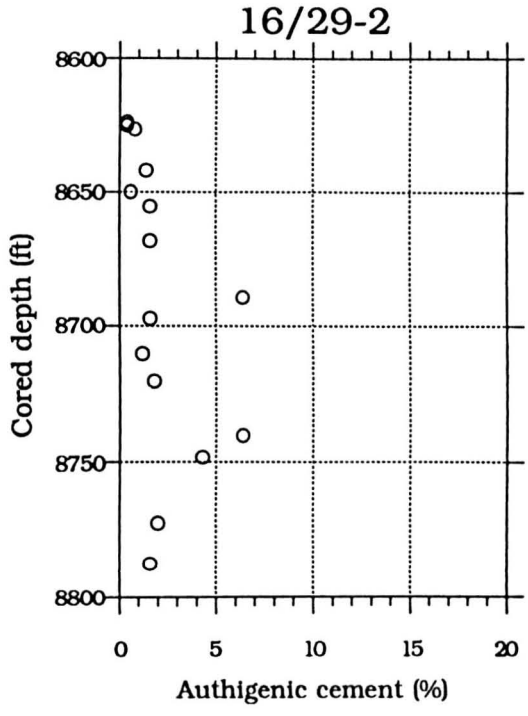

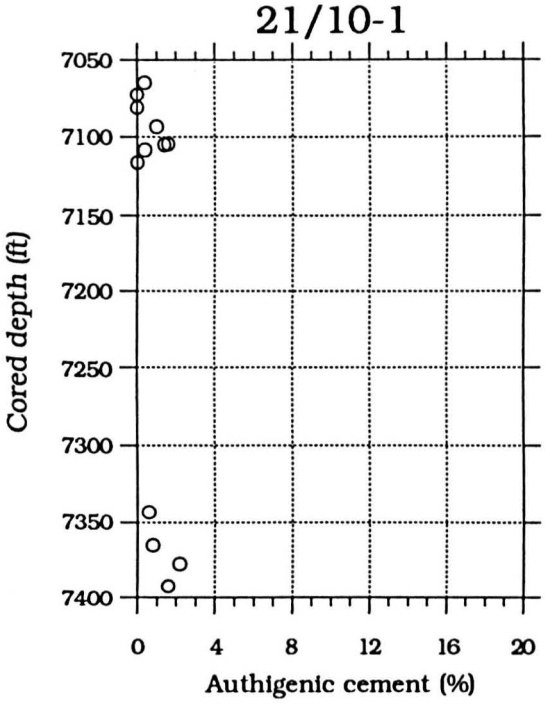

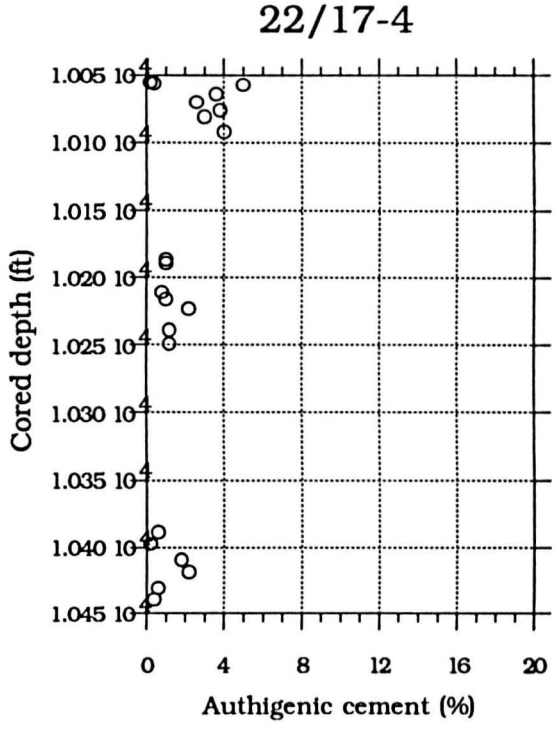

Figure 5.16a-d

Figure 5.17

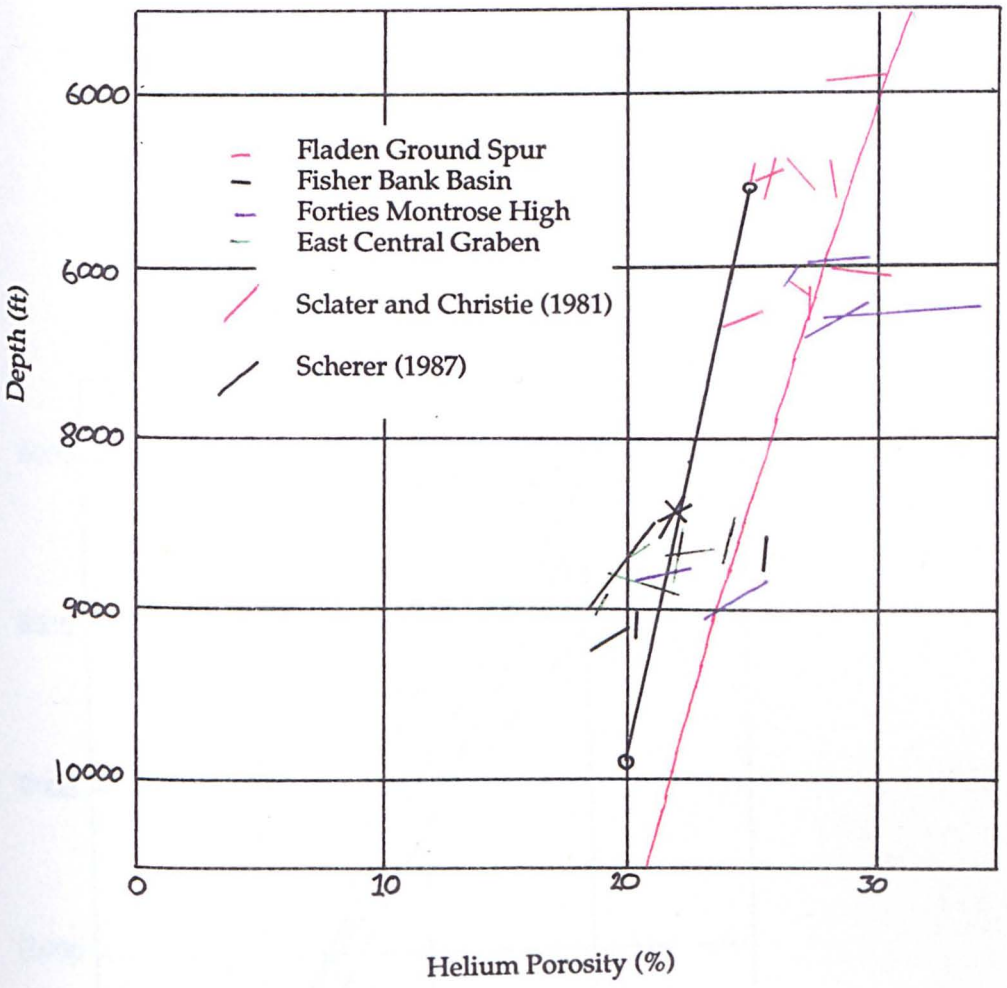
Fladen Ground Spur
Fisher Bank Basin
Forties Montrose High
East Central Graben
Sclater and Christie (1981)
Scherer (1987)
6000
8000
9000
10000
0
10
20
30
Depth (ft)
Helium Porosity (%)

Figure 5.18

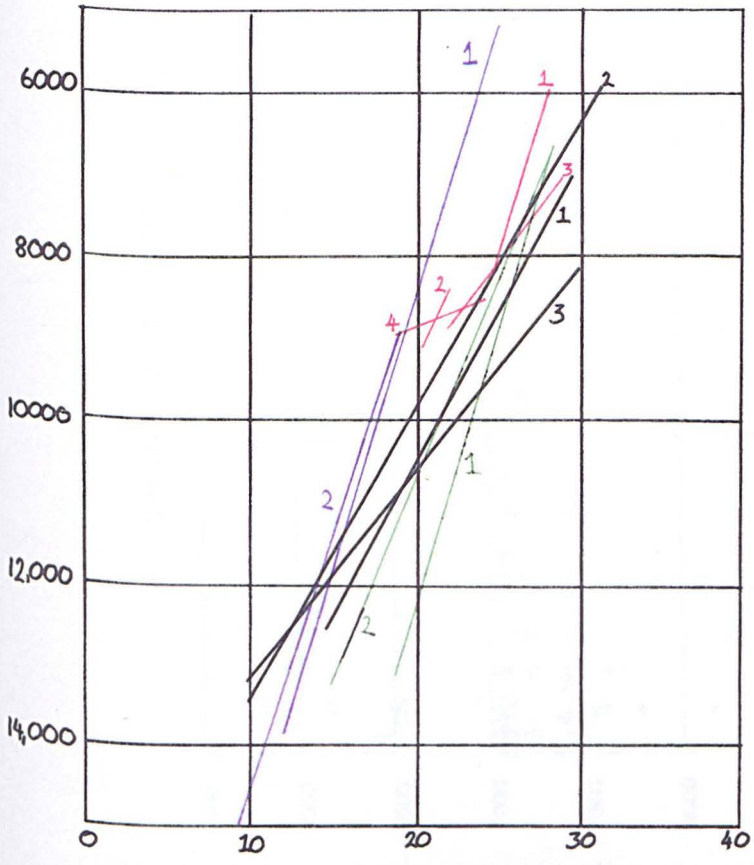

1 Fladen Ground Spur 1.69%/1000ft
2 Fisher Bank Basin 2.69%/1000ft
3 Forties Montrose High 4.04%/1000ft
4 East Central Graben 12.27%/1000ft

1 Central Graben, Ramm and Bjorlykke (1994)
2 Norwegian Shelf, Ramm and Bjorlykke (1994)

1 Etive Formation, Brent Group, Giles et al. (1992)
2 Ness Formation, Brent Group, Giles et al. (1992)
3 Statfjord, Hutton and Lyell Fields, Harris (1992)

1 Frio Formation, Loucks et al. (1984)
2 Wilcox Formation, Loucks et al. (1984)

Fig 5.19 Point count data: quartz overgrowth increase slowly with depth

CHAPTER 6 COMPARISON OF DIAGENESIS BETWEEN PALAEOCENE MONTROSE GROUP AND JURASSIC SANDSTONES, NORTH SEA, UK

CHAPTER 6: COMPARISON OF DIAGENESIS BETWEEN LOWER PALAEOCENE AND THE BRENT GROUP SANDSTONES, NORTH SEA, UK

6.1 Abstract

Palaeocene Montrose Group cores from the Central North Sea have been sampled and results have been compared to northern North Sea Brent Group data. For both sandstones; authigenic pyrite, microdolomite, quartz precipitation, and illitization of kaolinite are primarily controlled by burial depth; while authigenic kaolinite precipitation, calcite cementation are primarily controlled by pore-fluid changes. Enhanced quartz cementation is related to salt-diapirs and may be related to higher temperature resulting from salt high thermal conductivity or upwards migration of silica precipitating fluids from underlying sedimentary units.

Quartz cementation increases significantly at 2590m (8500ft) within Montrose Group sands and at 2740m (9000ft) within the Brent Group. Calcite cement origin is varied within both sandstones. Volumes of diagenetic kaolinite in Brent are much higher than Palaeocene except where delta progradation took place over shallow buried Montrose Group. Post-depositional meteoric flushing within Brent Group sandstones, recorded by the high volume of authigenic kaolinite can be ascribed to Montrose Group sandstones where kaolinite volumes are high. Where meteoric water influx is thought to have occurred to a lesser extent then kaolinite volumes are low. Secondary porosity forms a minor component within the Palaeocene. Fibrous illite begins to precipitate at depths greater than 2590m (8500ft) within the Palaeocene, a similar depth to the Brent.

6.2 Introduction

6.2.1 General information

Within the past 15 years over 30 papers have been published relating to the diagenesis of the mid-Jurassic Brent Group in the Northern North Sea (**Figure 6.1**) e.g. (Scotchman et al. 1987; Giles et al. 1992; Glasmann 1992; Haszeldine et al. 1992). The Brent Group, one of the most productive reservoir horizons within the North Sea, is often cored from between 2438m (8000ft) and 3810m (12,500ft)(Giles et al. 1992), where traps are present in tilted fault blocks. The vast quantity of data generated from core analysis has provided geologists with an opportunity to try and test their theories regarding processes of diagenesis. However, the mid- Jurassic at depths shallower than 2438m (8000ft) is rarely cored, (Gluyas & Coleman 1992; Osborne 1994) which results in uncertainty concerning shallow diagenetic processes within the North Sea basin.

This study examines core, poroperm data and rock samples from the Palaeocene clastic Montrose Group sandstones from 730m (2400ft) to 2743m (9000ft). This provides an opportunity to compare and contrast paragenetic sequences at similar depths with North Sea Middle Jurassic Brent sandstones, and also to examine diagenetic processes which have occurred at shallower depths.

The Palaeocene Montrose Group, although comparable to the Brent Group in terms of hydrocarbon resources, has not been studied diagenetically in similar detail until recently (Stewart et al. 1993; Watson 1993). This results from the relatively small effects that diagenesis has had on reservoir properties. However the increasing

importance of Palaeogene reservoirs in North Sea exploration and production should result in an increase in such studies. A regional study of the Palaeocene sandstones provides geologists with a control, to compare paragenetic schemes of proposed shallow/early Brent Group diagenesis.

6.2.2 Location

The Palaeocene clastic sequence subcrops extensively within the central North Sea and the flanks of the Viking Graben, **Figure 6.1, 6.2.** The Brent Group subcrops within the northern North Sea. Palaeocene sandstones are predominantly cored within the depth interval 1829m (6000ft) to 2743m (9000ft), while the Brent is cored generally between 2591m (8500ft) to 3810m (12,500ft) (Giles et al. 1992) though shallower cores for each interval do exist.

Montrose Group stratigraphy is initially based upon lithostratigraphy (**Figure 6.3, 6.4**). Deegan & Scull's (1977) terminology will be used in this paper. The biostratigraphic subdivision of the clastic sequence is hindered by the lack of microfossils, a consequence of the sand-rich nature of the sediments. This has been the recent focus of much debate (Mudge & Copestake 1992; Den Hartog Jager et al. 1993). The Montrose Group has been divided into three Formations (Maureen, Andrew and Forties Formations) which represent regional clastic aprons sourced from the East Shetland Platform and the Scottish Highland (Morton et al. 1993) and laid down in the Central North Sea, **Figure 6.2.** The sands were deposited in a subsiding basin and the three Formations represent second order changes in sea level resulting from three phases of uplift on the Scottish mainland and the East Shetland Platform (Deegan & Scull 1977; Stewart 1987). Underlying the Montrose Group is a Cretaceous sequence of chalks and chalk-rich sands. Within the Outer Moray Firth, the Montrose Group was succeeded by the Moray Group (Deegan & Scull 1977), a major deltaic complex which prograded over the Montrose sediments within the Moray Firth. The eastward limit of progradation is defined by the limit of coals deposited on top of the deltaic pile (Timbrell et al. 1993). Within the Central North Sea overlying the Montrose Group is a thick sequence of Tertiary marine mudstones.

6.2.3 Sedimentology

Sandstones were laid down by high-density turbidites sourced from the Scottish mainland (Rochow 1981). The underlying Maureen Formation contains resedimented chalk clasts. The main sandbody, the Andrew Formation, up to 700m thick (Den Hartog Jager et al. 1993), has a very high overall sand:mud ratio and was deposited within frequently meandering channel complexes (Den Hartog Jager et al. 1993). The lack of mud precluded stable levee banks constraining flow and so breaches in sand levee led to frequently migrating channels. The overlying Forties Formation, though only a mud with thin sandstone stringers in the Witch Ground Graben and Fisher Bank Basin, is up to 400m (1310ft) thick (Den Hartog Jager et al. 1993) in the Forties Montrose High area. Here overall sand:mud ratios decline enough for the formation of stable levee banks (Den Hartog Jager et al. 1993). Channel systems here were 3km wide and contain sandstones, encased in mudrock.

The dominant facies throughout the Montrose Group is massive sandstone resulting from the rapid deposition of high density turbidites. Other facies are thin bedded

sandstones and mudstones and muddy siltstones (Carman & Young 1974). The massive facies frequently makes over 80% of the cored clastic sequence.

Under petrographic examination, the massive sandstones consist of amalgamated beds of very fine to medium grained, poorly to moderately sorted sandstones. A pebbly lag is sometimes observed at the base of units. The sandstones vary from sublitharenites to litharenites. Lithic clasts, mainly schistose quartzites, reflect one ultimate provenance area i.e. Scottish Highland metamorphics. Occasionally some beds have a volcaniclastic component of basalt and volcanic glass. This deposit is frequently weathered, or diagenetically altered to clay. The detrital mud component is generally <5%.

6.3 Methodology

Eleven wells were sampled for petrographic and isotopic analyses from across the Central North Sea **Figure 6.2.** Wells were chosen to cover the study area as evenly as possible. Blue-stained epoxy- resin-impregnated thin-sections were made from core stubs. The slides were stained to identify carbonates with methods similar to Dickson (1965). The slides were examined under a petrographic microscope and point-counted (500 points per slide) to quantify detrital and diagenetic minerals. Rock stubs were examined by scanning electron microscope to observe the habit and morphology of diagenetic minerals. Back-scattered electron image analysis of polished thin-sections was used for major element analysis of authigenic phases.

Mineral separation was carried out for authigenic carbonate and kaolinite. Carbonate samples were crushed and purified by heavy mineral and magnetic separation. Purity was checked by X-ray diffraction. For small core-plug specimens whole-rock crushed samples were used. Strontium analysis of authigenic carbonates follows the methods outlined by Smalley et al. (1992)

Clay extraction follows the method of Jackson (1979); disaggregation of the rock, separation of the clay fraction, oxidation of organic material, deflocculation of the clays and separation into size fractions by settling and centrifugation. The 2-5μm and 5-10μm size fractions were selected for isotope analyses on the basis of a high kaolinite percentage estimated from X-ray Diffraction (XRD) analyses and visually by SEM. XRD traces of kaolinite and dickite standards were used to test for the presence of dickite. XRD traces indicated that most samples had less than 5% quartz contaminant. Rarely, samples were contaminated with 10% quartz but the measured isotope values have not been corrected for impurities. Oxygen isotopic analysis follows the method of Clayton & Mayeda (1963), and hydrogen analysis follows the method of Biegelman et al. (1952). All isotopic data are presented in per mil values with respect to Standard Mean Ocean Water (SMOW). The analytical error of laboratory standard δD and $\delta^{18}O$ values was 5‰ and 0.3‰ (2σ) respectively.

6.5 Diagenesis

Sample well depths range from 732m (2400ft) to 2743m (9000ft) from across the central North Sea. Paragenetic sequences can broadly be divided into early and late diagenesis, **Figure 6.5.** Overall volumes of diagenetic minerals are small outwith concretionary horizons and volumes are rarely >5%. The paragenetic sequence is broadly similar amongst wells.

Early diagenetic alterations consist of microcrystalline dolomite, pyrite, authigenic chlorite, microquartz, smectite resulting from K- feldspar dissolution, illite transformation from detrital illite- smectite, K-feldspar overgrowths, early calcite concretions, vermiform kaolinite and very thin quartz overgrowths. Late diagenesis consists of; albite overgrowths, minor dissolution of earlier concretions, blocky kaolinite, quartz overgrowths, illite and later carbonate concretions.

The major differences between wells relates to vermiform kaolinite and concretionary carbonates. Particularly large volumes of kaolinite cement are present within wells 15/26-3 and 15/26-4.

Compared with Jurassic sandstones (Giles et al. 1992; Glasmann 1992; Osborne 1994) **Figure 6.6**, the most obvious differences are in the larger volumes of kaolinite present (up to 22%bv) within shallow Jurassic sandstones at similar burial depths.

6.5.1 Pyrite

Pyrite is found with three habits:
i) small aggregates of framboids (each framboid <5μm), most often associated with detrital organic material and authigenic dolomite. In this case, the relationship with texturally early dolomite indicates that pyrite is likely to have precipitated as a result of sulphate reduction.
ii) Single framboids associated with the dissolution of Na-feldspar. Within secondary porosity created by the preferential dissolution of albite twins, pyrite is found. Unless feldspars were skeletal during deposition pyrite precipitation must post-date dissolution of feldspars. This implies that precipitation below the sulphate reduction zone. The source of sulphur for such pyrite is unknown.
iii) Rimming secondary pores created by the dissolution of detrital Fe-Mg minerals. This pyrite probably post-dates sulphate reduction as secondary pores maintain their shape implying that the rock matrix had ceased rapid compaction due to partial cementation.

6.5.2 Mn-calcite

Within well 15/20-4 is a concretionary layer 50cm (1996.50m cored depth) thick within a 1m mudstone layer. The central zone of the concretion is composed of rhodochrosite spherules (10μm in diameter) outlining burrows and trace fossils within an 15cm Mn-calcite concretion, **Figure 6.7**. Outwith the Mn-calcite are 15cm thickness of thin 1-2mm calcite cement layers interbedded with muds forming cone-in-cone structures. Point-count volumes of cement are >90% and the preservation of delicate trace fossils suggests that the concretions represent a syngenetic hard-ground similar to those found by Lallier-Verges & Alberic (1989). Isotopic analysis of the Mn-calcite concretion indicates that sulphate reduction was the method of carbonate precipitation, $\delta^{13}C$=-25 to -18‰PDB, **Figure 6.8, Table 6.1.** $\delta^{18}O$ values around -26‰PDB indicate precipitation at acceptable temperatures of 28°C within Palaeocene marine porewater. Precipitation within early Tertiary meteoric waters give non-sensical precipitation temperatures below 0°C.

6.5.3 Microdolomite

Within most wells microdolomite clusters a few microns across occur. These are associated with organic detritus and framboidal pyrite. They never comprise more than 1% of rock volume. Microdolomite is seen enclosed within calcite concretions and therefore likely precipitated before calcite growth, within the sulphate reduction zone.

6.5.4 Chlorite

Chlorite is found in restricted horizons containing detrital tuffaceous deposits. Chlorite coats detrital grains, perhaps precluding quartz overgrowth formation, **Figure 6.9.** Cored samples from 15/18-5 and 15/20-4 in which chlorite has precipitated are particularly friable compared with the rest of the core. The abundance of chlorite is less than 2% within these wells, but has a marked effect upon rock properties reducing permeabilities 10 times lower than expected values, see Chapter 5. $\delta^{18}O$ of chlorite separates ($\delta^{18}O$ =12.7 to 16.0‰SMOW) indicates that chlorite likely precipitated from cool (less than 20°C) marine waters **Figure 6.10, Table 6.2.**

6.5.5 Microquartz

In many wells, an early silica supersaturation resulted in microquartz crystallites, **Figure 6.11.** These crystals did not precipitate on the detrital grains but are associated with detrital clay. Such quartz could be associated with silica-releasing reactions such as smectite to illite reactions, K-feldspar dissolution or volcanic glass dissolution. The nucleation of quartz at many sites suggests rapid precipitation from supersaturated fluids. Bjorlykke et al. (1992) would suggest that such quartz originates from original chalcedony recrystallising.

6.5.6 Illite-smectite to illite.

Detrital clays smeared on grain surfaces have a boxwork habit perpendicular to grain surfaces, **Figure 6.12.** Back-scattered electron images suggest such detrital clays are rich in iron indicating a chloritic component. Transformation of detrital clay to boxwork habit appears to have been early as boxwork crystals predate concretion formation in wells 15/20-4 and also underly quartz overgrowths in this well. The boxwork habit of smectite is attributed to very early in-situ alteration or derivation by weathering of volcanic ash, high inputs of which are associated with rifting in the North Atlantic during the late-Cretaceous to early Tertiary.

Illite-smectite transformation has been noted as being coincidental with the Palaeocene-Eocene boundary within the Central North Sea (Pearson & Small 1988). These authors infer that transformation occurred as a result of a Tertiary thermal event. Illitisation releases silica and takes up Al and K. Dissolution of K-feldspar could probably the main source of K and Al.

Smectite + Al^{3+} + K^{+} = illite + Si^{4+} (Hower et al. 1976)

Rock temperature exceeding 90°C is thought to be a fundamental control on illitisation as well as controlling the supply of dissolution to provide solutes (Hower et al. 1976). However calculated temperatures through time (Pearson & Small 1988) indicate that present day burial up to 2400m results in no increase in maximum burial

temperatures since Palaeocene- Eocene boundary. Therefore, we must infer that this transformation of smectite to illite was supposed to have taken place after several hundred metres burial but not more than 1km. This would imply temperature gradients of more than 90°C/km. Such temperature gradients are difficult to conceive as hot- spring activity must have taken place to transport heat vertically in the basin by fluid motion. Consequently the hypothesis of temperature-driven illitisation is rejected. This illite is inferred to have grown by early diagenetic dissolution of unstable volcaniclastic debris, restricted to specific depositional layers (Dypvik 1983).

6.5.9 K-feldspar Overgrowths

K-feldspar has precipitated on detrital K-feldspars and on albite grains. Precipitation surfaces were clean of detrital clay. Dissolution of detrital K-feldspar often dissolved before dissolution of K-feldspar overgrowths, **Figure 6.13**. Quartz overgrowths from adjacent grains are seen to surround K-feldspar overgrowths, showing that K-feldspar overgrowth predates quartz overgrowths.

These K-feldspar overgrowths occur only as trace volumes to 0.8%BV. Volumes do not increase with depth. This is interpreted to indicate that precipitation is a shallow diagenetic phenomenon. Source of overgrowths is likely to be dissolution of previous K- feldspars.

6.5.7 Concretions

A common feature of Palaeocene massive sandstones is the presence of carbonate concretions. These are commonly 10's of cm thick. Small concretions appear to be oblate ellipsoids, long axes being perpendicular to core length. It is presumed that larger concretions are shaped in a similar manner. However concretions are also situated within resedimented chalk-rich layers and these are likely to be laterally continuous. Concretions within the Forties Formation have been described as permeability baffles (Emery & Robinson 1993), indicating that concretions can form extensive layers within the Montrose Group. Concretions can make up to 10% of core length but commonly are around 3 to 7% of core length, see Chapters 2 and 3.

The mineralogical composition of calcite concretions in the Montrose Group ranges from Fe-calcite, Mn-calcite, to non-ferroan calcites throughout the Central North Sea, see Chapter 2. However a texturally early concretion within well 15/26-3 (1879m) is ankeritic in composition. No zoning is seen in any concretion either by cathodoluminescence or by back scattered electron imaging. CL colours are a uniform dull to medium orange with bright orange patches identifying detrital carbonate grains. More luminescent carbonate is also seen associated with skeletal feldspars, it is difficult to say whether the feldspars were replaced by carbonate or whether calcite precipitated within secondary porosity.

However on the basis of minus-cement porosity and isotopic compositions concretions have been divided up into early (>37% minus-cement porosity) and late (e.g. <37% minus-cement porosity). The concretionary calcite cements completely fill any porosity and point count volumes of the carbonate are presumed to represent porosities during precipitation.

Calcite cemented zones within the sands have a wide range of carbon isotopic compositions. These can be divided into four general groups
i) Concretions from wells 15/26-3 and 15/26-4 are isotopically heavy ($\delta^{13}C$=-20 to +13‰PDB) and relate to fermentation processes. These concretions precipitated within predominantly marine waters at cool temperatures <35°C.
ii) Very negative $\delta^{13}C$ values (< -16‰PDB) of concretions from wells 15/20-4 relate to oxidation of hydrocarbons. These concretions precipitated within predominantly meteoric waters at cool temperatures <35°C .
iii) In well 14/13-3 negative values of $\delta^{13}C$ (-12 to -2‰PDB) relate to sulphate reduction within cool waters ($\delta^{18}O$=23 to 27‰SMOW) and a contribution from dissolution of detrital calcite ($\delta^{13}C$~0‰PDB). These concretions precipitated within predominantly meteoric waters at cool temperatures.
iv) Wells with $\delta^{13}C$ slightly negative to zero values (-9 to +3‰PDB) relating to inorganic reactions and chalk debris dissolution ($\delta^{13}C$~0‰PDB). These concretions precipitated within waters of marine water composition at temperatures greater than 60°C.

Calcite cement appears to be located as concretionary cements and not as dispersed authigenic grains. Using this information, over on hundred composite logs were examined to calculate the amount of concretions present within cores (Chapter 3). Concretions are relatively easy to identify from electric logs within the massive sands, although small concretions (<25cm thickness) would not be easy to identify. Percentage of concretions range from 0-10% of sand interval, see Chapter 3.

6.5.10 Kaolinite
Authigenic kaolinite in present in two habits
i) an early ragged vermiform shape
ii) later deeper more blocky form.

Kaolinite is present in three locations
I) as a pore filling habit (5-20μm),
ii) between splayed muscovite flakes (up to 200μm)
iii) filling secondary pores resulting from the dissolution of feldspars, **Figure 6.14.**

Texturally the porefilling kaolinite is seen to intergrown with and be overgrown by authigenic quartz. This suggests that these minerals were co-genetic during kaolinite precipitation.

Within deeper wells (7000ft, 2130m), and particularly away from the East Shetland Platform, kaolinite precipitation has taken on a more blocky habit. This is generally smaller, 5 to 10μm compared with earlier kaolinite (5 to 20μm). This later kaolinite is seen to overgrow early verms.

The kaolinite generally makes less than 5% of the rocks except for two wells where it forms up to 12%, wells 15/26-3 and 15/26-4 These two wells contain conspicuously more kaolinite than other sampled wells as a result of strong meteoric flow during early burial. (Figure 6.15)

Isotopic compositions of kaolinite are similar **Figure 6.16.** Oxygen isotope 25th percentiles is 13.2‰SMOW, 75th percentile is 16.8‰SMOW. Hydrogen compositions percentiles are δD=-70‰SMOW (25th percentile) to -55‰SMOW (75th percentile). On an interpretative δD-δ^{18}O cross plot this suggests that kaolinite precipitated from fluids of composition δ^{18}O = -6.5 to -3‰SMOW at temperatures between 43-75°C. This would be compatible with mixed meteoric and depositional seawater, Chapter 4.

6.5.11 Authigenic quartz

Quartz overgrowth habit is determined by the detrital clay content of the sands. Where sands have low detrital clay content and grain surfaces are clay-free, small incipient quartz has precipitated, **Figure 6.17.** Detrital clay coatings hinder precipitation and overgrowths take on a more blocky nature and grow over and above clay smeared surfaces.

Point counting of quartz overgrowths is hindered by the presence of reworked overgrowths and the lack of detrital mud in sands to provide clear dust rims Point counts are likely to be underestimates. Provenance studies indicate that sands are likely to be reworked Mesozoic sands. The thin reworked overgrowths, identified by the presence of double dust rims, and pitted and rounded overgrowths, indicate that sandstones were never deeply buried before reworking. Shallow burial of a sandstone source for the Montrose Group is suggested by Reynolds (1994), who calculated that only approximately 1km of uplift of the East Shetland Platform, the primary provenance area, is required so as to balance the sedimentary input to the Central North Sea.

Point-counted volumes of diagenetic quartz are insignificant (<2%) down to 2591m (8500ft) **Figure 6.18.** At greater depths, >2590m (8500ft), authigenic quartz forms up to 5% of rock volume. This increase is seen within Block 16/28 in the Fisher Bank Basin. In well 23/16-4 overgrowths make up more than 5%BV in the East Central Graben area at shallower depths (2150m to 2329m) than 2591m. By contrast other deep wells such as 16/29-2 (2623m to 2685m) and 22/17-4 (2515m to 2637m) do not have comparable volumes of authigenic quartz. In the case of 16/29-2 microcrystalline quartz may hinder overgrowths and in 22/17-4 illite-smectite coatings on clay probably precluded quartz overgrowths.

Pressure release from underlying overpressured Jurassic sandstones may result in quartz cementation from vertically migrating silica-rich fluids (Burley 1993). Palaeo-leakages of pressure would be more likely adjacent to major Mesozoic fault zones and Zechstein salt-domes. Wells 23/16-4 and 22/20-3 are immediately above salt domes where intense fracturing in the vicinity has been observed on seismic sections (Foster & Rattey 1993; Hoilnad et al. 1993; Platt & Philip 1993).

The alternative explanation for the link between salt-domes and quartz cement is heat-flow. Significantly higher heat-flows exist around salt-domes in the Central North Sea (Andrews-Speed et al. 1984). If temperature is the controlling factor for silicate dissolution, silica transport and precipitation then higher temperatures would increase the rate of quartz cementation. Sampled wells in the immediate vicinity of salt domes (23/16-4, 22/20-3) have anomolously high percentages of authigenic quartz. Silica veining, a feature that may be expected if silica-rich fluids are being transported into

the sands were not seen within sample wells and are neither mentioned within the literature. Hence enhanced quartz precipitation within Montrose Groups sandstones due to higher heat-flows around salt domes is the preferred option over introduction of silica-rich fluids.

6.5.12 Fluid inclusions in authigenic quartz overgrowths

Fluid inclusions are very small and difficult to observe. Three measurements were made on a fluid inclusion wafers from well 16/28-6. Homogenisation temperatures were 89, 90 and 92°C. These temperatures are close to present-day burial temperatures for this well (~90°C). Such high temperatures could indicate that i) fluid inclusions have only been formed during recent burial, ii) that the inclusions record a thermal event or iii) that the inclusions have been reset during burial. Recent work suggests that early irregular shaped inclusions may be reset during burial (Osborne & Haszeldine 1993) and this explanation is accepted here.

6.5.13 Platy/hairy illite

Platy/hairy illite only occurs in sandstones buried deeper than 2500m (>8202ft). The habit of this diagenetic clay occurs as illite growing on the edges of dissolving kaolinite. **Figure 6.19.** This cannot be seen petrographically and makes <1% of the rock volume and is only seen by SEM. At these depth detrital illite-smectite coats forms a distinctive illitic habit

6.5.14 Secondary porosity

Secondary porosity forms 0-12% of rock volume and is usually 0.5%. Because of the open framework of the sandstones outsize pores were difficult to interpret, and were not counted as secondary porosity unless relict clay rims were seen. There is no apparent trend with depth **Figure 6.20.** Secondary porosity results from the dissolution of detritus feldspars and the occasional igneous and lithic clast. Values of secondary porosity are fairly consistent and with the exception of wells 15/26-3 and 15/26-4, do not exceed 5% at any depth. These two wells have more than normal secondary porosity. These wells also have higher volumes of kaolinite. The silica and aluminium supplying kaolin are inferred to be sourced from the dissolving detrital feldspars within a closed system

6.6 Discussion: Comparison of Montrose Group and Brent Group

6.6.1 Carbonates

Isotopic compositional fields of Brent and mid-Jurassic concretions are shown in **Figure 6.21.** $\delta^{13}C$ and $\delta^{18}O$ compositions for Brent carbonates are highly variable (Giles et al 1992). The variety and polygenic origin of many carbonate cements within the Brent Group causes difficulty in unravelling the depth relationships of the carbonate cement types from petrographic data alone. The discussion will therefore concentrate on $\delta^{13}C$ and $\delta^{18}O$ compositions to compare and contrast origins of Palaeocene and Brent carbonate cements.

Within the Brent Group, marine sandstone Formations contain the most authigenic carbonate. Giles et al. (1992) found that the Rannoch Formation shore-face sandstones contained the most carbonate cement (5% average) whilst Haszeldine et al. (1992) found it was the Tarbert Formation. Bjorlykke et al. (1992) in their study of Norwegian Sector Brent Group found that the Rannoch and Etive Formations

contained the most carbonate cement (up to 7.4% average). The common feature is marine facies where detrital shell debris could be anticipated. That carbonate cements are dependent

That carbonate cements are dependent on facies suggests that the cement is derived dominantly from biogenic sources or early carbonate cements formed on the sea floor. Such a pattern would not be expected if carbonate cement was transported into a reservoir from an outside source (Bjorlykke et al 1992). However (Haszeldine et al. 1992) also found significant quantities of cement within the non-marine Ness and related this to cross-formational fluid flow.

Within the Brent, carbonates are found in a variety of forms, as sheetlike layers, e.g. Rannoch (Giles et al. 1992), or as isolated concretions. Sheet-like geometries could relate to stratified detrital carbonate dissolving out and then precipitating within source sands (Bjorkum & Walderhaug 1990). Palaeocene sands do not contain stratified storm deposits for this manner of depositional sorting of debris. However it is likely that sheet-like concretions exist within the lowermost formation, the Maureen Formation, as beds often have a basal unit rich in coarse-grained detrital chalk debris. Original detrital carbonate in the Maureen Formation, though now not present within the massive sands, was likely to have been mostly randomly distributed. However fluid escape structures, outlined by detrital fines, are likely to concentrate any carbonate fines, microfossils and micas (Lowe 1982). These could have provided nucleation points and an initial local source for concretions to precipitate.

Generally early diagenetic Brent concretions are non-ferroan or weakly ferroan calcites, and siderites (Giles et al. 1992) while late diagenetic Brent concretions are replacive ferroan calcites and ankerites (Harris 1992).

$\underline{\delta^{13}C}$ and $\underline{\delta^{18}}$ compositions

Early carbonate cements predating kaolinite precipitation within the Brent are characterised by $\delta^{18}O \sim -6$‰PDB with a range of $\delta^{13}C = -30$ to -3‰PDB in the Dunlin and Cormorant fields (Giles et al. 1992). In Haszeldine et al. (1992) early carbonates are around $\delta^{13}C = -12$ to +2‰PDB and $\delta^{18}O$ from -13 to -6‰PDB. Osborne (1994) found that early calcites have $\delta^{13}C = -4$ to -1 ‰PDB and $\delta^{18}O = -3$ to -4‰PDB. Early siderites have $\delta^{13}C$ of up to +20‰PDB (Giles et al. 1992).

Early carbonate cements within the Montrose Group exhibit a similarly wide variation in carbon isotopic composition. As with the Palaeocene sandstones, the carbon isotopic composition of Brent appear to be strongly related to the depositional environment. The negative $\delta^{13}C$ values within early carbonate cements are presumed to be indicative of sulphate reduction and/or oxidation of methane.

Deeper Brent carbonates are contemporaneous with silica diagenesis and have $\delta^{13}C$ compositions with higher proportions of ^{13}C. Dunlin and Cormorant Field concretions have values between -16 to -3‰PDB (Giles et al. 1992). In the Haszeldine et al. (1992) study of Dunlin Field carbonates, $\delta^{13}C$ values are between -7 and 0‰PDB. The increase in ^{13}C is interpreted to reflect the influx of isotopically negative carbon related to thermal decarboxylation of organic matter. The slightly

more positive values are possibly due to the inclusion of higher proportions of ^{13}C-rich methanogenic bicarbonate, or marine bicarbonate sourced from the dissolution of bioclasts. These later carbonates though compositionally different from diagenetically late Palaeocene carbonate cement form a very similar grouping to Palaeocene 'late' diagenetic carbonates $\delta^{13}C$ = -10 to +2‰PDB. This suggests that the same processes were responsible for both sets of carbonates.

Such $\delta^{18}O$ values found within early Brent carbonates are frequently interpreted as recording meteoric/brackish water during precipitation at less than 40°C. A predominantly meteoric composition is favoured for Palaeocene early carbonates at similar temperatures, Later Brent Group carbonates have more negative $\delta^{18}O$ compositions and are interpreted to have precipitated within brackish waters at higher temperatures around 60°C (Haszeldine et al. 1992). For Palaeocene late carbonate, a porewater of predominantly marine composition is favoured during precipitation. Temperatures of precipitation are assumed to be >60°C.

Strontium

Strontium ratios within Brent Group carbonates are particularly radiogenic compared to Montrose Group concretions **Figure 6.22** (Haszeldine et al. 1992). This radiogenic component has been shown to come from the dissolution of detrital silicate minerals. Haszeldine et al. (1992) concluded that in the non-marine Ness Formation, which is devoid of detrital carbonate, calcite $^{87}Sr/^{86}$ Sr ratios required fluid flow to transport ions between formations. Concretions from Palaeocene Montrose Group sandstones strontium ratios fall into two groups. A ratio similar to Palaeocene shells which relate to early concretions, and a ratio which has a radiogenic component which relates to late concretions. This source is unknown but the small rise in Sr ratios may indicate that the silicate dissolution may be internal rather than due to expulsion of fluids from the underlying Jurassic sequence.

6.6.2 Kaolinite

Kaolinite forms an important diagenetic phase of the Brent Fields forming 0-23%BV **Figure 6.15** (6.5% average, Giles et al. 1992; Osborne et al. 1994). Even the shallowest cored Jurassic sandstones can contain considerable volumes of kaolinite, e.g. Emerald Oilfield (1600m) contains up to 15%BV kaolinite (Osborne et al. 1994). Authigenic kaolinite within the Brent has long been recognised to have precipitated in two forms (Kantorowicz 1984; Brint 1989) an early vermicular form and a later blocky form. The only wells in the present study of Montrose Group which contain comparable volumes of kaolinite are wells 15/26-3 and 15/26-4. Their position is different in relation to other sampled cores as they are adjacent to predicted Palaeocene palaeoshorelines. The limit of progradation of a late Palaeocene delta-plain has been identified from overlying lignites in the Moray Group (Timbrell et al. 1993). This delta prograded over the East Shetland Platform and into the Moray Firth in the late Palaeocene.

Mass balance of kaolinite

Mass balance calculations by Osborne et al. (1994) indicate that overall bulk volume of authigenic kaolinite within Brent sandstones can be precipitated from the dissolution of detrital feldspar. Within the Montrose Group, trends with depth for

feldspar or secondary porosity are not apparent. Nor is a clear trend apparent within kaolinite percentage with depth. However using the closed system mass balance equation from Osborne (1994) it appears that silica has been preserved within the Montrose Group sandstones; see Chapter 4. A similar conclusion was noted in the shallow Brent sandstones at similar burial depths (Osborne 1994).

There is a general consensus from oxygen and hydrogen isotopic evidence that vermiform kaolinite precipitated within predominantly meteoric pore-fluids at moderate temperatures (25-70°C) (MacAulay et al. 1994; Osborne 1994) **Figure 6.23, 6.24, 6.25.** The attributed source of the meteoric pore-fluids varies, **Figure 6.26;**

i) Osborne et al. (1994) favour meteoric flushing through the Brent during the Palaeocene, sourced from the adjacent East Shetland Platform. The meteoric water flowed through the basement and along major graben faults to enter the reservoir sandstones. Haszeldine et al. (1992) from isotopic measurements of quartz cements suggested wide-scale flushing with meteoric water descending >3km along major faults before moving laterally from fault block to fault block. Larter & Horstad (1992) proposed easterly flowing meteoric water to explain degradation of oils within the Gullfaks Field. Though the exact location of the hydraulic head is unknown, flow is likely to have occurred within the early Tertiary at the earliest.

ii) Emery et al. (1990) identified an increase in porosity and increased kaolinite within 10m of the unconformity surface in the Magnus Field. Meteoric flushing occurred during the sub-aerial erosion of the emergent fault block crest.

iii) MacAulay et al. (1994) using reverse-flexural modelling, found no evidence of post-Brent emergence for the Cormorant block. To avoid meteoric water descending 2km before rising up major faults, these authors suggested that trapped depositional meteoric pore- waters had been mixed with compactional marine fluid from surrounding muds.

<u>Montrose meteoric water influx</u>
Did meteoric water flushing take place within Montrose Group sandstones? As Palaeocene sandstones were never sub-aerially exposed, meteoric water most likely was introduced by flushing from palaeo-shorelines. Reconstructions of palaeo-shorelines and the reconstruction of now-eroded landscapes are fraught with problems. Palaeobathymetry of the early Tertiary sea ranged from 300m to 800m (Knox et al.1981 and Reynolds 1994). Therefore meteoric water would have to descend to these depths, plus the burial depth of sands which would have been an additional 10's to 100's of metres.

The Montrose Group sandstones are generally well connected by depositional geometries within proximal graben axes. Outwith depositional axes and towards distal areas, the sand/shale ratios drop and sands were funnelled along leveed channel complexes with a resultant drop in connectivity (Den Hartog Jager et al. 1993). However these Palaeocene sandstones are not overpressured today (Crawford et al. 1991), implying a good fluid connection to surface. Also in the distal Maureen Field, interbedded mudstones do not restrict flow of oil within the reservoir, also implying

good connectivity on a local scale between the sandbodies (Cutts 1991). The distance required to flush meteoric water laterally through the Montrose Group is high. Meteoric water can travel many kilometres through an aquifer with only a small hydraulic head. Smalley et al. (1994) found that in the 40m thick Lincolnshire Limestone with a meteoric water head of only 50m, meteoric water was able to flow at least 25km from surface outcrop. Another example of extensive modern day meteoric flow is from the coast of Florida where meteoric water flows 120km through Tertiary carbonate aquifers (Manheim 1967). The depth of penetration of meteoric water can also be considerable, in the Great Artesian Basin of Australia the meteoric water lies at depths up to 2000m (Habermahl 1980). Thus lateral flow of meteoric water for tens of kilometres within the Montrose Group is feasible.

During the late Palaeocene delta progradation of the Moray Group, meteoric water would have become rich in organic acids if the water percolated through the thick peat deposits. This acid may have rapidly been neutralised by the dissolution of detrital carbonate and feldspar within the Montrose Group sandstones. Thus such acidic pore-water influxes are buffered by the bulk composition of the rock.

Early Tertiary introduction of meteoric water has been proposed by several other authors. Osborne (1994) explained the presence of vermiform kaolinite as the result of intense shallow meteoric water flushing into Jurassic sands, 4km from a palaeo-shoreline. Barnard & Bastow (1992) explained the present day geographical variation of degraded hydrocarbons in terms of a Tertiary meteoric flushing period. In the Gullfaks Field the east to west increase in degraded oil has been interpreted as a Tertiary meteoric water flushing event bringing oxygenated waters into the reservoir from the west (Larter & Horstad 1992). In this case meteoric water may have travelled 60km eastwards and up to 3km deep through Mesozoic deposits to reach Gullfaks.

Blocky kaolinite has a variety of origins. Precipitation of booklet kaolinite/alteration of vermiform kaolinite occurs at 50°C (Osborne et al. 1994), or 80 to 100°C (MacAulay et al. 1994). Two opposed types of processes have been envisaged.
i) According to Hurst & Irwin (1982) kaolinite precipitated in a vermiform manner from rapid feldspar dissolution, within cool flowing meteoric water. As temperature increased the mineral took on a blocky form with slower precipitation.
ii) Osborne et al (1994) identified vermiform kaolinite as a consequence of low supersaturation regardless of flow rates but also requiring low feldspar dissolution. Consequently, precipitation required nucleation points such as mica surfaces. Blocky kaolinite precipitated within highly supersaturated solutions resulting from rapid dissolution of feldspars triggered by the decay of oxalate. This is considered to be more likely.

Within deeper Palaeocene wells, kaolinite is predominantly 5-10μm and blocky in nature, though the crystal habit is not as well defined as deep Brent Group blocky kaolinite. Blocky kaolinite clearly overgrows vermiform kaolinite in 15/20-4 thus post dating it. Thus the processes of Montrose Group kaolin growth are similar to those which operated in the Brent Group.

6.6.3 Quartz cement

Quartz forms an important authigenic phase within the Brent Group sandstones forming up to 0-27%BV and is responsible for most of the porosity loss at depths greater than 2740m (9000ft) (Bjorlykke et al. 1992), **Figure 6.18.** Shallow Brent quartz overgrowths form 1-2% of rock volume at 5300-5600' within the Emerald Field (Osborne 1994). Within the Brent Group quartz overgrowths form low percentages until 2740m (9000ft) (Giles et al. 1992). Below this depth quartz overgrowths form an increasingly important authigenic phase up to 27%BV.

Such low point-counted volumes at shallow depths are consistent with most of the Montrose Group Palaeocene sandstones. At 2590m (8500ft) depth in the Palaeocene, quartz overgrowths begin to form >2% of rock volume.

The consistent low volumes (<5%) of quartz overgrowths above 2590m (8500ft) in the Montrose Group, and 2740m (9000ft) within the Brent Group and the significant increase deeper than this, may reflect two processes acting as sources of silica:- a shallow source and a deep source. Several sources for available silica during burial have been put forward;

i) dissolution of K-feldspar at shallow depth. Some feldspar dissolution is apparently early as skeletal grains are seen within early concretions. Within the Palaeocene, as in the Brent Group, feldspar dissolution resulting in secondary porosity does not increase markedly with depth until 2740m, 9000ft (Giles et al. 1992). The lack of increase in this feldspar dissolution may result from;
a) continued compaction of skeletal grains destroying diagnostic secondary porosity textures.
b) one stage dissolution at shallow depth.
c) errors in point counting are so high that data are only useful to indicate that values are small; i.e. are qualitative.

ii) pressure solution of thin beds of siltstones. As the volume of quartz overgrowths in the Brent Group cannot be supplied by the dissolution of feldspars alone (Giles et al. 1992), pressure solution of siltstones and shales are proposed as a silica source. Silica cannot be transported very far (Giles 1987), and cross formational silica transport is not envisaged. Palaeocene sandstone facies are predominantly massively-bedded and silt stringers are rarely found within cores. Thus, this process may not be relevant.

iii) pressure solution of detrital quartz grains - temperature cannot be held simply responsible for quartz overgrowths as Statfjord sandstones at 2.5km burial only has 1-3% quartz overgrowths (Bjorlykke et al. 1992). The Statfjord sandstones are however overpressured to equivalent to 1 to 1.5km burial pressure. Quartz overgrowths with oil inclusions must require silica to be internally derived as external silica would have limited mobility within oil saturated pores (Walderhaug 1990).

iv) smectite-illite reactions, Smectite-illite to illite transformation releases silica. There is little evidence for great volumes of volcanic detritus in Brent sandstones. However smectite-illite is locally common as a detrital clay in Palaeocene sands. Transformation reactions appear to be taking place during burial in the Montrose

Group, as visually from the SEM, the volume of boxwork habit authigenic illite-smectite increases with depth. The volumes of silica that can be generated from this reaction are patently too small to generate more than a fraction of a percent silica as detrital clays rarely make more than a few percent of bulk volume.

v) dissolution of volcanic glass. Volcanic glass shards are preserved within muddy sandstones. Dissolution of volcanic detritus is seen within cleaner sands. Dissolution is apparent because secondary pores are lined with opaque minerals. This is likely to have taken place early during burial of the Montrose Group in restricted horizons and may be a source for microquartz.

vi) dissolution of feldspar by organic acids. Introduction of organic acids from deep buried Kimmeridge clays into the Jurassic may have resulted in dissolution of feldspars (MacLaughlin et al. 1994). In the Montrose Group, interbedded muds can be organic-rich especially within the Forties Formation. Burial of these muds to 2591m (8500ft) has only recently taken them to temperatures around 90°C. It is unlikely that these muds were a local source for organic acids in the geological past. In different parts of the basin introduction of organic acids from the underlying Kimmeridge through the chalk during oil migration may have taken place. Present day pore-waters in some localities of the Palaeocene are particularly saline. These salinity measurements from Norwegian Sector Central North Sea sandstone pore-waters indicate that highly saline porewaters from nearby Zechstein salt diapirs in the Central Graben area. The strongly faulted zones around the diapirs provide a pathway for hydrocarbon migration into the Tertiary section (Foster & Rattey 1993). The porewaters from the Arbroath and Montrose fields (Crawford et al. 1991) are highly saline 135,000 and 111,000mg/l respectively but are 25km away from salt diapirs which pierce the base Cretaceous (Sears et al. 1993). Presently underlying Zechstein salts are on the order of hundreds of metres below Lower Palaeocene sandstones in this area (Penge et al. 1993). Movement of saline fluids must have been either vertically along faults within the Mesozoic section or horizontally along the Lower Palaeocene sandstones where salt diapirs come into contact with the Montrose sandstones. This movement of saline fluids is limited as porewaters within Montrose Groups oilfields in the Witch Ground Graben are only slightly more saline than seawater.

Salinity measurements of Central North Sea sandstone pore-waters indicate that highly saline porewaters within the Tertiary do not exist at depths <2200m (Bjorlykke & Gran 1994). This preculdes large scale mixing of formation porewater within the Central North Sea but does permit limited mixing of porewaters in the vicinity of diapirs. Bjorlykke & Gran (1994) suggest that saline waters, 100s of metres directly away from diapirs, result from diffusion processes. Highly saline waters are present within the Montrose and Arbroath Fields (Crawford et al. 1991). These fields are several kilometres away from salt diapirs which have punctured the Tertiary section which indicates that perhaps pore-fluid transfer, as opposed to simply secondary oil migration, from the deep basin to shallower Montrose Group has taken place over a limited distance.

Salt-diapirs and quartz cementation - The connection between salt diapirs and increase in quartz cementation within the Montrose formations may be due to

conditions other than change in porewater composition. Salts have substantially higher conductivities (Zechstein k=71$Wm^{-1}C^{-1}$ Andrews Speed et al 1984) than sandstones (Jurassic k=2.4-3.6$Wm^{-1}C^{-1}$) or shales k=2.9$Wm^{-1}C^{-1}$. Although it has been demonstrated that elevated heat alone does not result in quartz cementation (Bjorlykke et al 1992), the combination of enhanced burial temperatures and pressure solution may result in a rise of quartz precipitation.

Conclusion:- Diagenetic quartz in the Montrose Group and Brent Group precipitated throughout burial with an increase in the percentage of quartz at present day burial of 8500-9000ft. Precipitation was not due to an unusual thermal event, which is not recorded in shallow Brent Group or deep Montrose Group sandstones. However within the Montrose Group sandstones, adjacent to salt-diapirs, enhanced quartz overgrowths are present at depths less than 2590m (8500ft). This may be due to higher formation temperatures resulting from salts' high heat conductivity or the introduction of porewaters containing organic acids from the underlying Jurassic sequence.

6.6.4 Secondary porosity

Migration of organic acids from source rocks (Surdam et al. 1984) and acid dissolution by meteoric waters (Emery et al. 1990) are commonly held responsible for the creation of secondary porosity.

The lack of a secondary porosity trend with depth in Montrose Group sandstones **Figure 6.20** may indicate that some secondary porosity was created <6000ft (70°C). However kaolinite precipitation must have also taken place deeper than that because of change in kaolinite morphology with depth. Another explanation is that secondary porosity is being continuously created by dissolution. This secondary porosity is also being continually destroyed by compaction which crushes skeletal grains and oversized pores maintaining optimum porosity for depth (Wilkinson et al, in prep). In a poor-moderately sorted sand such fragments would be very difficult to identify.

Secondary porosity within the Brent Group is also well developed within shallow reservoirs though the total volume of secondary porosity does not significantly increase with depth, e.g. at depth 2400m to 3600m (7870ft to 11800ft)(Harris 1992) **Figure 6.20**. Giles et al. (1992) however show a linear decrease of feldspar abundance beginning at 2740m (9000ft). They link the increase in proportion of secondary porosity relative to overall porosity with this decrease of feldspar. Porosity creation by this method is largely redistributional in nature (Giles & De Boer, 1990). Glasmann (1992) indicates that at depth >3700m (12140ft) reservoir horizons are characterised by the complete diagenetic removal of detrital K- spar. Feldspar volume within the Lower Palaeocene does not vary with depth although 15/26-4 has lower proportions of feldspar. There is no need to invoke introduction of organic acids which aggressively dissolve feldspars at 3km (9843ft) burial depth.

6.6.5 Illite

Illite forms a noticeable diagenetic component of Brent Group sandstones at depth greater than 3200m (10,500ft) burial (Giles et al. 1992). Illitic clays are apparent within the iron-rich mixed layer detrital clay that occur within the Palaeocene sandstones. Illite also occurs precipitating upon the edge of fraying kaolinite. This is

seen at depths >2500m (8200ft). The proportion is too small to be point- counted and forms less than 1%. Studies show that kaolinite can become unstable and illitized during burial (Kantorowicz 1984). Illite can also precipitate upon the already existing illitic coatings. Therefore the lack of illite in the Montrose Group is consistent with the kinetic barrier to illite stabilisation unless temperatures exceed 80 to 110°C (2150 to 3000m) (Eslinger and Peavar 1988).

6.8 Conclusions

Although the paragenesis of the Montrose Group and Brent Group sandstones are different, the same processes can be recognised.

1) In both sandstones early concretions have a wide range in carbon isotopic compositions (-30 to +20‰PDB) relating to organic mediated reactions, while later concretion $\delta^{13}C$ is restricted to -10 to 0‰PDB resulting from thermal decarboxylation reactions.

2) Shallow early kaolinite close to palaeo-shorelines of Palaeocene Montrose Group has a similar habit to Brent kaolinites which resulted from meteoric flushing. Deep late blocky kaolinites from the Montrose Group and the Brent Group have compositions which could be interpreted as precipitating from a mixed marine-meteoric water.

3) Quartz overgrowths within Palaeocene and Brent become volumetrically important at depths greater than 2591m (8500ft), and increase progressively with depth.

4) Secondary porosity is present within Palaeocene and Brent Group sandstones at shallow burial depths. Compaction eliminated diagenetic textures to reduce recognition of secondary porosity.

5) Illite is not present in Montrose Group sandstones in volumetrically important volumes as burial depths have not exceeded -2500m (80 to 100°C) where illite forms a stable mineral phase.

References

Andrews-Speed C.P., Oxburgh E.R. and B.A. Cooper 1984 Temperature and depth-dependent heat flow in western North Sea. *Bulletin of the Amercian Association of Petroleum Geologists*, **68**, 1764-1781.

Barnard P.C. and M.A. Bastow 1992 Hydrocarbon generation, migration alteration, entrapment and mixing in the Central and Northern North Sea. In: *Petroleum Migration*, W.A. England and A.J. Fleet (eds), *Geol. Soc. Spec. Publ.* **59**, 167-190.

Biegelman J., Perlman M. L.and H.C. Prosser (1952) Conversion of hydrogenic materials to hydrogen for isotopic analysis. *Anal. Chem.* **24**, 1356.

Bjorkum P.A. and O. Walderhaug 1990 Lateral extent of calcite-cemented zones in shallow marine sandstones. In: *North Sea Oil and Gas Reservoirs-II*, The Norwegian Institute of Technology, Graham and Trotman, 331-336.

Bjorlykke K. and K. Gran 1994 Salinity variations in North Sea formation waters: implications for large-scale fluid movements. *Marine and Petroleum Geology*, **11**, 5-9.

Bjorlykke K., Nedkvitne T., Ramm M. and G.C. Saigal. 1992 Diagenetic processes in the Brent Group. In: *Geology of the Brent Group*, . A.C. Morton, R.S. Haszeldine, M.R. Giles and S. Brown (eds) *Geol. Soc. Spec. Publ.*, **61**, 263-289.

Brint J.F. 1989 *Isotope diagenesis and palaeofluid movement; Middle Jurassic Brent sandstones, North Sea.* Ph.D Thesis, University of Strathclyde.

Burley S.D. 1993 Models of burial diagenesis for deep exploration plays in Jurassic fault traps of the Central and Northern North Sea. In: *Petroleum Geology of Northwest Europe: Proceedings of the 4th Conference*, J.R. Parker (ed) Geol. Soc., London, 1353- 1375.

Carman R. and N.R. Young 1981 Reservoir Geology of the Forties Oilfield. In: *Petroleum Geology of North-West Europe*, J. Brooks and K.Glennie (eds), Graham and Trotman, London, 371-379.

Crawford R., Littlefair R.W. and L.G. Affleck 1991 The Arbroath and Montrose Fields, Block 22/17,18 UK North Sea. In: *United ICingdom Oil and Gas Fields, 25 Years Commemorative Volume*, I.L. Abbotts (ed), *Geol. Soc. Mem.* **14**, 211-217.

Cutts P.L. 1991 The Maureen Field, Block 16/29a, UK North Sea. In: *United Kingdom Oil and Gas Fields, 25 Years Commemorative Volume*, I.L. Abbotts (ed), *Geol. Soc. Mem.* **14**, 347-352.

Deegan C.E. and B.J. Scull. 1977 A standard lithostratigraphic nomenclature for the central and northern North Sea. *Inst. Geol. Sci. Bull. Report* 77/25.

Den Hartog Jager D., Giles M.R. and G.R. Griffiths 1993 Evolution of Paleogene submarine fans of the North Sea in space and time. In: *Petroleum Geology of Northwest Europe: Proceedings of the 4th Conference*, J.R. Parker (ed) Geol. Soc. London, 59-71.

Dickson J.A.D. 1966 Carbonate identification and genesis as revealed by staining. *Journal of Sedimentary Petrology*, **36**, 491-505.

Emery D. and A. Robinson 1993 Porosity and permeability. In: *Inorganic Geochemistry: Applications to Petroleum Geology*, D. Emery and A. Robinson (eds), Blackwell Scientific Publications, London, 129-169.

Eslinger E. and D. Peavar 1988 *Clay Minerals for Petroleum Geologists and Engineers.* Society of Economic Palaeontologists and Mineralogists: *Short Course Notes*, 22.

Foster P.T. and P.R. Rattey 1993 The evolution of a fractured chalk reservoir: Machar Field, UK North Sea. In: *Petroleum Geology of Northwest Europe*:, J.R. Parker (ed), Geol. Soc. London, 1445-1452.

Giles M.R. 1987 Mass transfer problems of secondary porosity creation in deeply buried hydrocarbon reservoirs. *Marine and Petroleum Geology*, **4**, 188-204.

Giles M.R. and R.B. deBoer 1990 Origins and significance of redistributional secondary porosity. *Marine and Petroleum Geology*, **4**, 188-204.

Giles, M.R., Stevenson S., Martin S.V., Cannon S.J.C., Hamilton P.J., Marshall J.D., and G.M. Samways 1992 The reservoir properties of the Brent Group: a regional perspective. In: *Geology of the Brent Group*, . A.C. Morton, R.S. Haszeldine, M.R. Giles and S. Brown (eds) *Geol. Soc. Spec. Publ.*, **61**, 289-327.

Glasmann, J.R. 1992 The fate of feldspar in Brent Group reservoirs, North Sea: a regional synthesis of diagenesis in shallow, intermediate and deep burial environments. In: *Geology of the Brent Group*, A.C. Morton, R.S. Haszeldine, M.R. Giles and S. Brown (eds) *Geol. Soc. Spec. Publ.*, **61**, 329-350.

Gluyas, J. and M. Coleman. 1992 Material flux and porosity changes during sediment diagenesis. *Nature*, **356**, 52-54.

Habermahl, M.A. 1980 The Great Artesian Basin, Australia. *J. Australian Geol. Geophys.*, **5**, 9-38.

Harris N.B. 1992 Burial diagenesis of Brent sandstones: a study of Statfjord, Hutton and Lyell fields. In: *Geology of the Brent Group*, . A.C. Morton, R.S. Haszeldine, M.R. Giles and S. Brown (eds) *Geol. Soc. Spec. Publ.*, **61**, 351-376.

Haszeldine, R.S., Brint J.F., Fallick A.E., Hamilton P.J. and S. Brown. 1992 Open and restricted hydrologies in Brent Group diagenesis: North Sea. In: *Geology of the Brent Group*, . A.C. Morton, R.S. Haszeldine, M.R. Giles and S. Brown (eds) *Geol. Soc. Spec. Publ.*, **61**,. 401-419.

Hoilnad O., Kristensen J. and T. Monsen 1993 Mesozoic evolution of the Jaeren High area, Norwegian Central North Sea. In: *Petroleum Geology of Northwest Europe*, J.R. Parker (ed), Geol. Soc. London, 1189-1195.

Hower J., Eslinger E.V., Hower M.E. and E.A. Perry. 1976 Mechanism of burial metamorphism of argillaceous sediment: 1. Mineralogical and chemical evidence. *Geol. Soc. Amer. Bull.*, **87**, 160-165

Jackson M.L. 1979 *Soil chemical analyses-advanced course* 2nd edition. Published by the author, Madison, Wisconsin.

Kantorowicz J.D. 1984 The nature, origin and distribution of authigenic clay minerals from Middle Jurassic Ravenscar and Brent Group Sandstones. *Clay Minerals*, **19**, 359- 375.

Knox R.W.O'B., Morton A.C. and R. Harland 1981 Stratigraphic relationships of Palaeocene sands in the UK Sector of the central North Sea. In: *Petroleum Geology of the Continental Shelf of North West Europe*, L.V. Illing and G.D. Hobson (ed), Institute of Petroleum, Heyden and Son, 267-281.

Lallier-Verges E. and P. Alberic 1989 Burrowing: a major process in the Mn-Ni enrichment of red clays. *Marine Geology*, **86**, 75-79.

Larter S. and I. Horstad 1992 Migration of petroleum into Brent Group reservoirs: some observations from the Gullfaks Field, Tampen Spur area, North Sea. In: *Geology of the Brent Group*, . A.C. Morton, R.S. Haszeldine, M.R. Giles and S. Brown (eds) *Geol. Soc. Spec. Publ.*, **61**, 441-463.

Lowe D.R. 1982 Sediment gravity flows: II. Depositional models with special reference to the deposits of high-density turbidity currents. *Journal of Sedimentary Petrology*, **52**, 279-297.

MacAulay G.E., Burley S.D., Fallick A.E. and N.J. Kusznir 1994 Palaeohydrodynamic fluid flow regimes during diagenesis of the Brent Group in the Hutton-NW Hutton reservoirs: constraints from oxygen isotope studies of authigenic kaolin and reverse flexural modelling. *Clay Minerals*, **29**, 609-626.

MacLaughlin O.M., Haszeldine R.S., Fallick A.E. and G. Rogers 1994 The case of the missing clay, aluminium loss and secondary porosity, South Brae oilfield, North Sea. *Clay Minerals*, **29**, 651-663.

Manheim F.T. 1967 Evidence for submarine dishcharge of water on the Atlantic continental slope of the southern United States. *Trans. New York Acad. Sci.*, **11**, 829- 835.

Morton A.C., Halsworth C.R. and G.C. Wilkinson 1993 Stratigraphic evolution of sand provenance during Palaeocene deposition in the Northern North Sea area. In: *Petroleum Geology of Northwest Europe: Proceedings of the 4th Conference*, J.R. Parker (ed), Geol. Soc., London, 73-84.

Mudge D.C. and P. Copestake 1992 Revised Lower Palaeocene lithostratigraphy for the Outer Moray Firth, North Sea. *Marine and Petroleum Geology*, **9**, 53-69.

Osborne,M. 1994 *The effect of differing hydrogeological regimes on sandstone diagenesis: Brent Group oilfields, UK North Sea.* PhD Thesis, University of Glasgow.

Osborne M. and R.S. Haszeldine 1993 Evidence for resetting of fluid inclusion temperatures from quartz cements in oilfields. *Marine and Petroleum Geology*, **10**, 271- 278.

Osborne M., Haszeldine R.S. and A.E. Fallick 1994 Variation in kaolinite morphology with growth temperature in isotopically mixed pore-fluids, Brent Group, UK North Sea. *Clay Minerals*, **29**, 591-608.

Pearson M.J. and J.S. Small 1988 Illite-smectite diagenesis and palaeotemperatures in northern North Sea Quaternary to Mesozoic shale sequences. *Clay Minerals*, **23**, 109- 132.

Penge J., Taylor B., Huckerby J.A. and J.W. Munns 1993 Extension and salt tectonics in the East Central Graben. In*: Petroleum Geology of Northwest Europe: Proceedings of the 4th Conference*, J.R. Parker (ed) Geol. Soc. London, 1197-1209.

Platt N.H. and P. Philip 1993 Comparison of Permo-Triassic and deep structures of the Forties-Montrose and Jaeren Highs, Central Graben, UK and Norwegian North Sea. In: *Petroleum Geology of Northwest Europe*, J.R. Parker (ed), Geol. Soc. London, 1221-1230.

Reynolds T. 1994 Quantitative analysis of submarine fans in the Tertiary of the North Sea Basin. *Marine and Petroleum Geology*, **11**, 202-207.

Rochow K.A. 1981 Seismic stratigraphy of the North Sea 'Palaeogene' deposits. In*: Petroleum Geology of the Continental Shelf of North- West Europe*, I.V. Illing and G.D. Hobson (eds), Heyden, London, 225-266.

Scotchman, I.C., L.H. Johns, and R.S. Miller. 1987 Clay diagenesis and oil migration in Brent Group sandstones of NW Hutton field, UK North Sea. *Clay Minerals*, **24**, 339- 374.

Sears R.A., Harbury A.R., Protoy A.J.G. and D.J. Sterwart 1993 Strucutral styles from the Central Graben in the UK and Norway. In: *Petroleum Geology of Northwest Europe*, J.R. Parker (ed), Geol. Soc. London, 1231-1243.

Smalley P.C., Lonoy A. and A. Raheim 1992 Spatial $^{87}Sr/^{86}Sr$ variations in formation water and calcites from the Ekofisk chalk oil field: implications for reservoir connectivity and fluid composition. *Applied Geochemistry*, **7**, 341-350.

Smalley P.C., Bishop P.K., Dickson, J.A.D. and D. Emery 1994 Water-rock interaction during meteoric flushing of a limestone: implications for porosity development in karstified petroleum reservoirs. *Journal of Sedimentary Research*, **64**, 180-189.

Stewart I.J. 1987 A revised stratigraphic interpretation of the Early Palaeogene of the Central North Sea, In: *Petroleum Geology of North West Europe*, J. Brooks and K.W. Glennie (eds), Graham and Trotman, London, 557-577.

Stewart R.N.T., Haszeldine R.S., Fallick A.E., Anderton R. and R. Dixon. 1993 Shallow calcite cementation in a submarine fan: biodegradation of vertically migrating oil? *American Association of Petroleum Geologists Annual Convention,* New Orleans, Louisiana, 186.

Surdam R.C., Boese S.W. and L.J. Crossey 1984 The chemistry of secondary porosity. In: Clastic Diagenesis, D. MacDonald and R. Surdam (eds*), Association of American Petroleum Geologists Memoir* **37**, 127-151.

Timbrell G. 1993 Sandstone architecture of the Balder Formation depositional system, UK Quadrant 9 and adjacent areas. In: *Petroleum Geology of Northwest Europe: Proceedings of the 4th Conference*, J.R. Parker (ed), Geol. Soc. London, 107-121.

Walderhaug O. 1990 A fluid inclusion study of quartz-cemented sandstones from offshore mid-Norway: possible evidence for continued quartz cementation during oil emplacement. *Journal of Sedimentary Petrology*, **60**, 203-210.

Watson R.S. 1993 *The Diagenesis of the Tertiary Sands from the Forth and Balmoral Fields*. PhD Thesis, University of Aberdeen.

Figure captions

Figure 6.1 Structural framework of the North Sea, Brent Group Province and study area of Montrose Group sandstones illustrated.

Figure 6.2 Central North Sea location map for study wells

Figure 6.3 Lithostratigraphy for Palaeogene stratigraphy, Deegan & Scull 1977.

Figure 6.4 Cartoon cross-section of Central North Sea illustrating relationship between the Montrose Group and Moray Group sandstones (Deegan & Scull 1977)

Figure 6.5 Paragenetic sequence for Montrose Group sandstones, Central North Sea, WGG - Witch Ground Graben. Derived from authors petrographic studies.

Figure 6.6 Paragenetic sequences for Brent Group sandstones a) a-shallow Brent fields <2800m, b-intermediate depth Brent fields 2800-3700mn c-deep Brent fields >3700m from Glasmann 1992, b) from Giles et al. 1992.

Figure 6.7 Back-scattered photomicrograph of rhodochroisite replacing trace-fossils; bright patches are pyrite, surrounded by 50-100μm rhodochroisite spherules, dark grey is calcite and vertical dark grey is a calcite vein, (15/20-4 1996.5m)

Figure 6.8 Carbon and oxygen sotopic values of manganese carbonate concretion with depth.i

Figure 6.9 Photomicrograph of authigenic chlorite. Chlorite precipitates as grain coating crystallites -2μm across. Sandstones containing chlorite cement are particularly friable. (15/20-4 2013m)

Figure 6.10 Oxygen isotopic values of chlorite separates vs precipitation temperature.

Figure 6.11 Photomicrograph of microcrystalline quartz. Quartz forms euhedral crystals up to 10μm and is associated with detrital clay. (16/29-2 8625ft).

Figure 6.12 Photomicrograph of detrital illite-smectite. A boxwork habit of illite-smectite clay forms perpendicular to grain surfaces. This is seen within all wells regardless of depth(16/28-6 2631m), b) Boxwork habit clays precipitating adjacent to K-feldspar overgrowths (15/20-4 1991.7m).

Figure 6.13 Photomicrograph of K-feldspar overgrowths. Authigenic K- feldspar is more resistant to dissolution and is overgrown by quartz overgrowth (15/20-4 1986.8m). b) K-feldspar overgrowth and detrital grain fractured during compaction (15/20-4 2002.6m).

Figure 6.14 Photomicrograph of kaolinite. Up to 12% rock volume of kaolinite is present within wells 15/26-3 and 15/26-4. Kaolinite is present as pore-filling ragged verms (15/26-4 2070.2m), b) Within deeper and more distal wells a blocky habit of kaolinite predominates (23/16-4 2309.6m).

Figure 6.15 Kaolinite % with depth. Kaolinite forms less than 4% rock volume for most wells. Within wells close to late Palaeocene shorelines (15/26-3 and 15/26-4) substantially more kaolinite is present, up to 12% rock volume. Derived from authors point counts and BP sedimentological reports b) Kaolinite % for Brent Group sandstones from Giles et al. (1992). At similar depth 5000ft to 9000ft, there is more kaolinite present within Brent Group sandstones but volumes decline gradually at depths greater than 9500ft burial.

Figure 6.16 $\delta^{18}O$(kaolinite) with depth for Montrose Group sandstones. $\delta^{18}O$ values stay relatively constant between deep wells and shallow wells indicating similar conditions during precipitation.

Figure 6.17 Photomicrographs of quartz overgrowths

Figure 6.18 Quartz overgrowth % with depth. Volumes of authigenic quartz remain small <2% until burial greater than 8000ft. Anomalous well 23/16-4 (and 22/20-3) have enhanced quartz overgrowths and are adjacent to salt-diapirism. Derived from authors own point counts and BP sedimentological reports. b) Authigenic quartz % with depth from Giles et al. (1992). Authigenic quartz volumes remain low (<2%) until burial depths of 8500ft is reached. Then volumes gradually increase to up to 24% volume at depth-12000ft.

Figure 6.19 Photomicrograph of fibrous illite. At depth greater than 2500m burial, illite forms an important though volumetrically small (<1% volume) authigenic phase. Boxwork smectite-illite clays become more plate-like (22/17T-4 10186ft) and b)kaolinite flakes begin to fray and illite precipitates upon plates (16/28-6 2631m).

Figure 6.20 Secondary porosity with depth. a) Volumes of secondary porosity in the Montrose Group do not vary much with depth, they are normally <4% volume. Data from authors point-counts and BP data; b) Brent Group volumes of secondary porosity (Harris 1992). Volumes of secondary porosity are not much different from Montrose Group sandstones although dissolution of feldspars is happening progressively with depth. It is likely that secondary porosity is continuously destroyed by compaction during burial form optimum 4% secondary porosity.

Figure 6.21 $\delta^{13}C$- $\delta^{18}O$ crossplot of carbonates. Cross plot illustrates groupings of Montrose Group carbonates. 1- contains carbonates formed during shallow sulphate reduction within depositional marine porewaters. 2 - concretions in this file precipitated during oxidation of migrating hydrocarbons within meteoric porewaters. 3 - concretions within this field precipitated as a result of fermentation of organic material within meteoric porewaters. 4 - compositions of late concretions within deep and distal wells plot in this field as a result o decarboxylation and reprecipitation of detrital carbonate. b) compositions of Brent Group carbonates. The distribution of Brent Group carbonate are broadly similar to that of Montrose Group sandstones. This provides geochemical evidence that similar precipitation processes operated although the volumes of cement do vary.

Figure 6.22 $^{87}Sr/^{86}Sr$ -$\delta^{13}C$ crossplot of carbonates. Plot shows that Montrose Group concretions are not as radiogenic as Brent Group carbonates. We deduce that there is less feldspar and silicate dissolution within the Montrose Group,

Figure 6.23 $\delta^{18}O$ SMOW (kaolinite) frequency plot of Montrose Group sandstone data and published data from the Middle Jurassic Brent Group sandstones; Brint (1989), samples from the Thistle Field (211/18, the Murchison field (211/19) and the Dunlin Field (211/13 and 211/23): Osborne et al. (1994), samples from the emerald Field (2/10 and 3/11): Macaulay e al. (1994), samples from the Hutton and NW Hutton Fields (211/27 and 211/28): Glasmann et al. (1989), samples from the Heather Field (2/5). Montrose Group data falls on the vermiform side of Brent Group data.

Figure 6.24 δD SMOW (kaolinite) frequency plot of Montrose Group sandstone data and published data from the Middle Jurassic Brent Group; Brint (1989), samples from the Thistle Field (211/18), the Murchison field (211/19) and the Dunlin Field (211/13 and 211/23): Osborne et al.(1994), samples from the Emerald Field (2/10 and 3/11): Macaulay e al. (1994), samples from the Hutton and NW Hutton Fields (211/27 and 211/28): Glasmann et al. (1989), samples from the Heather Field (2/5). There does not appear to be any correlation between habit and δD values.

Figure 6.25a $\delta^{18}O$ - δD crossplot of kaolinite values. Kaolinites from both Brent and Montrose Groups have precipitated within mixed meteoric-marine porewaters over a range of temperatures. Macaulay et al.'s (1994) blocky and vermiform data and Glasmann et al.'s (1989) blocky morphology kaolinite precipitated at temperatures >60°C. There is very little compositional difference apparent in the oxygen and hydrogen isotopic values of Macaulay et al vermiform and blocky kaolinite data. Osborne et al.'s (1994) and Brint's (1989) kaolinite data suggests that precipitation took place at cooler temperatures of <60°C. Montrose Group kaolinite oxygen and hydrogen data suggests that precipitation took place over a range of temperatures (35°C to 80°C) within porewaters of between -6.5 to -4‰SMOW.
Figure 6.23b Illustrates Montrose Group data only.

Figure 6.26 Meteoric component of porewaters. There are three hypothesis about introduction of meteoric porewaters into the Brent: 1) Porewaters were meteoric during the deposition and porewater composition was maintained during burial (MacAulay et al. 1994), 2) Meteoric porewater was introduced into the Brent Group during subarial erosion of tilted fault-blocks during the Kimmeridgian Unconformity (Macaulay et al. 1993), 3) Meteoric water was introduced from the adjacent East Shetland Platform during relative sealevel fall (Haszeldine et al. 1992).
b) flushing could have happened within the Montrose Groups during the late Palaeocene as a result of the progradation of the overlying Moray Group deltaic system and relative sealevel fall (Reynolds 1994).

Table 6.1 Oxygen isotope values from Mn-calcite concretion, 1996.5m cored depth.

Length along concretion	δ^{13}CPDB	δ^{18}OPDB	δ^{18}OSMOW
10cm	-18.3	-5.6	25.1
9cm	-18.4	-12.0	18.6
8cm	-18.8	-10.1	20.5
8cm	-25.1	-9.1	21.5
7cm	-19.0	-5.2	25.6
6cm	-18.3	-4.1	26.7
2cm	-18.3	-4.9	25.8
1.5cm	-21.1	-8.4	22.2

Table 6.2 Oxygen isotope values from chlorite separates, 15/20-4, cored depth 1968m

δ^{18}OSMOW	Grain size (μm)
17.0	5
12.7	5
15.1	2
15.2	2
13.0	2
14.9	0.5

Table 6.3 Point count data

Well	Cored depth (ft)	Cored depth (m)	Quartz overgrowth (%)	Secondary porosity (%)	Kaolinite (%)
15/20-4	6482.2	1975.8	1.0	1.2	0.2
	6499.7	1981.1	0.6	1.2	1.6
	6518.5	1986.8	0.4	0.6	0.8
	6534.5	1991.7	0.4	0.6	0.2
	6534.9	1991.8	0.6	0.2	0.2
	6535.1	1991.9	0.57	0.0	0.3
	6525.3	2019.4	1.2	1.0	0.6
15/26-3	6162.4	1878.3	0.6	0.4	1.4
	6217.8	1895.2	0.0	0.2	0.2
	6150.6	1874.7	0.0	3.2	5.2
	6151.3	1874.9	0.0	3.0	11.0
	6153.2	1875.5	0.0	2.6	11.0
	6154.9	1876.0	0.0	2.8	9.6
	6157.2	1876.7	0.0	2.6	8.2
	6176.5	1882.6	0.0	1.4	9.2
	6189.3	1886.5	0.0	2.2	10.0
	6202.8	1890.6	0.0	2.0	7.4
	6204.1	1891.0	0.0	2.4	7.2
	6236.1	1900.8	0.0	1.8	11.0
	6249.0	1904.7	0.0	3.6	6.2
	6265.1	1909.6	0.0	2.6	5.4
	6285.3	1915.7	0.0	1.4	6.6
	6302.5	1921.0	0.0	3.4	4.0

	6305.8	1922.0	0.0	2.4	4.2
	6328.7	1929.0	0.0	3.8	0.6
15/26-4	6759.8	2060.4	0.0	2.6	4.0
	6791.3	2070.0	0.0	2.0	3.0
	6799.9	2072.6	0.6	2.4	4.6
	7236.7	2205.7	0.0	2.6	12.0
	7315.3	2229.9	0.0	7.6	11.0
	7383.2	2250.4	0.0	0.2.	0.8
	7416.3	2260.5	0.2	6.8	3.8
	7450.0	2270.7	0.0	4.6	8.8
	7484.8	2281.4	0.2	3.2	7.6
	7508.5	2288.6	0.0	1.6	9.4
	7551.7	2301.8	0.0	3.0	9.0
	7565.6	2306.0	0.0	2.4	6.6
	7574.8	2308.8	0.0	3.8	0.0
16/28-4	8420.9	2566.7	7.0	-	3.0
	8425.2	2568.0	0.0	-	1.0
	8426.8	2568.5	3.0	-	0.5
	8431.8	2570.0	2.0	-	2.0
	8438.3	2572.0	1.0	-	2.0
	8443.2	2573.5	2.0	-	1.0
	8453.1	2576.5	0.5	-	2.0
	8460.1	2578.6	1.0	-	2.0
	8463.8	2579.8	0.0	-	0.0
	8466.2	2580.5	2.0	-	1.0
	8471.1	2582.0	3.0	-	2.0
16/28-5	8471.8	2582.2	0.0	-	5.0
	8479.3	2584.5	0.0	-	0.0
	8553.2	2607.0	5.0	-	2.0
	8569.6	2612.0	2.0	-	0.5
	8586.0	2617.0	2.0	-	5.0
	8602.4	2622.0	0.5	-	0.5
	8611.6	2624.8	2.0	-	3.0
	8618.8	2627.0	3.0	-	0.0
	8636.8	2632.5	1.0	-	1.0
	8649.1	2636.3	0.0	-	2.0
	8653.2	2637.5	1.0	-	0.0
	8654.9	2638.0	0.5	-	0.0
	8668.8	2642.3	0.5	-	3.0
	8671.3	2643.0	1.0	-	3.0
	8677.0	2644.8	0.0	-	1.0
	8691.0	2649.0	4.0	-	0.5
	8706.7	2653.8	0.5	-	3.0

	8726.9	2659.9	0.5	-	1.0
16/28-6	8483.5	2585.8	1.8	2.0	4.4
	8483.9	2585.9	2.2	4.0	2.6
	8484.3	2586.0	1.0	3.4	4.4
	8525.9	2598.7	1.8	3.2	1.0
	8579.7	2615.1	0.5	1.4	1.7
	8632.6	2631.2	0.8	0.8	2.2
	8679.1	2645.4	2.8	3.2	8.0
	8679.5	2645.5	0.8	0.4	1.2
	8727.7	2602.2	0.6	1.6	1.8
	8778.6	2675.7	1.6	2.2	2.4
	8803.5	2683.3	1.2	1.2	2.4
	8824.5	2689.7	0.0	1.0	1.6
	8877.0	2705.7	2.6	1.2	1.8
	8925.6	2720.5	1.0	0.2	1.8
	8971.5	2734.5	1.6	1.4	1.6
16/29-2	8607.0	2623.4	24	0.2	0.0
	8623.9	2638.6	0.4	0.0	0.0
	8625.0	2628.9	0.2	0.8	0.2
	8626.6	2629.4	0.4	1.2	0.4
	8642.0	2634.1	0.8	1.4	0.4
	8650.0	2636.5	0.4	1.4	0.2
	8655.2	2638.2	0.0	1.0	1.6
	8668.0	2642.0	0.2	1.8	1.4
	8689.0	2648.4	2.0	0.8	3.4
	8697.0	2650.8	0.6	0.8	1.0
	8710.0	2654.8	0.6	0.8	0.6
	8720.0	2657.9	0.2	1.0	1.6
	8740.0	2663.9	0.4	1.0	1.2
	8748.1	2666.4	0.2	0.8	1.8
	8772.0	2673.7	0.2	0.8	1.8
	8787.0	2678.3	0.2	1.6	1.4
	8810.3	2685.4	0.2	1.4	2.4
21/10-1	7065.0	2153.4	0.0	0.2	0.4
	7072.5	2155.7	0.0	0.0	0.0
	7080.7	2158.2	0.0	0.0	0.0
	7093.0	2161.9	0.0	2.4	0.4
	7104.0	2165.3	0.6	1.6	1.0
	7104.5	2165.4	0.2	2.8	1.2
	7116.0	2169.0	0.0	0.4	0.0
	7343.0	2238.1	0.0	2.4	0.6
	7357.0	2242.4	0.0	0.0	0.2
	7365.0	2244.8	0.0	1.8	0.8

	7377.0	2248.5	0.4	3.0	0.0
	7392.0	2253.1	0.8	2.8	0.2
21/10-FB55	7552.5	2302.0	0.5	-	0.5
	7585.3	2312.0	0.5	-	0.0
	7678.5	2343.7	0.0	-	1.0
	7718.2	2352.5	0.0	-	0.0
	7785.4	2373.0	0.5	-	2.0
	7815.0	2382.0	0.0	-	0.5
	7857.6	2395.0	0.0	-	1.0
	7026.5	2416.0	0.0	-	0.0
	7979.0	2432.0	0.0	-	0.0
	8047.9	24530	0.0	-	0.5
	8129.1	2477.7	0.0	-	0.5
	8152.1	2484.7	0.5	-	0.0
22/12-5	7553.2	2302.2	0.5	2.9	5.0
	7559.1	2304.0	0.5	2.0	4.0
	7575.5	2309.0	0.0	1.7	2.5
	7593.5	2314.5	0.5	2.9	1.0
	7600.7	2316.7	1.0	3.3	1.0
	7613.2	2320.5	0.0	1.4	2.0
	7623.0	2323.5	0.0	0.0	0.5
	7642.8	2329.5	0.0	1.4	0.5
	7648.4	2331.2	0.0	1.9	0.0
	7652.6	2332.5	0.0	0.5	3.5
22/12-7	8481.6	2585.2	2.5	3.2	0.5
	8484.9	2586.2	3.0	5.2	0.5
	8495.9	2589.6	4.0	7.0	2.0
	8515.9	2595.6	0.0	0.0	0.0
	8532.8	2600.8	4.0	11.0	1.0
22/17T-4	10055	2667.0	0.0	0.4	0.2
	10056	2667.3	0.0	0.6	0.4
	10057	2667.6	0.0	1.4	1.8
	10064	2669.8	1.0	2.8	2.6
	10070	2671.6	0.8	2.0	1.8
	10076	2673.4	0.6	4.6	2.2
	10081	2675.0	0.0	2.6	3.0
	10092	2678.3	0.2	3.4	3.8
	10186	2707.0	0.2	2.2	0.8
	10190	2708.2	0.0	1.7	0.8
	10193	2709.1	0.0	2.0	1.2
	10212	2714.9	0.6	2.4	0.2
	10216	2716.1	0.4	1.8	0.4

	10224	2718.5	0.4	3.8	1.8
	10250	2726.4	0.4	2.2	0.8
	10240	2723.4	0.2	1.8	1.0
	10388	2768.6	0.4	1.6	0.2
	10397	2771.3	0.0	0.4	0.0
	10410	2775.2	0.2	1.6	1.6
	10419	2777.9	0	0.8	2.2
	10430	2781.3	0.2	2.2	0.4
	10439	2784.1	0.0	0.4	0.4
22/20-3	8823.5	2689.4	3.4	2.4	1.4
23/16-4	7054.5	2150.2	0.4	1.2	0.8
	7073.4	2156.0	0.2	0.0	0.2
	7034.4	2156.0	0.0	0.0	0.2
	7075.1	2156.5	0.0	0.8	1.2
	7075.2	2156.5	0.0	0.0	0.2
	7075.2	2156.5	0.2	0.0	0.0
	7092.0	2161.6	0.0	0.6	1.8
	7093.6	2162.1	0.0	1.0	0.6
	7094.3	2162.3	0.6	1.6	2.2
	7094.9	2162.0.	5.0	0.0	1.8
	7095.4	2162.7	0.2	0.2	1.0
	7105.3	2165.7	0.0	1.6	0.6
	7225.6	2202.4	0.2	1.0	0.8
	7229.6	2203.6	0.2	10	0.0
	7227.2	2202.9	0.0	0.0	0.0
	7425.8	2263.4	0.0	1.0	0.8
	7425.8	2263.4	1.0	2.2	1.8
	7437.8	2267.0	0.0	1.6	1.2
	7577.6	2309.6	0.0	1.4	2.0
	7580.2	2310.4	0.0	0.0.	0.8
	7022.0	2140.3	2.0	0.1	0.0
	7024.4	2141.0	2.0	0.1	1.0
	7025.7	2141.4	0.2	0.0	0.0
	7037.6	2145.1	6.5	0.9	2.5
	7056.3	2150.7	1.0	0.8	2.0
	7062.8	2152.8	3.5	0.5	2.5
	7075.1	2156.5	0.5	0.0	0.0
	7078.1	2157.4	1.0	0.5	3.0
	7092.4	2161.7	0.2	0.1	2.0
	7094.8	2162.5	0.5	1.0	0.5
	7116.9	2169.2	3.0	0.4	1.5
	7131.2	2173.6	4.5	0.1	2.5
	7154.0	2180.5	1.5	0.5	1.0
	7166.8	2184.4	7.0	0.5	0.5

	7170.3	2185.5	4.5	0.9	1.5
	7187.6	2190.8	0.2	0.5	1.5
	7220.4	2200.8	1.5	1.3	1.0
	7224.5	2202.0	1.0	0.45	1.0
	7227.8	2203.0	1.0	0.0	0.0
	7419.9	2261.6	0.2	0.0	1.5
	7424.2	2262.9	3.0	0.5	3.5
	7439.3	2267.5	1.5	0.1	1.0
	7442.8	2268.6	0.5	0.5	2.5

Figure 6.1

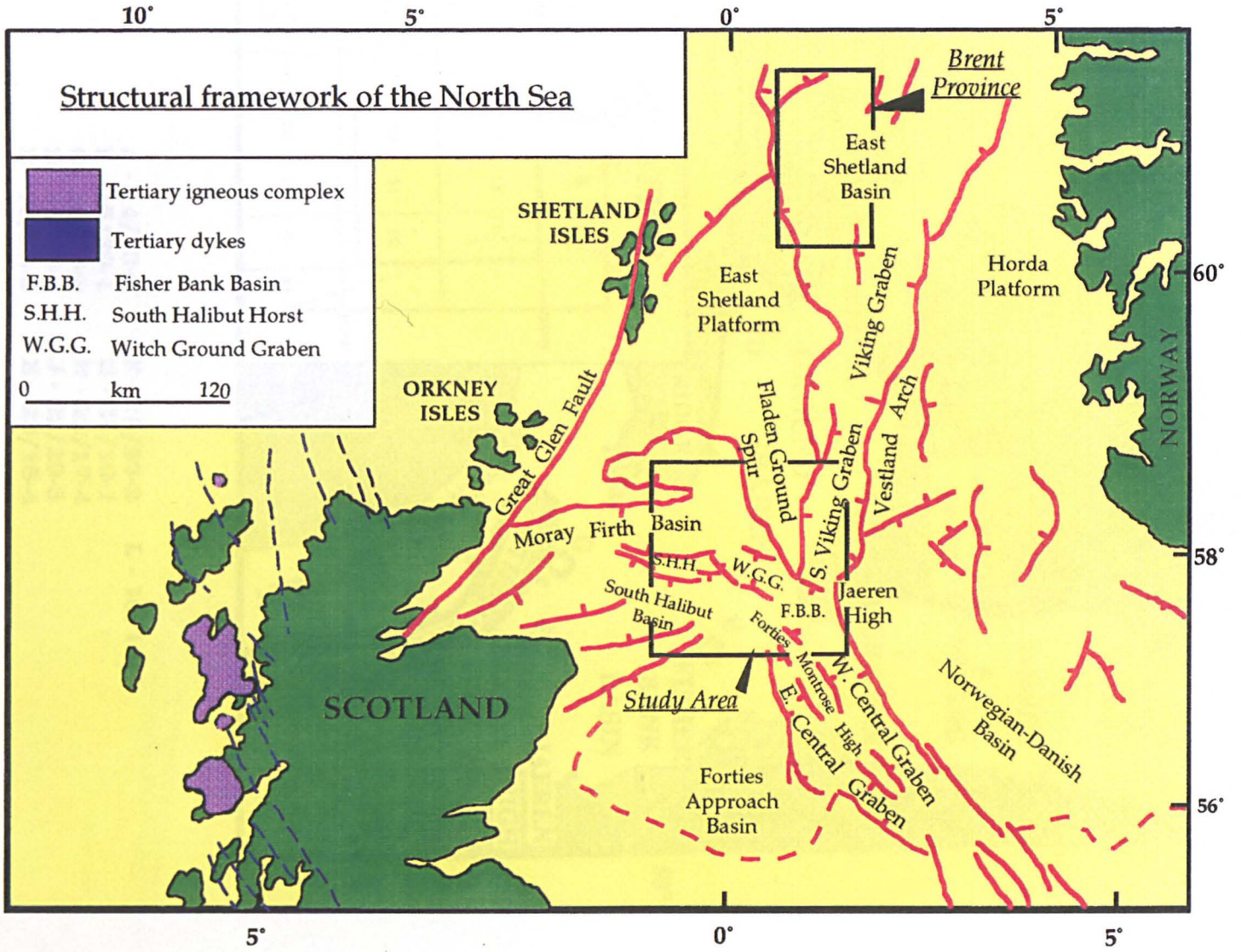
Structural framework of the North Sea
Tertiary igneous complex
Tertiary dykes
F.B.B. Fisher Bank Basin
S.H.H. South Halibut Horst
W.G.G. Witch Ground Graben
0 km 120
10°
5°
0°
5°
60°
58°
56°
5°
0°
5°
Brent Province
East Shetland Basin
SHETLAND ISLES
East Shetland Platform
Viking Graben
Horda Platform
NORWAY
ORKNEY ISLES
Great Glen Fault
Fladen Ground Spur
Vestland Arch
S. Viking Graben
Moray Firth Basin
S.H.H.
W.G.G.
South Halibut Basin
F.B.B.
Jaeren High
Forties Montrose High
W. Central Graben
E. Central Graben
Norwegian-Danish Basin
SCOTLAND
Study Area
Forties Approach Basin

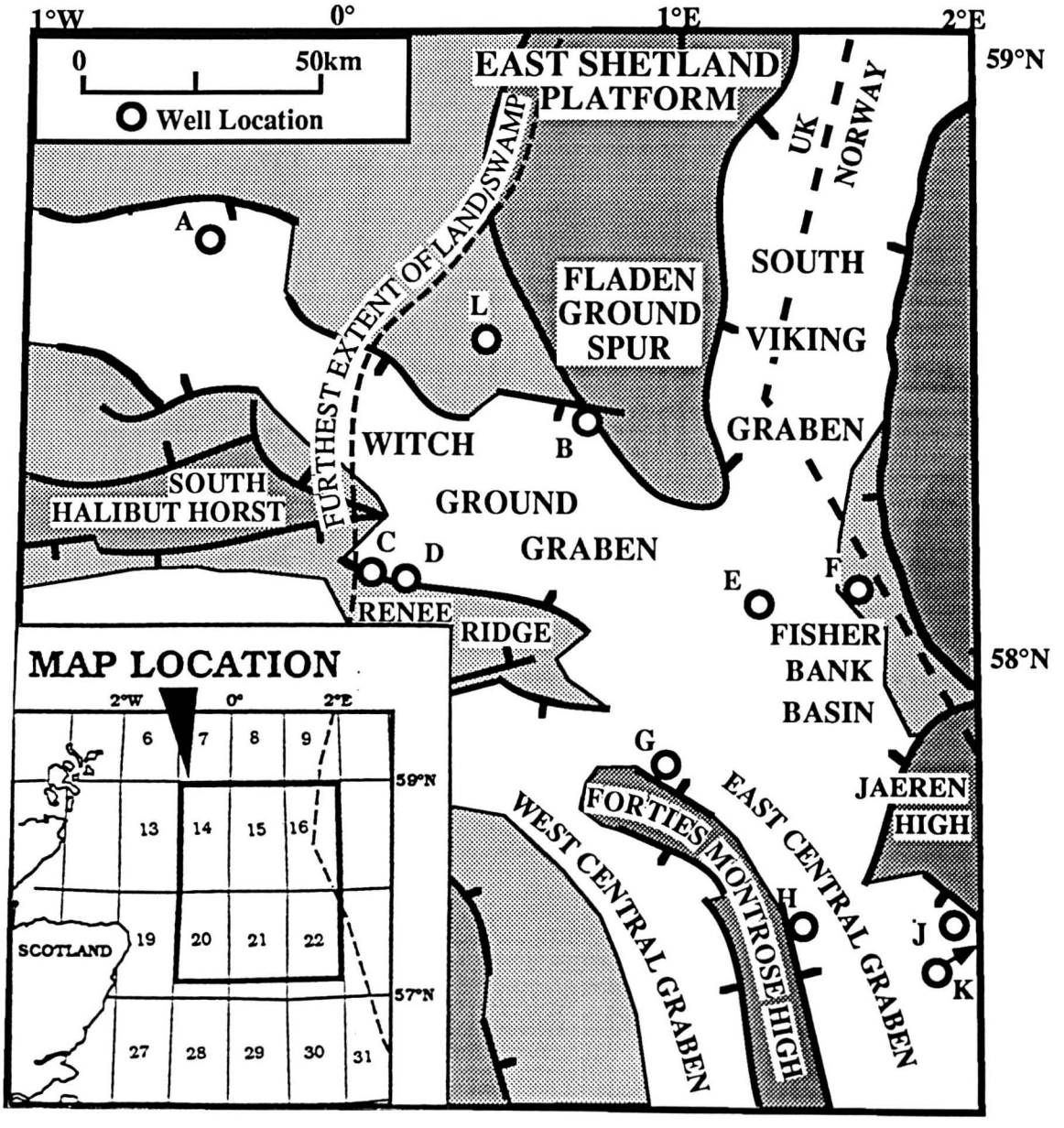

A - 14/13-3
B - 15/20-4
C - 15/26-3
D - 15/26-4
E - 16/28-6
F - 16/29-2
G - 21/10-1
H - 22/17-4
J - 22/20-3
K - 23/16-4
L - 15/18-5

Figure 6.2

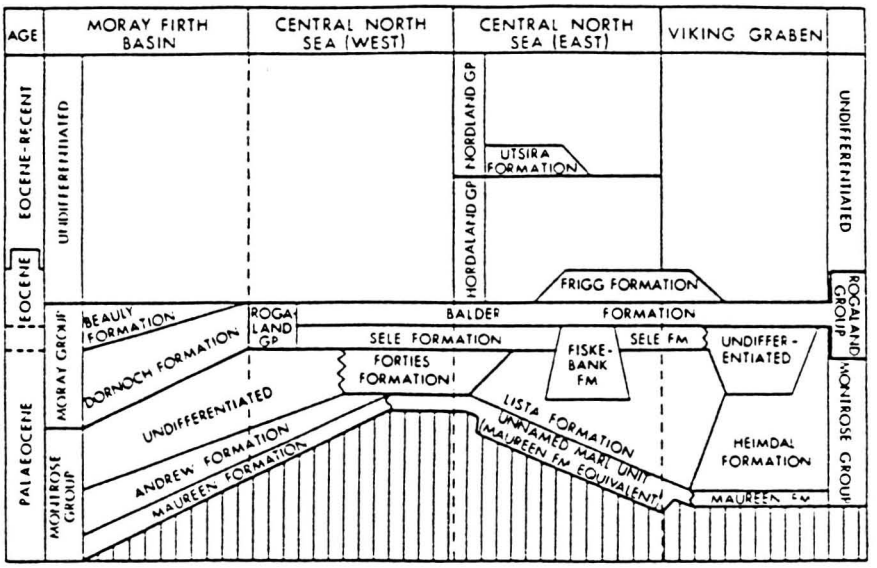
AGE
MORAY FIRTH BASIN
CENTRAL NORTH SEA (WEST)
CENTRAL NORTH SEA (EAST)
VIKING GRABEN
EOCENE-RECENT
UNDIFFERENTIATED
HORDALAND GP
UTSIRA FORMATION
UNDIFFERENTIATED
EOCENE
FRIGG FORMATION
ROGALAND GROUP
BEAULY FORMATION
DORNOCH FORMATION
MORAY GROUP
ROGALAND GP
BALDER FORMATION
SELE FORMATION
FORTIES FORMATION
FISKE-BANK FM
SELE FM
UNDIFFER-ENTIATED
MONTROSE GROUP
UNDIFFERENTIATED
ANDREW FORMATION
MAUREEN FORMATION
LISTA FORMATION
UNNAMED MARL UNIT
(MAUREEN FM EQUIVALENT)
HEIMDAL FORMATION
PALAEOCENE
MONTROSE GROUP
MAUREEN FM

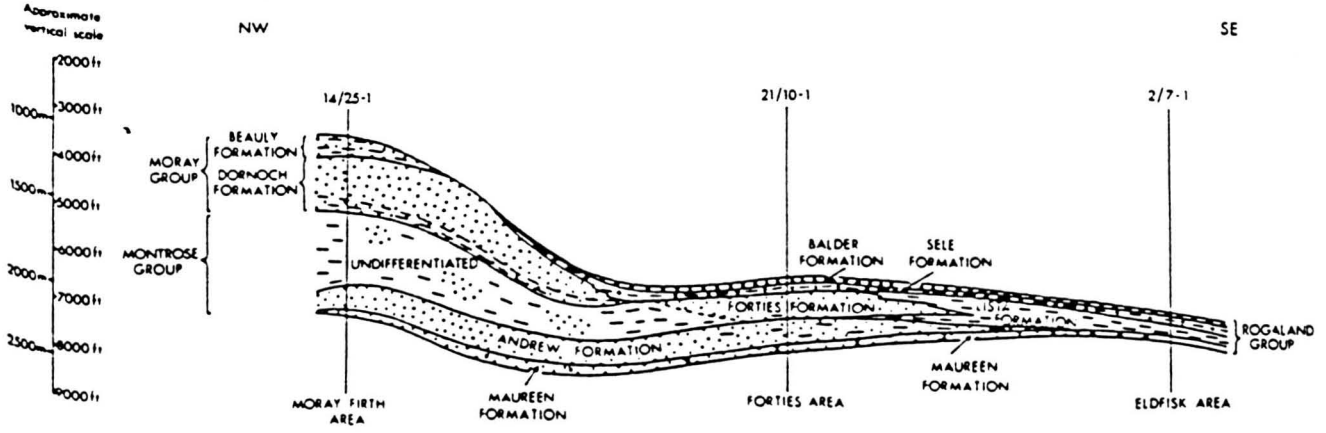
Approximate vertical scale
2000 ft
1000 m
3000 ft
4000 ft
1500 m
5000 ft
6000 ft
2000 m
7000 ft
8000 ft
2500 m
9000 ft
NW
SE
14/25-1
21/10-1
2/7-1
MORAY GROUP
BEAULY FORMATION
DORNOCH FORMATION
MONTROSE GROUP
UNDIFFERENTIATED
BALDER FORMATION
SELE FORMATION
FORTIES FORMATION
LISTA FORMATION
ANDREW FORMATION
MAUREEN FORMATION
ROGALAND GROUP
MORAY FIRTH AREA
MAUREEN FORMATION
FORTIES AREA
ELDFISK AREA

Figure 6.3

Figure 6.4

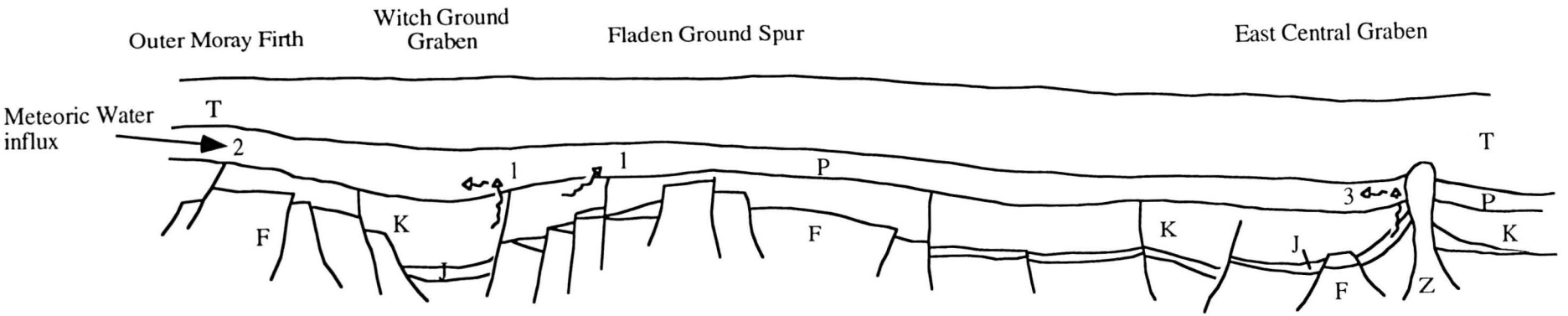
Outer Moray Firth
Witch Ground Graben
Fladen Ground Spur
East Central Graben
Meteoric Water influx
T
2
1
1
P
3
T
P
K
F
K
J
F
K
J
F
Z

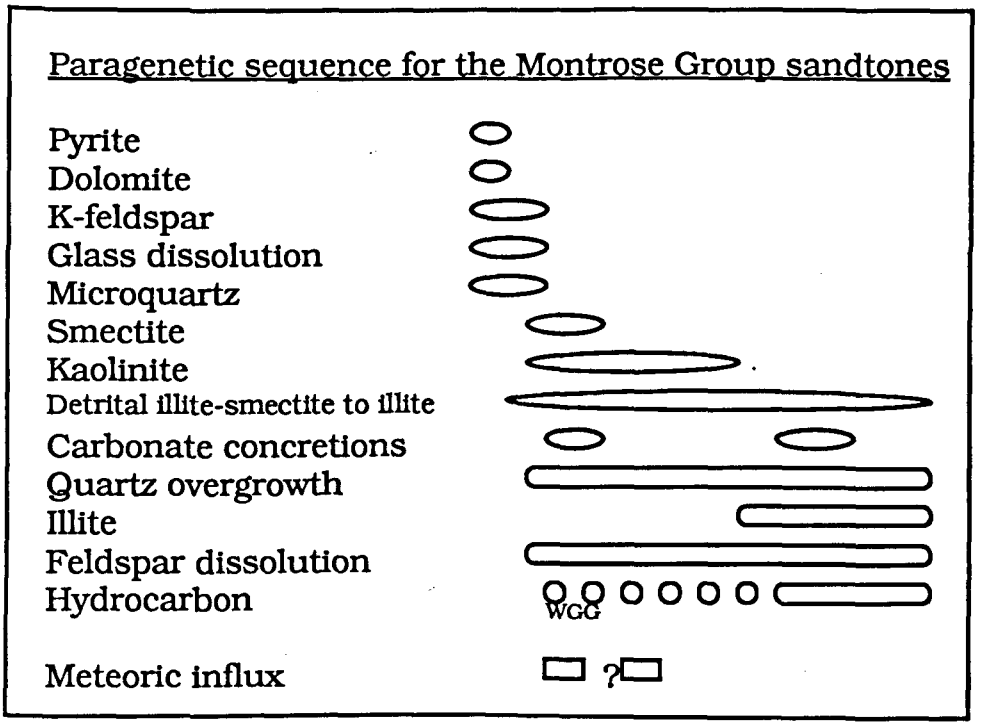
Paragenetic sequence for the Montrose Group sandtones
Pyrite
Dolomite
K-feldspar
Glass dissolution
Microquartz
Smectite
Kaolinite
Detrital illite-smectite to illite
Carbonate concretions
Quartz overgrowth
Illite
Feldspar dissolution
Hydrocarbon
WGG
Meteoric influx
?

Figure 6.5

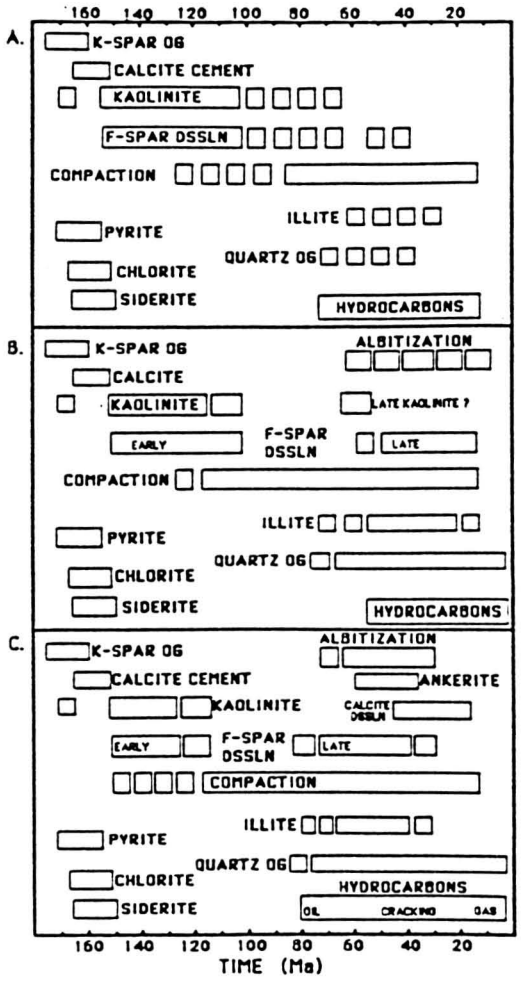
160 140 120 100 80 60 40 20
A.
K-SPAR OG
CALCITE CEMENT
KAOLINITE
F-SPAR DSSLN
COMPACTION
ILLITE
PYRITE
QUARTZ OG
CHLORITE
SIDERITE
HYDROCARBONS
B.
K-SPAR OG
ALBITIZATION
CALCITE
KAOLINITE
LATE KAOLINITE ?
EARLY
F-SPAR DSSLN
LATE
COMPACTION
ILLITE
PYRITE
QUARTZ OG
CHLORITE
SIDERITE
HYDROCARBONS
C.
K-SPAR OG
ALBITIZATION
CALCITE CEMENT
ANKERITE
KAOLINITE
CALCITE DSSLN
EARLY
F-SPAR DSSLN
LATE
COMPACTION
ILLITE
PYRITE
QUARTZ OG
CHLORITE
HYDROCARBONS
SIDERITE
OIL
CRACKING
GAS
160 140 120 100 80 60 40 20
TIME (Ma)

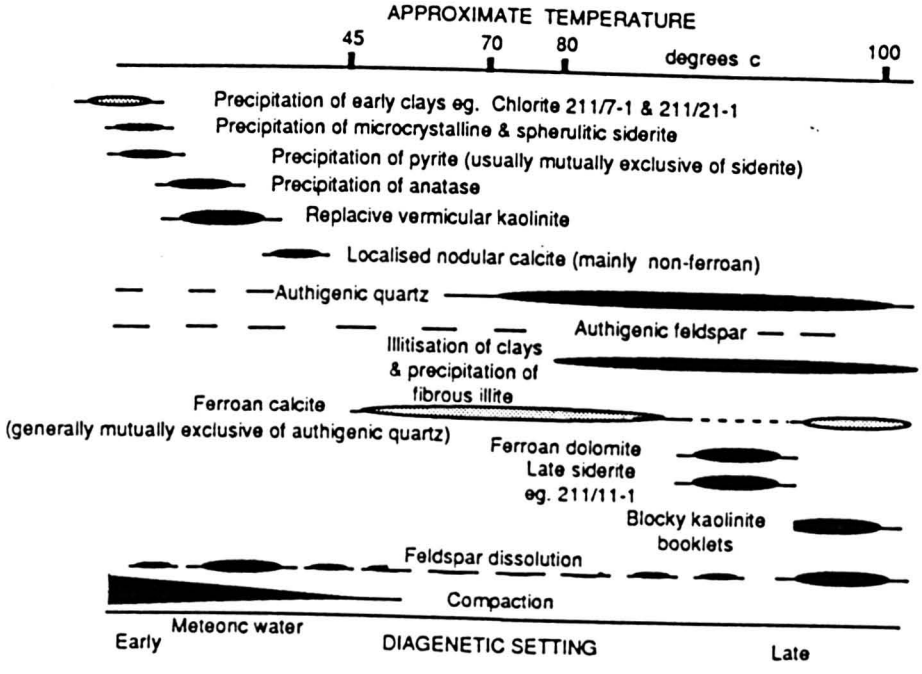
APPROXIMATE TEMPERATURE
45
70
80
degrees c
100
Precipitation of early clays eg. Chlorite 211/7-1 & 211/21-1
Precipitation of microcrystalline & spherulitic siderite
Precipitation of pyrite (usually mutually exclusive of siderite)
Precipitation of anatase
Replacive vermicular kaolinite
Localised nodular calcite (mainly non-ferroan)
Authigenic quartz
Authigenic feldspar
Illitisation of clays & precipitation of fibrous illite
Ferroan calcite
(generally mutually exclusive of authigenic quartz)
Ferroan dolomite
Late siderite eg. 211/11-1
Blocky kaolinite booklets
Feldspar dissolution
Compaction
Meteonc water
Early
DIAGENETIC SETTING
Late

Figure 6.6a,b

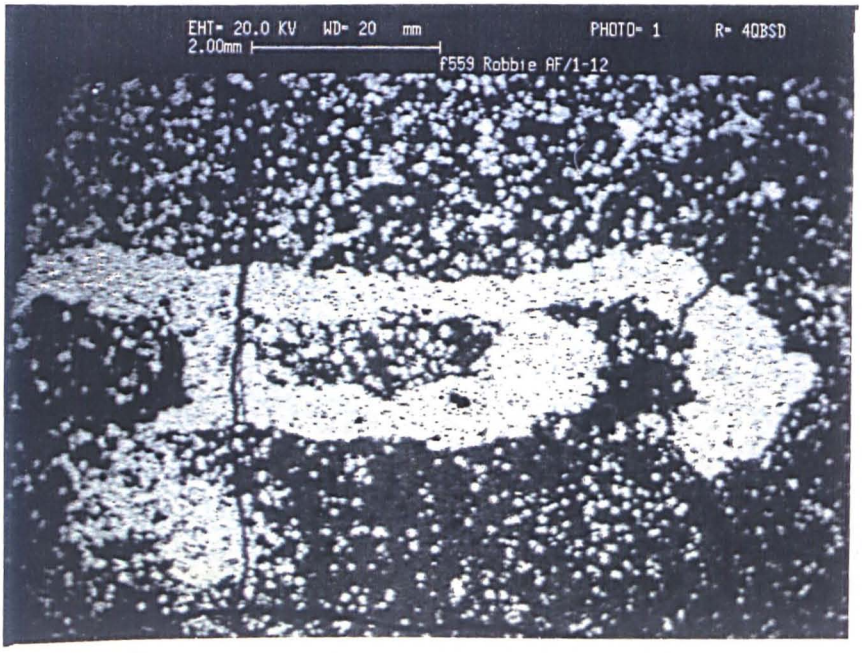

Figure 6.7a

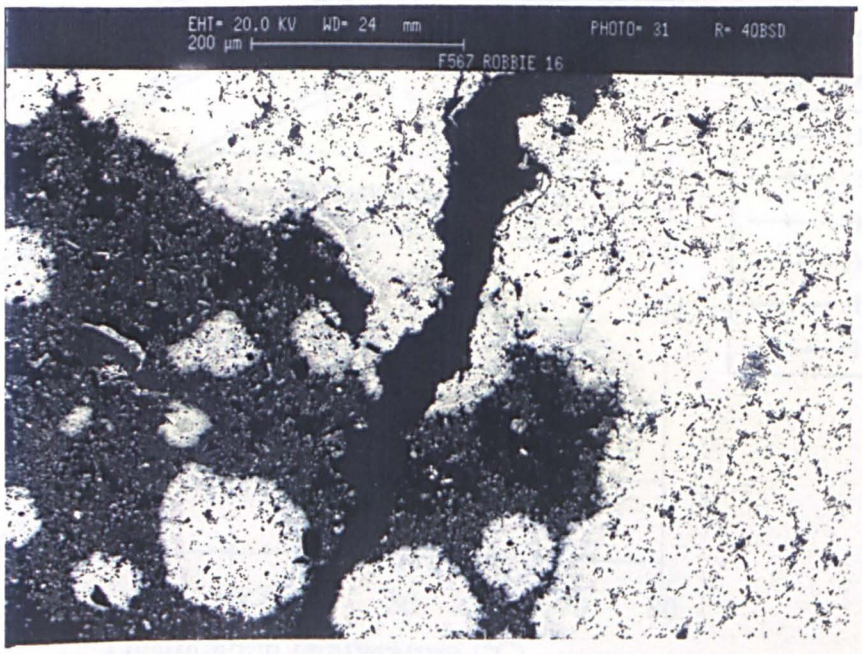

Figure 6.7b

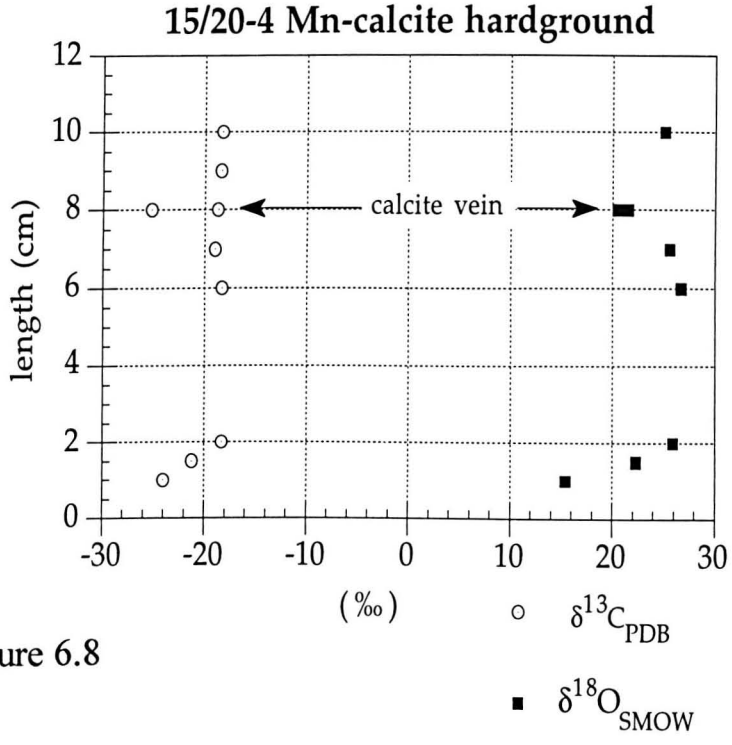

Figure 6.8

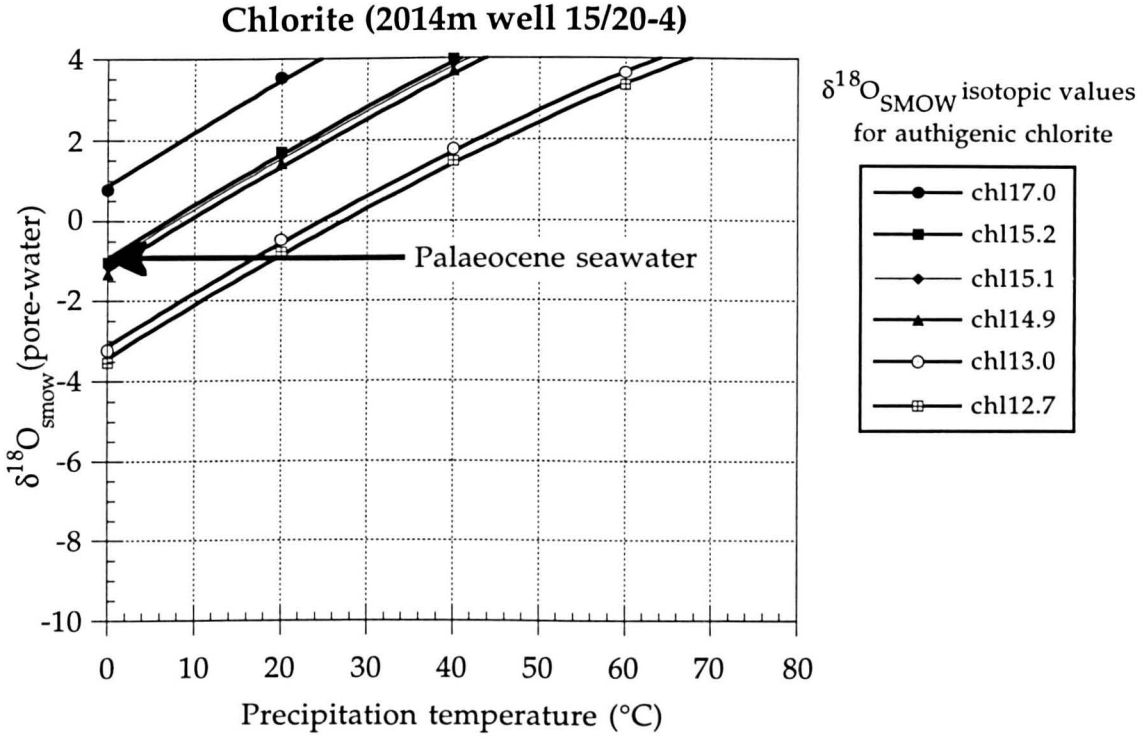

Figure 6.10

Figure 6.15

Kaolinite with depth

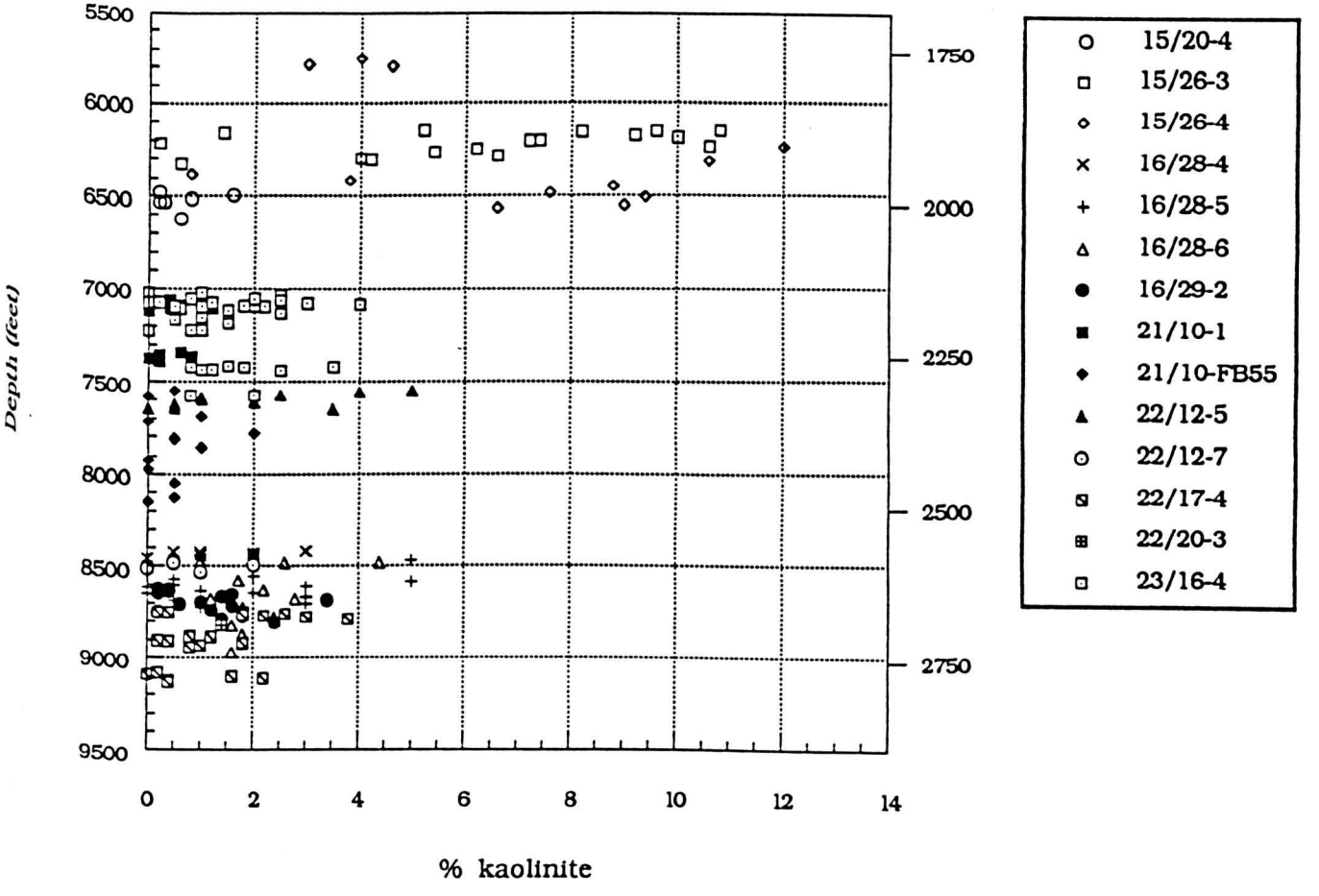

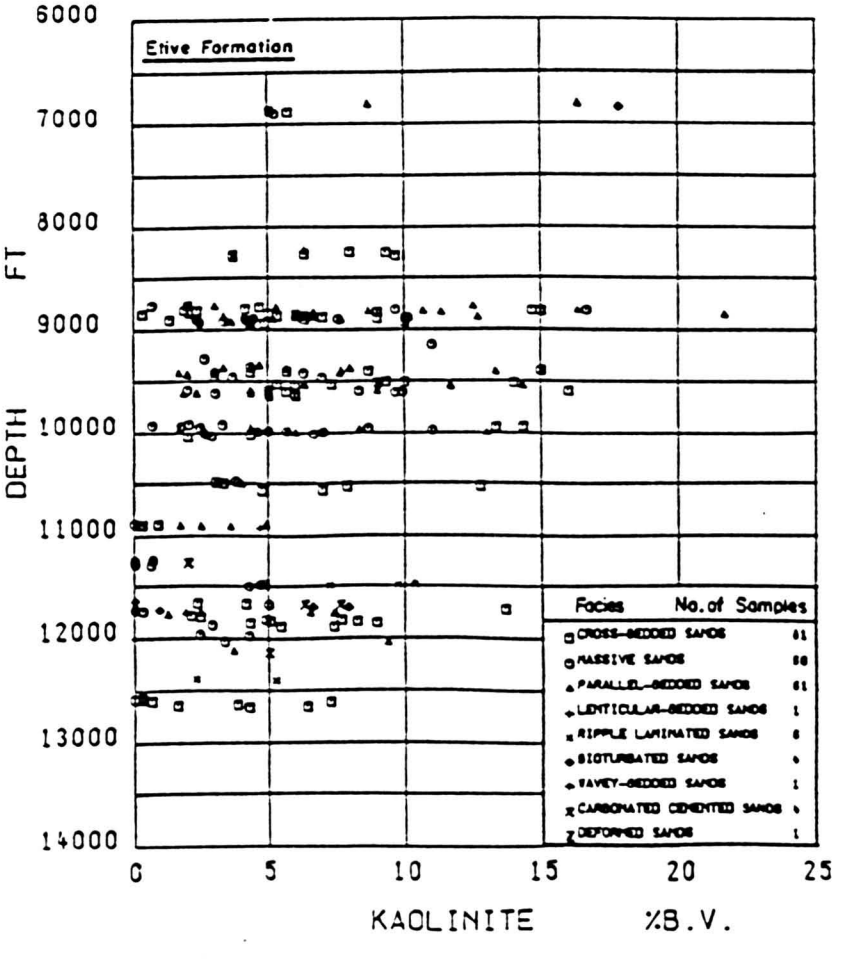

Figure 6.9

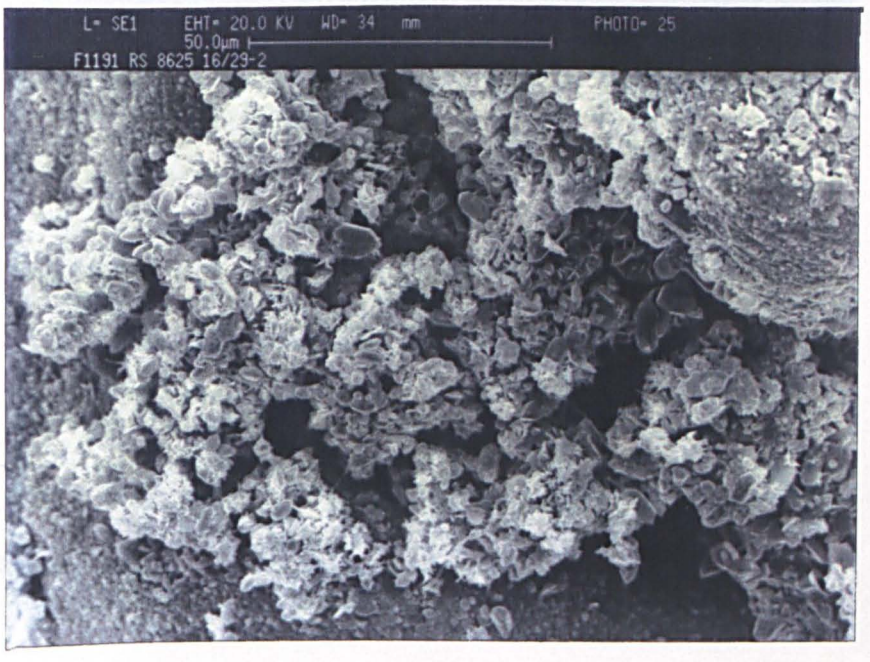

Figure 6.11

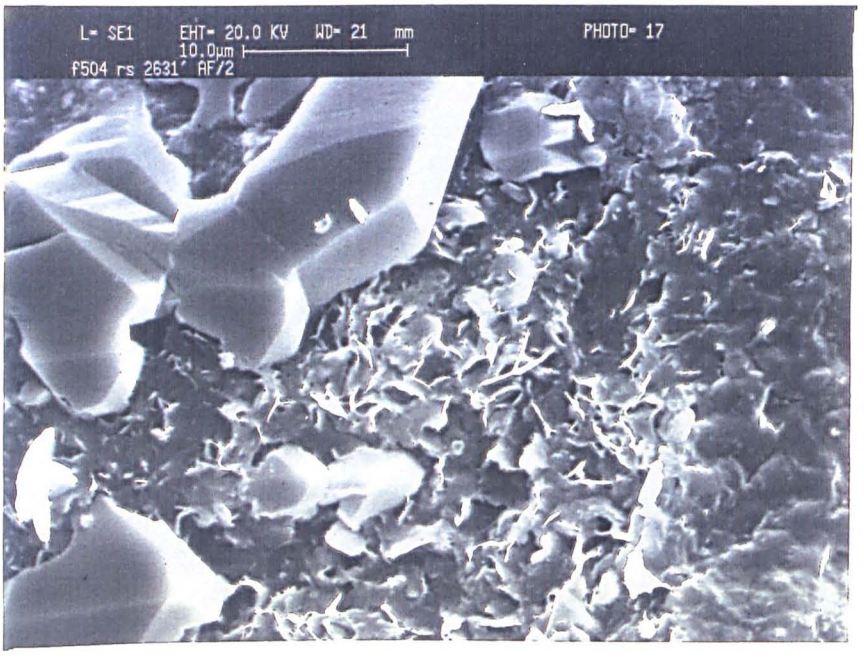

Figure 6.12a

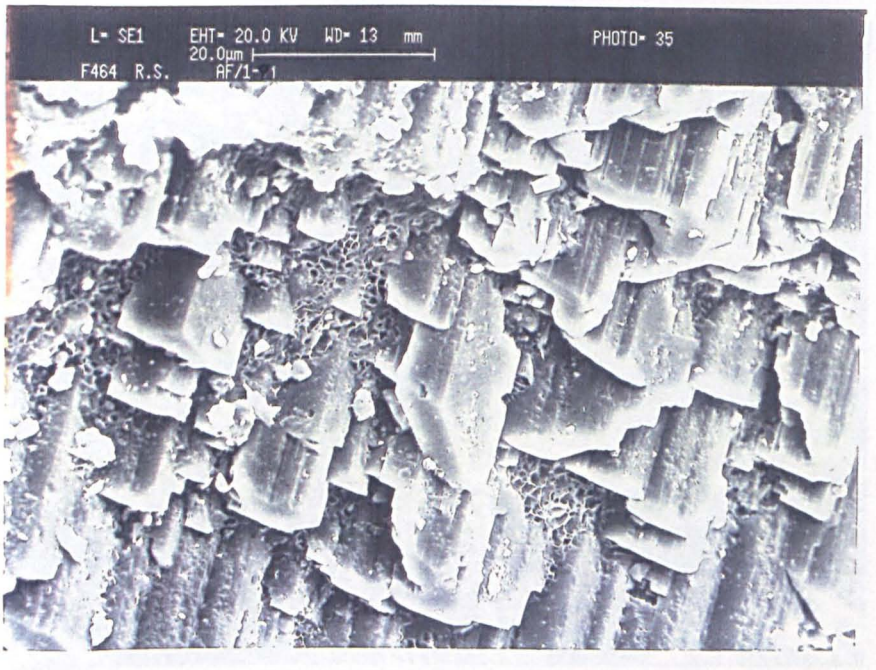

Figure 6.12b

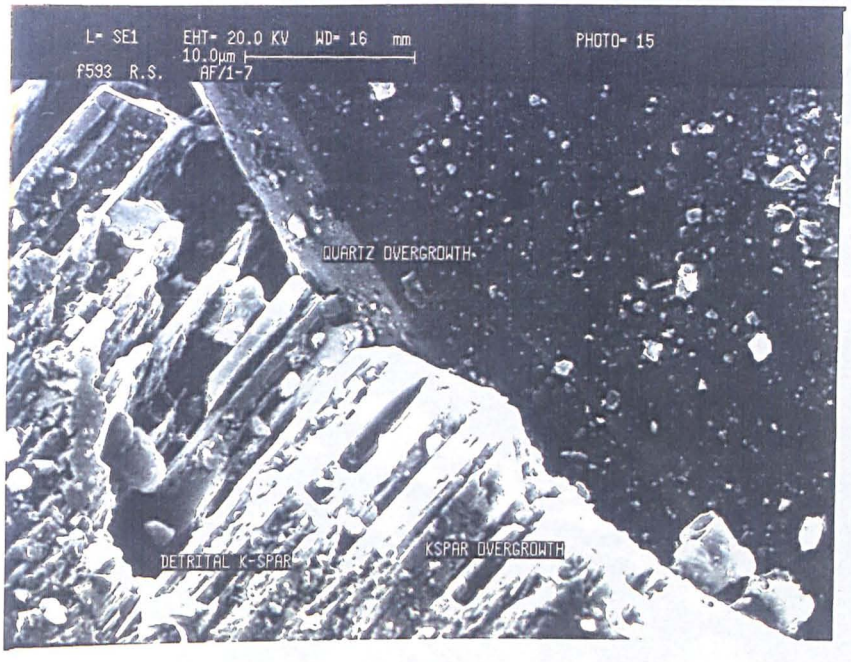

Figure 6.13a

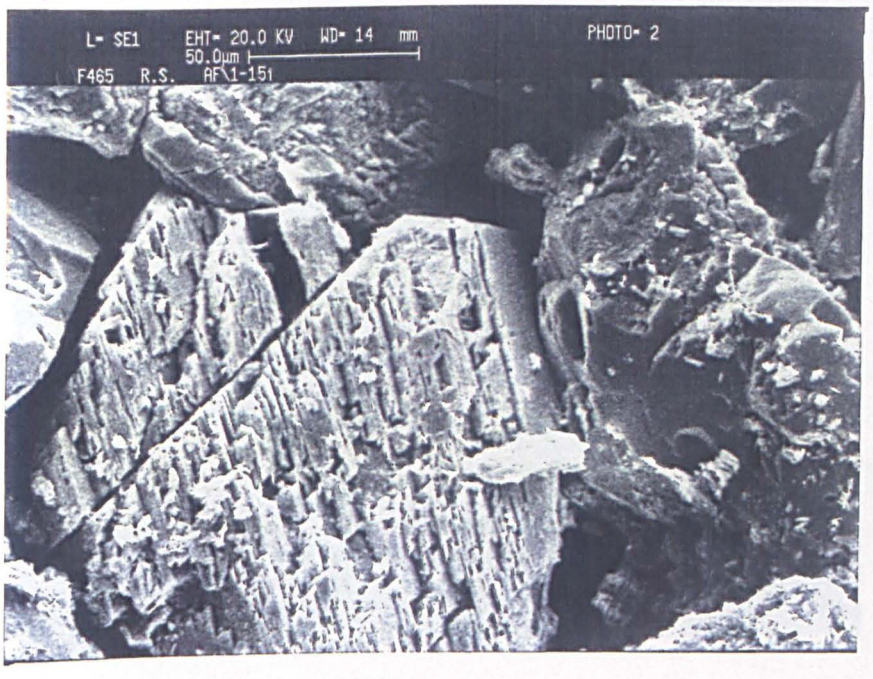

Figure 6.13b

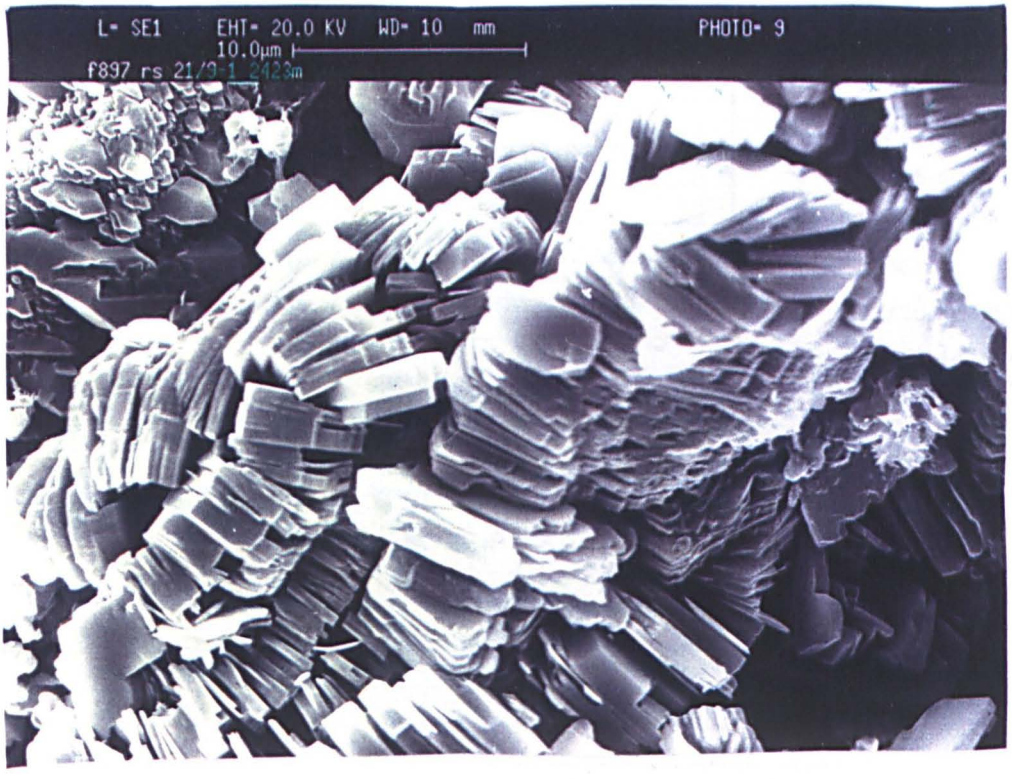

Figure 6.14a

Figure 6.14b

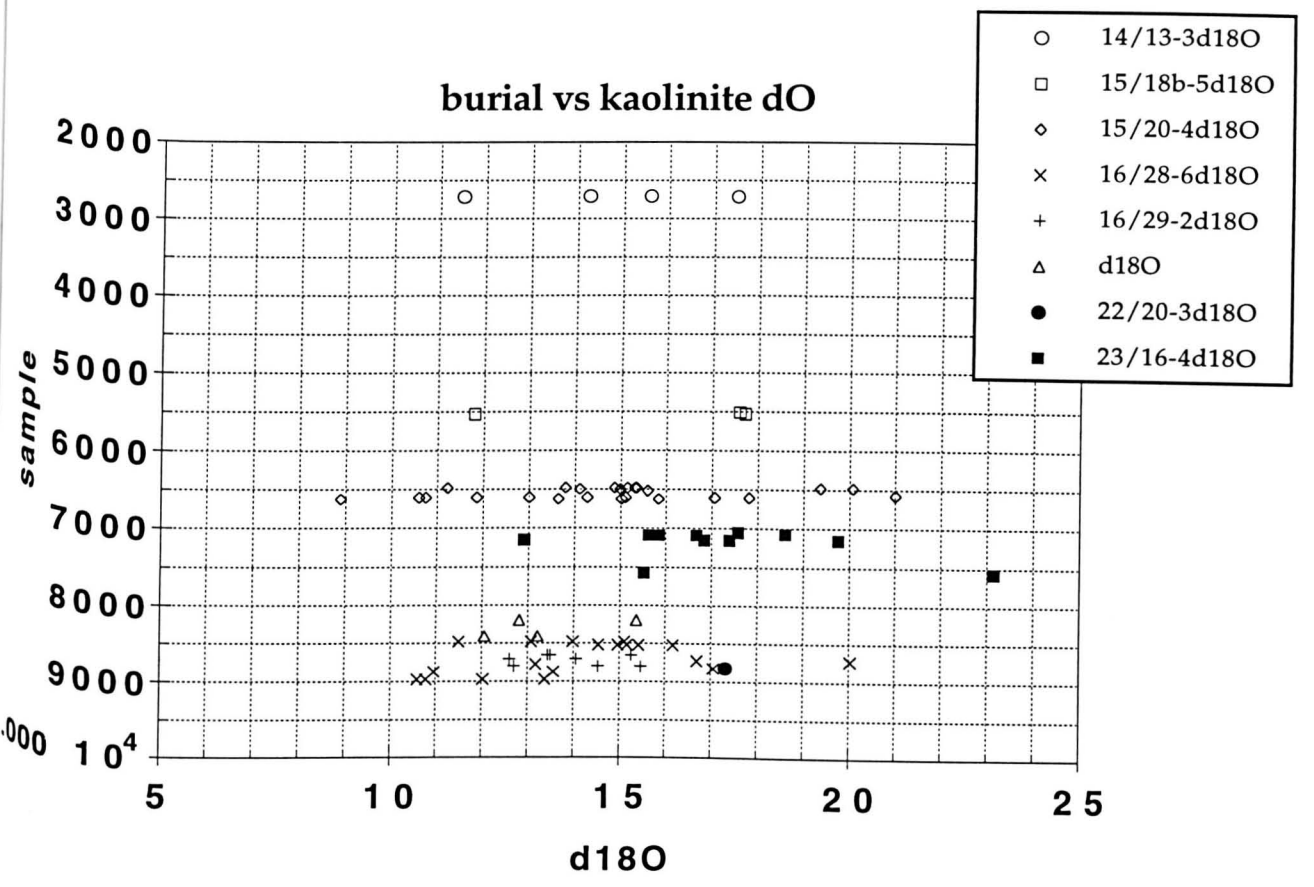
burial vs kaolinite dO
14/13-3d18O
15/18b-5d18O
15/20-4d18O
16/28-6d18O
16/29-2d18O
d18O
22/20-3d18O
23/16-4d18O
2000
3000
4000
5000
6000
7000
8000
9000
10^4
sample
5
10
15
20
25
d18O

Figure 6.16

Figure 6.17a

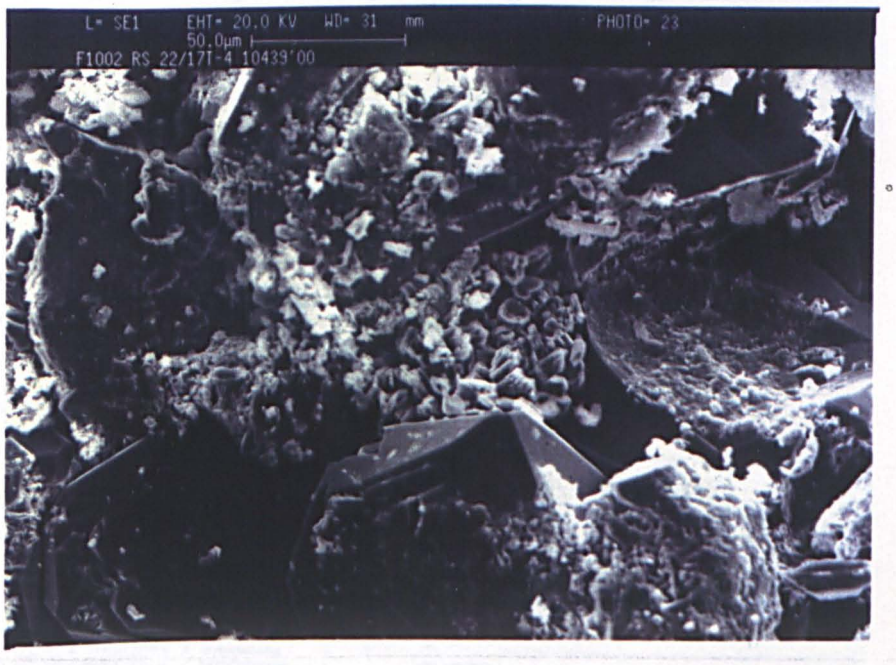

Figure 6.17b

Figure 6.18

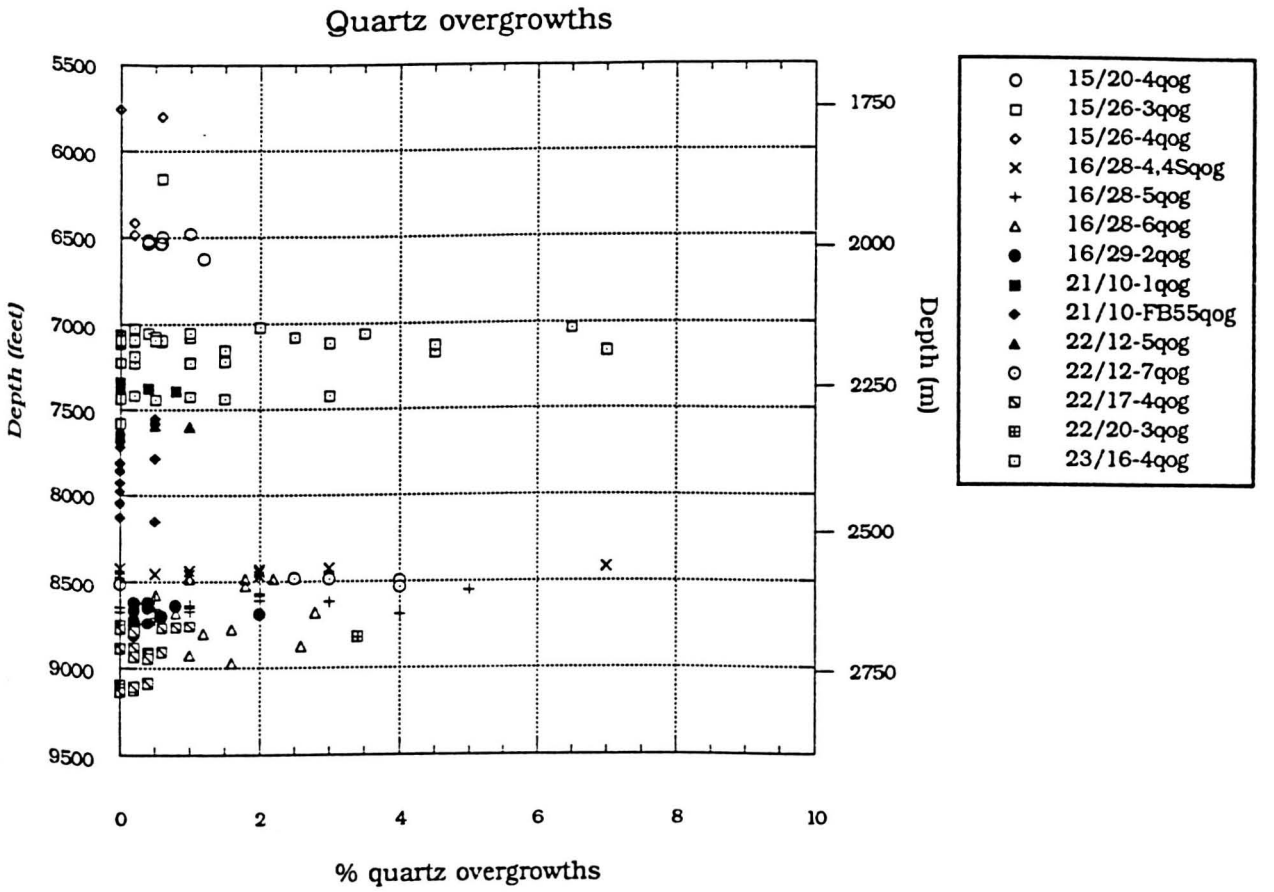
Quartz overgrowths
Depth (feet)
Depth (m)
5500
6000
6500
7000
7500
8000
8500
9000
9500
1750
2000
2250
2500
2750
0
2
4
6
8
10
% quartz overgrowths
15/20-4qog
15/26-3qog
15/26-4qog
16/28-4,4Sqog
16/28-5qog
16/28-6qog
16/29-2qog
21/10-1qog
21/10-FB55qog
22/12-5qog
22/12-7qog
22/17-4qog
22/20-3qog
23/16-4qog

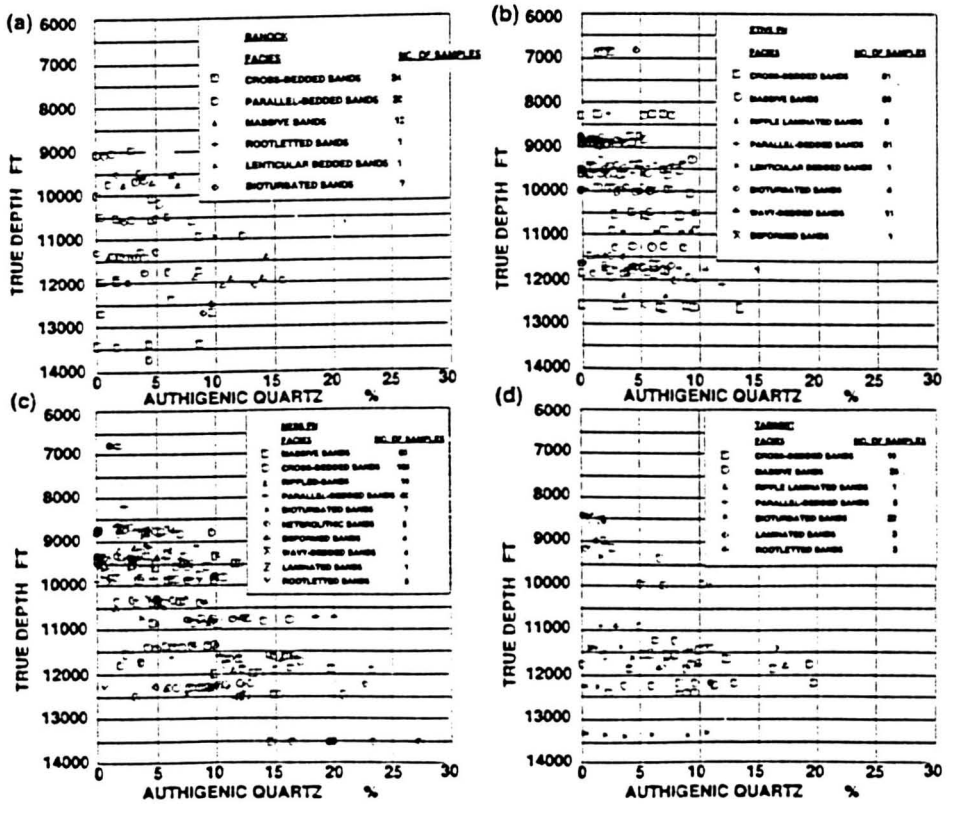
(a)
(b)
(c)
(d)
TRUE DEPTH FT
AUTHIGENIC QUARTZ %
6000
7000
8000
9000
10000
11000
12000
13000
14000
0
5
10
15
20
25
30

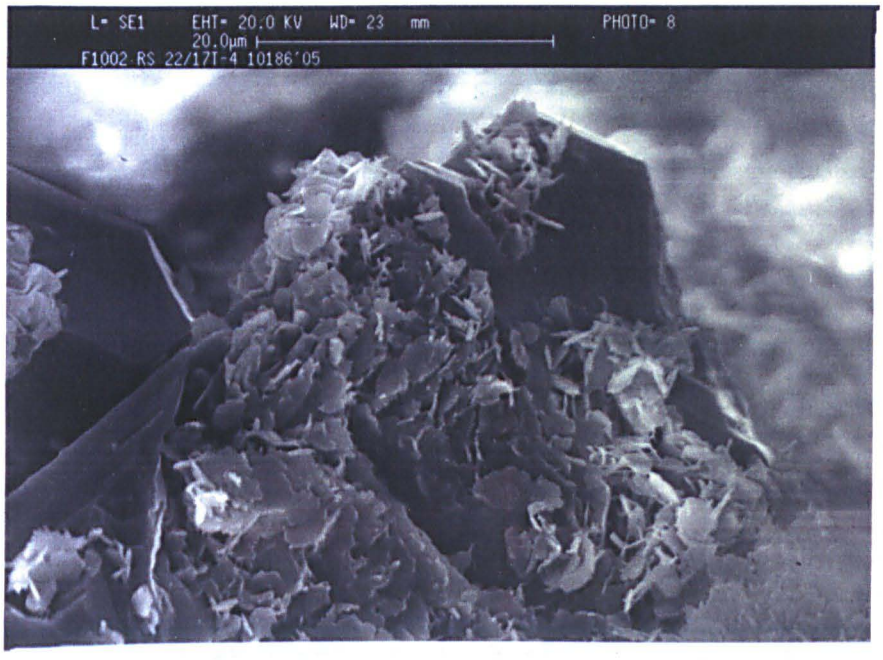

Figure 6.19a

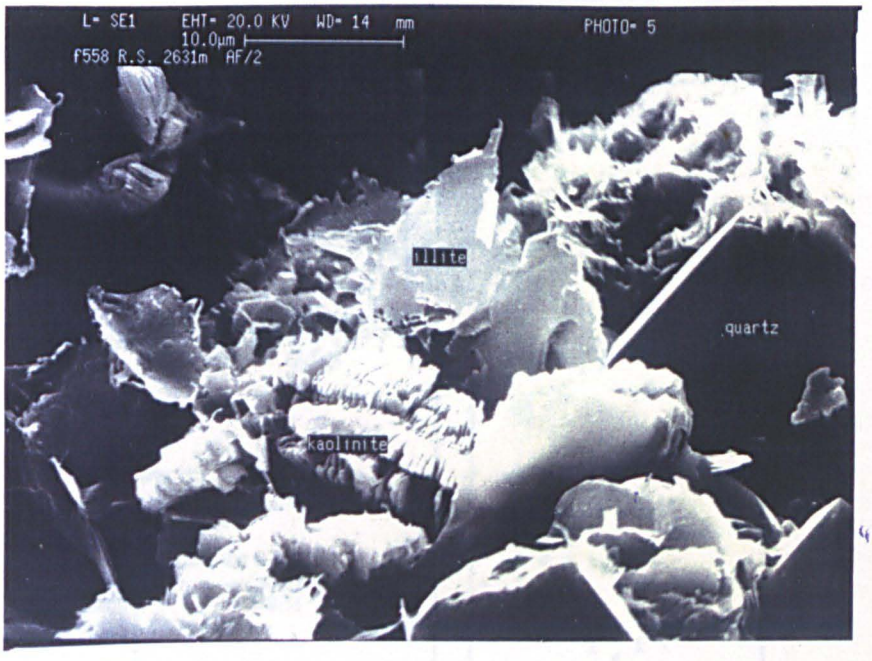

Figure 6.19b

Figure 6.20a,b

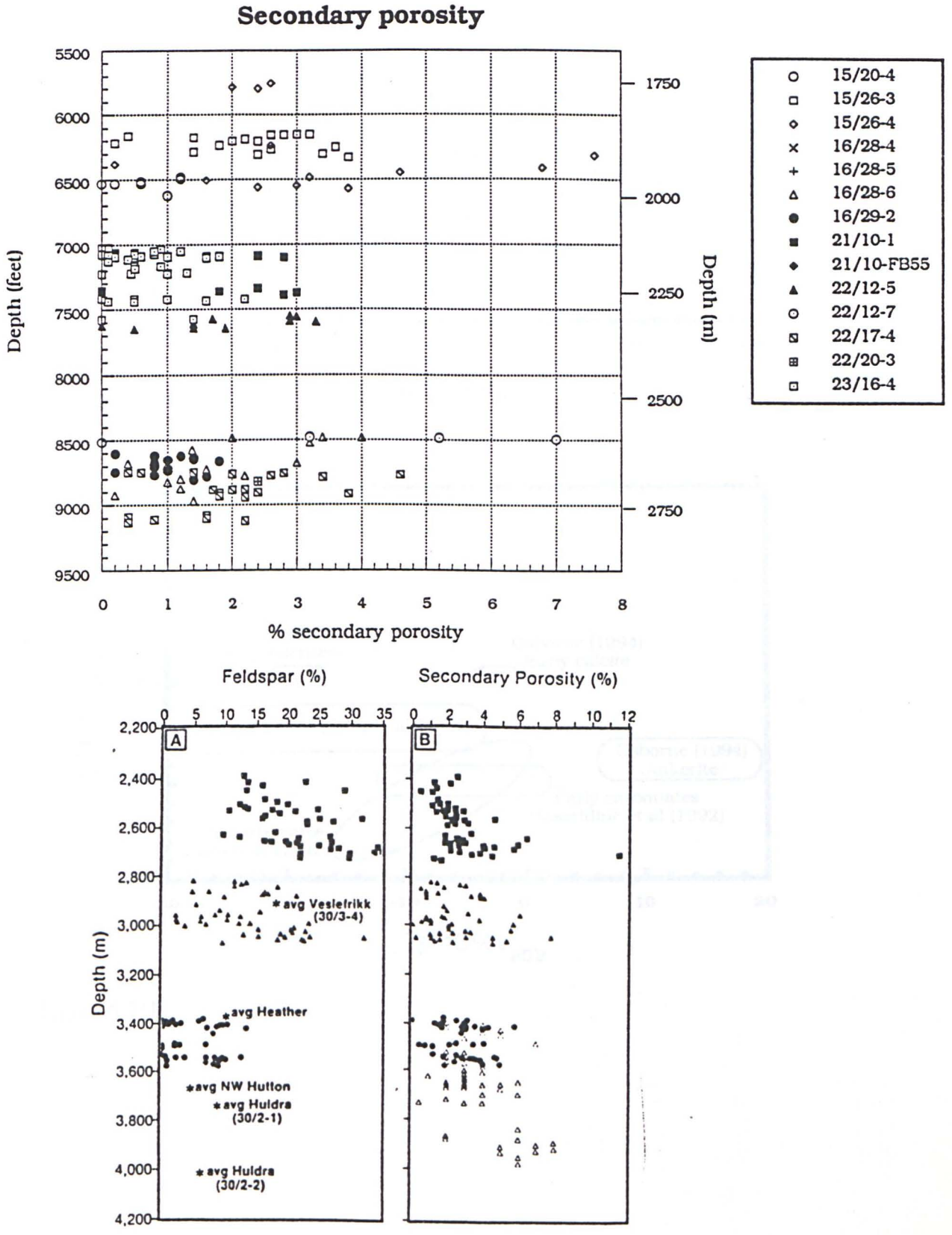

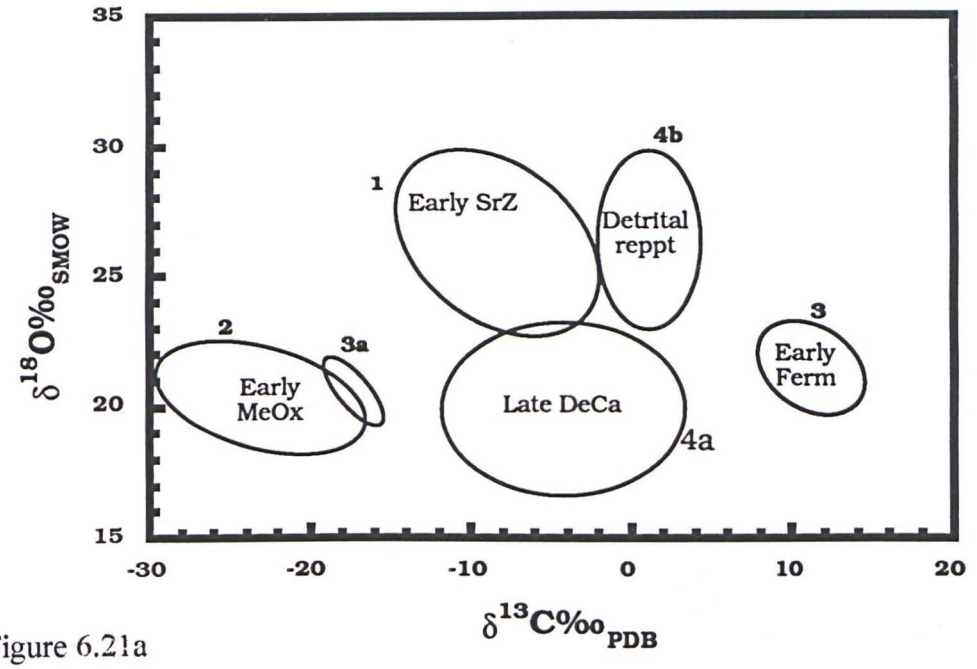

Figure 6.21a

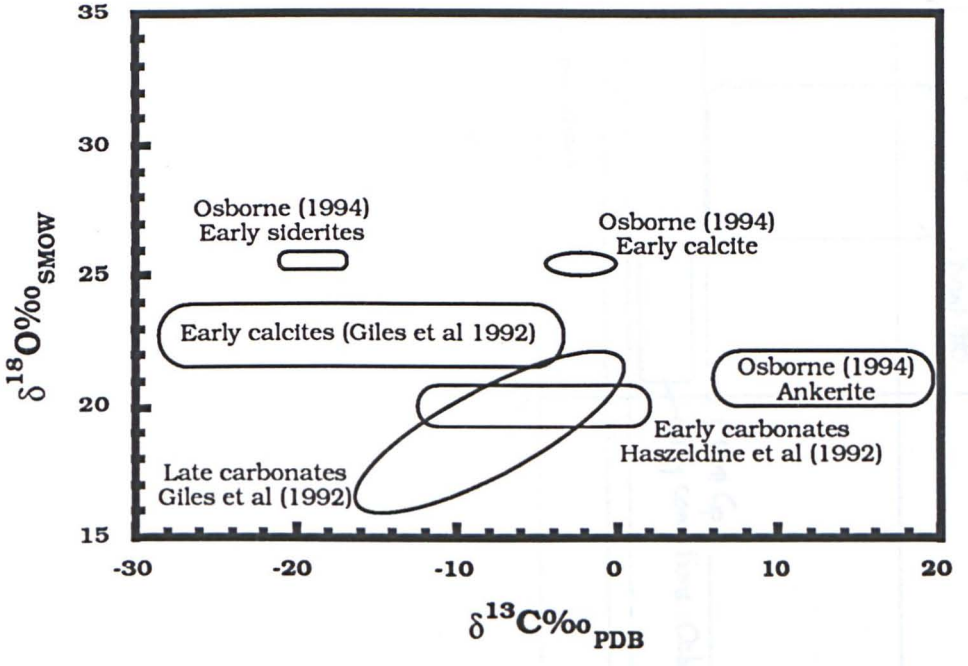

Figure 6.21b

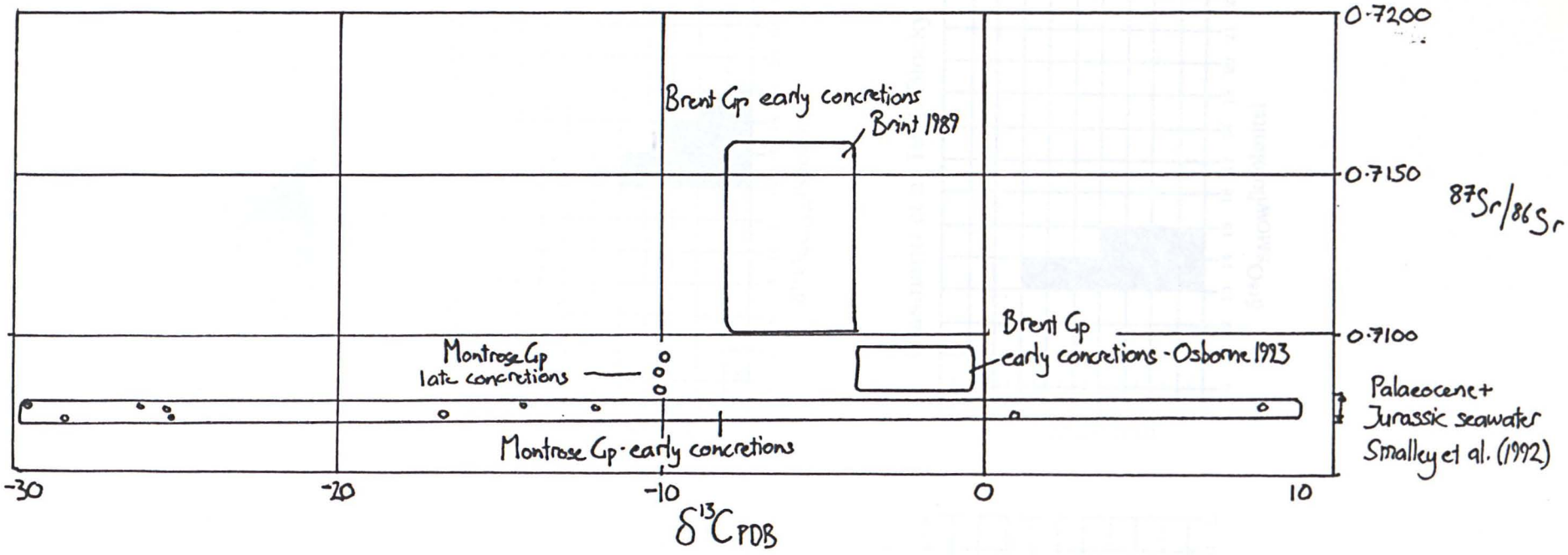
0·7200
0·7150
0·7100
87Sr/86Sr
Brent Gp early concretions
Brint 1989
Brent Gp
early concretions - Osborne 1993
Montrose Gp
late concretions
Montrose Gp - early concretions
Palaeocene+
Jurassic seawater
Smalley et al. (1992)
-30
-20
-10
0
10
δ13C PDB

Figure 6.22

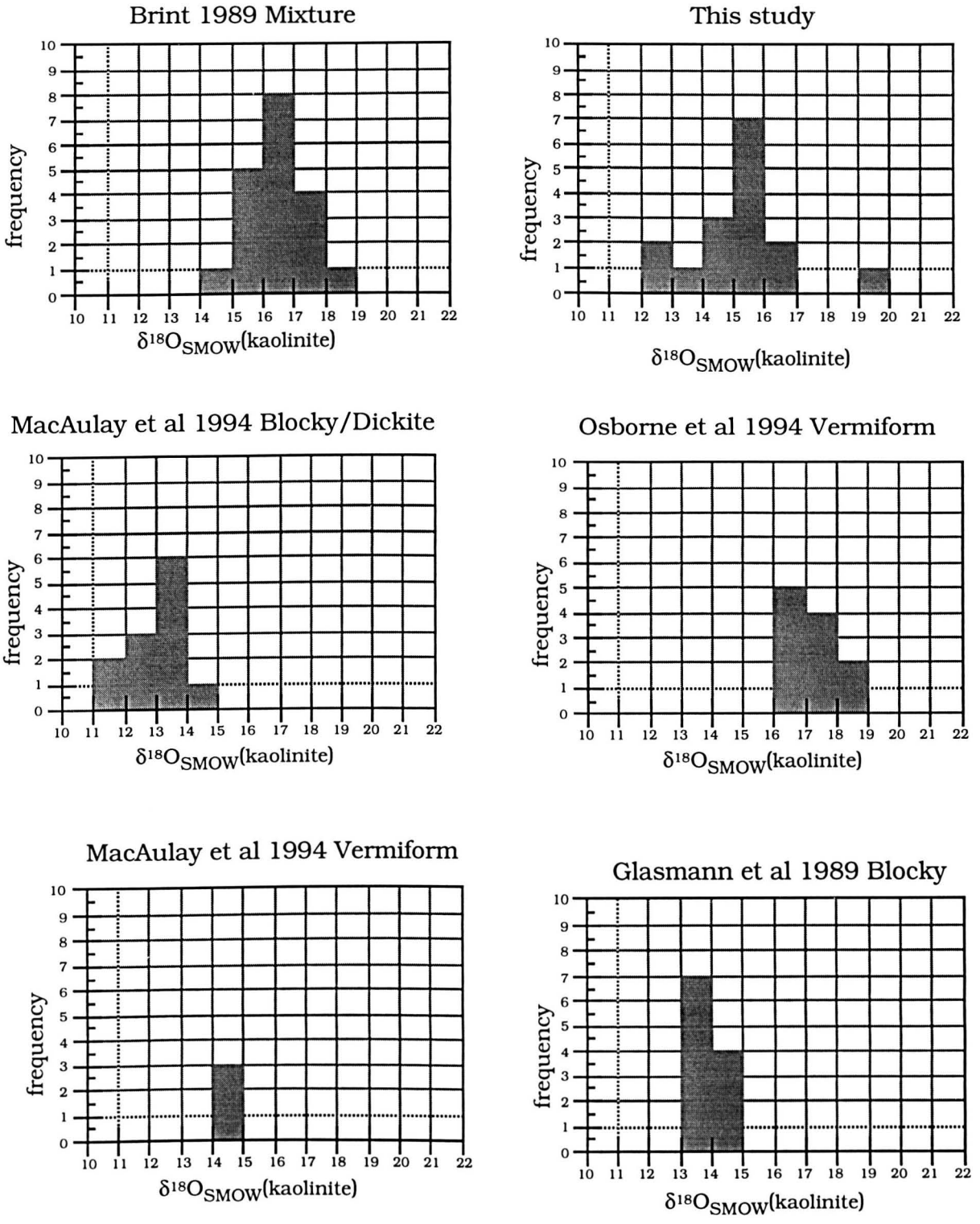
Brint 1989 Mixture
This study
MacAulay et al 1994 Blocky/Dickite
Osborne et al 1994 Vermiform
MacAulay et al 1994 Vermiform
Glasmann et al 1989 Blocky
frequency
δ18OSMOW(kaolinite)

Figure 6.23

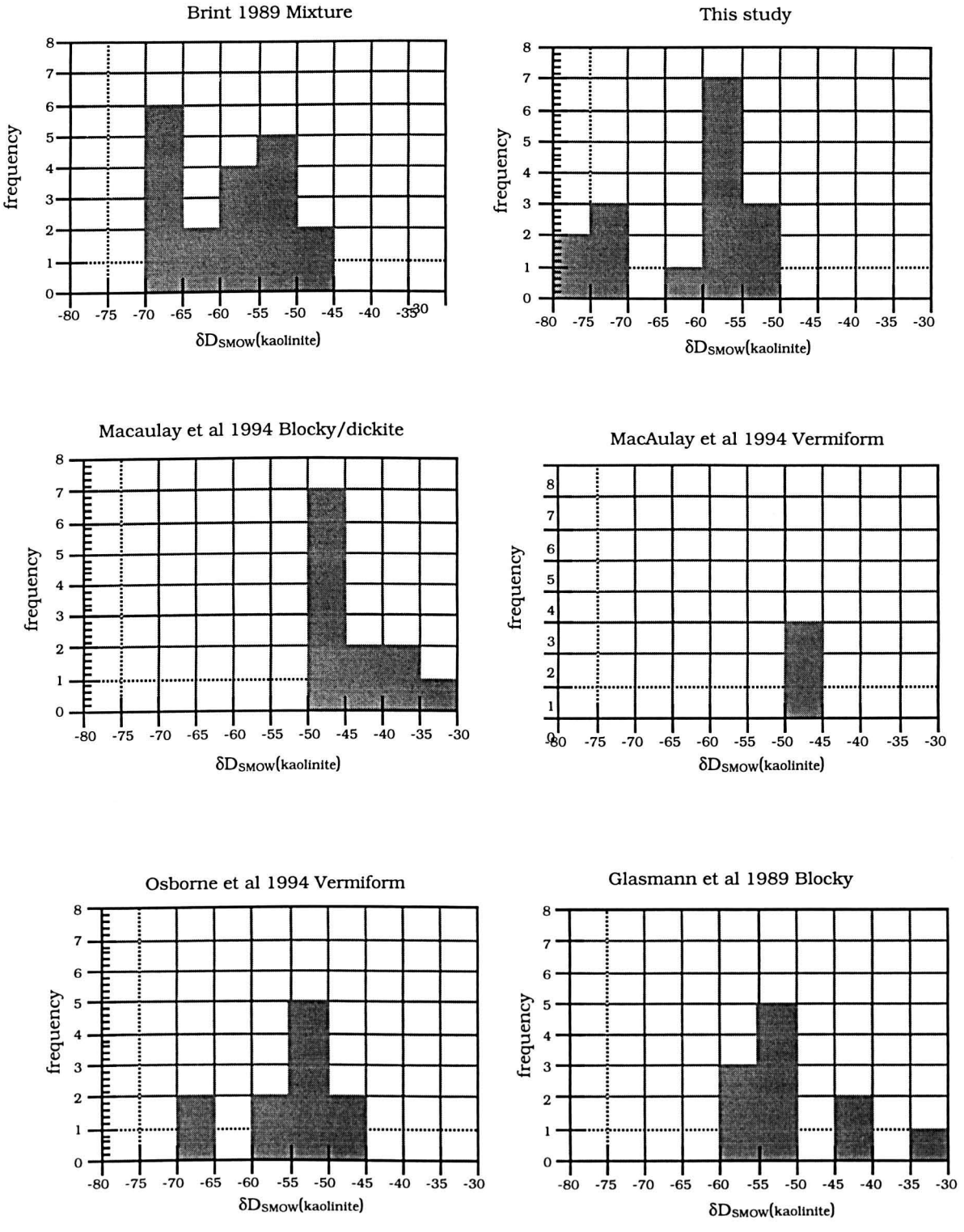
Brint 1989 Mixture
This study
Macaulay et al 1994 Blocky/dickite
MacAulay et al 1994 Vermiform
Osborne et al 1994 Vermiform
Glasmann et al 1989 Blocky
frequency
δDSMOW(kaolinite)
-80 -75 -70 -65 -60 -55 -50 -45 -40 -35 -30
0 1 2 3 4 5 6 7 8

Figure 6.24

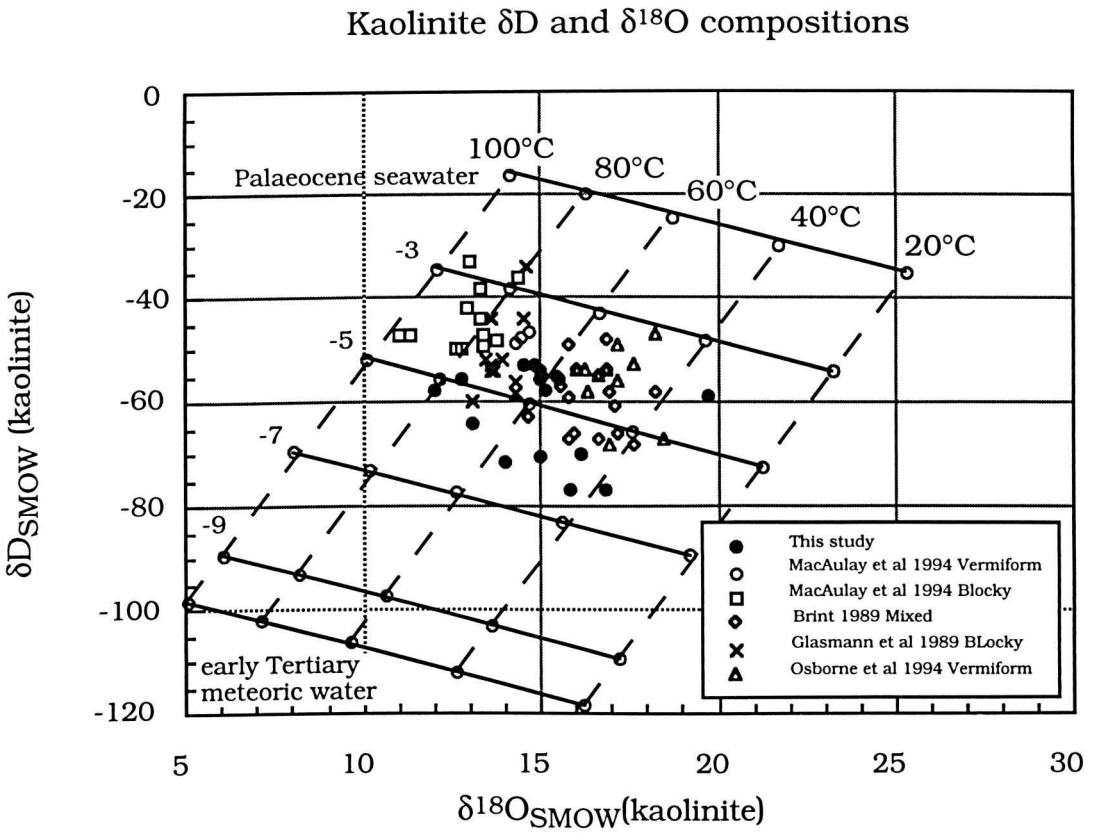

Figure 6.25a

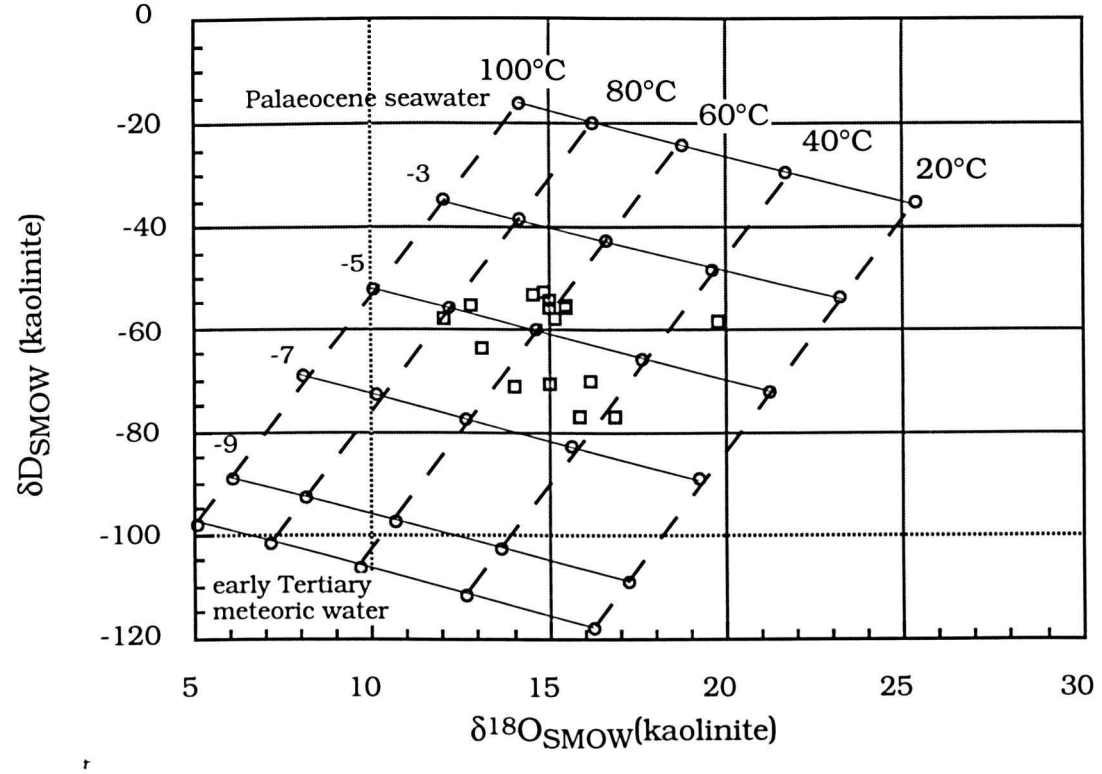

Figure 6.25b

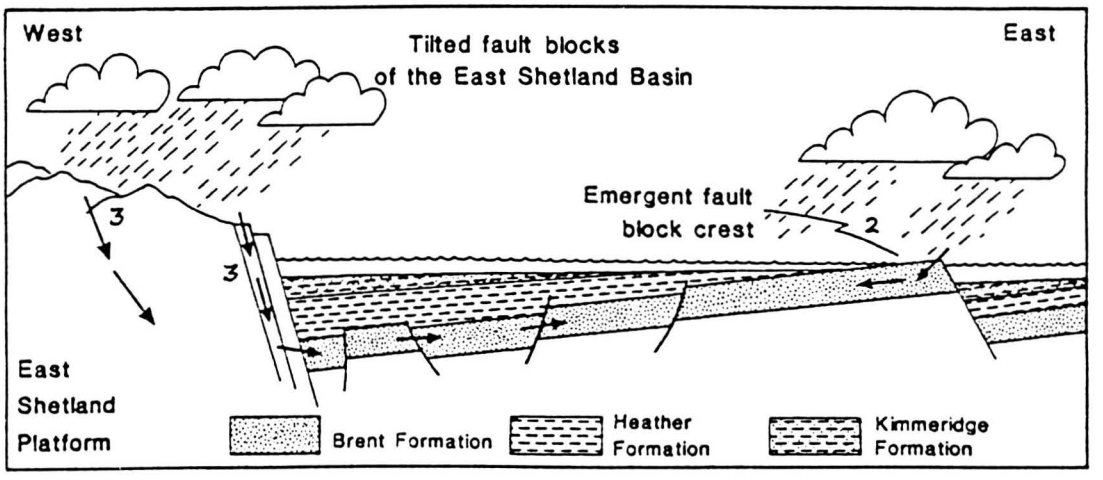

Figure 6.26a

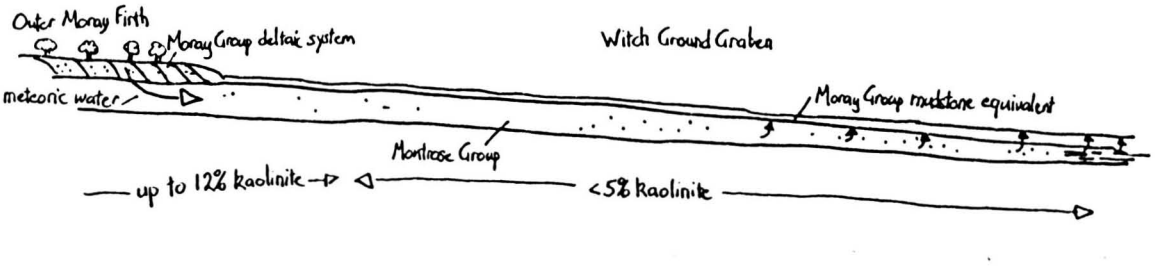

Figure 6.26b

CHAPTER 7 CONCLUSIONS

7.1 General overview

This chapter provides a summary and synthesis of the observations and deductions in earlier chapters. A diagenetic model is presented. (**Figure 7.1** Location map)

Palaeocene Montrose Group sandstones were laid down within the subsiding Central North Sea by high-density turbidity currents from the East Shetland Platform and Scottish mainland. The three formations (Maureen, Andrew and Forties Formations) form sand-rich aprons; their areal extent is controlled by the underlying Mesozoic graben system. Regionally the dominant facies is a massive-bedded sandstone forming thick (10's m) amalgamated units.

Meteoric flushing of these marine sandstones occurred early on during deposition of Montrose Group sandstones as Palaeogene basinward tilting exposed proximal Lower Palaeocene deposits, and progradation of Moray Group deltaic deposits in the Outer Moray Firth (Milton et al. 1990). An early diagenetic effect recording this porewater change has been the precipitation of carbonate cements. Structural control on carbon source is obvious from the regional groupings of early concretionary compositions.

Authigenic kaolinite isotopic compositions also recorded meteorically influenced porewaters. Wells sited close to the entrance point of meteoric water have up to 12% rock volume vermiform kaolinite, which may have directly precipitated during active flow. Most kaolinite within the sandstones comprises only <4% rock volume and appears to have grown over a considerable period during burial. Isotopic signatures indicate that precipitation took place within mixed meteoric-marine pore-fluids.

The isotopically heavier compositions of oxygen in pore-waters during late carbonate precipitation are likely to be due to introduction of porewaters from surrounding mudstones. Carbon isotopic compositions of late concretions within deeper buried wells indicate precipitation resulting from decarboxylation. The radiogenic strontium component and high manganese content within concretions is similar to that of published carbonate cements within the underlying chalks. Although this can be related to vertical fluid flow from the underlying Jurassic sandstones, resulting from overpressure release, the occurrence of the Mn-rich and radiogenic Sr-ratios can be sourced internally within the Montrose Group. An increase in quartz overgrowths also appears to be related to the structural proximity of salt diapirs. These cements may be linked to release in overpressure from underlying Jurassic sediments charging the Palaeocene sandstones with organic acids or ^{87}Sr-rich fluids. However if temperature is the main control on quartz cementation and overpressuring is absent then, the proximity to salt-diapirs can be explained by the higher heat conductivities of salt locally raising geothermal gradients accelerating geochemical reaction responsible for quartz precipitation. Major quartz cementation commenced at 8500ft by similar processes to the Brent Group. Overall porosity decline is approximately 2%/km

7.2 Carbonates and implications

Early concretions, identified by their high minus-cement porosities, have distinctive carbon and oxygen isotopic compositions resulting from specific organic reactions.

Of particular interest are concretions with very low $\delta^{13}C$ values ($\delta^{13}C$= -30 to -17‰PDB). A similar range of values occurs in cements associated with hydrocarbon oxidation. These calcite cements texturally post-date dolomites formed in the sulphate reduction zone. The presence of bituminous stains within concretions also record anaerobic oxidation of early migrating hydrocarbons and provide supporting evidence that this was the source of carbon.

Concretion thicknesses compiled from composite logs of massive channel sandstones enable the construction of a distribution map of concretions within the Central North Sea **Figure 7.2.** This map indicates that concretions generally makes 3-7% of sandstone thickness, i.e. 1.2-2.8% rock volume. These values may be close to the proportion of detrital carbonate originally in the sands. However anomalous areas of enhanced cementation are identified. These are generally deeper into the graben system, along graben flanks and along the axes of grabens.

Implications

Rapid burial within the Witch Ground Graben during the early Tertiary resulted in early maturation of Kimmeridge Clays in this area (Barnard & Bastow 1992). The timing and method of migration of these oils are problematic, i.e. when did they migrate, how did they enter the Lower Tertiary and by what pathway did they migrate in the Tertiary. The combination of isotopic compositions of carbonate cements and distribution of carbonate cements can be used to speculate that the enhanced cementation identifies palaeo-oil migration pathways. Where meteoric water, entering the Montrose Group from the palaeo-landmass to the west, mixed with hydrocarbons, the hydrocarbons were degraded. Degradation products included CO^{3-} which was utilised for calcite precipitation **Figure 7.3.** The hydrocarbons preferentially migrated up the graben flanks and through the depositional axes of the Witch Ground Graben and the Fisher Bank Basin on **Figure 7.2.** Extensive carbonate cements within a similar geological setting have been recognised within Palaeocene sandstones in UK Quadrant 9 (R. Dixon, BP, Dyce pers. comm. 1994). Here and in the Eocene Forth Field (Watson 1993) tilted 'bright spots', resulting from tight cemented sandstones, on seismic sections identified palaeo-pooling of hydrocarbon. After these cements had grown, the trap was later tilted basin-ward and the hydrocarbons migrated updip. Enhanced carbonate cementation in the more depositionally distal area may record late cements related to vertically underlying salt intrusion or salt-related activity, areas 2 and 3 on **Figures 7.2, 7.4.** There is evidence in high salinities in Montrose Group oilfield porewaters in the East Central Graben that vertical movement of fluid from the deep Jurassic to Palaeocene sediments has occurred. The carbon isotopic compositions (-10 to -5permill PDB) would appear to suggest that the carbon source is not simply reflect remobilisation of detrital carbonate but includes a component of carbon from a more negative source. Decarboxylation is the preferred process to supply carbon and is a late phase likely to be influenced by the proximity of heat-conducting salt diapirs.

7.3 Quartz and implications

Authigenic quartz cement precipitated from early burial onwards. Initially the quartz precipitated as small incipient overgrowths a few microns wide overlying detrital clays. It forms less than 2% of rock volume throughout burial. Deeper in burial depth, a gradual increase in quartz cementation is seen, **Figure 7.5.** The

silica is thought to precipitate from processes of pressure solution within the sandstone. Anomalous individual wells also occur; one well 23/16-4 has up to 7% quartz overgrowth volumes at depths around 2200m (7220ft). Although the processes supplying this silica are not known, this well overlies a Zechstein salt-dome, **Figure 7.4.** Though the composition of pore-waters from this well is not known, pore-waters from deep Montrose Group Arbroath & Montrose Oilfields in the Central Graben are known to be highly saline (Crawford et al. 1991). This is considered to have resulted from cross formational fluid flow from Zechstein salt. Anomalous increases in quartz overgrowths within Upper Jurassic and Brent Group sandstones have been noted by Emery et al (1993); these have been related to synchronous cementation and oil migration. Salt tectonics are not likely to have been responsible for this within this Brent Group area as Zechstein evaporites are not present within the Northern North Sea.

Implication

At depth authigenic quartz is volumetrically the most important cementing phase within the Brent Group, Northern North Sea. However, in shallow Brent sandstones, quartz cements form similar low volumes, as observed in the Montrose Group. These volumes however start to increase rapidly from burial depths of 2740m (~9000ft)(Giles et al. 1992). Although Giles et al. (1992) were not able to confidently identify the source of silica increase, they suspected that this was sourced by both local feldspar dissolution, and by pressure solution within siltstones. The resulting silica was transported a short distance into the sandstones. Emery et al. (1993) discovered that gradients of porosity decline vary from structure to structure within Mesozoic sandstones in the Northern North Sea. They attribute porosity decline gradients higher than standard to cementation synchronous with hydrocarbon charging of the structure. Quartz cementation was consequently reduced in oil bearing sandstones with cementation enhanced in the water leg. It is difficult to relate this process directly to the Montrose Group as no oilfields form in large tilted-fault block structures within this area as in the Brent province. The coincidence of increased quartz cement over a salt-dome (well 23/16-4) may be an analogous effect, and perhaps relates to cementation with hydrocarbon and pore-water migration vertically from the deep basin. These underlying fluids may have altered mineral equilibria, triggering silica-release reactions. Silica-bearing fluids rising up are not suspected as silica veining is not noted within publications which deal with petrographic descriptions and diagenetic alteration of chalk reservoirs within this area (Taylor & Lapre 1987, Smalley et al. 1992). It is likely that raised geothermal gradients around salt diapirs accelerated feldspar dissolution/quartz precipitation reactions.

7.4 Kaolinite and implications

Kaolinite usually forms 0 to 4.5% of the sandstones, and kaolinite separates from several wells have been isotopically analysed. Two morphologies of kaolinites are present within the Montrose Group; a vermiform kaolinite habit and a booklet kaolinite habit. The two habits are not mutually exclusive. Booklet kaolinite appears to overgrow earlier vermiform kaolinite within deeper wells. Kaolinite morphology changes with depth and therefore with distance from depositionally proximal areas. Anomalously abundant kaolinite makes up to 12% by volume of sandstones in wells 15/26-3 and 15/26-4.

Isotopic compositions (δD and $\delta^{18}O$) of kaolinite in the Montrose Group throughout the Central North Sea are very similar. The simplest interpretation from a δD-$\delta^{18}O$ cross-plot would indicate that the kaolinite grew within mixed waters, $\delta^{18}O$= -6.5 to -3‰SMOW, at moderate temperatures, 35 to 80°C. The assumption is made that post-growth isotopic exchange with pore-fluids did not occur.

Implications

The similarity of compositions for kaolinite separates suggests an overlapping spread of pore-water compositions and temperatures of precipitation for both kaolinite morphologies. However, the data may also conceal a long period of slow rates of kaolinite growth under gradually changing circumstances. The implication is that pore-waters were mixed. This implies that meteoric water had flushed through the Palaeocene sands at some stage of burial. The most likely timing is throughout the Palaeocene itself as basinward tilting exposed earlier deposited Lower Palaeocene sediments when the North Sea suffered a remarkable fall of relative sea-level (54.8Ma, Milton et al. 1990), which resulted in delta progradation of the Moray Group into the Moray Firth, **Figure 7.6**. The meteoric head must have been sufficient to have flushed the sands at this time. Meteoric signature was present during kaolinite precipitation after marine transgression had sealed off proximal end of Montrose Group within the Outer Moray Firth.

Kaolinite precipitation within wells 15/26-3 and 15/26-4 may have precipitated in response to this active introduction of meteoric water, though unfortunately there is no isotopic data from these wells. The temperatures of up to 80°C deduced from isotopic data suggest that pore-fluids still had a noticeable meteoric influence long after closure of the system to shallow meteoric flow. This mixture of meteoric-marine pore-waters is in contrast to late calcites which post-date kaolinite in the distal areas of the Montrose Group. Late concretions have $\delta^{18}O$ compositions that are satisfactorily explained by precipitation within pore-water isotopically similar to marine compositions.

7.5 Late carbonate and implications

Late concretions within distal areas of the Montrose Group have $\delta^{18}O$ values that are consistent with precipitation from pore- fluids with a marine composition. Carbon isotopic compositions indicate precipitation from a combination of decarboxylation and detrital carbonate dissolution. Concretions post-date quartz cements and kaolinite, **Figure 7.7**. $^{87}Sr/^{86}Sr$ ratios of late carbonate indicate that a radiogenic component was present during precipitation. Late carbonate concretions are also enriched in manganese.

Implications

Present day pore-waters within the Forties Field 21/10, (Emery & Robinson 1993), have $\delta^{18}O$ values of -0.7 to +1.7‰SMOW and δD values of -25.5 to -13.8‰SMOW, with very low sulphate concentrations (1-42ppm). These pore-waters are enriched in ^{18}O even compared with Palaeocene sea-water. The enrichment in ^{18}O is puzzling as there has not been sufficient precipitation of low ^{18}O authigenic minerals to enrich pore-waters in ^{18}O from end member meteoric values.

Sandstone pore-waters must have mixed with fluids introduced after flushing to attain their present day composition. These may have been:-
i) Zechstein pore-fluids, the highly saline nature of some deep Montrose Group pore-fluids (135,000ppm salinity Montrose Field, Crawford et al. 1991) attest to the introduction of connate waters. Porefluids outside the East Central Graben have normal salinities.
ii) Fluids from overpressured overlying Upper Tertiary muds; Carbonate and pyritic veins within mudstones overlying the Montrose Group attests to fluid flow through this sequence. The release of overpressuring by downwards fluid movement may have introduced modified saline pore-waters into the clastic Palaeocene sequence. Present day profiles of formation pressure, derived from mud weight logs, show that the Montrose Group forms a hydrostatically pressured regional aquifer, and pressures in overlying muds gradually increase away from this sandstone.
iii) Jurassic pore-fluids; Strontium ratios of authigenic calcites within underlying chalks are more radiogenic than depositional chalks, and strontium ratios increase with depth. Enrichment of the radiogenic strontium component results from the dissolution of silicate minerals. Such pore-waters may have risen up fractures overlying the Jurassic during overpressure release. Once in the Palaeocene sandstones, these fluids could have moved laterally outwards from the basin centre.

7.6 Proposals for future work

7.6.1 Concretions

Data from composite logs have been entered into Stratamodel 3D computer modelling program. Computer generated graphics of separate Palaeocene Formations are envisaged creating a more accurate portrayal of carbonate distribution. It will be possible to determine whether sand/mud ratios have influenced precipitation of carbonate. Transit times have also been recorded, from these it is hoped that it will be possible to identify depths where silica cements precipitate, in the form of a sudden regional drop in transit times.

7.6.2 Kaolinite

Sampling from wells in a transect across the palaeo-shoreline should enable workers to shed more light on the processes which resulted in the precipitation of kaolinite. It would be interesting to know whether the isotopic compositions of kaolinite separates from wells 15/26-3 and 15/26-4 fall within the Osborne et al (1994) vermiform field on the $\delta^{18}O$-δD crossplot, and hence grew at similar times to the majority of kaolinite. Different $\delta^{18}O$ and δD values would confirm different fluids and timing of fluid change.

7.6.3 Overpressure leak points

Perhaps the most intriguing question concerns the cause of quartz cementation at depth. What is the link between maturation, oil migration or Zechstein breakthrough? Research could take the form of sampling wells around a diapir structure, and tabulating; $^{87}Sr/^{86}Sr$ ratio of carbonates, quartz overgrowth percentage, fluid inclusion analysis of quartz overgrowths to determine petroleum composition, and making Ro measurements from organic samples.

7.7 Diagenetic model for exploration

Throughout the whole Montrose Group, sandstones regionally have good porosities and permeabilities. However there are variations in these qualities which relate to diagenetic processes, **Figure 7.8.** The main porosity reducer within sandstones is the presence of carbonate concretions. These can fill up to 10% whole rock volume of producing sandstones (see composite logs of Balmoral Field, Tonkin & Fraser 1991). They can also result in partial compartmentalisation of reservoirs. The areas of higher carbonate cement are situated within the axis of the Witch Ground Graben, the north flank of the Witch Ground Graben. These are tentatively associated with biodegradation of early migrating hydrocarbons within meteoric porewaters. High percentages of carbonates are also found along the east side of Quadrant 22 and within block 16/28. These areas are associated with salt diapirism. Higher percentages of concretions are also found along the axis of the East Central Graben

Kaolinite generally does not precipitate in sufficient volumes to affect production. However close to palaeo-shorelines, kaolinite forms up to 12% of rock volume as a result of meteoric influx. Such volumes may cause problems with clay migrating during production. Biodegradation of early migrating oil within the cool meteoric water would also have taken place.

Areas in proximity to salt diapirs also have anomalously higher percentages of diagenetic quartz, up to 7% rock volume, compared with an average of ~2% rock volume. In sandstones with 25% porosity, this reduces porosity by a fifth. The best prospects for drilling are areas away from salt diapirism, away from areas of early migrating oil within meteoric waters and away from direct meteoric influx.

A more common problem in Palaeocene may be not too much diagenetic cements, but too little. This can result in loose sand being pumped up during production. Such loose sands are common in chlorite-cemented zones. These are controlled by depositional axes and inputs of volcanic debris.

References

Barnard P.C, and Bastow M.A. 1992 Hydrocarbon generation, migration, alteration, entrapment and mixing in the Central and Northern North Sea. In: *Petroleum Migration,* W.A. Fleet (ed), *Geol. Soc. Spec. Publ.* **59,** 167-190

Crawford R., Littlefair R.W. and Affleck L.G. 1991 The Arbroath and Montrose Fields, Block 22/17,18 UK North Sea. In: *United Kingdom Oil and Gas Fields, 25 Years Commemorative Volume,* I.L. Abbotts (ed)., *Geol. Soc. Lond. Mem.* **14,** 211-217.

Emery D., Smalley P.C., and Oxtoby N.H. 1993 Synchronous oil migration and cementation in sandstone reservoirs demonstrated by quantitative description of diagenesis. *Phil. Trans. R. Soc. Lond.* **344,** 115-125.

Emery D. and Robinson A. 1993 Petroleum Recovery In: Emery D. and Robinson A, (eds). *Inorganic Geochemistry: Applications to Petroleum Geology* Blackwell Scientific Publications, Oxford, 213-230.

Giles M.R., Stevenson S., Martin S.V., Cannon, J.C., Hamilton P.J., Marshall J.D. and Samways, G.M. 1992 The reservoir properties of the Brent Group: a regional perspective. In: *Geology of the Brent Group,* A.C. Morton, R.S Haszeldine, M.R. Giles and S. Brown (eds) *Geol. Soc. Spec. Publ.* **61,** 289-327.

Milton N.J., Bertram G.T. and I.R. Vann 1990 Early Palaeogene tectonics and sedimentation in the Central North Sea. In: *Tectonic Events Responsible for Britain's Oil and Gas Reserves*, R.F.P. Hardman and J. Brooks (eds), *Geol. Soc. Spec. Publ.* **55**, 339-351.

Platt N.H. and Philip P. 1993 Comparison of Permo-Triassic and deep structure of the Forties-Montrose and Jaeren highs, Central Graben, UK and Norwegian North Sea. In: *Petroleum Geology of Northwest Europe: Proceedings of the 4th Conference*, J.R. Parker (ed), Geol. Soc., London, 1221-1230.

Smalley P.C., Lonoy A., and Raheim A. 1992 Spatial $^{87}Sr/^{86}Sr$ variations in formation water and calcites from the Ekofisk chalk oil field: implications for reservoir connectivity and fluid composition. *Applied Geochemistry*, **7**, 341-350.

Taylor S.R. and J.F. Lapre 1987 North Sea chalk diagenesis: its effect on reservoir location and properties. In: *Petroleum Geology of North West Europe*, J.R. Parker (ed), Geol. Soc., London, 107-121.

Tonkin P.C., Fraser A.R. 1991 The Balmoral Field, Block 16/21, UK North Sea. In: *United Kingdom Oil and Gas Fields, 25 Years Commemorative Volume*, I.L. Abbotts (ed), *Geol. Soc. Lond. Mem.* **14**, 237-243.

Watson R.S. 1993 *The Diagenesis of Tertiary sands from the Forth and Balmoral Fields*. PhD Thesis, University of Aberdeen.

Figure Headings

Figure 7.1 Location map of the Central North Sea showing major tectonic features of the base Cretaceous.

Figure 7.2 Map of percentage diagenetic carbonate within Montrose Group sandstones. Data was compiled from 101 composite logs. Areas 1 to 4 contain anomalous amounts of concretions. In area 1, concretions precipitated as a result of hydrocarbon biodegradation within cool meteoric waters sourced from the northwest. This area along the axis of the Witch Ground Graben and north flank of the witch Ground Graben also potentially identifies the location of early oil migration paths. Area 2 identifies an area of salt- diapirism. The geochemical and isotopic composition of the late Montrose Group concretions can be related to cross-formational fluid movement from the underlying Cretaceous sequence. Areas 3 and 4 contain late concretions with similar geochemical compositions as area 2 and are thought to be related to similar processes.

Figure 7.3 Cartoon illustrating the Witch Ground Graben during the late Palaeocene. Meteoric water sourced from a prograding delta system interacts with early migrating hydrocarbons. Biodegradation of the hydrocarbons resulted in the precipitation of early calcite concretions.

Figure 7.4 Illustrative cross-section from Platt & Philip (1993) across the Jaeren High shows the effect of Zechstein salt-diapirism on the overlying sediments. Late Mn-calcites within the Montrose Group have a radiogenic Sr component which is similar to that found in Central North Sea chalks (Smalley et al. 1992). This enriched Sr is likely to have come from Jurassic formation water as a result of fracturing around the salt-dome, which encouraged fluid escape from overpressured Jurassic

formations. Arrows show inferred directions of fluid movement. Evidence for cross-formational flow can be summarised as:- - high salinities recorded within deep buried Montrose Group sandstones e.g. Montrose 111,000mg/1 salinity, Arbroath 135,000mg/1 salinity (Crawford et al 1991). Such salinities could only have resulted from dissolution of Zechstein evaporites. - radiogenic $^{87}Sr/^{86}Sr$ ratios within late carbonates in Montrose Group sandstones. (Authigenic calcites in underlying chalks also have a radiogenic component which increases with depth, Smalley et al. 1994). Radiogenic components within chalks implies that Sr resulting from dissolution of silicates was imported from underlying Jurassic clastic sequence. - Mn enrichment within late carbonate within the Montrose Group is similar to that noted in chalk sequences. The manganese may have been imported into the chalks and the Montrose Group sandstones. - Anomalous increase in quartz cementation within Montrose Group sandstones in proximity to salt-diapirs. The process which causes this is not understood, nevertheless enhancement in silica of up to 7% is seen wells adjacent to salt structures.

Figure 7.5 Percentage quartz overgrowth with depth. At burial depths >8500ft (2.4km) the percentage of quartz overgrowths increase above 2%. In wells adjacent to salt diapirs anomalous increase in quartz overgrowth is seen e.g. 23/16-4. This is related to movement of fluids from underlying overpressured Jurassic formation, perhaps related to oil expulsion resulting in silica- releasing reactions within the Montrose Group sandstones.

Figure 7.6 Cartoon illustrating meteoric influx into the Montrose Group. During the late Palaeocene, drastic sea-level fall resulted in the progradation of the deltaic Moray Group across the Outer Moray Firth. Maximum progradation of clastic deposits is denoted by the present day eastward limit of lignite's. Close to palaeo-shorelines two wells contain anomalously high proportions of kaolinite, up to 12% rock volume. Regionally the average kaolinite is <4% rock volume. This enhanced kaolinite percentage is related to the rapid flow of water through the sandstones in this area,

Figure 7.7 Photomicrograph from well 22/20-3. This well is situated above a salt diapir. The photo illustrates the high percentage of quartz overgrowth now tightly cemented by late carbonate.

Figure 7.8: Diagenetic exploration map of the Central North Sea.
Area 1 Poor area resulting from meteoric flushing; Any hydrocarbons which migrated into this area are likely to have been severely degraded, high percentages of kaolinite may cause blocking of sand pore if clay migrates during oil production.
Area 2 Poor area resulting from high amounts of carbonate concretions; These concretions may fill up to 10% of reservoir horizon and create permeability baffles. Early migrating oil may be degraded as well.
Area 3 Poor area resulting from salt-diapir related diagenesis; Increasing quartz cementation (up to 7%) reduces porosity. Also enhanced volumes of late carbonates substantially reduce porosity within sandstones.
Area 4 to 5 Poor area; concretions from these areas have similar geochemical compositions as area 3, though percentages of quartz cementation is not altogether clear as a result of lack of samples.

Best areas for exploration are situated; i) Away from meteoric water influence, and ii) within late oil migration routes, up dip from salt-diapirs. Forties Field 21/10 and 22/6 is situated in such a position.

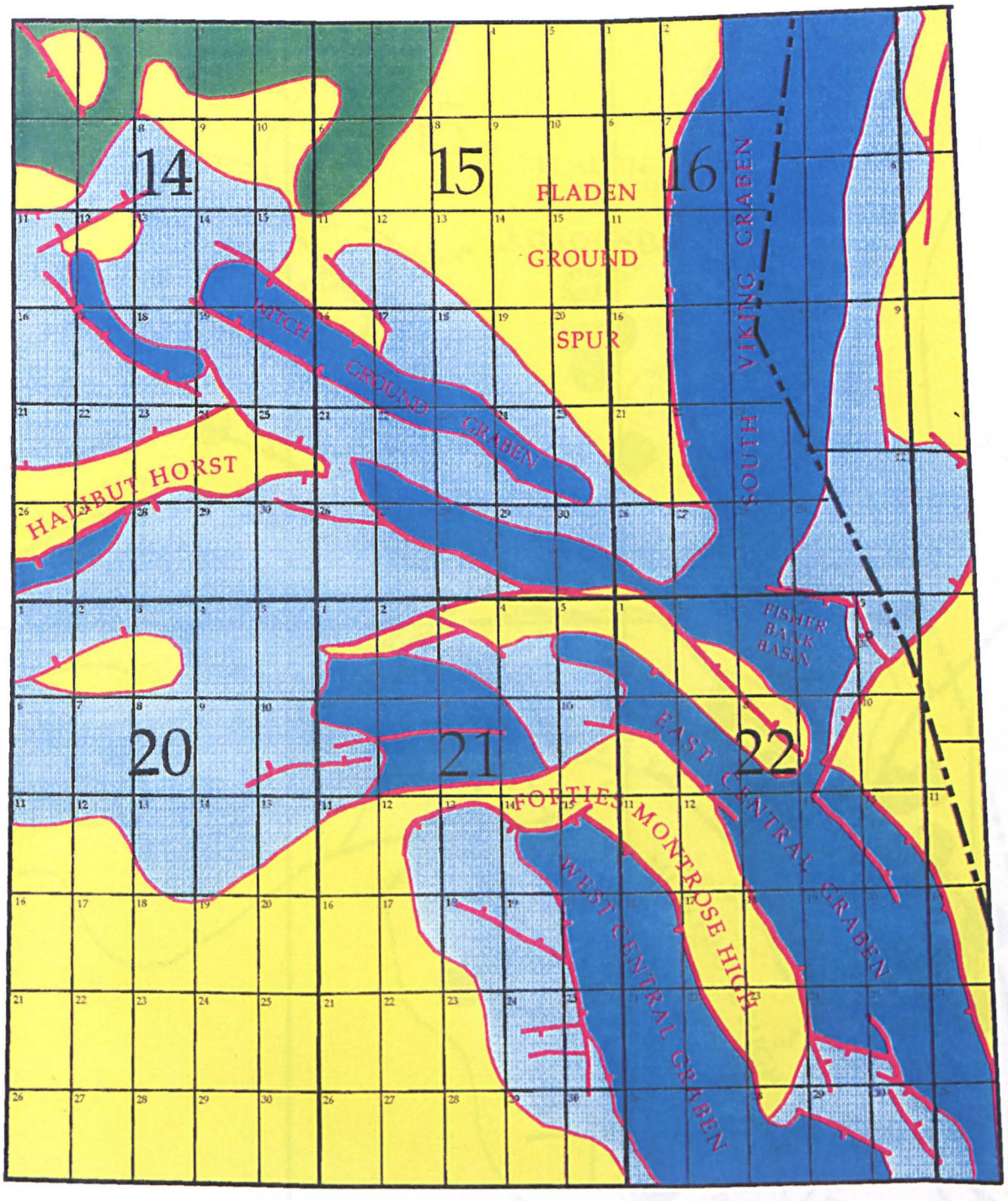

Figure 7.1 Location Map

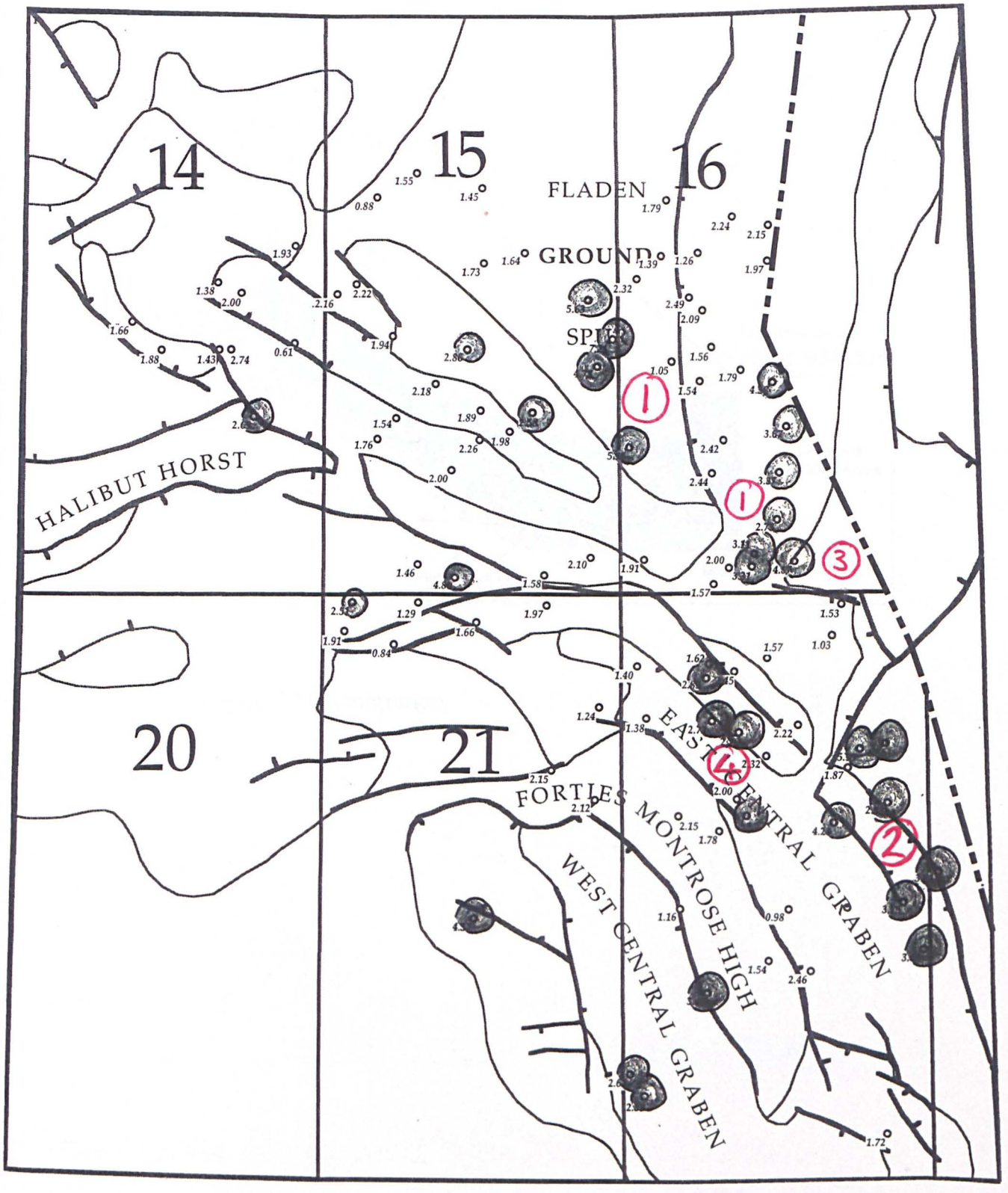

Figure 7.2
cf. Section 2.12

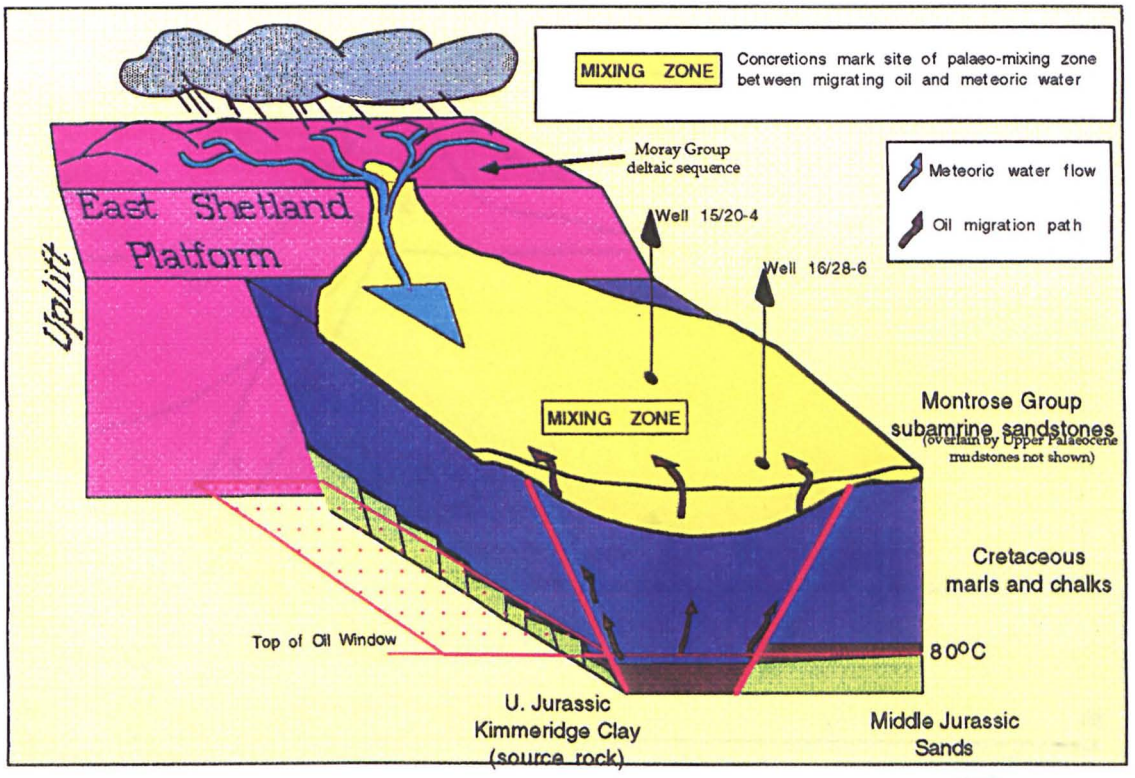

Figure 7.3 Oil migration

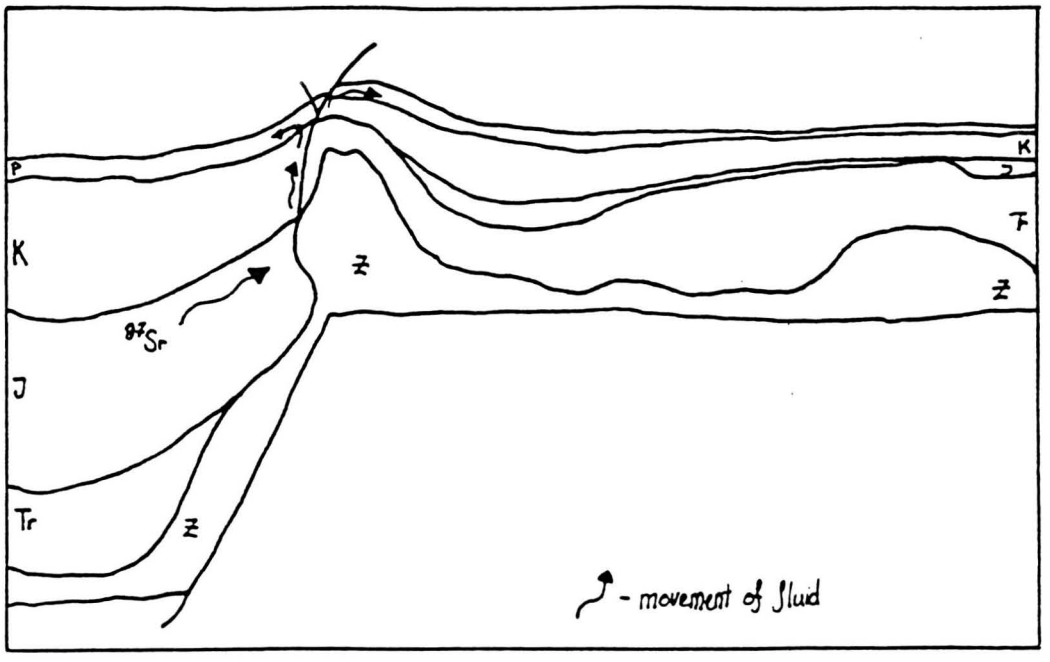
P
K
J
Tr
Z
^{87}Sr
- movement of fluid

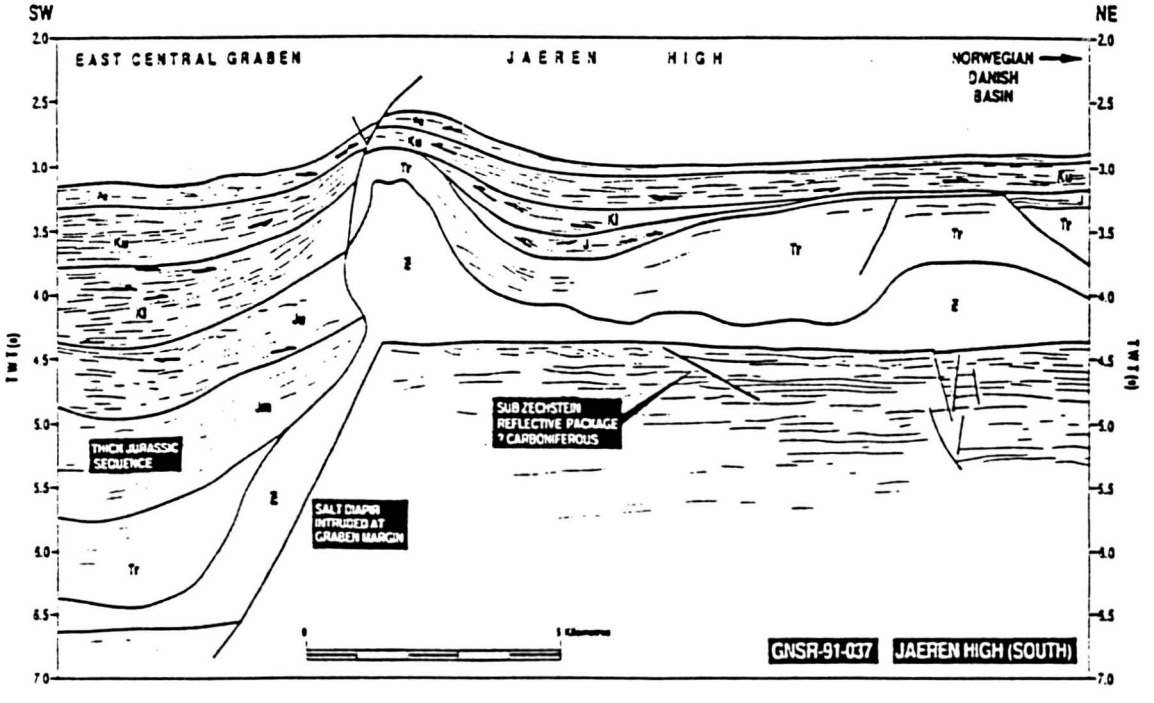
SW
NE
EAST CENTRAL GRABEN
JAEREN HIGH
NORWEGIAN DANISH BASIN
TWT (s)
THICK JURASSIC SEQUENCE
SALT DIAPIR INTRUDED AT GRABEN MARGIN
SUB ZECHSTEIN REFLECTIVE PACKAGE ? CARBONIFEROUS
GNSR-91-037
JAEREN HIGH (SOUTH)

Figure 7.4

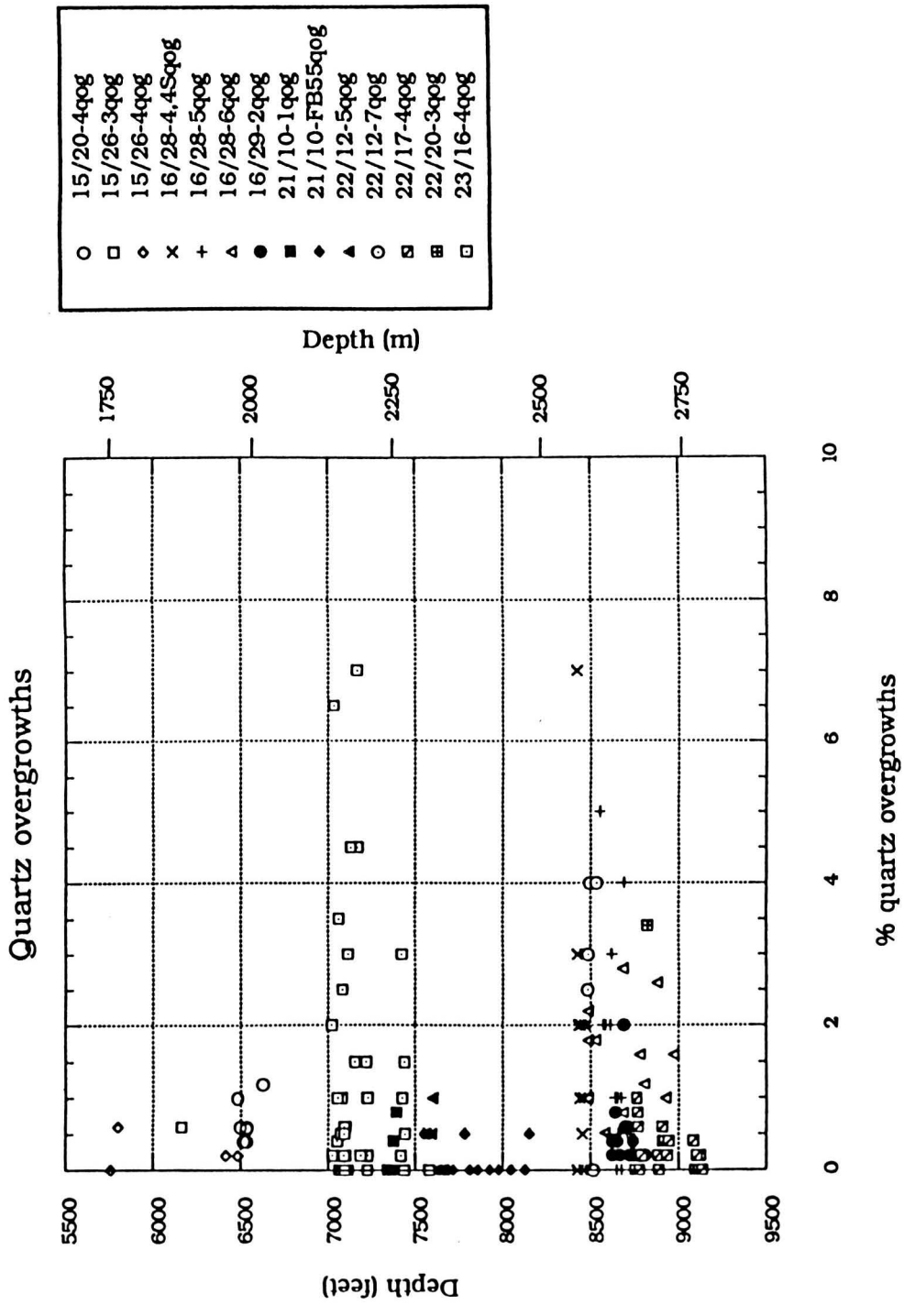

Fig 7.5 Point count data: quartz overgrowth increases slowly with depth

Figure 7.6 Isotopic data from carbonate separates indicate that pore-waters within Montrose Group submarine sandstones were influenced by a meteoric influx. During late Palaeocene a relative sea-level drop of 900m (Reynolds 1994) resulted in the progradation of a deltaic system (Moray Group) over the Outer Moray Firth. Introduction of meteoric water is inferred to have occurred during this period. Maps illustrate Sequence 3 and 8 (Andrew Formation and Moray Group equivalent) Stewart 1987. Meteoric flushing must have occurred before compaction of overlying Tertiary muds resulting in a regional seal.

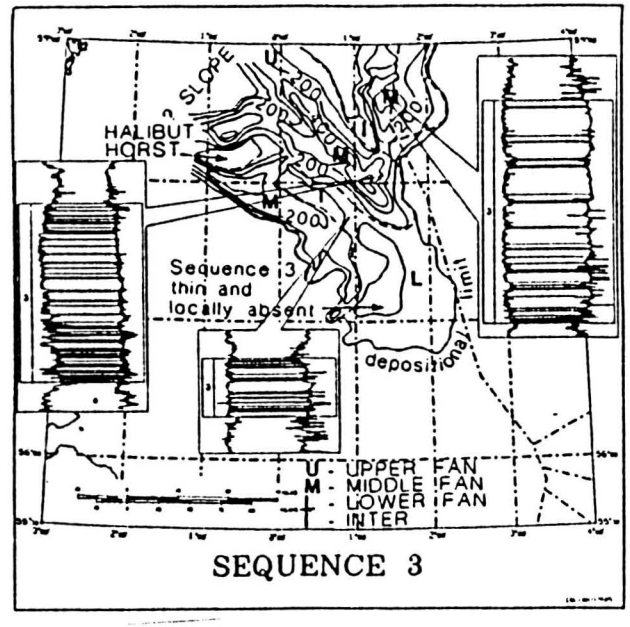

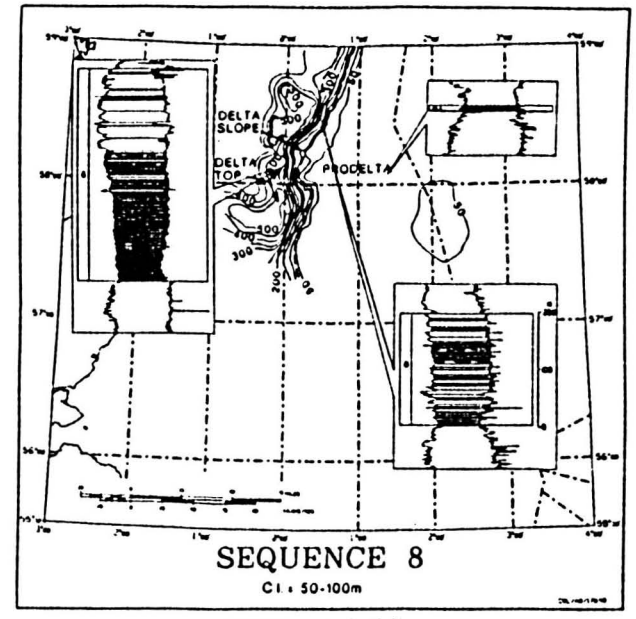

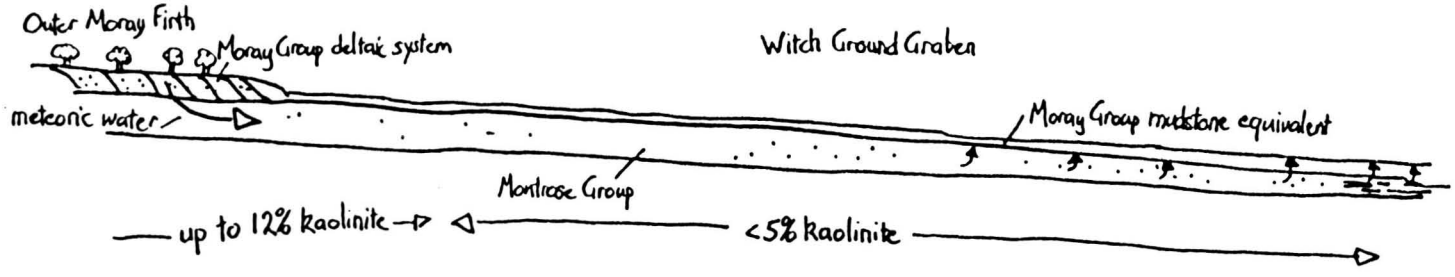

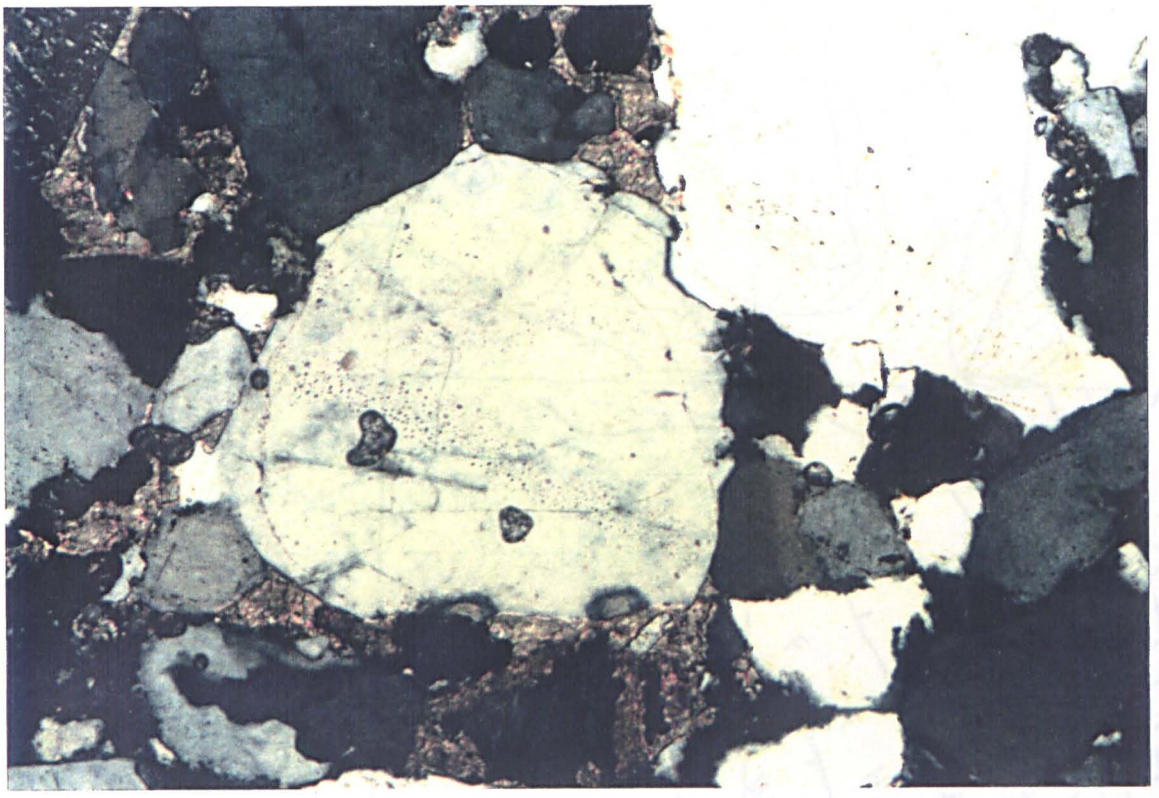

Figure 7.7 Photomicrograph of late calcite enclosing kaolinite and quartz overgrowths, well 22/20-3, 2645.7m. Photo is 250μm across.

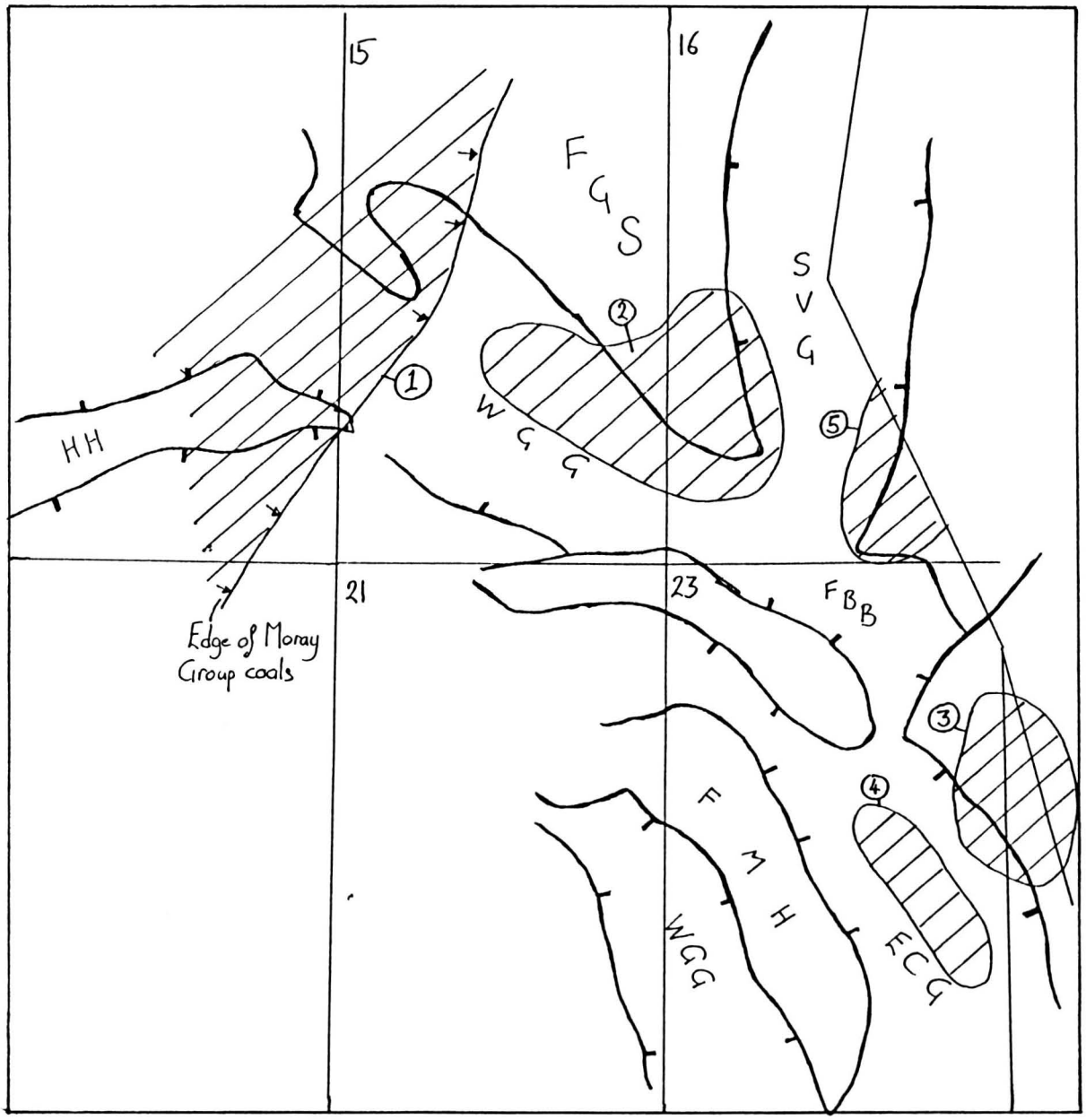

Figure 7.8